THÈSE

Pour obtenir le grade de

DOCTEUR DE L'UNIVERSITÉ GRENOBLE ALPES
et de l'UNIVERSITE Joseph KI-ZERBO

École doctorale : STEP - Sciences de la Terre de l'Environnement et des Planètes
Spécialité : Sciences de la Terre et de l'Environnement
Unité de recherche : Institut des Sciences de la Terre et Laboratoire de Microbiologie et Biotechnologie Microbienne

Impact de l'orpaillage sur les écosystèmes aquatiques et les populations au Burkina Faso et en Guinée

Impact of gold mining on aquatic ecosystems and populations in Burkina Faso and Guinea

Présentée par :

Djamilatou DABRE

Direction de thèse :

Stéphane GUEDRON Université Grenoble Alpes	Directeur de thèse
Ynoussa MAIGA Université Joseph KI-ZERBO	Co-Directeur de thèse
Jacques GARDON Hydrosciences Montpellier	co-Directeur de thèse
Ousséni OUÉDRAOGO Université Joseph KI-ZERBO	co-encadrant de thèse

Rapporteurs :

David AMOUROUX DIRECTEUR DE RECHERCHE, CNRS	Université de Pau et des Pays de l'Adour
Vera SLAVEYKOVA FULL PROFESSOR	University of Geneva

Thèse soutenue publiquement le **04 Mars 2026**, devant le jury composé de :

Stéphane GUEDRON DIRECTEUR DE RECHERCHE, IRD	Directeur de thèse
Ynoussa MAIGA Professeur Titulaire, UJKZ	Co-Directeur de thèse
David AMOUROUX DIRECTEUR DE RECHERCHE, CNRS	Rapporteur
Vera SLAVEYKOVA FULL PROFESSOR	Rapportrice
Birane NIANE Maître de conférences, Université Iba	Examinateur
Valérie LAPERCHE Chercheur au BRGM	Examinatrice
Géraldine SARRET Directrice de recherche CNRS	Présidente du Jury

THÈSE

UNIVERSITÉ GRENOBLE ALPES et UNIVERSITÉ JOSEPH KI-ZERBO

École doctorale des sciences de la Terre, de l'environnement et des planètes/ École doctorale Sciences et Technologie

Présentée par

Djamilatou DABRE

Pour l'obtention du grade de docteur de l'Université Grenoble Alpes et de l'Université Joseph KI-ZERBO

Sujet de la thèse :

Impact de l'orpaillage sur les écosystèmes aquatiques et les populations au Burkina Faso et en Guinée

MEMBRES DU JURY

RAPPORTEURS

- David AMOUROUX — Université de Pau et des Pays de l'Adour, France
- Vera SLAVEYKOVA — Université de Genève

EXAMINATEURS

- Birane NIANE — Université Iba Der THIAM de Thiès
- Valérie LAPERCHE — Chercheur au BRGM, France

DIRECTEURS

- Stéphane GUÉDRON — Université Grenoble Alpes, France
- Ynoussa MAÏGA — Université Joseph KI-ZERBO, Burkina Faso

ENCADRANTS

- Odile BRUNEEL — Hydrosciences Montpellier, France
- Jacques GARDON — Hydrosciences Montpellier, France
- Ousséni OUÉDRAOGO — Université Joseph KI-ZERBO, Burkina Faso
- Hamed A. KONATÉ — Université Mine et Géologie de Boké, Guinée

Abstract

Artisanal and small-scale gold mining (ASGM) is a major source of environmental pollution, which remains poorly documented in West Africa. In Burkina Faso and Guinea, this mining activity has expanded dramatically over the past few decades. The use of chemicals for gold recovery, including mercury (Hg) and cyanide (CN) leads to major contamination of the environment. In addition, soil reworking can lead to the remobilization of geogenic contaminants like Hg, lead (Pb) and arsenic (As) naturally present in these soils. This study aims to quantify and characterize metal contamination, with a focus on Hg speciation and its environmental and health impact in Burkina Faso and Guinea. To this end, soil, sediment, surface water, groundwater, and pore water samples, as well as fish, were collected on and downstream of gold mining sites and compared with control sites. The results show that soils are major Hg sinks, with concentrations reaching up to 4,500 ng g^{-1} in Burkina Faso and 18,000 ng g^{-1} in Guinea, compared to 1–20 ng g^{-1} in bedrock and 63 ± 14 ng g^{-1} in reference soils. Hg speciation in soil analysed by thermodesorption shows that in contaminated soils, the proportion of elemental (Hg0) can reach 62 to 75% Total Hg (THg) in Guinea, whereas it is never exceed 10% in Burkina Faso. Such high Hg0 levels in Guinean soil can results in possible significant re-emission into the atmosphere. Furthermore, ASGM also appears to be a source of Hg-enriched particles in rivers, where THg in surface waters reach concentrations up to 239 ng L^{-1} and 350 ng L^{-1}. Sediments downstream of ASGM sites contain up to 7.8 µg g^{-1} in Burkina Faso and 700 ng g^{-1} in Guinea. Furthermore, selective extractions show that organic matter (OM) and amorphous iron oxides (amFe) are major Hg carrier phases, accounting for 18–42% and 16–61% of THg respectively in soil. In river sediment, Hg_{OM} remained within a comparable range (11–35% of THg), whereas the proportion of Hg associated with amFe decreased markedly to 24–36%. This latter phase has been shown to promote the availability of Hg for methylating microorganisms in sediments, decreasing with an increase in the proportion of methylmercury (MeHg) from 0.03–0.04% to 0.23–2.2% THg from soil to sediment. In specific locations, groundwater pumping for ASGM activities was found to remobilize geogenically enriched As groundwater with levels exceeding WHO standards of 10µg L^{-1}.

Finally, bioaccumulation and biomagnification of (Me)Hg in fish was found significant in the Niger River, with 18% of collected fish exceeding USEPA standards of 300 ng g^{-1} (wet weight). This suggests potential health risk for communities whose diet relies on fish.

This work provides new insights on baseline levels and speciation of Hg and contaminants in sites impacted by ASGM activities. It also documents the fate of Hg between different environmental compartments impacted by ASGM activities, as well as its potential impact on human health through fish consumption and inhalation of Hg0.

Résumé

L'exploitation minière artisanale et à petite échelle de l'or est une source majeure de pollution environnementale, qui reste mal documentée en Afrique de l'Ouest. Au Burkina Faso et en Guinée, cette activité minière s'est considérablement développée au cours des dernières décennies. L'utilisation de produits chimiques pour l'extraction de l'or, notamment le mercure (Hg) et le cyanure (CN), entraîne une contamination importante de l'environnement. En outre, le remaniement des sols peut entraîner la remobilisation de contaminants géogéniques tels que le Hg, le plomb (Pb) et l'arsenic (As) naturellement présents dans ces sols.

Cette étude vise à quantifier et à caractériser la contamination par les métaux, en mettant l'accent sur la spéciation du Hg et son impact sur l'environnement et la santé au Burkina Faso et en Guinée. À cette fin, des échantillons de sol, de sédiments, d'eau de surface, d'eau souterraine et d'eau porale, ainsi que des poissons, ont été prélevés sur et en aval des sites d'exploitation aurifère et comparés à des sites témoins. Les résultats montrent que les sols sont des puits importants de Hg, avec des concentrations atteignant 4500 ng g^{-1} au Burkina Faso et 18000 ng g^{-1} en Guinée, contre 1 à 20 ng g^{-1} dans le substrat rocheux et 63 ± 14 ng g^{-1} dans les sols de référence. La spéciation du mercure dans le sol analysé par thermodésorption montre que dans les sols contaminés, la proportion de Hg d'élémentaire (Hg0) peut atteindre 62 à 75 % du Hg total en Guinée, alors qu'elle ne dépasse jamais 10 % au Burkina Faso. Ces niveaux élevés de Hg0 dans le sol guinéen peuvent entraîner d'importantes réémissions dans l'atmosphère. En outre, l'orpaillage semble également être une source de particules enrichies en Hg dans les systèmes hydrologiques, où le Hg total dans les eaux de surface atteint des concentrations allant jusqu'à 239 ng L^{-1} et 350 ng L^{-1}. Les sédiments en aval des sites orpaillés contiennent jusqu'à 7,8 µg g^{-1} au Burkina Faso et 700 ng g^{-1} en Guinée. De plus, des extractions sélectives montrent que la matière organique (OM) et les oxydes de fer amorphes (amFe) sont les principales phases porteuses du Hg, représentant respectivement 18 à 42 % et 16 à 61 % du THg dans le sol. Dans les sédiments, le Hg_{OM} est resté dans une fourchette comparable (11 à 35 % du THg), tandis que la proportion de HgamFe a considérablement diminué, passant à 24-36 % du THg. Il a été démontré que cette dernière phase favorise la disponibilité du Hg pour les micro-organismes méthylants dans les sédiments, leurs abondances diminuant avec l'augmentation de la proportion de méthylmercure (MeHg) de 0,03-0,04 % à 0,23-2,2 % du THg du sol aux sédiments. Dans certains endroits spécifiques, le pompage des eaux souterraines pour les activités d'orpaillage remobilise les eaux souterraines géogéniquement enrichies en As, avec des niveaux dépassant les normes de l'OMS de 10 µg L^{-1}.

Enfin, la bioaccumulation et la bioamplification du (Me)Hg dans les poissons se sont avérées significatives dans le fleuve Niger, avec 18 % des poissons collectés dépassant les normes de l'USEPA de 300 ng g^{-1} (poids humide). Cela suggère un risque potentiel pour la santé des communautés dont l'alimentation repose sur le poisson.

Ces travaux apportent de nouvelles informations sur les niveaux de référence et la spéciation du Hg et des contaminants dans les sites touchés par les activités d'orpaillage, et documentent le devenir du Hg entre les différents compartiments environnementaux affectés par les activités d'orpaillage, ainsi que son impact sur la santé humaine via la consommation de poisson et l'inhalation de Hg0.

Aknowledgments

Montaigne wrote: “A well-formed mind is better than a well-filled mind.” This thesis is the result of a continuous learning process, built step by step through mistakes, challenges, and progress. Over the past three years, I have experienced many periods of uncertainty and faced difficult setbacks; however, the most important lesson has always been to learn how to move forward. In this sense, Montaigne's words take on their full meaning: learning means understanding, transforming, and reorganizing one's thoughts in order to think and write more effectively.

Throughout this thesis, perseverance, which Victor Hugo described as “the secret of all triumphs” has been constantly put to the test. This manuscript would never have seen the light of day without the support of rigorous and demanding individuals who, although sometimes severe, have always shown great kindness. Through their advice, questions, and trust, they imparted much more than scientific knowledge, giving meaning to my efforts and contributing profoundly to my scientific and personal development.

First of all, I would like to express my deep gratitude to my thesis advisor, Stéphane Guédron, who supported me from the beginning of the project to its completion. His advice was essential not only for the scientific basis of this work, but also for obtaining funding and preparing field missions. I would also like to extend my warmest thanks to his family, who always welcomed me with great generosity. During my thesis, I spent many months at their home, especially when I returned from the field and did not always have a place to stay. Their kindness and hospitality were an invaluable support, far beyond the academic setting.

Thank you to my scholarship organization ACE-Partner for providing funding and to IRD for its administrative support. I would also like to sincerely thank my co-advisor, Ynoussa, who agreed to accompany me on this adventure even though he didn't know me. I would like to thank all my other supervisors, Odile, Jacques, and Ousséni, for their constant support. Their trust, especially during difficult times, their help in finding funding, and the attention they paid to my writing were crucial throughout this thesis. I would also like to extend my warmest thanks to my supervisor in Guinea, Hamed Konaté, who always facilitated the shipment and transit of samples, thereby enabling the analyses and smooth running of field research. I would also like to express my gratitude to the epidemiologist who agreed to be the principal investigator (PI) for the epidemiological project. Although this project did not ultimately come to fruition, his commitment and availability were instrumental in the completion of the written project. My thanks also go to Robert Mason for his training in fish analysis techniques at his laboratory in Connecticut, USA. Thank you to the members of my CSI (Céline Duwig, Corinne Casiot-Marouani, Marc Vinches) for their various pieces of advice over the past three years.

I would like to give special thanks to my co-worker Naomi for her unwavering support, her careful proofreading of this manuscript, and the valuable advice she gave me throughout the writing process. Thank to the engineers and technical staff (Sylvain, Sarah, Sabine, Delphine, Jonathan, Simona, etc.) whose support has been both scientific and personal. Their availability, patience, and training in laboratory techniques have greatly contributed to the quality of this work.

Finally, I would also like to thank my interns (Perrine and Lahna) for their determination to learn and their help in achieving certain results. I would like to express my sincere gratitude to the members of my thesis committee for agreeing to review, examine, and chair my dissertation. I am especially thankful for the attention they devoted to my work and for the richness of the discussion we had during the defense. I would also like to extend a special thank you to everyone at LAMBM, and especially to Compaoré and Palé for their support and for making room for me during my time at the laboratory in Burkina Faso. Finally, thank you to my friends and family for their support, in particular, my mother, who has always believed in me, and my fathers (DABRE Youssoufou and Sanou Raoul), who watch over me from above with their prayers and protection.

Table of contents

Abstract i
Résumé ii
Aknowledgments iii
Table of contents iv
List of Figures vii
List of Tables x
List of Abbreviations xi
General introduction 1
Origin of the research project 1
The objectives of the thesis 2
Thesis document structure 4
I. Chapter I. Current state of knowledge 6
I.1. Gold mining in West Africa 7
I.1.1. History of gold mining on Burkina Faso and Guinea 7
I.1.2. Geology 11
I.1.3. West Africa gold mining practices 12
I.2. Impact of ASGM 16
I.2.1. Mercury 16
I.2.2. Cyanide (use, chemistry, and health/risk/exposure) 23
I.2.3. Geogenic contamination (As, Pb) of groundwater and health/ exposure issues 23
I.3. Study sites and sampling strategy 25
I.3.1. Burkina Faso study site 25
I.3.2. Guinea Republic study sites 32
I.3.3. Sampling strategy and methodological approach 37
II. Chapter II. Transfer and Transformation from Mine Soil to River Sediment: The Potential Role of Amorphous Iron Oxides in Methylation Processes in Southern "Burkina Faso" 42
II.1. Introduction 47
II.2. Material and methods 49
II.2.1. Environmental settings 49
II.2.2. Sample collection and conditioning 51
II.2.3. Soil and sediment characterization 52
II.2.4. Chemical analyses 52

II.2.5. Statistical analysis 54
II.3. Results and interpretations 54
II.3.1. Mercury, arsenic and lead contents in surface and groundwater 54
II.3.2. Mercury, arsenic and lead levels in soils and sediments 57
II.3.3. Mercury speciation and carrier phases in soils and sediments 59
II.3.4. Comparison between thermodesorption and selective extractions 61
II.4. Discussion 62
II.4.1. Impact of ASGM activities on mercury and arsenic contamination of surface water 62
II.4.2. Partitioning of mercury species onto soil carrier phases in ASGM context. 63
II.4.3. Fate of Hg carrier phases and implication on MeHg accumulation in river sediment 65
II.5. Conclusion 67
II.6. Supplementary information 69
III. Chapter III. Transfer of mercury contamination from mine to village in Guinea: the case of artisanal and small-scale goldmining. 81
III.1. Introduction 85
III.2. Material and methods 87
III.2.1. Environmental settings and sampling strategy 87
III.2.2. Soil collection and conditioning 89
III.2.3. Groundwater sampling and conditioning 89
III.2.4. Samples characterization and chemical analysis 89
III.2.5. Statistical analysis, mapping, and calculation 91
III.3. Results and interpretations 92
III.3.1. Hg distribution in soil profiles: evidence for topsoil contamination 92
III.3.2. Hg carrier phases in ASGM and village topsoil: elemental Hg contamination 93
III.3.3. Hg levels and speciation in ground water 95
III.4. Discussion 97
III.4.1. Transfer of mercury contamination from mine to village: a mass balance 97
III.4.2. Potential health risk of Hg exposure in miner's villages 101
III.5. Conclusion 102
III.6. Supplementary information 105
IV. Chapter IV. Impact of artisanal and small-scale goldmining on (methyl)mercury contamination of the Niger River in Guinea Republic: insights from sediment and fish bioaccumulation. 120
IV.1. Introduction 124
IV.2. Materials and Methods 126
IV.2.1. Environmental settings and sampling sites 126
IV.2.2. Sample collection and conditioning 127

IV.2.3. Analytical methods 128
IV.3. Results and interpretation 130
IV.3.1. Spatial distribution of mercury species and cyanide in surface water 130
IV.3.2. Spatial distribution of mercury species in river sediments 132
IV.3.3. Mercury and methylmercury levels in fish 135
IV.4. Discussion 137
IV.4.1. Particulate transport drive mercury contamination from ASGM in the Niger River 137
IV.4.2. Link between Hg carrier phases and MeHg levels in the river 138
IV.4.3. Hg levels in fish and potential health risks for local population 139
IV.5. Conclusion 140
IV.6. Supplementary information 142
V. Chapter V. Summary of the main results and presentation of new research questions and perspectives 153
V.1. Summary of key results 154
V.2. Scope and level of response to the research questions 155
V.3. Practical recommendations 156
V.4. Perspectives 157
References 159
VI. VI. Appendices 187
VI.1. Appendix 1 : Synthèse en Français « Impact de l'orpaillage sur les écosystèmes aquatiques et les populations au Burkina Faso et en Guinée » 188
VI.1.1. Introduction 189
VI.1.2. Description des sites d'étude 191
VI.1.3. Méthodes analytiques 196
VI.1.4. Résultats 200
VI.1.5. Conclusion générale, recommandations et perspectives 211
VI.2. Appendix 2 : Protocole d'étude épidémiologique 212
VI.2.1. Introduction 216
VI.2.2. Méthodologie 220
VI.2.3. Question 1 : Evaluer les connaissances, attitudes et pratiques de la population sur l'utilisation du mercure dans les sites d'extraction artisanale des mines à Kouroussa 221
VI.2.4. Question 2 : Quelles sont les niveaux d'expositions des populations au mercure sur les sites miniers à Kouroussa : 223
VI.2.5. ANNEXE 232
VI.3. Appendix 3 : Article on master's thesis work: "Source, fate, and budget of mercury species in the high-altitude watershed of a fast-developing Andean city (El Alto, Bolivia)" 238

List of Figures

Figure I.1. West Africa's share of global gold production between A) 1990 and B) 2017 (modified from Atlasocio.com and Natural Environmental Research Council, British Geological Survey). https://atlasocio.com/classements/economie/ressources-naturelles/classement-etats-par-production-or-afrique_1990.php. 10
Figure I.2. Geological map of the West African Craton (modified from Milési et al. (2004); Block et al. (2015)) 12
Figure I.3. Photographs (credit D. Dabré) illustrating the two techniques used to extract gold at Burkina and Guinea mining sites: amalgamation and cyanidation. 13
Figure I.4. Artisanal gold mining processes in West Africa 16
Figure I.5. Mercury (Hg) bio-geochemical cycle in West Africa context. Based on Boudou et al. (2006) and Wasserman et al. (2003), pngtree.com. SR indicates sulfate reducing and IR indicates iron reducing. 18
Figure I.6. Geological maps of Burkina Faso with artisanal gold mines location 25
Figure I.7. Historical and modern trends in gold production in Burkina Faso from 1995 to 2024. Sources: (Sba-Ecosys, 2011; Côte, 2013; MME and Par-Gs, 2014; Zabsonré et al., 2016; ENZO, 2017; Côte and Korf, 2018; MOORE, 2018; OCDE, 2018). 28
Figure I.8. Picture of the mining site in southwestern Burkina Faso showing A) the mining village of Djikando, B) the Memer1 settling basin, C) the visible environmental impact of the Djikando mining site on the Poni River in Djikando. 31
Figure I.9. Geological maps of Guinea with artisanal gold mines location. 32
Figure I.10. Historical and modern trends in gold production in Guinea from 1995 to 2024. Sources: (Levin Sources, 2017; MEEF and PAN, 2018; PROJEG, 2018; MMG, 2019, 2020; FMI, 2021; MEEF, 2021; ASFF, 2022; ITIE, 2022). 34
Figure I.11. Picture on the Saman mining site showing A) crossing the Niger River in a fishing canoe, B) the artisanal mining site at Saman showing the mine shaft and the number of miners (5), C) the mine shafts observed by Satellite at the Saman site, D) the cyanidation site at Saman. 37
Figure I.12. Summary of the mining environment compartments sampled during this thesis. Adopted from (Crespo-Lopez et al., 2021; Gerson et al., 2022). 39
Figure II.1. Map of the study site with A) The location of Burkina Faso within Africa. B) Geological map of Burkina Faso showing the greenstone belt, the Mouhoun and Poni rivers, and the three studied mining districts: Boromo, Dano and Gaoua. C) Zoomed in excerpt. D) synthetic information for all studied sites about the type of ASGM extraction process (mercury and or cyanidation), the number of miners, year of set-up, surface area at the date of sampling, and source of water used in the mining process. 50
Figure II.2. From left to right: methylmercury (MeHg) and total mercury (THg) concentrations. Proportions of THg (%) released by thermodesorption at 80°C (Hg0), 180°C (Hg_{180}) and the difference between 180 and 550°C (Hg_{Res}), NH_4OH (Hg_{OM}) or ascorbate (Hg_{amFe}) selective extraction in soil away from ASGM sites (top); ASGM-influenced soil (middle) and river sediment (bottom). Stars indicate pristine environment, i.e., soil samples at Boromo, Dano and Gaoua (Site B1-3, B4-3 and B5-5, respectively) were collected few km downstream the ASGM site, and sediment samples were collected upstream the ASGM site at Dano (sites B3-3 and B3-4). All Gaoua sediment samples (site B5) were collected downstream the ASGM site. 60
Figure II.3. ASGM soils. Biplots between Hg released by thermal desorption at 180°C (Hg_{180}) and A) Hg_{OM} (extracted by NH_4OH; B) Hg_{amFe} (extracted by ascorbate), and C) the sum of Hg_{OM} plus Hg_{amFe} ($Hg_{OM+amFe}$). 61

Figure II.4. ASGM soil. Biplots between A) Hg_{OM} (extracted with NH_4OH) and total sulfur, B) MeHg concentration versus organic carbon (C_{org}). 64
Figure II.5. Synthesis figure showing the environmental processes involved in gold mining and the percentages of different mercury compounds in soils and sediments downstream of mining sites in Burkina Faso. 65
Figure III.1. Map of study area showing A) Guinea in Africa; B) study region location; C) study sites locations and D) sites characteristics. 88
Figure III.2. Mercury (top) and organic matter (bottom) in soil profile in A) pristine; B) Mine sites where ore is extracted; C) Village at the periphery and D) Village where amalgamation occurs and E) Grain size distribution in pristine soils (top), Saman (middle) and Dionko (bottom). 92
Figure III.3. From left to right: A) Methylmercury (MeHg) and Total mercury (THg) concentration, with the distances of pristine sites from Kouroussa in green (top) and the proportion of MeHg in THg shown in light blue (bottom), on the right side of the figure. B) Proportion of Hg0 released by thermodesorption at 80°C (Hg0), 180°C (Hg_{OM}+ $Hg_{ascorbate}$) and the difference between 180 and 550°C (Hg_{Res}). 94
Figure III.4. Boxplot of mercury levels and speciation in filtered water on the left with A) THg_F and B) $MeHg_F$, and unfiltered water on the right with C) THg_{UNF} and D) $MeHg_{UNF}$. Upper and lower end of the box show the 25th and 75th percentile, full lines indicate the mean, minimum and maximum of each data set (N is the number of samples). 96
Figure III.5. IDW (Inverse Distance Weighted) interpolated map of mercury concentrations in surface soils at Dionko and Saman. Top: map showing the location of the two villages in relation to the Niger River. Bottom left: interpolated soil map of Dionko village in the background, with unfiltered water superimposed in blue. Bottom right: interpolated soil map of the village and Saman mine with unfiltered water superimposed in blue. 98
Figure IV.1. Map of study area showing A) Guinea in Africa; B) the study region Kouroussa location in Guinea and C) Sampling sites along the main studied rivers. 126
Figure IV.2. Spatial distribution of total mercury concentration in A) filtered (THg_F) and unfiltered (THg_{UNF}) surface water; and metylmercury in C) filtered ($MeHg_F$) and D) unfiltered ($MeHg_{UNF}$) surface water. 131
Figure IV.3. Concentration and speciation of mercury (Hg) in surface sediment with A) total mercury; B) elemental Hg, and Hg associated to organic matter and non-crystalline Fe oxides, and Hg bound to refractory minerals, and C) methylmercury. 133
Figure IV.4. Depth profiles of mercury concentrations in sediment cores collected in the Niger River (left), the Saman River1 (middle), and the Niandan River (right). For the Niger river caption, Fa + Km represents the distance from Faranah (Fa) along the Niger River, and for the Saman and Niandan tributaries Ng+ Km represents the distance to the confluence with Niger River (Ng). 134
Figure IV.5. Mercury (A) and methylmercury (B) concentrations in sediment porewater. 135
Figure IV.6. Biplots of A) total mercury and B) methylmercury concentrations in fish species sampled in the Niger river. C) Bioaccumulation factor (BAF) vs fish weight. 136
Figure VI.1. Carte du site étudié avec A) La localisation du Burkina Faso en Afrique. B) Carte géologique du Burkina Faso montrant la ceinture de roches vertes, les fleuves Mouhoun et Poni, et les trois districts miniers étudiés : Boromo, Dano et Gaoua. C) Extrait agrandi. 193
Figure VI.2. Carte de la zone d'étude montrant A) la Guinée en Afrique ; B) la région d'étude, située à Kouroussa en Guinée, et C) les points d'échantillonnage avec les principaux cours d'eau. 196
Figure VI.3. De gauche à droite : concentrations de méthylmercure (MeHg) et de mercure total (THg). Proportions de THg (%) libérées par thermodésorption à 80°C (Hg0), 180°C (Hg180) et la différence entre 180 et 550°C (HgRes), extraction sélective par NH_4OH (HgOM) ou ascorbate (HgamFe) dans le sol loin des sites d'orpaillage (en haut) ; sol influencé par l'orpaillage (au milieu) et sédiments fluviaux (en

bas). Les étoiles indiquent un environnement vierge, c'est-à-dire que les échantillons de sol à Boromo, Dano et Gaoua (sites B1-3, B4-3 et B5-5, respectivement) ont été prélevés à quelques kilomètres en aval du site orpaillé, et les échantillons de sédiments ont été prélevés en amont du site d'orpaillage à Dano (sites B3-3 et B3-4). Tous les échantillons de sédiments de Gaoua (site B5) ont été prélevés en aval du site d'orpallage..... 202
Figure VI.4. Figure de synthèse illustrant les processus environnementaux liés à l'exploitation aurifère et les pourcentages des différents composés du mercure dans les sols et les sédiments en aval des sites miniers au Burkina Faso. 204
Figure VI.5. Mercure (en haut) et matière organique (en bas) dans le profil du sol dans A) un site vierge ; B) des sites miniers où le minerai est extrait ; C) un village situé à la périphérie et D) un village où se produit l'amalgamation et E) distribution granulométrique dans les sols vierges (en haut), Saman (au milieu) et Dionko (en bas). 206
Figure VI.6. Carte interpolée IDW (Interpolation par Pondération Inverse de la distance) des concentrations de mercure dans les sols superficiels à Dionko et Saman. En haut : carte indiquant l'emplacement des deux villages par rapport au fleuve Niger. En bas à gauche : carte interpolée des sols du village de Dionko en arrière-plan, avec l'eau non filtrée superposée en bleu. En bas à droite : carte interpolée des sols du village et de la mine de Saman avec l'eau non filtrée superposée en bleu. 207
Figure VI.7. Répartition spatiale de la concentration totale en mercure dans A) les eaux non filtrées (THg_{NF}); B) les sédiments de surface. Spéciation du Hg dans les sédiments de surface avec C) phases porteuses du mercure, D) méthylmercure. E) méthylmercure dans les eaux porales. Concentration totale du mercure F) et méthylmercure G) dans les poissons. 209

List of Tables

Table II-1. Physico-chemical parameters and metal(loïdes) concentrations in filtered and unfiltered water at Boromo, Dano and Gaoua districts. * indicate pristine river collected 3 km away from mining Dano site. ° Indicate sites where river water is used for ore processing whereas the others use groundwater. The SEM only appear when there are at least two values. N.D indicate not determined. 56
Table II-2. Concentrations of metal(loïds) in crushed rock, soils, sediments, concentrate, concentrate to which mercury has been added, and waste material for sites in the districts of Boromo, Dano and Gaoua. Concentrations are given in dry weight. N.D indicates not determined, and < DL indicates below detection limits. The SEM only appear when there are at least two values. * indicate all three studied districts (Boromo, Dano and Gaoua). 58
Table III-1. Total and elemental mercury stock per surface unit at the two mining sites and villages in Saman (1.05km^2) and Dionko (0.12 km^2). 99

Tableau VI-1. Informations synthétiques pour tous les sites étudiés concernant le type de processus d'extraction de l'orpaillage (mercure et/ou cyanuration), le nombre de mineurs, l'année de création, la superficie à la date de l'échantillonnage et la source d'eau utilisée dans le processus d'extraction A) au Burkina Faso et B) en Guinée. N.D signifie non déterminé. Les coordonnées sont exprimées en UTM où X correspond à l'abscisse est et Y à l'abscisse nord. Au Burkina Faso, les coordonnées UTM sont exprimées en zone 30N (WGS84). Les sites étudiés dans la région de Kouroussa (Haute Guinée) sont situés en zone UTM 29N (WGS84). 194
Tableau VI-2. Sites potentiels de l'étude en Guinée Conakry à Kouroussa 220
Tableau VI-3. Synthèse du nombre d'échantillon à considérer 225

List of Abbreviations

AAS: atomic adsorption spectroscopy

amFe: amorphous iron oxide

ANEEMAS: agence nationale d'encadrement des exploitations minières artisanales et semi-mécanisées

As: arsenic

ASGM: artisanal and small-scale gold mining

CN: cyanide

C_{org}: organic carbon

CVAFS: cold vapour atomic fluorescence spectroscopy

DOC: dissolved organic carbon

FMI: fond monetaire international

Hg: mercury

Hg0: elemental mercury

Hg_F: filtered mercury

HgII: divalent mercury

Hg_{UNF}: unfiltered mercury

ICP-AES/MS: *Inductively Coupled Plasma Atomic Emission Spectroscopy/* mass spectrometry

ITIE: Initiative pour la Transparence dans les Industries Extractives

MEEF: Ministère de l'environnement et des eaux et forêt

MeHg: methylmercury

MME: Ministère des Mines et de l'Energie

MMG: ministère des mines et géologie

OM: organic matter

Pb: lead

PCA: principal comporant analysis

SOM: soil organic matter

TEM: Transmission Electron Microscopy

TOC: total organic carbon

UNEP: United Nation Environmental Programme

USEPA: U.S.Environmental Protection Agency

XRD: X-ray diffraction

General introduction

Origin of the research project

According to Hauptmann and Klein, (2009), one of the oldest gold mines ever discovered located in Georgia, Asia dates back to the fourth or third millennium BCE, attesting to the long history of gold mining. This mining activity continues to thrive today throughout the world, with artisanal and small-scale gold mining (ASGM) production accounting for around an estimated 20% of global gold production (AMAP/UNEP, 2019). ASGM in West Africa, particularly in Burkina Faso and Guinea, has experienced significant growth for over a decade. This vital income source, practiced since the 9th century, has become widely democratized and has reached unprecedented levels in recent years, driven by rising gold prices, and political and economic crises (Choquet, 2018). Burkina Faso, a major gold producer in Africa, saw its artisanal production fluctuate between 0.1 and 0.5 tons in 2014, rising to 8.1 tons in 2024 (ATI, 2025). Meanwhile, Guinea, rich in geological resources, is experiencing sustained expansion of ASGM, particularly in Upper and Forest Guinea (Bortnikov et al., 2024; WAXI Africa, 2023), with artisanal gold exports increasing from 5 tons in 2013 to 83 tons in 2021 (MMG, 2022).

ASGM is an informal, poorly regulated gold mining process in these two countries. The mining process typically involves vein-based extraction, crushing, grinding, washing, and gold (Au) amalgamation with mercury (Hg) (Donkor et al., 2006; Telmer and Veiga, 2009). The amalgam is then burned in the open air, releasing Hg vapors that can be inhaled by workers and local populations (Noble et al., 2016). Part of this Hg condenses and is redeposited onto soil, causing long-term contamination and potential re-emission, while another fraction escapes into the global atmosphere (Fu et al., 2010; Tomiyasu et al., 2012; Yu et al., 2014). Burkina Faso is experiencing intense mercury use (IGF, 2022), with an estimated annual consumption of 78 tons of Hg in 2020 (PAN, 2020)

Gold mining in the watercourses and catchment areas of Guinea and Burkina Faso increases the risk of contaminants transfer to aquatic ecosystems. These environments are particularly vulnerable to Hg pollution originating from mining discharges or soil erosion. Once deposited in river sediment, Hg can be converted into methylmercury (MeHg) by microbial metabolism (Clarkson and Magos, 2006; Ullrich et al., 2001; Parks et al., 2013; Eagles-Smith et al., 2016).

This toxic compound bioaccumulates in aquatic organisms, including fish at the top of the food chain, posing a direct threat to human populations whose diet relies mainly of fish (Boischio and Henshel, 2000; Ouédraogo and Amyot, 2013). Another technique for recovering gold by cyanidation of amalgamation sludge residues can lead to the formation of stable dissolved Hg-CN complexes that can significantly increase the solubility and mobility of Hg in aquatic environments (Tulasi et al., 2021). Other contaminants such as arsenic (As) and lead (Pb), naturally occurring in rocks and sediment at

elevated levels (geogenic origin), can be mobilized during ore extraction and can be found in high concentrations in groundwater, exposing local communities to chronic health risks when concentrations exceed WHO drinking water standards [10 µg L^{-1} (Hilson, 2002; UNEP, 2013; Bretzler et al., 2017)]. These co-contaminants may also be discharged into the surface water system if enriched groundwater is pumped for ore washing.

Soils play a crucial role in contamination dynamics, acting as long-term sinks and sources of pollutant transfer to surface and groundwater (Aleksander-Kwaterczak and Ciszewski, 2016). Although, ASGM in West Africa is vital for local socio-economic growth, it also poses significant environmental and health risks. Data regarding Hg dynamics, carrier phases, the impacts of Pb and As, and their effects on human health and aquatic ecosystems are limited.

Understanding Hg speciation and distribution in soils, its reactivity, and methylation precursors in sediments is therefore essential for understanding the health risks associated with gold mining activities in West Africa.

The objectives of the thesis

This doctoral thesis, jointly supervised by University Joseph KI-ZERBO (UJKZ) and Grenoble-Alpes University (UGA), is funded through the African Centers of Excellence (ACE-Partner) network, which brings together the World Bank, the Association of African Universities (AAU), the French Development Agency (AFD), the French National Institute for Research in Computer Science and Control (INRIA) and the Institute of Research for Development (IRD). The thesis project was developed in line with the scientific project of the African Centers of Excellence (ACE), including the Emerging Center for Mines and Society (CEMS) at the Higher Institute of Mines and Geology of Boké (ISMG) in Guinea and the Center of Excellence on Water and Environmental Engineering (2IE) in Burkina Faso. Both CEA CEMS and 2IE aim to train qualified local experts locally in the exploration and development of mineral resources and the resolution of societal and environmental issues related to mining in Guinea and Burkina Faso. In order to meet the requirements of both Centers of Excellence, these two countries were selected as study sites because of their rich geogenic resources, including primary and alluvial gold, with gold mining being practiced throughout Burkina Faso and mainly in the north-eastern regions of Guinea.

The overall objective of this study was to evaluate the environmental fate of metal contaminants associated with gold mining and their ecological and human health risk in Burkina Faso and Guinea. To address this objective, the following specific objectives, scientific questions, and hypotheses were formulated:

I- Determination of the background levels of contaminants and the impact of the ASGM activities on their concentrations in the environmental compartments.

To distinguish anthropogenic inputs from naturally occurring pollutant levels, it is essential to have a clear understanding of the natural geochemical background levels of these pollutants. This distinction is particularly important in areas affected by artisanal and small-scale gold mining (ASGM), as mining activities can both introduce so-called anthropogenic pollutants and remobilize naturally occurring contaminants known as geogenic pollutants. This objective raises five scientific questions and hypotheses:

What are the geochemical background concentrations of Hg species, CN, As, and Pb in environmental compartments (water, soil, sediment, and fish) in Burkina Faso and Guinea?

Are they naturally elevated in groundwater?

What is the impact of ASGM activities on Hg and CN levels?

Does the use of ground water in ASGM practices remobilize geogenic contaminants (As and Pb) to the surface?

What factors influence the concentrations of these contaminants?

The hypotheses formulated were that Hg and CN concentrations are higher in recent and active ASGM sites than in older or natural sites, and that the type and duration of mining influence the distribution and speciation of metals in the different environmental compartments.

II- Study the reactivity and transfer of Hg from ASGM sites to rivers and miner's villages.

Due to its high mobility and its ability to transform into hazardous forms such as methylmercury, mercury is a major pollutant that requires careful study in areas of artisanal and small-scale gold mining (ASGM). Since its reactivity and toxicity depend on its chemical forms, it is therefore essential to study its speciation and transport pathways to understand its ecological impact and fate in the environment. Three scientific questions and hypotheses arise from this specific objective:

What is the impact of ASGM on the Hg contamination and the remobilisation of geogenic Hg?

What are the Hg species and the main carrier phases or ligands that carry Hg?

What is their behaviour and fate when transferred into aquatic compartments?

The hypotheses formulated were that depending on its speciation and the reactivity of its carrier phases, Hg will either be immobilized in river sediment or transformed into more available and toxic species that can bioaccumulate in trophic chains (methylmercury).

III- Assess the risk of population exposure.

In regions where artisanal and small-scale gold mining (ASGM) takes place, and where local communities rely heavily on natural resources for their food supply, it is essential to assess human exposure in order to determine the public health implications of this contamination. This raised two scientific questions and hypotheses:

Do the measured concentrations of As, CN, and Pb present health risks to local populations through the use of water as drinking water?

What are the main routes of Hg exposure (fish consumption, direct contact, inhalation)?

The hypotheses formulated were that if the concentrations of contaminants exceed the limit values recommended by the WHO and other international organizations, they may pose a risk to human health; and that fish consumption and inhalation of dust and Hg vapor may also constitute important routes of human exposure.

Thesis document structure

The results presented in this PhD thesis concern the study of two ASGM sites located along the Mouhoun River in the southwestern Burkina Faso, and along the Niger River in Upper Guinea, Republic of Guinea. The manuscript is organized in the form of a thesis article with an introductory chapter describing the current state of knowledge (Chapter I), followed by three articles that have been published or are in the process of being submitted (Chapter II to IV), and a chapter on conclusions and perspectives (Chapter V). The content of these four chapters is as follows:

- Chapter I provides an overview of current knowledge on the issue of gold mining in West Africa. The biogeochemical cycle of Hg is described, and the impact of ASGM on the Hg, CN, As and Pb pollution are discussed. The bioaccumulation of Hg in food chains and the impacts on human health are also discussed. Finally, the context of the thesis, the description of the study sites, and the sampling strategy are presented.

- Chapter II assesses mercury levels and speciation in mining soils and river sediments in southwestern Burkina Faso. It also examines arsenic and lead levels in water, soil, and sediments. Emphasis is placed on the role of non-crystalline iron oxides in methylation processes in river sediments.

- Chapter III assesses the level of Hg contamination of ASGM sites and miner's villages, and the exposure of populations to Hg vapor in Guinea. This chapter discusses mining practices specific to Guinea that result in the transfer of Hg contamination from mines to villages. Possible contamination of groundwater by soil is also discussed.

- Chapter IV focuses on the impact of ASGM on the Hg contamination of the Niger River and its tributaries, and the potential health risk for local populations in Guinea. This chapter discusses the

partition, mobility, and bioaccumulation of Hg in sediment and fish in the Niger River. It discusses the spatial distribution of Hg species through the mapping of contamination levels and the vertical distribution of Hg in sediment cores. The bioaccumulation of (methyl)Hg in fish species is also discussed.

- Chapter V summarizes the main results and presents new research questions and perspectives.

Finally, three appendices at the end of this manuscript present i) a summary of the main results of this work (Appendix 1), ii) the epidemiological protocol drafted for submission to the Ethics Committee of the Republic of Guinea to address the epidemiology (human exposure) aspects of this thesis (Appendix 2), and iii) an article on my master's thesis work and results, comparable to the work in this PhD thesis, entitled “Source, fate, and budget of mercury species in the high-altitude watershed of a fast-developing Andean city (El Alto, Bolivia)” (Appendix 3).

Chapter I.

Current state of knowledge

I.1. Gold mining in West Africa

I.1.1. History of gold mining on Burkina Faso and Guinea

I.1.1.1. Historical context

Artisanal and small-scale mining (ASM) has played a central role in the economic and political history of West Africa especially in large empires such as Ghana (8th-11th century) and Mali (11th-15th century) (Sylla and Ngom, 1997). Since the era of the great empires of Mali, gold has constituted a strategic resource, fuelling both prosperity and regional influence (Keita, 2001). Ghana, Mali, Guinea, Ivory Coast and Burkina Faso derived much of their power from gold exploitation, with major deposits located in areas such as Bouré in Guinea, Bambouk in Mali and Senegal, Lobi in Burkina Faso and Côte d'Ivoire, and the Akan region spanning Côte d'Ivoire and Ghana (Mbodj, 2011; Dessertine et al., 2022). The exploitation of these gold-bearing zones fostered dense commercial networks that connected West Africa to the Arab-Muslim world and, later, to Europe, remaining dynamic until the early twentieth century (Mbodj, 2009, 2011). This gold-based wealth was embodied by prominent historical figures such as Kaya-Magan Cissé, known as the "master of gold," in Ghana and Kankou Moussa, the emperor of Mali (Mbodj, 2011). The famous pilgrimage to Mecca by King Kankan Moussa in 1325 CE highlights the importance of gold production. Gold production in Mali and Ghana is difficult to estimate, but it was used as currency between 1471 and 1880 CE, with over 443 tons produced earning the country the nickname "Côte de l'Or" by its first exploiters (Keita, 2001). In Burkina Faso, documented practices date back to the fifteenth century, particularly in the Lobi and Gourounsi regions (Bohbot, 2017; Kiethega and Mauny, 1985). In Guinea, the practice is even older, as early as the ninth century. Populations in Upper Guinea, especially in the Bouré and Séké regions, were already engaged in seasonal gold mining activities, often undertaken as a complement to agriculture (Sidam-Minorex, 1998; Mbodj, 2009). These longstanding traditions, deeply embedded in local socio-economic systems, help explain the resilience and vitality of artisanal gold mining in both countries today.

I.1.1.2. The recent expansion and scale of ASGM

Over the past three decades, Burkina Faso has experienced a rapid expansion in gold mining activities. From 70 artisanal sites and a single industrial mine in 2003, the country expanded to 149 artisanal sites by 2012, and 12 to 17 industrial sites by 2012 and 2020, respectively (MME and Par-Gs, 2014; Tao, 2020). This increase in industrial mines, has fuelled a sharp increase in export revenues, from 974 billion CFA francs (1.75 billion US$) in 2016 to 1.42 billion CFA francs in 2019 (2.56 billion US$) (Tao, 2020).

Guinea has followed a similar trajectory experiencing what can be described as a genuine gold rush. Although the exact number of mining sites remains difficult to quantify, more than 200 ASGM sites have been identified in five districts in the eastern part of the country, with gold exports representing

over half of industrial exports in 2016 (Choquet, 2018). The ASGM sector directly involves more than one million people across the country (UNECA, 2011), and provides livelihoods for more than 250,000 individuals today, representing over 5% of the national population (Levin Sources, 2017; Petit-Roulet, 2025). Since 2022, gold has become Guinea's leading export commodity (MMG, 2022). At the sub-regional level, artisanal and small-scale mining (ASM) has intensified since the early 2000s, reflecting both historical continuity and deep socio-economic embeddedness (Grätz, 2004).

Both in Burkina Faso and Guinea, this gold expansion is closely linked to the sharp rise in international gold prices, which has reinvigorated historical mining areas while encouraging the opening of new sites through the diffusion of technological innovations (Bolay, 2016). The persistence and scale of ASM in West Africa illustrate its dual nature: as both a traditional livelihood strategy rooted in long-standing practices, and as a modern response to global market dynamics.

I.1.1.3. Social implications

The rapid expansion of gold mining in West Africa cannot be dissociated from the broader socio-economic transformations triggered by the structural adjustment programs in the 1980s and 1990s. Promoted by international financial institutions such as the World Bank and International Monetary Fund (IMF), these reforms privatized and liberalized national economies, leading to massive job losses and the collapse of public enterprises (Hilson and Potter, 2003, 2005). In this context of rising unemployment and poverty, artisanal and small-scale mining (ASM) emerged as a vital survival strategy for a growing share of the population (Hilson and Potter, 2003; Banchirigah, 2008). Environmental pressures further reinforced this shift. Indeed, in sub-Saharan Africa particularly in Burkina Faso, Ghana, Niger, and Benin, recurring droughts and declining agricultural productivity have driven farmers to abandon subsistence farming for gold mining (Razack, 2002; Hilson and Pardie, 2006; Yonlihinza, 2017; Hilson et al., 2018). In North-eastern Guinea, the collapse of cotton cultivation in the 1990s accelerated the adoption of ASGM as an alternative income source (Gerardeaux and Kourouma, 1998). Similar trend is observed in 2009 in Burkina Faso, where cotton was abandoned in favor of ASGM, leading the country becoming the continent's fourth largest gold producer in 2012 (Werthmann, 2013; PRPRSS, 2024). Since the early 2000s, agricultural land has been progressively neglected in favour of gold mining, with estimates suggesting that approximately 362 hectares of agricultural land are lost each year (Levin Sources, 2017).

Beyond its economic role, ASGM is deeply embedded in social organization and cultural practices. In Guinea, for instance, ore extraction follows a strongly gendered division of labor: men (*Djatis*) are primarily responsible for extraction, transport, and crushing, while women dominate the subsequent stages of washing, amalgamation, and burning, often carried out in huts or in the open air (Hilson and

Potter, 2003). This system not only structures production but also reshapes household dynamics, granting women an active role in local economies. At the national scale, ASGM represents both a major source of livelihood and a significant contributor to state revenues. In Burkina Faso, more than one million people were engaged in ASGM across over 448 sites in 2016, contributing 230 billion CFA francs (approximately 414 million US$) to the national economy (MME, 2017). In Guinea, more than 221,000 individuals were directly involved in ASGM in 2017 (Levin Sources, 2017). ASGM, while providing resilience and income to marginalized populations, also drives structural transformations that undermine agriculture and reconfigure gender relations.

I.1.1.4. Geographical distribution and the role of West Africa at the global scale

West Africa has emerged as one of the world's most significant gold-producing regions. In 2017, North Africa ranked as the second gold-producing zone on the continent, after South Africa. The annual output of 70 tons of gold in 2017, positioned South Africa ahead of Mali and Burkina Faso (Fig.1B) (Chevrillon-Guibert and Magrin, 2018). Today, West Africa is considered the third-richest gold-bearing region in the world. Ghana has become its leading producer, with 147 tons extracted in 2019, followed by Mali (73 tons) and Burkina Faso (64 tons) (World Gold Council, 2021). In Burkina Faso, gold has overtaken cotton as the country's principal export commodity, elevating the nation to the position of the fourth-largest gold producer in Africa, after South Africa, Ghana, and Mali (Airault, 2012; Nicolas et al., 2014). This rapid ascent is due to both the expansion of industrial operations and the intensification of ASGM, which has spread across virtually all regions of the country.

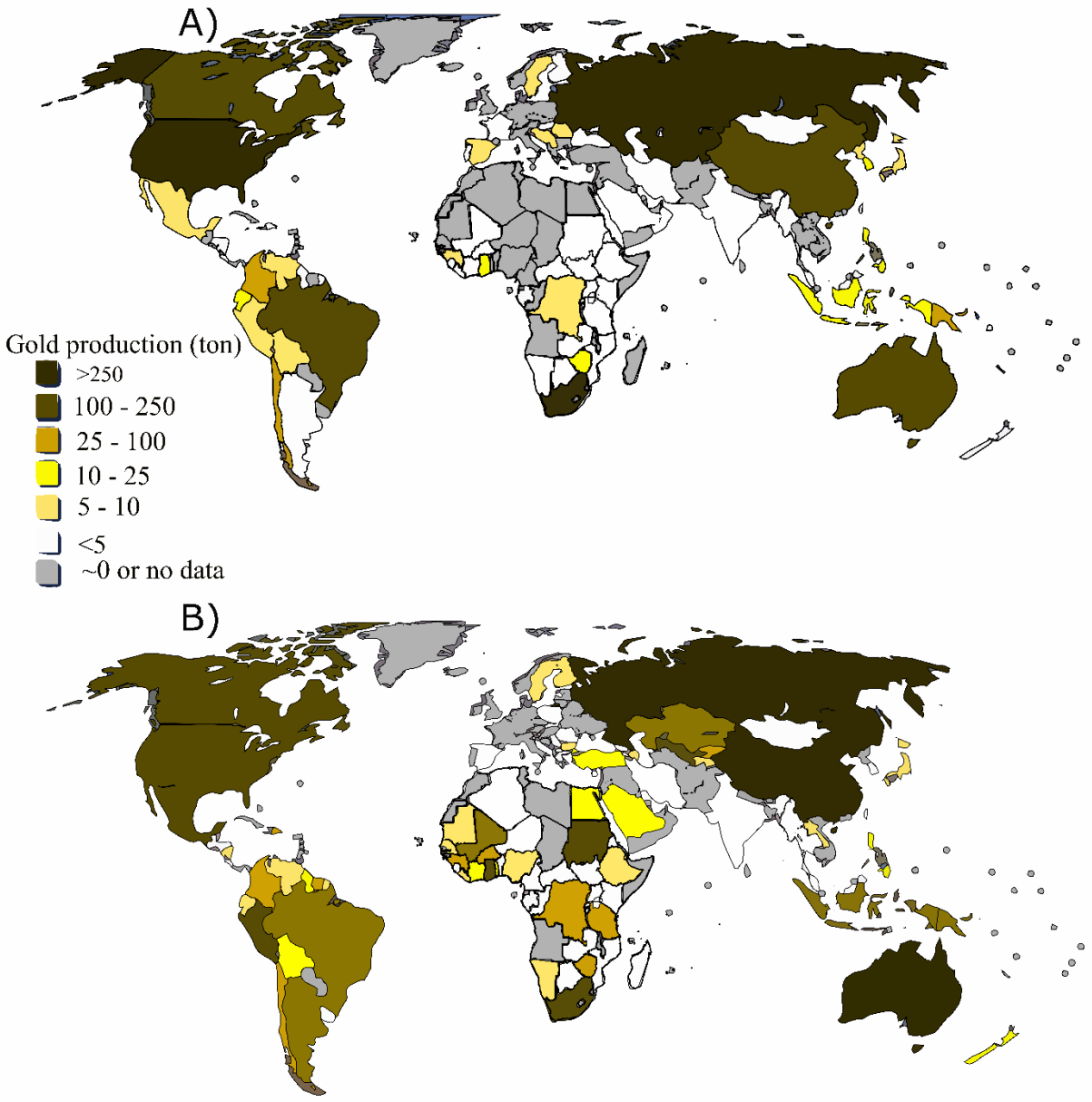


Figure I.1. *West Africa's share of global gold production between A) 1990 and B) 2017 (modified from Atlasocio.com and Natural Environmental Research Council, British Geological Survey). https://atlasocio.com/classements/economie/ressources-naturelles/classement-etats-par-production-or-afrique_1990.php.*

The expansion of gold production is much more visible in Burkina Faso, which went from <5 tons in 1990 to 45.5 tons in 2017 [**Figure I.1** A and B (OCDE, 2018)]. Although Guinea is not among the top ten global producers, its output remains significant within the African context and is steadily growing increasing from a total production of between 5 - 10 tons in 1990 to 25 - 100 tons in 2017 (**Figure I.1**.A and B). Estimates suggest that artisanal production accounts for nearly one-third of Guinea's total gold exports (Verbrugge and Geenen, 2020), which reached close to 57 tons in 2020 (World Gold Council, 2021), thus demonstrating that, the mining sector plays an equally pivotal role in the national economy. Indeed, since 1997, between 20 and 25 percent of the country's GDP (Gros Domestic

Product) has been directly linked to mining activities (Porgo and Gokyay, 2017; Choquet, 2018; AFRODAD, 2020). With 22% contribution in GDP in 2019, gold remains a cornerstone of Guinea's extractive economy, alongside bauxite (Fonds monétaire international, 2021). Notably, in 2023, Guinea ranked as the sixteenth-largest gold-producing country, with approximately 71 tons, sitting close behind South Africa and ahead of Mali and Burkina Faso (Papadopoulos, 2023; Tri Santosa, 2025).

At the continental level, ASGM accounted for approximately 54 % of Africa's total gold production in 2022, highlighting West Africa's particularly dynamic contribution to this segment (Ummel and Schulz, 2024). West Africa represent a particularly dynamic zone thanks to favourable geological conditions and new discoveries. These developments place the region alongside traditional global producers such as Australia, Russia, South Africa, and China, positioning West Africa as a fast-growing contributor to the international gold economy (Dokua Sasu, 2025). The expansion of gold production clearly visible in Burkina Faso and Guinea (**Figure I.1** A and B), shows that these two countries have a dominant position reflecting a dualistic model: industrial-scale operations controlled by international corporations, and informal ASGM that sustains millions of local livelihoods. Together, these two sectors underscore West Africa's strategic and complex role in the international gold economy.

I.1.2. Geology

Most of the gold deposits in West Africa are associated with Birimian greenstone belts in the West African craton (**Figure I.2**) dating from 2230 Myr to 2060 Myr (for younger magmatic roks) (Béziat et al., 2008; Vic and Billa, 2015). These belts are favourable for orogenic gold (quartz veins, stockworks, etc.) (Béziat et al., 2008). The Birimian belt covers 22% of Burkina Faso's territory, while it covers 11% of Guinea's, according to Ibrahim Sory N'Diaye in the Harmattan collection (N'Diaye, 2015; AFRODAD, 2020; Kaboré, 2023). Milési et al. (1992); Mignot et al. (2014) identified two gold deposits in Burkina Faso, Diénémera-Gongondy of the Gaoua district, a deposited of tholeiitic volcanic rock and metasedimentary rock, and Poura, a mesothermal quartz vein deposit controlled by shear structures located in the "boucle du Mouhoun" region. Gold is therefore present in almost all parts of Burkina Faso, particularly in the northeast, north, and southwest of the country (**Figure I.2**). In Guinea, the majority of gold deposits are located in the north-eastern part of the country in Upper Guinea (**Figure I.2**), where the Precambrian formations are found, in the prefectures of Siguiri, Dinguiraye, Kouroussa, Mandiana, and Kankan (ITIE-BDO, 2018; Levin Sources, 2017). This geological resource contains 10,000 tons of gold, as well as other resources such as iron, diamonds, and bauxite (AFRODAD, 2020).

The host rocks are volcano-sedimentary sequences reshaped by deformations related to the Eburnean orogeny, often of greenschist facies, and affected by strong hydrothermal alterations (Fontaine et al., 2017), leading to two types of mineralization. The first type corresponds to quartz veins, often deformed and accompanied by sulphides such as pyrite and a borosilicate mineral such as tourmaline,

as observed in the Youga deposit. There are also two types of gold deposits in Guinea that lead to two types of artisanal gold mining. Primary deposits (quartz veins, schists, stockworks, etc.) and the secondary deposits (eluvial on the surface and alluvial ores on the riverbeds and terraces of rivers) (ITIE-BDO, 2018; ITIE, 2022). Primary and eluvial deposits are the richest and dominate with 71% of sites and the alluvial represents only 22% of sites in Guinea (Levin Sources, 2017). The grades and dimensions of the veins vary by location. In Siguiri, the primary veins are typically 1 to 3 cm thick with gold grades ranging from 1 to 25 g m^{-3}. In Kouroussa, the primary Gobele and Blue veins reach 0.4 to 2.3 m and 400 m thick. The eluvial veins, found on the Siguiri plateau and the Niandan chain are 8 to 10 m thick and contains 1 to 2 g m^{-3} gold (Levin Sources, 2017).

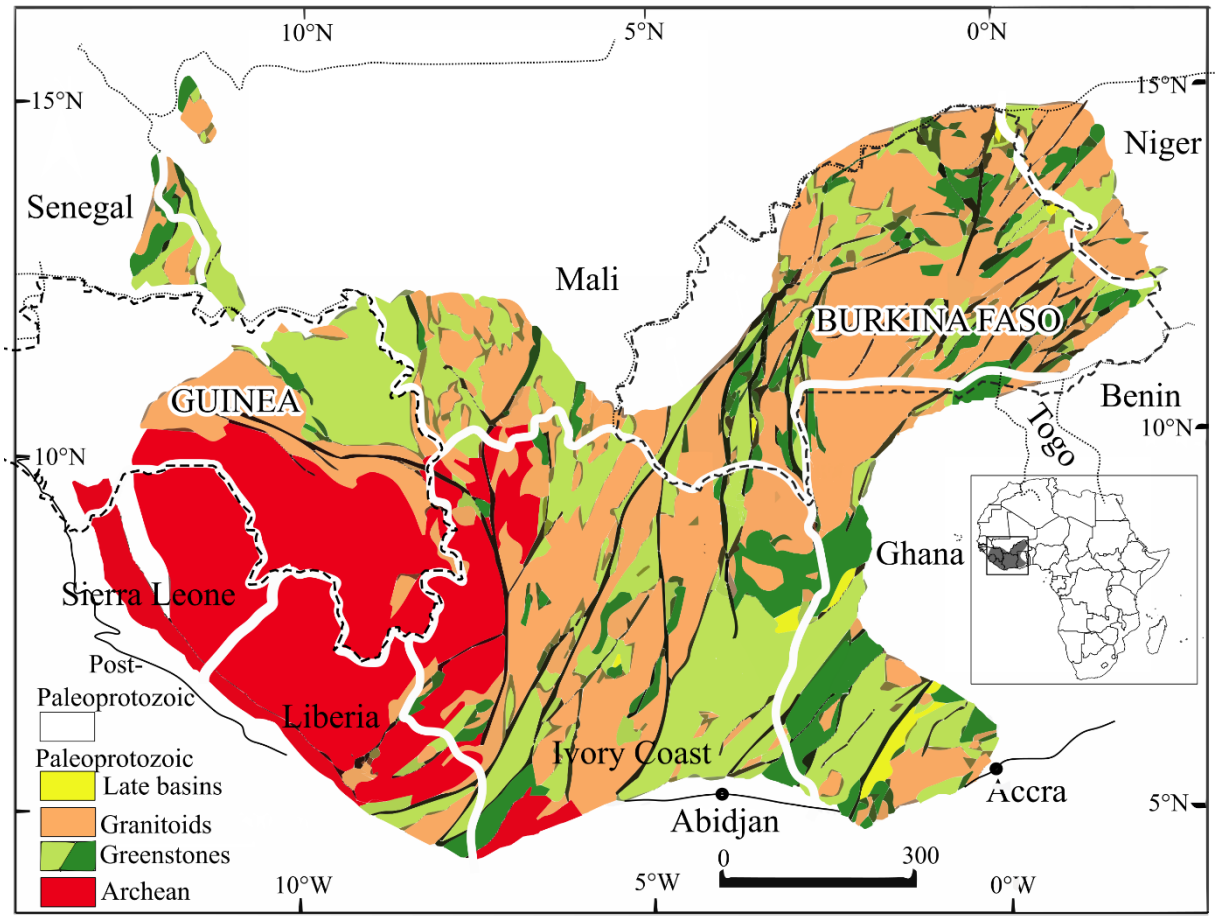


Figure I.2. *Geological map of the West African Craton (modified from Milési et al. (2004); Block et al. (2015))*

I.1.3. West Africa gold mining practices

Gold mining involves extracting ore (rock from the Earth's crust) and recovering the metal it contains. Open-pit, underground mining and the dredging of waterways are the three techniques used exclusively to extract gold from deposits. Open-pit mining involves removing overburden and excavating the surface to access the ore, while underground mining involves creating pits and tunnels below the surface at depths of between 0 and 100 meters to extract the ore from the deposit. Dredging

involves sucking up sand and gravel from the bottom of waterways that may contain gold. ASGM dominates in West Africa, where ore is extracted from vertical cylindrical pits often reaching depths of up to 400 meters using wooden supports to access deeper eluvium and veins, highlighting the rudimentary and dangerous nature of this activity (Vasters and Schütte, 2023). Once extracted from the holes, the ore is then crushed manually and mechanically ground into a fine powder of approximately 0.75 mm (**Figure I.3**) (Sawadogo, 2011; Roamba, 2014; Kouadio et al., 2025). Then, the gold is concentrated by gravimetric washing, a manual process based on differences in mineral density. According to Roamba, (2014), this “sluice” technique generally uses an inclined wooden board, approximately 2.5 m long and 0.4 m wide (Kohio et al., 2024), covered with cotton and wool mats (Veiga et al., 2006), designed to capture high-density gold particles while allowing lighter materials to be washed away.



Figure I.3. Photographs (credit D. Dabré) illustrating the two techniques used to extract gold at Burkina and Guinea mining sites: amalgamation and cyanidation.

At most sites, women are primarily in charge of this phase of mineral processing, applying practical methods to separate gold from mud while reusing water to minimize water waste due to its scarcity or unavailability at certain sites (Sawadogo, 2011; Roamba, 2014). The device consists of a board placed over a barrel filled with water, raising the opposite end for effective washing. The gold-bearing material is sifted, mix with water to form a slurry and poured along the board. The gold particles are

retained in the fibers of the cotton or wool mats, while the lighter sediment and clay are discharged into a pit (**Figure I.3**). Once the washing cycle is complete, the mats are rinsed in a basin of water to recovered the gold concentrate, highlighting the ingenuity and limitations of artisanal processing methods (Roamba, 2014; PAN, 2020). Another type of ore preconcentration known as the "panning" is often used directly at the mining site to test whether the ore contains gold. This technique involves washing the ore contained in pan (calabash) in a basin of water while rotating it counter-clockwise (Konate et al., 2025). This motion removes fine materials, allowing the denser gold particles to settle at the bottom of the pan.

Gold recovery from ore concentrate obtained by gravity washing often uses mercury amalgamation, a chemical process that involves adding mercury to the gold concentrate, whereas the pan technique does not use any chemicals (Veiga et al., 2006). According to Roamba, (2014), this amalgamation process uses 14.4 g of liquid elemental mercury (Hg0) to amalgamate the concentrate extracted from washing 50kg of crushed ore. Once formed, the amalgam is heated with a blowtorch to evaporate the mercury and recover the purified gold (Tomicic et al., 2011; OMS, 2017). This combustion stage releases mercury vapor into the atmosphere, contributing significantly to local and global environmental contamination (Tomicic et al., 2011; Black et al., 2017). In Guinea, intermediaries known as "Djatis" assist miners by purchasing and refining gold amalgams, often using borax as a smelting aid to improve gold recovery and reduce dependence on mercury (Keita, 2019). However, this alternative technique remains underused due to a lack of training and awareness. As Hilson et al. (2007); Velásquez-López et al. (2011), emphasized that a better understanding of the chemical and physical processes involved in ore processing can lead to improved practices and reduced negative impacts, while a lack of technical knowledge encourages harmful practices in artisanal mining.

Since mercury only allows for the recovery of 30 to 40% of the gold (Velásquez-López et al., 2011), some miners resort to cyanidation, a technology that uses sludge residues from amalgamation, resulting in a gold recovery rate of approximately 98% (Velásquez-López et al., 2011; Verbrugge et al., 2021). The cyanidation process, mainly carried out by men, involves purchasing the slurry residues from the gold amalgamation and ore washing processes prior to amalgamation which are carried out by women (Ouédraogo, 2020; Lanzano and Arnaldi Di Balme, 2021). The process involves soaking gold ore residues in a sodium cyanide solution for 24 hours, after which the gold is recovered using methods such as zinc precipitation (Merrill-Crowe process) or column adsorption on charcoal (CIC) (Tankari Dan-Badjo et al., 2015; Drace et al., 2016). The following reactions occur during cyanidation (Torkaman and Veiga, 2023):

$$4Au + 8CN^- + O_2 + 2H_2O = 4Au(CN)_2^- + 4OH^-$$

$$2Au(CN)_2^- + Zn = 2Au + Zn(CN)_4^{2-}$$

In artisanal cyanidation sites, excavated installations typically measured around 4 m long, 2 m wide, and 0.5 m deep (Kohio et al., 2024). These excavations are arranged in pairs around a larger central basin commonly called “Pool” (Lanzano and Arnaldi Di Balme, 2021). The pre-dried slurry residues are placed into flat basins, with bottoms and walls covered by a plastic film with limited waterproofing (Kouadio, 2016; Knoblauch et al., 2020). These regular basins slope towards the central basin, which is equipped with a drainage pipe to collect leachate during cyanidation. Between 1 and 1.5 kg of sodium cyanide (NaCN) are mixed with 400-600 litres of water (Balma and Aka, 2016; Knoblauch et al., 2020). The mixture is then added to 4,500 to 6,000 kg of dry tailings in the two twin ponds, allowing the cyanide to dissolve the gold particles for 24 hours (Verbrugge et al., 2021). After this time, the water containing the Au-CN leachate is collected in the central basin via the pipe. The process is repeated with the mixture of water and CN solution if the tailings used are very rich in gold (Sanoussi, 2020). Once the CN-Au leachate is obtained, zinc chips are used according to the Merrill-Crowe process at our study sites in Burkina Faso and Guinea (**Figure I.3**). The zinc chips are fed into the paired pipes in the form of elbows from the paired basins to the central basin. After three days of reaction and fixation of the gold on the zinc by precipitation, the chips are recovered and placed in a sulfuric acid solution (unknown concentration), which will dissolve the gold absorbed on the zinc. Nitric acid is added to the mixture to remove impurities and excess zinc by releasing hydrogen cyanide. The resulting solution is then decanted and the precipitate or pellets are heated by calcination to evaporate the water and excess cyanide in order to obtain a powder rich in gold, which will be melted to obtain purified gold (Velásquez-López et al., 2011; Tankari Dan-Badjo et al., 2015; Verbrugge et al., 2021). The zinc method is used not only on riverbanks at around 200 meters, but also in open-pit mines (Keita, 2019; Sanogo et al., 2019).

The second method of gold recovery (CIC), using elution and electro-extraction of the gold precipitate on activated carbon is not used in artisanal gold mining (Stapper et al., 2021). The various extraction and recovery techniques used in gold mining in Burkina Faso and Guinea are summarized in **Figure I.3** and **Figure I.4**.

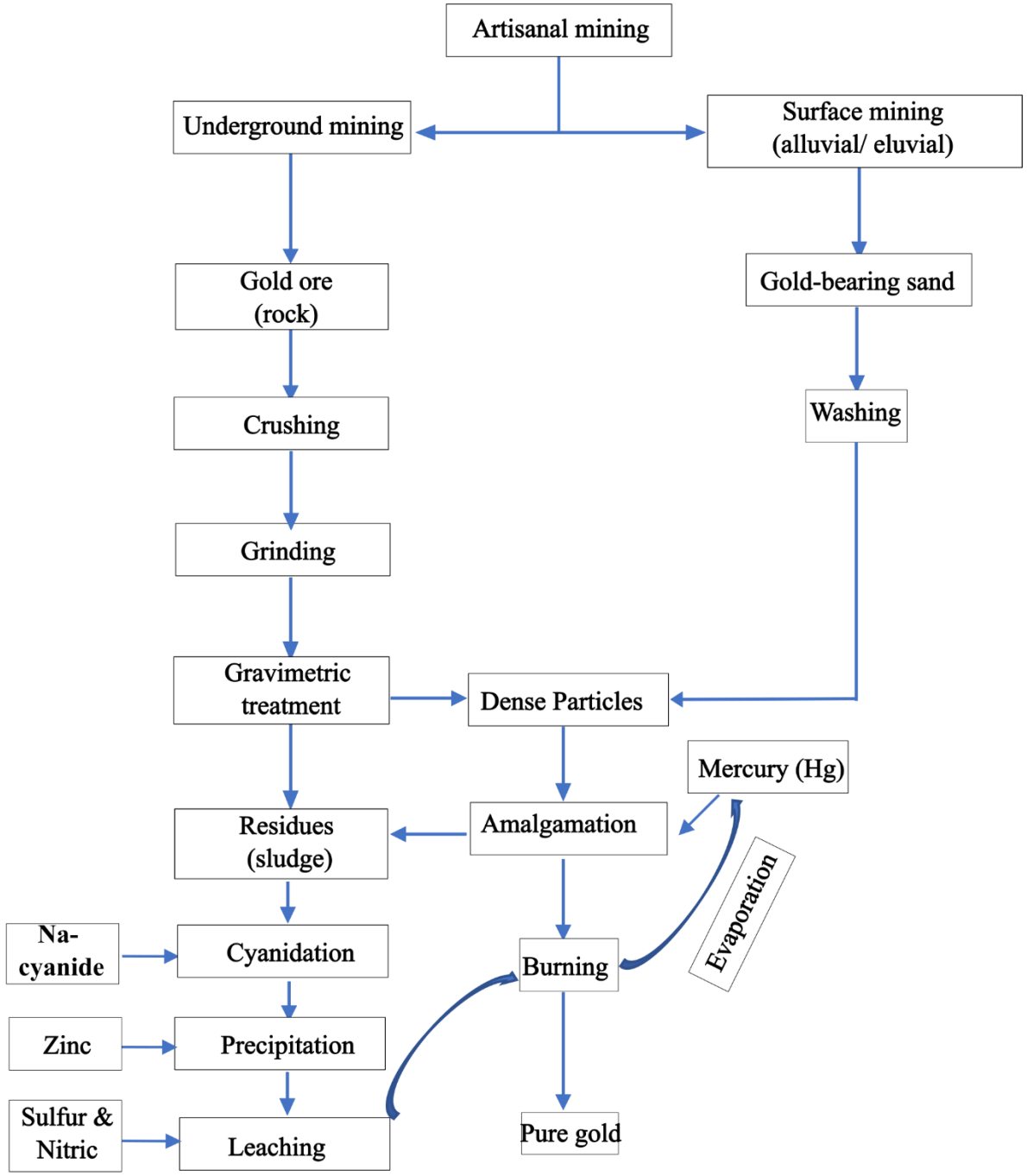


Figure I.4. Artisanal gold mining processes in West Africa

I.2. Impact of ASGM

I.2.1. Mercury

I.2.1.1. Mercury biogeochemical cycle in the West African context

Artisanal and small-scale gold mining is booming in developing countries such as Burkina Faso and Guinea leading to intensive and unregulated use of elemental Hg for gold amalgamation. The origin of the anthropogenic Hg is still poorly documented, but it appears to come mainly from Togo, destined for countries in West Africa and Burkina Faso (Benkadi, 2021). Mercury, which is used in the recovery

of gold, is released in large quantities into the environment, profoundly altering its biogeochemical cycle (Sonke et al., 2023). Its biogeochemical cycle makes it exists in various forms in the environment, namely in elemental form (Hg0) and inorganic divalent mercury (Hg^{2+} or HgII)), and in the organic form; methylmercury (MeHg). The elemental form (Hg0) is mainly found in the environment in gaseous form, but also in liquid form used in amalgamation by miners. Methylmercury exists in two forms being monomethylmercury (CH_3Hg^+ or MMHg) and dimethylmercury ($(CH_3)_2Hg$). Unlike Amazonian tropical soils, where Hg can be of natural origin, resulting from the degradation of ferralitic soils and leading to Hg accumulation in ecosystems (Roulet and Lucotte, 1995; Grimaldi et al., 2008), in the tropical regions of West Africa, mercury is mostly exogenic due to anthropogenic input. Indeed, the high mercury levels [0.1 to 41 µg g^{-1} (Rajaee et al., 2015a; Niane et al., 2019b; Thiombane et al., 2023)] found in West African soils were found to be mainly from anthropogenic inputs (Marshall et al., 2018; Schudel et al., 2018). This Hg released by ASGM is mainly deposited in the form of Hg(0) droplets, which accumulate in soils near amalgamation sites due to its low reactivity, slow solubility in water (60 mg L^{-1} at 25°C), high density, and slow oxidation rate (Ariya et al., 2015). Part of the Hg emitted during the combustion of gold-mercury amalgam volatilizes and disperses into the atmosphere, where it can be transported over long distances before falling back to the ground and water as dry (dust-aerosols) and/or wet (rain) depositions (Lyman et al., 2009; Zhang et al., 2009; Liu et al., 2011). Dry deposition time can be particularly long for particles smaller than 2.5 µm, which are deposited more frequently through episodic wet deposition events (Lin et al., 2006). Another part of this atmospheric Hg (Hg0 and/or Hg^{2+}) is then absorbed or adsorbed by tree leaves and subsequently incorporated into the soil via litter, thus constituting the source of exogenic Hg input into these soils (Jiskra et al., 2015), in addition to Hg0 droplets deposited during amalgamation (Guedron et al., 2009), as shown in Amazonia. Thus, high levels of Hg up to 670 ng g^{-1} have been reported in the leaves of food plants at mining sites in West Africa (Ahiamadjie et al., 2011), probably due to the deposition and adsorption of atmospheric Hg onto the leaves (Naharro et al., 2020). All these processes of burning and dispersing Hg0 into the environment expose burners and other miners to health risks, as well as a more diffuse risk to surrounding populations through inhalation of dust and Hg0 vapor (Tomicic et al., 2011; Black et al., 2017) (**Figure I.5**). Once Hg0 is oxidized, HgII reincorporates into the soil matrix and binds either preferentially to organic matter (OM) and/or to iron oxides and sulfur compounds (Hg^{2+}-OM and Hg^{2+}-Fe oxides), which influence its mobility and bioavailability (Biester and Scholz, 1997; Biester et al., 2002; Guedron et al., 2009). Following episodes of runoff after precipitation, these Hg-rich particles are drained into aquatic ecosystems, constituting a significant source of contamination in these environments (Grimaldi et al., 2015; Niane et al., 2019b). Several studies have shown that ASGM is the main source of Hg contamination in aquatic environments in West Africa (Donkor et al., 2006; Ouédraogo and Amyot, 2013; Niane et al., 2014; Asare-Donkor and Adimado, 2016; Niane et al., 2019b;

Kouadio et al., 2025). Once deposited onto riverbed sediment, mercury undergoes chemical transformations during sediment early diagenesis. During this process, inorganic Hg can be converted by sulfate-reducing (SR), iron-reducing (IR) bacteria, as well as methanogenic archaea and other anaerobic bacteria carrying the *hgcA* and *hgcB* genes into methylmercury (CH_3Hg^+), a toxic compound that accumulates and bioamplifies in food chains (Parks et al., 2013; Bravo et al., 2018; Mason et al., 2019; Compaore et al., 2020). This toxic compound thus enters terrestrial food webs, moving up the food chain and exposing local wildlife and human populations that consume fish to significant health risks (Grandjean et al., 1997; Bonzongo et al., 2004; Clarkson and Magos, 2006; Grandjean et al., 2010; MEEF, 2018). During this same diagenesis process, demethylation can occur through the conversion of methylmercury into inorganic mercury by the same bacteria that carry the methylation genes, thereby regulating the net concentration of methylmercury produced in these environments (Clarkson and Magos, 2006). ASGM therefore disrupts the Hg balance by increasing its source, intensifying its transformation, and dispersing it throughout ecosystems.

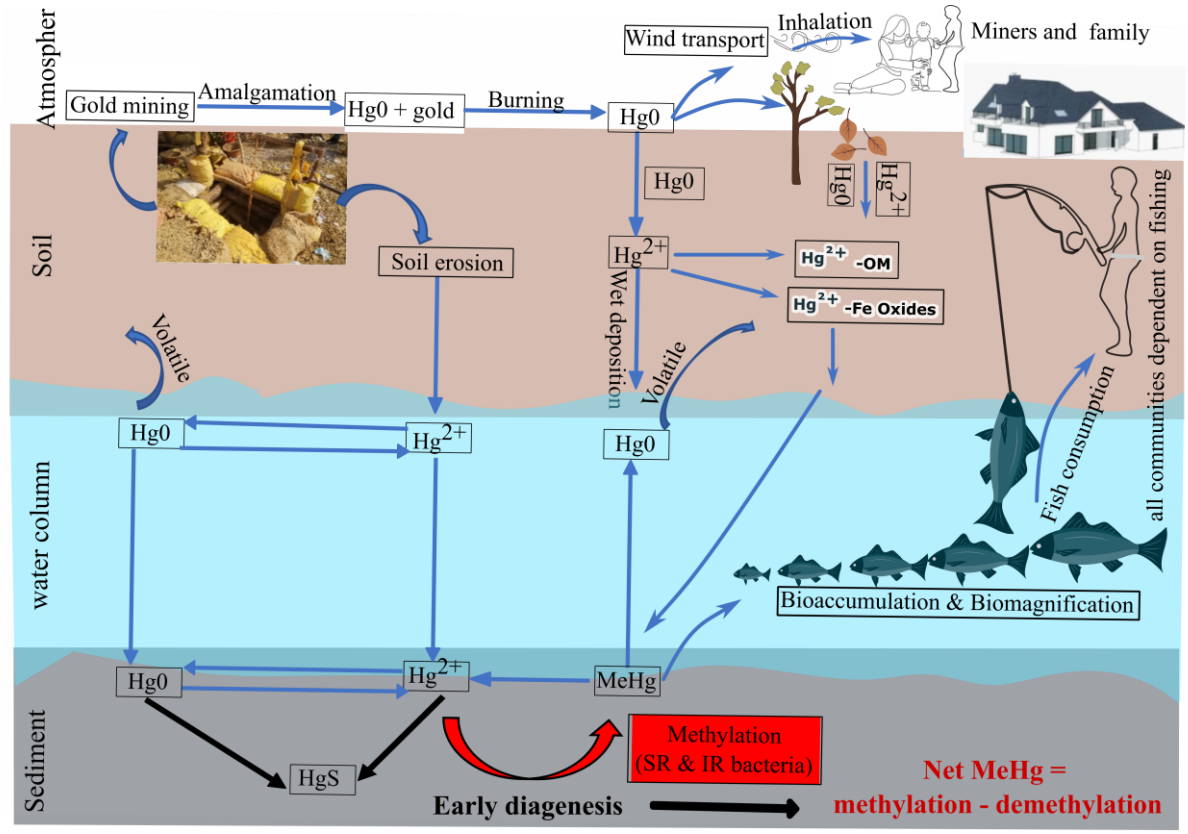


Figure I.5. Mercury (Hg) bio-geochemical cycle in West Africa context. Based on Boudou et al. (2006) and Wasserman et al. (2003), pngtree.com. SR indicates sulfate reducing and IR indicates iron reducing.

It is important to note that gold mining is not the only activity influencing the Hg cycle in West Africa. Coal-fired power plants and industries, as well as cement factories, contribute to anthropogenic Hg deposits in soil and water (UNEP, 2013, 2018). Informal waste treatment such as recycling and

incineration releases enormous quantities of Hg into the soil (0.1 to 7.6 µg g^{-1}), as is the case in Ghana (Amponsah et al., 2023). The Gulf of Guinea and the Niger Delta in particular, the oil sector also mobilizes Hg, contaminating groundwater up to 6 µg L^{-1} THg and aquatic hydrosystems with THg concentrations between 10 and 529 µg g^{-1} found in sediments (Aleku et al., 2025).

I.2.1.2. Mercury in soil

Mercury is naturally present in rock substrates (igneous, sedimentary, and metamorphic rocks) (Eawag-EPFL, 2019). Its concentrations in Amazonian rock substrates are very low at 2.1±0.7 ng g^{-1} (Goix et al., 2019). No data on Hg levels in rocks are available for West Africa. Its presence in soils may therefore be of natural or anthropogenic origin. Several studies have documented high Hg levels in West African tropical soils impacted by ASGM, as documented previously in section 1.2.1.1 (Rajaee et al., 2015a; Niane et al., 2019b; Gerson et al., 2018; Sako and Nimi, 2018; Adewumi and Laniyan, 2020; Thiombane et al., 2023), but very few mention background levels in soils not impacted by ASGM. Among the few studies available, generally low Hg concentrations have been reported in pristine tropical African soils (5–80 ng g^{-1}) (Tetteh et al., 2010; Akoto et al., 2017; Sako and Nimi, 2018; Akanchise et al., 2020), compared to Amazonian tropical soils where concentrations can be naturally higher, ranging from 100 to 900 ng g^{-1} (Leiva G. and Morales, 2013; Figueiredo et al., 2018; Fostier et al., 2023; Guedron et al., 2009). Hg has a strong affinity for specific soil components, notably organic matter (OM) and iron (Fe) oxides, which influence its retention, mobility, and bioavailability in soils (Ravichandran, 2004; Skyllberg et al., 2006). OM forms stable complexes with reduced sulfur groups, making it a key binding phase for Hg (Skyllberg et al., 2006). In addition, iron oxides can adsorb inorganic Hg effectively under oxic conditions (Schuster, 1991; Wiatrowski et al., 2009). Together, OM and Fe oxides are recognized as the primary carriers of Hg in various soil types, especially in tropical and forested ecosystems (Grimaldi et al., 2001; Grigal, 2002; Guedron et al., 2009).Very few studies have investigated the interaction between Hg and organic matter and iron oxides in West African soils. Among the few studies conducted, relatively low OM concentrations (between 4 and 10%), and iron oxides (0–3%) are assigned to West African soils in Burkina Faso and Senegal (Niane, 2014; Compaore et al., 2019; Niane et al., 2019b). However, several studies define OM and iron oxides as the major carrier phases in tropical soils in the Amazon (Grimaldi et al., 2001; Guedron et al., 2009). No link between OM and Hg has yet been found in West African tropical soils, probably due to the rapid renewal of OM leading to the development of a thin organic layer dominated by compounds with limited affinity for Hg. This restricts the availability of functional groups capable of binding strongly to Hg, and thus limiting Hg accumulation in these soils. On the other hand, in pristine soil profiles, Hg concentrations of 5–60 ng g^{-1} have been found to correlate with sulfur and clay, illustrating the strong affinity of this Hg for the sulfur groups of OM associated with the fine clay rich fraction of the soil

(Niane et al., 2019b). To date, these data have always been compared to Hg concentrations in pristine soil profiles around the world ranging from 20 to 250 ng g^{-1} (Adriano, 2001; Ndzana et al., 2023), thus showing a lack or low availability of studies on Hg background levels in pristine soil surfaces and profiles in West Africa. Very little data is available on MeHg levels in west African soils. Among the data that is available, MeHg levels around 0.3 ng g^{-1} are found in undisturbed soils in West Africa, representing less than 0.5% of THg (Gerson et al., 2018). MeHg has been found to be uncorrelated with THg concentrations in soils, thus showing that geochemical processes other than the amount of Hg are responsible for the production and accumulation of MeHg (Gerson et al., 2018).

I.2.1.3. Mercury in water

In West African groundwater unaffected by gold mining, where water-rock interactions tend to control geochemistry and where turbidity is generally low, total Hg is usually found in dissolved form at very concentrations [<10 ng L^{-1} (Fréèze and Cherry, 1979; Sunkari et al., 2022; BRGM, 2024; Aleku et al., 2024)]. However, there are virtually no reliable empirical data establishing baseline levels of total filtered Hg in groundwater in West Africa except for a single study conducted in Nigeria where levels <10 ng L^{-1} were reported (Aleku et al., 2025). On the other hand, generally low background levels in undisturbed aquifers (0.5–5 ng L^{-1}) have been reported worldwide (Krabbenhoft and Babiarz, 1992; Kowalski et al., 2007; Szymczycha et al., 2013; Kowalski et al., 2018). Groundwater used as drinking water by local communities can be degraded by gold mining through Hg-rich particle contamination, as high levels of total Hg ranging from 4 µg L^{-1} to 7 mg L^{-1} have been reported in unfiltered groundwater in Ghana and Burkina Faso (Rajaee et al., 2015a; Somé et al., 2016). There is almost no MeHg data in groundwater in west Africa. MeHg concentrations of <0.01 to 0.8 ng L^{-1} have been reported in the filtered fraction of groundwater in a study conducted in the United States (Black et al., 2009; Wang et al., 2020).

In West Africa, rivers are not always perennial, with seasonal rivers dominating in some regions (Koussoubé et al., 2018; Gnazou et al., 2018; Bianchi et al., 2023; Wannous et al., 2024; Adeotan et al., 2025). In pristine West African hydrosystems, THg varies between 5 and 20 ng L^{-1}, with between 75 and 85 % of Hg bound to the particles (Meili, 1997; Ouédraogo and Amyot, 2013; Niane et al., 2019b). Previous studies conducted in rivers and reservoirs unaffected by gold mining in Senegal and Burkina Faso have reported unfiltered Hg levels ranging from 0.4 to 22 ng L^{-1}, while the filtered fraction remained relatively low between 0.05 and 5.6 ng L^{-1} (Ouédraogo and Amyot, 2013; Niane et al., 2019b; Bokar et al., 2020). In the same hydrosystems, MeHg concentrations in the filtered fraction have been reported to range between 0.01 to 0.2 ng L^{-1}, and around 0.2 ng L^{-1} in the unfiltered fraction (Ouédraogo and Amyot, 2013; Niane et al., 2019b). In rivers impacted by ASGM activities, Hg contamination can occur hundreds of kilometres from a watercourse if the mining site is located near

that water source (Hill, 2016). Approximately 70% of the Hg is bound to particles, with the particulate fraction ranging from 38 to 726 ng g^{-1} in aquatic systems impacted by ASGM in Côte d'Ivoire (Mason et al., 2019). In addition, pond waters studied in Senegal revealed similar levels of MeHg (3.6 ±1.7 ng g^{-1}) with higher levels of THg up to 9 µg g^{-1} due to increased MeHg production, which could become a source of MeHg contamination in adjacent rivers. This means that MeHg production is not only linked to the total amount of Hg, but also to geochemical conditions (anoxia, presence of sulfato-reducing bacteria, etc.) and the bioavailability of Hg (Niane et al., 2019b).

I.2.1.4. Mercury in River sediment

Baseline concentrations in pristine sediments from rivers in Mali and Senegal have been reported to range between 15.5±7.1 ng g^{-1} to 30±6 ng $g^{-1}$for THg and 2.3 ±2.2 ng g^{-1} for MeHg (Niane et al., 2019b; Bokar et al., 2020). Sediment can be contaminated by anthropogenic Hg used in ASGM activities. In ASGM impacted aquatic hydrosystems in West Africa, reported levels range from 0.02 to 2.4 µg g^{-1} in river sediments in Côte d'Ivoire and Senegal, with MeHg levels ranging from 0.5 to 16 ng g^{-1} (Mason et al., 2019; Niane et al., 2019b). Mercury in sediments exists in various chemical forms, including inorganic Hg bound to sulfide minerals (like HgS or FeS), complexed with organic matter, adsorbed onto mineral surfaces, or as dissolved species in pore waters (Guedron et al., 2009; Skyllberg et al., 2006). The distribution of these species is affected by factors such as redox conditions, pH, sulfide concentration, and organic matter content, causing variability over time and space in sediments and pore waters (Sunderland et al., 2006). Mercury methylation in sediments occurs during early diagenesis under anoxic conditions, with microbial activity transforming inorganic Hg to MeHg through anaerobic microorganisms like sulfate-reducing and iron-reducing bacteria, as well as methanogenic archaea (Benoit et al., 1999; Bravo et al., 2018). The distribution of Hg species, which includes inorganic Hg bound to sulphides, organic matter, and iron oxides, is crucial for understanding its bioavailability to methylating bacteria (Sunderland et al., 2006). Faster analytical methods such as thermodesorption for determining Hg bound to organic matter (Rumayor et al., 2013, 2016) and more specific methods such as sequential and selective chemical extraction (Kostka and Luther, 1994; Rodríguez Martín-Doimeadios et al., 2000; Bloom et al., 2003; Raiswell et al., 2010), X-ray absorption spectroscopy (XAS) (Bacon and Davidson, 2008), and species-specific isotope techniques are used to analyze Hg speciation, which informs predictions of methylation processes and mobility (Kim et al., 2003).

I.2.1.5. Mercury in food chains and humans

Once in the hydrosystem, Hg and MeHg in water can enter and be accumulated in the food chain. Highest concentrations are generally found in top predator fish, which makes predatory fish bioindicators of Hg contamination in aquatic ecosystems (De Paula Gutiérrez and Agudelo, 2020; Maury-Brachet et al., 2020). According to a study conducted by the USEPA (1997), baseline Hg levels

of 100 to 200 ng g^{-1} are found in uncontaminated freshwater fish. In a study by de Kwaansa-Ansah et al. (2011), despite the impact of ASGM on the Yeji basin in Ghana, relatively low concentrations of Hg (3 to 90 ng g^{-1}) were found in fish from the White Volta River. This is likely due to their diet and trophic position (non-carnivorous species), which limits Hg bioaccumulation. In contrast, Hg levels found in piscivorous fish in major rivers in West Africa indicated ASGM and predation as major factors responsible for high Hg levels in fish in this region (Oppong et al., 2010; Ouédraogo and Amyot, 2013; Niane et al., 2015; Ouédraogo et al., 2015; Mason et al., 2019, 2022). MeHg accounts for approximately 90% of the total Hg in piscivorous fish due to its high assimilability, low elimination, and high biomagnification (Mason et al., 2022; Ouédraogo and Amyot, 2013).

Locally and globally, apart from inhalation of Hg vapor, which exposes populations, fish consumption remains the major source of human exposure to Hg, as fish consumption represents a significant part of the diet of West African populations (FOA, 2025; Mason et al., 2022). Very few reliable studies exist on Hg levels in humans in West Africa. Amongst available data, a study conducted in Tanzania and Zimbabwe established baseline levels of Hg in urine (0.58±0.54 µg L^{-1}), blood (2.9±2.2 µg L^{-1}), and hair (1.4±0.8 µg g^{-1}) in individuals living in areas where no mining activity was taking place (Bose-O'Reilly et al., 2008). In West Africa, a study conducted in Senegal revealed baseline Hg levels of 0.4±0.3 µg g^{-1} in the hair of control populations and reported a link between Hg concentrations in populations whose diet rely mainly on fish at mining sites and the consumption of contaminated fish (Niane et al., 2015). According to the WHO, Hg exposure among miners and their communities appears to be mixed, with recent exposure to MeHg via fish resulting in the presence of Hg in the blood, and exposure to inorganic forms of Hg (among people living near gold mining areas) resulting in elevated Hg levels in the urine (OMS, 2003). MeHg concentrations in blood have been found to correlate with concentrations in hair, making this latter an accessible biomarker widely used to describe population exposure to Hg from food sources (Budtz-Jørgensen et al., 2004). Low Hg concentrations (<1 µg g^{-1}) were found in the hair of people who consume fish no more than once a week (Castaño et al., 2015) in Europe. In contrast, concentrations of between 15 – 20 µg g^{-1} were found in highly fish consumers in the Amazon (consuming 4 to 14 times fish a week), while concentrations between 2.6 –7.7 µg g^{-1} were found in fish consumers Côte d'Ivoire and Senegal in West Africa (Barbieri and Gardon, 2009; Niane et al., 2015; Claon et al., 2024). Fish consumption can contribute to increased blood Hg levels, but miners are mainly exposed to Hg0 vapor through inhalation, resulting in blood Hg concentrations above 5 µg L^{-1} in 54% of people working in mining sites in Ghana (Afrifa et al., 2018). Another study conducted in Ghana showing high concentrations of Hg in chicken kidneys and livers as well as sheep kidneys seems to indicate that human exposure is also possible through the consumption of poultry and sheep (Bortey-Sam et al., 2015).

I.2.2. Cyanide (use, chemistry, and health/risk/exposure)

Virtually absent from mining extraction techniques in West Africa, cyanidation first appeared in the 2000s and began to spread rapidly from 2010 onwards (Knoblauch et al., 2020; Lanzano and Arnaldi Di Balme, 2021; Verbrugge et al., 2021). Recent studies conducted in Burkina Faso, Guinea, and Mali have shown the dominant and exacerbated scale of this technique between 2015 and 2025, especially at artisanal and semi-mechanized sites (Brugger et al., 2018; Kohio et al., 2024). Cyanide, is increasingly used in ASGM, generally in the form of salt (sodium cyanide), dissolves gold by forming an $Au(CN)^{2-}$ complex, which is potentially toxic in its free form (CN^-) or in the form of volatile hydrocyanic acid (HCN) (Tissot and Pichard, 2005; INERIS, 2018). In Kokumbo, Côte d'Ivoire, mining waste from cyanidation contained between 1.9 and 100 µg g^{-1} of cyanide, with less than 3% available in the form of free cyanide (CN^-) (Kouadio et al., 2025). Due to the proximity of cyanidation sites to rivers and episodes of rainfall, these tailings are leached and end up in surface water systems. This is the case in Burkina Faso, where high concentrations of free cyanide in water (up to 2 mg L^{-1}) and soil (up to 9 µg g^{-1}) have been linked to significant risks of human exposure through water ingestion, inhalation, skin contact, fish consumption, and consumption of contaminated tubers (Kohio et al., 2025). The use of cyanide has been linked to potential neurological effects leading to short-term memory loss with high levels of biomarkers of cyanide exposure (blood lactate) in miners using cyanide (Knoblauch et al., 2020). In addition, human and environmental exposure (agriculture, livestock farming, fishing) through intensive and inappropriate use of cyanide has been reported by Koné (2021).

I.2.3. Geogenic contamination (As, Pb) of groundwater and health/ exposure issues

In West Africa, the digging of deep wells and the pumping of groundwater during underground gold mining can remobilize geogenic contaminants such as arsenic (As) and lead (Pb) (Smedley and Kinniburgh, 2002). As can be present in ores in high concentrations ranging from 20 to 30 g kg^{-1} in cobalt (Co), lead (Pb), and gold (Au), up to 110 g kg^{-1} in copper (Cu) ores (Lombi et al., 2000). As levels in soils ranging from 6 to 936 µg g^{-1} have been reported in Mali (Bokar et al., 2020), while concentrations of 16.7 to 122 µg g^{-1} have been reported in Kokumbo, Côte d'Ivoire (Kouadio et al., 2025). The main geogenic sources of arsenic are sulfides such as arsenopyrite, commonly found in thermal deposits, volcanic-sedimentary and magmatic rocks, whose weathering leads to two levels of arsenic oxidation into arsenite (As(III)) and then arsenate (As(V)) in oxic water resources (Smedley et al., 2007; Hug et al., 2020). Particularly in semi-arid environments, arsenic mobilization is much greater in the form of arsenate (As(V)) under oxic conditions and at basic pH (>8) (Bretzler et al., 2019; Hug et al., 2020). This is the case in Burkina Faso, where dissolved As was mainly present in the form of arsenate (As(V)) in groundwater that appeared to be mainly oxygenated (Smedley et al., 2007). Exposure to arsenic has been linked to skin lesions, skin cancer risk, and cardiovascular disease

(BARRO-TRAORE et al., 2005; States et al., 2009; Obiri et al., 2010). Since drinking water consumption is the main route of contamination for populations, most studies on As have focused on groundwater and surface water in West Africa. This is the case in Burkina Faso, where Birimian rocks, which are particularly As rich sulfides, can cause As to be released into groundwater, with 14.6% exceeding the WHO standard of 10 µg L^{-1} (Bretzler et al., 2017). In addition, As concentrations between 0 and 5 µg L^{-1} have been reported in 70% of wells in the Bambouré mineralization zone in Burkina Faso, groundwater in Kokumbo, Côte d'Ivoire, and Kamabangou, Niger, while levels of up to 100 µg L^{-1} have been reported in boreholes in Burkina Faso (Sako et al., 2016; Tankari Dan-Badjo et al., 2019; Kouadio et al., 2025). In West Africa, very little information exists on background levels of As in surface water and sediments. Background levels of 0.1 to 44.8 µg g^{-1} in sediments and 0.5 to 29 ng L^{-1} in water have been reported in Morila, Mali (Bokar et al., 2020). A study conducted in surface waters in Kokumbo, Côte d'Ivoire, reveals levels between 0.03 and 2.4 µg L^{-1} with average concentrations of 85. 3±54.7 µg g^{-1} in sediments, showing the adsorption of arsenic on iron oxy(hydro)oxides, resulting in its low mobility in water (Kouadio et al., 2025).

Concentrations ranging from 9.1 to 45.4 µg g^{-1} of as lead (Pb), another geogenic contaminant have been reported in soils at gold mining sites in Kokumbo, Côte d'Ivoire (Kouadio et al., 2025). high concentrations of Pb in soil (<100 to 34700 µg g^{-1}), and sediments (<100 to 2360 µg g^{-1}) leading to chronic exposure to lead in well water (<10 to 165 µg L^{-1}) and surface water pond (<10 to 475 µg L^{-1}), has been linked to cognitive delays in children, renal and cardiovascular effects, in Zamfara in Nigeria (UNEP/OCHA, 2010). In West Africa, Pb concentrations in groundwater and surface water are generally low (<5 µg L^{-1}) (Lapworth et al., 2017), as is the case in groundwater in Kokumbo, Côte d'Ivoire, where concentrations of 0.01 to 0.09 µg L^{-1} have been found (Kouadio et al., 2025). However, substantial enrichments of up to 11 µg L^{-1} have been observed in groundwater in the Bamboré mineralization zone in Burkina Faso (Sako et al., 2016). As lead is geochemically immobile under neutral conditions, average concentrations of 4.8 to 30 µg g^{-1} and 21.5±6.7 µg g^{-1} were found in sediments, with concentrations of 0.1 to 4.0 µg L^{-1} and 0.02 to 0.19 µg L^{-1} in surface water and a pH of 7.3±0.3 in Morila, Mali, and Kokumbo, Côte d'Ivoire, respectively (Bokar et al., 2020; Kouadio et al., 2025). To date, very few reliable studies exist on baseline levels and contamination of lead and arsenic in soil, groundwater, surface water, and sediments in West Africa, particularly in Guinea, where there are none. With mining being practiced intensively and expanding rapidly in Guinea and Burkina Faso, monitoring these two co-contaminants with a high adverse effect on human health, is important in mining areas and their surroundings. Other co-contaminants such as cadmium (Cd), antimony (Sb), chromium (Cr), copper (Cu), and zinc (Zn) can be released into surface and groundwater through the weathering of shales and arsenopyrite and the exposure of rocks during artisanal gold mining, as is the case in Côte d'Ivoire (Sako et al., 2016; Kouadio et al., 2025).

I.3. Study sites and sampling strategy

I.3.1. Burkina Faso study site

I.3.1.1. Geology, hydrography, climate context, and gold-bearing zones

Burkina Faso is a flat country with an average altitude of 400 m, with Mount Ténakourou as the highest peak at 749 m, located in the south-west of the country. (Seguin, 2005; Courtois et al., 2010). Two geological units are found in the country: the crystalline basement, which covers 82% of the territory, and the sedimentary zone (MARAH, 2023). The crystalline basement consists of metamorphic and igneous rocks and covers the main gold deposits, which are primarily epigenetic and closely associated with quartz veins (**Figure I.6**) (Béziat et al., 2008). Burkina Faso is known for its soil heterogeneity due to its long geomorphological evolution and diverse geological cover. The country has three main types of soil: iron and manganese sesquioxide-containing (39%), poorly developed (26%), and hydromorphic (13%) (MARAH, 2023).

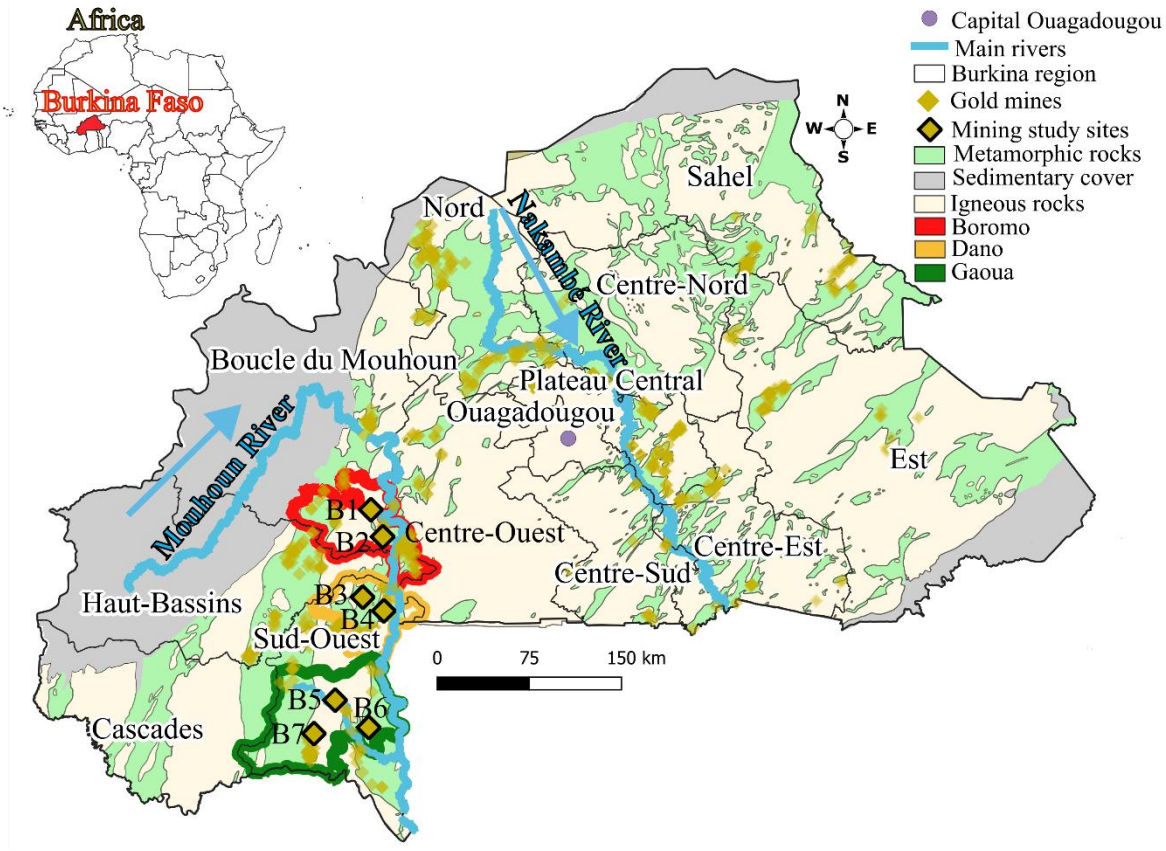


Figure I.6. *Geological maps of Burkina Faso with artisanal gold mines location*

The country has a tropical climate divided into two main seasons: the rainy season from June to October and the dry season from November to May, with peak temperatures (T°C>40°C) from March to May (Barbé et al., 2002; Sultan and Janicot, 2003; Fowe et al., 2015). It is influenced by three climatic zones: the Sahelian zone in the north with average rainfall of 600 mm/year, the Sudano-Sahelian zone

in the center with average rainfall of 600 to 900 mm/year, and the Sudanese zone in the south, which is more humid with 900 to 1200 mm/year (Lemoalle and De Condappa, 2009; Balma and Aka, 2016). This climate is influenced by air masses from the south crossing the ocean and laden with water vapor, known as the monsoon, and a drier, warmer air mass from the north crossing the Sahara Desert, known as the Harmattan (Lafore et al., 2010). As a result, these three climatic zones give the country three types of vegetation. The Sahelian zone features arboreal steppe in the north and wooded steppe in the south, while the Sudano-Sahelian zone is characterized by savannah with arboreal and woody grasses. Finally, the Sudanese zone is characterized by wooded savannah, open forests, and forest galleries (Balma and Aka, 2016).

The country's groundwater is linked to rock fissuring, fracturing, and weathering. Flow rates are generally low, averaging 5 m^3 $hour^{-1}$, with frequent negative drillings throughout the territory (Seguin, 2005; MARAH, 2023). On average, aquifers in Burkina Faso are recharged at a rate of 1 to 50 mm/year, with dolomitic limestone aquifers that can be karstified in the north of the country, resulting in good flow rates of 100 m^3 $hour^{-1}$ (Seguin, 2005). The country's hydrographic network is governed by three major basins: the Comoé basin in the southwest, the Volta basin in the Center, and the Niger basin in the northeast, with a small part in the west. The Volta basin is the largest in the country, covering 178,000 km^2 of a total area of 274,223 km^2 (Sanogo et al., 2014). This vast Volta basin covers three main rivers, two of which flow through Burkina Faso and Ghana, and the last of which flows only through Ghana. Among these rivers, the Mouhoun River, formerly known as the Black Volta, is perennial and originates in the Sudano-Guinean zone, with a total length of 1,000 km in Burkina Faso, characterized by its loop shape (**Figure I.6**) (Lemoalle and De Condappa, 2009; Balma and Aka, 2016). The Mouhoun River reached flows of 308,219 m^3 $hour^{-1}$ in 1990 and 1,757,991 m^3 $hour^{-1}$ in 2004 in the southwestern part of the country, where one of its largest tributaries, the Poni River, is located (Fig. 6) (Lemoalle and De Condappa, 2009). The north-south precipitation gradient is clearly visible in the region. The second river, the Nakambé, historically known as the White Volta (**Figure I.6**), has a very low flow during the dry season (average flow of 42,237 m^3 $hour^{-1}$) towards the north and may even dry up locally. Downstream, the river becomes perennial again thanks to the additional water supply from the Bagré dam located in the lower part (average flow of 970,320 m^3 $hour^{-1}$) (Lemoalle and De Condappa, 2009).

As mentioned above, mining sites in Burkina Faso are concentrated in the crystalline basement, which is home to a dozen deposits including gold, zinc, manganese, copper, bauxite, silver, nickel, aluminum, dolomite, marble, peat, and lead (Seguin, 2005). Gold is currently the most mined mineral in Burkina Faso, with three types of mining operations: industrial, semi-mechanized, and artisanal, commonly referred to as gold mining (Balma and Aka, 2016; Benkadi, 2021). ASGM and industrial gold mining sites coexist, generally located in the Southwest, Boucle du Mouhoun, Center-West, Cascades, and

Hauts-Bassins regions (**Figure I.6**). From 12 industrial mining sites in 2012 (MME and Par-Gs, 2014), Burkina Faso increased to 17 in 2019, including 16 gold mines and one zinc mine in operation (Benkadi, 2021). In addition, in 2017, 448 gold mining sites (artisanal and semi-mechanized) were reported in twelve (12) administrative regions, including 53 in the East, 34 in the Sahel, 34 in the Upper Basin, 25 in the Cascades, 17 in the Center-East, 110 in the Centre-North, 22 in the Boucle du Mouhoun, 14 in the Centre-West, 12 in the Central Plateau, 5 in the Centre-South, 61 in the North, and 61 in the South-West (ENZO, 2017). In 2019, the number of artisanal mining sites was estimated at 51, with 74,637 gold miners in the southwestern part of the country (Benkadi, 2021), This is undoubtedly due to the abandonment of certain ASGM sites following the emergence of terrorist groups since June 5, 2015, bringing the total number of ASGM sites to 440. To date, the number of gold mining sites is not yet well known in 2025, due to the inaccessibility of certain area for security reasons since 2015, with only the southwestern area remaining accessible until 2023.

I.3.1.2. Artisanal gold mining and gold production in Burkina Faso

The evolution of gold mining sites in Burkina Faso between 1995 and 2023 is closely linked to fluctuations in the international gold market and the gradual transformation of the national mining sector (**Figure I.7**). This evolution of gold mining sites was conceived by compiling information from national reports and articles published between 2011 and 2018 and should be considered an approximation (Sba-Ecosys, 2011; Côte, 2013; MME and Par-Gs, 2014; Zabsonré et al., 2016; ENZO, 2017; Côte and Korf, 2018; MOORE, 2018; OCDE, 2018).

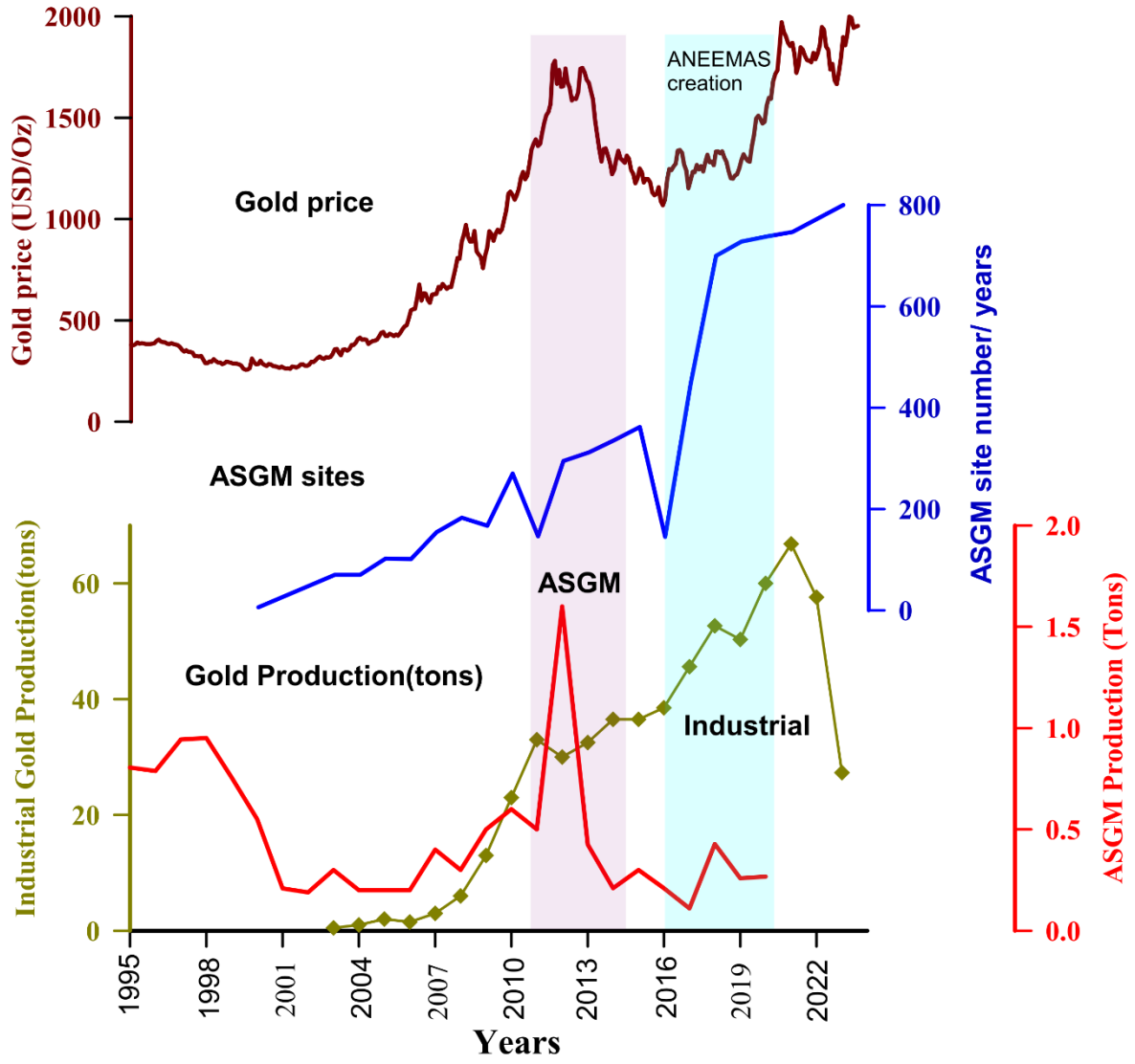


Figure I.7. *Historical and modern trends in gold production in Burkina Faso from 1995 to 2024. Sources: (Sba-Ecosys, 2011; Côte, 2013; MME and Par-Gs, 2014; Zabsonré et al., 2016; ENZO, 2017; Côte and Korf, 2018; MOORE, 2018; OCDE, 2018).*

Before the 2000s, artisanal gold production was in sharp decline until 2001, when it fell below 0.5 tons with fewer than 200 gold mining sites. After the mid-2000s, the steady rise in the price of gold coincided with a rapid expansion in the number of gold mining sites, which reached 400 in 2012, with artisanal production tripling to 1.6 tons. This gold rush is driven by the economic appeal of gold. At the same time, industrial production experienced sustained growth between 2008 and 2010 with the opening of several industrial mines and production rising to over 30 tons. This industrial production fluctuates and continues to grow until 2020, when it reaches 60 tons, then declines rapidly until 2022, when production returns to around 20 tons. On the other hand, artisanal production experienced more irregular growth, depending on both international price fluctuations and local operating conditions, as well as the creation of ANEEMAS (National Agency for the Supervision of Artisanal and Semi-

Mechanized Mining Operations) established by Decree No. 2015-1420/ PRES-TRANS/PM/MEF/MME of November 30, 2015.

The creation of ANEEMAS, now known as the National Precious Substances Company (SONASP) since August 9, 2023, coincides with a doubling of the number of gold mining sites to 800 in 2022, with artisanal production remaining low at less than 0.5 tons. As the gold mining sector is highly informal, these figures only represent the quantities of gold extracted recorded by Burkina Faso's gold and precious metals trading chambers. The rest of the gold is traded informally in neighbouring countries, notably through international gold-trading hubs such as Lomé and Dubai (OCDE, 2018). This reflects the problem of channelling gold transactions, already observed since the colonization period between 1925 and 1960, as described by Bantenga (1995), still visible and relevant today. The decline in the quantity of gold extracted by artisanal means can also be explained by the emergence of terrorism since 2015, which has led miners to abandon gold mining sites in order to prioritize their survival. In fact, 48 gold mining sites were abandoned in 2016, one year after the emergence of insecurity (Balma and Aka, 2016). These trends highlight a mining sector undergoing rapid change, where small-scale artisanal production coexists with more structured industrial production. This reflects the economic, social, and environmental challenges associated with gold mining in Burkina Faso and the need to formalize this activity.

I.3.1.3. Description of Burkina Faso study sites

In Burkina Faso, due to insecurity, it was impossible to work in the Sahel or eastern regions. In this context, the southwestern region, including the municipalities of Gaoua and Poura, which have numerous gold mining sites, were deemed more suitable for conducting this study. These two locations were selected for the study, and the sites were chosen based on current events and insecurity during the first year of the thesis in 2022. Thus, due to the insecurity in Burkina Faso in 2022, the locality of Poura was still in the classified as a “red zone” and therefore inaccessible, leading to a change in the regions of interest for this study over time. We therefore focused on three (3) localities in Burkina Faso, considering the security situation, mining potential, and ASGM techniques used in these regions. Thus, the regions of Boromo, Dano, and Gaoua were identified jointly with the ANEEMAS for sampling as part of this thesis. These study sites, located along the Mouhoun River from upstream to downstream (see **Figure I.6**), include: i) the first study site, Boromo, capital of the province of Balé, located in the Mouhoun loop in the center of the country, halfway between Bobo-Dioulasso and Ouagadougou. ii) the second study site, called Dano, is a commune and the capital of Ioba province. iii) the third study site, located in Gaoua, is a commune in Poni province in the southwestern region of Burkina Faso. All information on characteristics (GPS coordinates, year of creation, number and type of mines, and mining practices) can be found in Appendix1, Appendix1, **Tableau VI-1**A. These characteristics are

reported according to the ANEEMAS census and information received directly from mining site managers.

i) The first study area, in the Boromo region, located 175 km from Ouagadougou, has a rural population of 20,193, with 9.6% of the population living in urban areas throughout the Mouhoun loop, comprising eight villages, according to the 2022 national census (Insd-RGPH, 2022). It is located in the Sudano-Guinean zone, the second wettest area in the country according to the agro-climatic subdivision. Three types of soil are found in Boromo, namely raw mineral soil, ferruginous or gravelly soil, and hydromorphic soil (PIF, 2017). Two gold mining sites were sampled in the commune of Boromo. The Siby ASGM site (named B1, Appendix 1, **Tableau VI-1**) is the first study site created in 2009, located 13 km from the town of Boromo. This mining site is located near the Siby River, where miners use the water to wash their ore. Siggnoghin is the second gold mining site (B2) created in 2006, located in Boromo. The Signoghin mining site is located less than one kilometer from the village of Signoghin, which is 4 km from the town of Boromo.

ii) Located in southwestern Burkina Faso, the second study area, known as Dano commune, capital of the province of Ioba, is located 117 km from Gaoua, 280 km from Ouagadougou, and 150 km from Bobo-Dioulasso. Covering an area of 669 km², the commune of Dano is bordered to the east, west, and south by the communes of Coper, Guéguéré, and Dissin, respectively; to the north and northeast by those of Koti and Fara; and to the northwest by the commune of Oronkuaa (KI, 2009). Two ASGM sites were sampled in this region. The Gnikpière ASGM site (B3), which is much more recent, was created in 2019 (Balma and Aka, 2016). The second ASGM site is Memer 1 (B4), created in 1997. The latter is a pilot site for artisanal mining operated by ANEEMAS, located in a small village about 20 km west of Dano with a population of about 1,231 according to the 2006 General Population and Housing Census (RGPH).

iii) Located 395 km from Ouagadougou (capital of Burkina Faso) and 150 km from Bobo Dioulasso, Gaoua, the third study area, covers an area of 874 km². The municipality of Gaoua is at the crossroads of two countries. It is approximately 124 km from the Ghanaian border, accessible via the unpaved Gaoua-Batié-Kpuéré road, and 70 km from the Ivory Coast border, accessible via the paved Gaoua-Kampti-Frontière road. Geographically, Gaoua is bordered to the east by the municipality of Boussera; to the west by the municipality of Lorépéni; to the north by Bourom-Bouroum and Nako; and to the south by the municipality of Midebdo. It has a Sudanese climate, characterized by a dry season lasting about six (06) months from mid-November to mid-May and a winter season from mid-May to mid-November. This municipality receives abundant rainfall with a hydrographic network consisting of two perennial rivers and several secondary rivers. The municipality of Gaoua is composed of eight urban areas and 56 villages (MUH, 2011).



Figure I.8. *Picture of the mining site in southwestern Burkina Faso showing A) the mining village of Djikando, B) the Memer1 settling basin, C) the visible environmental impact of the Djikando mining site on the Poni River in Djikando.*

The fifth ASGM site of interest, called Djikando (**Figure I.8**.A), is the oldest site created in 1995 and located in the village of Djikando (B5) (AMR, 2021). Djikando is located about 3 km from the town of Gaoua, which is home to the largest gold mining site in the municipality. A large river runs through the village; the Poni River, which is a tributary of the Mouhoun River (Fig. 8C). In addition, in May-June 2018, Rober Mason sampled two ASGM sites, B6 and B7 (**Figure I.6**), in the Gaoua region. These are the gold mining sites known as Quadaradouo (B6) and the three small neighboring sites Bandediera, Banfara, and Poniro (named B7). No information is available on the creation, the number of miners, date of creation, or surface area. These latest samples have been analyzed since 2018 and have never been published. They are therefore included in this thesis in order to provide further documentation on the Gaoua region.

At all of these sampled mining sites, Hg amalgamation is the only technique used, except at the Siggnoghin site in Boromo, where cyanidation is used in addition to amalgamation.

I.3.2. Guinea Republic study sites

I.3.2.1. Geology, hydrography, climate context, and gold-bearing zones

Guinea is a country divided into four major regions: Maritime Guinea or Lower Guinea, Middle Guinea, Upper Guinea, and Forest Guinea. Its altitude varies depending on the region, ranging from 750 m to 1,200 m in some parts of Middle Guinea and an average altitude of 500 m in Upper Guinea (FAO and ONU, 2005). The geology of Guinea is dominated by Archean formations and the Precambrian basement. The northeast of the country is mainly composed of metamorphic formations, while the southeast is a vast eruptive zone cover by igneous rock and sedimentary deposits cover the northwest of the country (**Figure I.9**) (Mamedov et al., 2010).

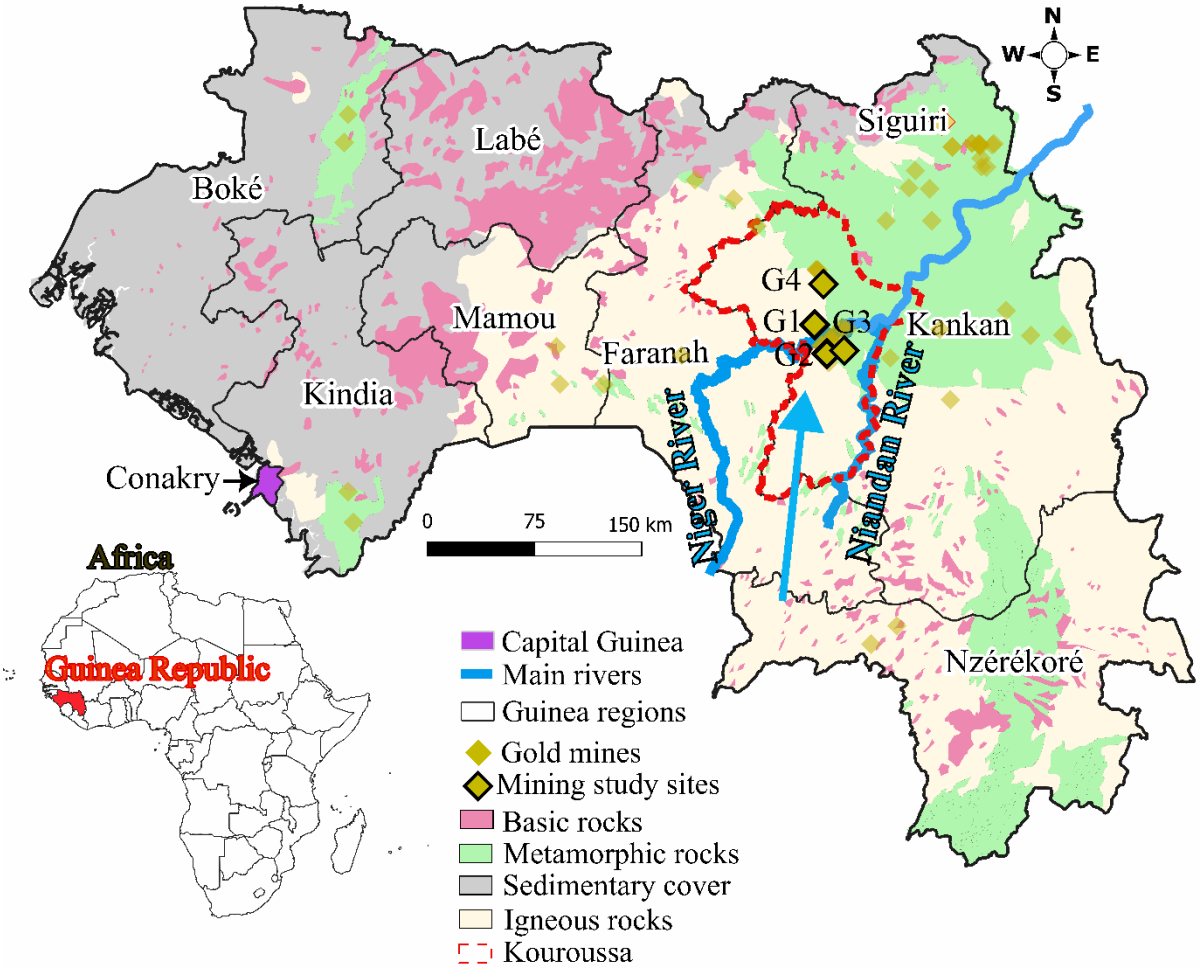


Figure I.9. *Geological maps of Guinea with artisanal gold mines location.*

Guinea has a variety of soils, including ferruginous lateritic soils in the southwest in Conakry, and clayey, silty, and sandy lateritic soils in the northwest in Labé. In the center and the North, in Siguiri and Faranah, there are clayey lateritic soils, and in the south, in N'zérékoré, there are silty and clayey lateritic soils (INS, 2021). The climate is tropical, dry, and warm, equatorial to monsoon, with average annual rainfall between 1,100 and 1,900 mm, reaching 2,000 to 4,000 mm in Boké and Conakry. There

are two distinct seasons: the dry season from November to May and the wet season from June to October. The dry season is particularly influenced in January and February by a hot, dry wind blowing from the northeast called the harmattan. Temperatures range from 15°C at night in December to 40°C during the day in April (FAO and ONU, 2005; Mamedov et al., 2010; INS, 2021). Guinea has a diversity of vegetation ranging from mangroves, dry forests, dense rainforests to savannahs, which account for more than 70% of the vegetation cover (Bah and Jean, 1996; Liu et al., 2016). Gold mining has greatly impacted the land cover between 2011 and 2013 in Siguiri region, with a loss of 36 % of the total area, which fell from 62% to 26%, leaving bare soil representing 37.9% of the total area (Oularé et al., 2025). The hydrography is generally characterized by fissured/fractured and volcanic (Phanerozoic) hydrogeological structures found near Mamou and Labé in the northeast of the country. Aquifers have a recharge rate of between 100 and 300 mm per year throughout the country, except in the southern part of Forest Guinea and Kindia, where recharge rates can reach up to 600 mm per year (Seguin, 2005). Considered as the water reservoir of West Africa, Guinea has abundant surface water resources, with several rivers originating there. Crossed in the center by the vast Niger River, the country's hydrographic network originates in the Fouta-Djalon mountain range and the Guinean ridge (Bah and Jean, 1996; FAO and ONU, 2005).

Guinea's subsoil is very rich and abounds in many minerals, including bauxite, iron, and gold. Guinea's gold production is primarily concentrated in the Upper Niger Basin, particularly at Siguiri, Kouroussa, Kankan, Mandiana, and Dinguiraye which have high gold grades ranging from 5 to 10 g/ton (**Figure I.9**) (Mamedov et al., 2010). Gold is also found in the southern part of the country in N'Zérékoré with grades between 1 and 4 g/ton. The third gold zone, Amamou-Faranah, is located between the Kaba and Mongo rivers, with relatively low grades. The fourth gold zone, Kindia, is along the Méyenkené and Kibesso rivers near Boko. Guinea's gold is of very good quality, ranging from 85 to 98% purity, or 20 to 23.5 carats. Three large mining companies have a monopoly on gold mining in Guinea, two in Siguiri (SMD and SAG) and one in Kourousa (Semafo) (MMG, 2022). However, there are 39 ASGM sites that have been officially studied and documented in the country in 2018, spread across the regions of Siguiri, Kankan, Mandiana, Kouroussa, Dinguiraye, Kindia, and Macenta (MEEF and PAN, 2018). Of these 39 gold mining sites, 9 are located in Kouroussa. The same source reports that in 2016 there were 73 gold mining sites, compared to 291 in 2021, demonstrating the informal and poorly monitored nature of gold mining in the country. The Niger River, which flows through the center of Kouroussa, has perennial tributaries such as the Niandan River on the right bank and the Mafou River on the left bank. Intermittent rivers, including the Saman and Dionko, named after the villages they flow through, also exist in this region.

I.3.2.2. Changes in ASGM sites and gold mining production in Guinea

The evolution of ASGM sites and mining production between 1995 and 2024 in Guinea is closely linked to the price of gold. The following **Figure I.10** was constructed by compiling official national reports published by state institutions and shows the evolution of artisanal and industrial production, as well as the number of gold mining sites in 2016 and 2021 (Levin Sources, 2017; MEEF and PAN, 2018; PROJEG, 2018; MMG, 2019, 2020; FMI, 2021; MEEF, 2021; ASFF, 2022; ITIE, 2022). These figures should be treated with caution, given the informal nature of gold mining. The rise in the price of gold on the London international market in the 2000s coincided with a significant increase in industrial gold production and a rapid expansion in the number of artisanal gold mining sites.

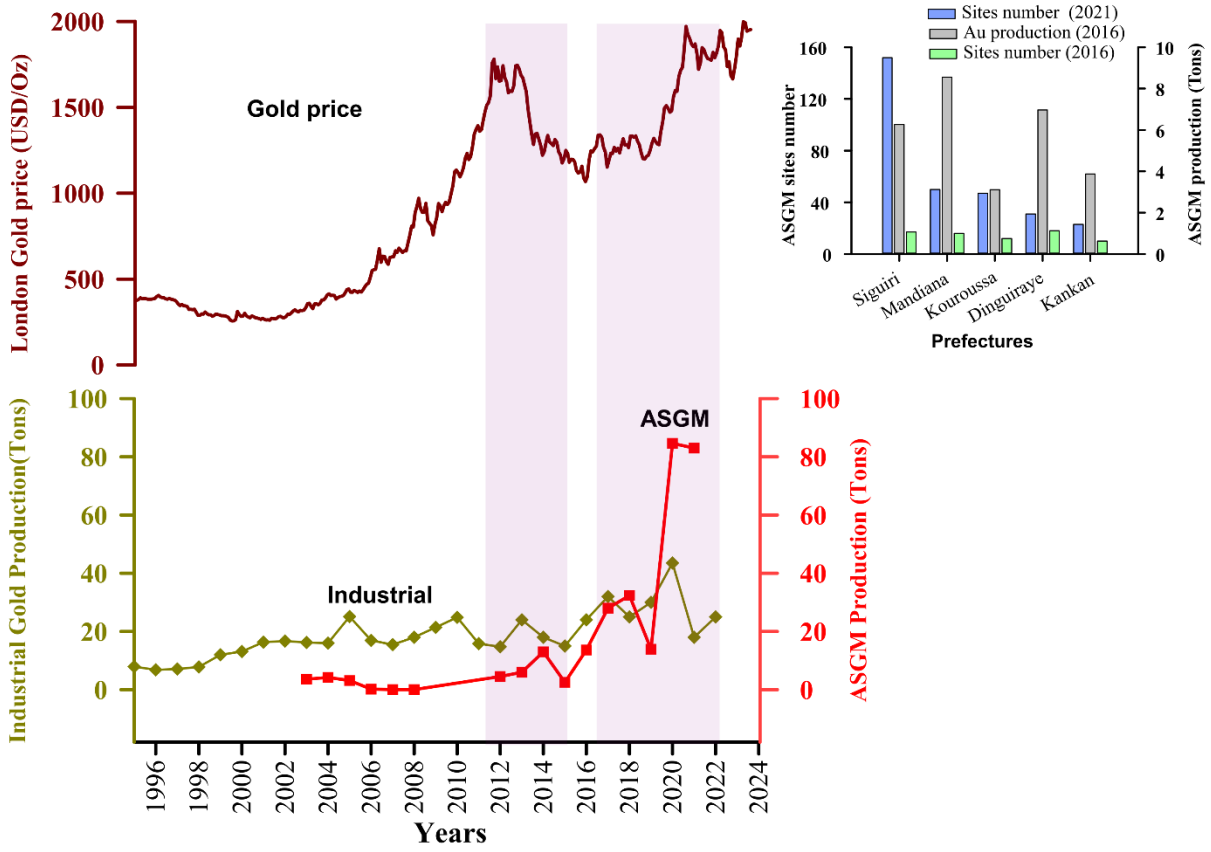


Figure I.10. *Historical and modern trends in gold production in Guinea from 1995 to 2024. Sources: (Levin Sources, 2017; MEEF and PAN, 2018; PROJEG, 2018; MMG, 2019, 2020; FMI, 2021; MEEF, 2021; ASFF, 2022; ITIE, 2022).*

Thus, from 73 gold mining sites in 2013, Guinea has grown to 291 mines in 2021, coinciding with an increase in artisanal gold mining production from less than 20 tons in 2019 to around 80 tons in 2021 (MEEF and PAN, 2018). In 2018, approximately 10 tons of artisanal gold were officially registered at BCRG counters (ITIE-BDO, 2018). With total production estimated at 21 tons in 2016, only 12.5 tons are recorded by the official counter, showing that 40% of production passes through the informal channel (Levin Sources, 2017), making it difficult to quantify revenues in ASGM. Among the five

prefectures, Siguiri has the most gold mining sites in 2021, with production amounting to 6 tons in 2016 (**Figure I.10**). According to a study by ITIE-BDO (2018) the total potential production of artisanal gold in Guinea is estimated at between 10 and 15 tons per year, and between 33 and 66% of the value of ASGM exports is thought to come from informal income. Since 2021, Guinea's gold production, primarily attributed to ASGM, accounted for 74% of total production in 2023, reaching 78 tons, underscoring the significant role of this sector in the country.

I.3.2.3. Description of Guinea study sites

In Guinea, due to insecurity in 2023 caused by the proximity of the site of interest in Siguiri to the Malian border, I was not allowed to access the sites. I therefore shifted the study site to the Kouroussa zone in Upper Guinea, which was more accessible and secure. According to Mamedov et al. (2010), Upper Guinea is a region of Guinea bordered by the Fouta Djallon plateau to the north and northwest, and by Forest Guinea to the south and southeast. Its morphology is flattened, with a gradual descent from 600-650 m in the southwest to 350-400 m in the northeast, following the slope of the Niger River bed. The landscape is cut by gently sloping, shallow valleys of current watercourses. Upper Guinea is a classic savanna that transitions to shrub savanna in the southwest, home to 19.8% of the country's population and the lowest density of any part of Guinea. The total population of Kouroussa is 268,630, with an average population per mining village of 3,720, including 1,336 women, 1,009 men, and 1,375 children. Burkinabè (29%) and Malians (38%) living in Guinea are the main miners practicing cyanidation at the sites we studied (Levin Sources, 2017). In Kouroussa, we studied four gold mining sites in Marsh-April 2023, three of which are concentrated along the Niger River in the Center of Kouroussa, and one in the Sanguiana prefecture, more than 5 km away from the Niger River. All information on characteristics (GPS coordinates, year of creation, number and type of mines, and mining practices can be found in Appendix 1 and **Tableau VI-1**). Four mining sites were studied in the region; i) Bankan (G1), ii) Djaraguela (G2), iii) Saman (G3) and iv) Dionko (G4). In April 2024, another sampling campaign was carried out at the G3 and G4 ASGM sites in Saman and Dionko, respectively. All four mining sites use only amalgamation (Hg), except for the Saman site, which also uses cyanidation. To date, no studies have focused on these four gold mining sites in Kouroussa explaining the very limited information available on these sites.

Located 550 km from Conakry, the artisanal gold mine in Kouroussa, named after the village of Bankan and Djaraguela ASGM sites, were established in 2021. The Saman mining site, named after the village of Saman, was created in 1983 and is home to two rivers, the Saman 1 and Saman 2, which flow until April. According to villagers, these two intermittent rivers dry up in places around May, which was clearly visible during the fieldwork when the drying up of the Saman 2 river was observed in April. The population of this mining site uses water from the river to wash their ore. Average rainfall is 789 mm

per year and average temperatures are 27.6°C. The mining village of Dionko, located in the Sanguiana area of Kouroussa, was created in 1993, and is home to a river called Dionko, which is very intermittent and was dry during the month of April when we visited. All of these mining villages were established following the discovery of gold, and the ore is extracted at the mining sites during four days, but then transported to the villages where it is processed for two days (crushing, grinding, washing) and amalgamated. At the Saman site, cyanidation takes place on the banks of the Niger River, less than 100 meters from the village. Given that there is no structure such as ANEEMAS in Burkina Faso that trains and monitors artisanal miners in order to track developments at mining sites, the number of miners (**Tableau VI-1**.B, appendix1) has been calculated based on the number of pits visible at mining sites (**Figure I.11**.B and **Figure I.11**.C). In Guinea, a system has been set up by the council of elders in each mining village. This is the "tomboloma", which ensures that the rules are applied, marks the boundaries of the mines, marks the points where the pits will be dug, draws up a site development plan, and collects taxes (Lanzano and Arnaldi Di Balme, 2018; Konaté et al., 2025a; Petit-Roulet, 2025). On some sites where tomboloma was not available or did not have information on the number of miners, we estimated the number by counting the pits, considering that each pit consists of four miners plus the team leader, making a total of five (Konaté et al., 2025a). The case of the Saman mining site is shown in **Figure I.11**.B below.



Figure I.11. *Picture on the Saman mining site showing A) crossing the Niger River in a fishing canoe, B) the artisanal mining site at Saman showing the mine shaft and the number of miners (5), C) the mine shafts observed by Satellite at the Saman site, D) the cyanidation site at Saman.*

We counted approximately 105 mine pits on this site using Satellite image (**Figure I.11**.C), which is roughly the same number we counted on the ground (approximately 101, .B, appendix1) during sampling campaigns on site in 2023 and 2024 (**Figure I.11**.B). This system, which preserves the traditional village chieftaincy and the creation of tomboloma, clearly demonstrates the absence of state regulation of these mining sites and the informal nature and extent of gold mining in Upper Guinea.

I.3.3. Sampling strategy and methodological approach

I.3.3.1. Complexity of the field survey: sampling methodology and strategy

From the beginning of the thesis in September 2022, we adopted a collective approach in preparing for the fieldwork. Indeed, as this was a joint thesis between three universities (France, Burkina Faso, and Guinea), and with two campaigns to be conducted in these two countries, in a context of insecurity, a very well-structured methodological approach was essential. As mentioned above, the areas of Poura in Burkina Faso and Siguiri in Guinea, which were the first sites to be studied, were classified in the red (high danger/restricted area) and yellow (increased vigilance/moderate security risk) zones, respectively by the authorities. We therefore turned our attention to the regions of Southwest Burkina Faso and Kouroussa in Guinea. For the sampling mission in Burkina Faso, we contacted an organization that supports artisanal miners called ANEEMAS.

Currently known as SONASP (Société Nationale des Substances Précieuses), ANEEMAS is responsible for environmental monitoring, including the supervision of artisanal miners and the regulation of informal gold trading. With offices in all regions of Burkina Faso, ANEEMAS was constantly informed of the security situation at mining sites. This is how we chose the mining sites in the Southwest in Boromo, Dano, and Gaoua, where ANEEMAS had offices. Before going to the mining sites, the office managers of the various mining sites organize a meeting or gathering with the village chief of the mining site to explain our mission and the reasons for our sampling before the mission. Once the village chief's agreement was obtained, we were able to carry out the mission. Once on site, a second meeting was organized between the scientists and the village chief, who delegated someone to accompany us during the sampling to avoid any conflict with the gold miners, who can be very suspicious of strangers. During this meeting with the village chief and his spokespeople, we give a brief presentation of our study and its scope. This process is carried out for each mining site (five in our case), so five meetings with local stakeholders and village chiefs from these sites were held during the sampling campaign in Burkina Faso in 2022.

In Guinea, the same process was adopted but was slightly more complex, as we needed the Prefect's approval, without which even the village chiefs would not allow us to take samples. Before the field campaign, the IRD helped us organize everything, including vehicle rental. Once in Conakry, the capital of Guinea, we had to travel 571 km, which took two days because all the roads were under construction and in very poor condition. Once in Kouroussa, we went to the prefecture to give a brief presentation on the reason for our visit, the study being conducted, and its importance for the population. We then obtained written agreement from the prefect and sub-prefect to sample the four mining sites (Bankan, Djaragbela, Saman, and Dionko). Once in each village, another meeting was held with the village chiefs of each mining site in order to delegate a native of each village to accompany us during the first days of sampling for reasons of safety and to gain the trust of the miners. All these processes and strategies clearly demonstrate the importance of customs and respect for local actors at each mining site in each country, despite the presence of the government. Specifically, in Kouroussa, which is crossed by the Niger River right through the center, every day we cross the Niger River in fishermen's canoes to reach the mining sites downstream (**Figure I.11**.A).

I.3.3.2. Sampling strategy

I.3.3.2.1. General sample collection

To get a comprehensive view of the environment, the sampling strategy was developed taking into account the entire mining ecosystem, from the mine itself to the associated hydrosystem, and mining villages (**Figure I.12**). Details for the sampling procedure are given in chapters II, III and IV.

Briefly, in all study sites in Burkina Faso and Guinea, water was collected on ASGM sites, including the mine drainage water collected from gold mining pits and the settling basins at mining sites, groundwater was collected in mining villages from wells and boreholes, and surface water samples (filtered and unfiltered) were also collected in all studied rivers. In the Niger river sediment, porewater samples were collected using microporous polymer tube samplers (Rhizon).

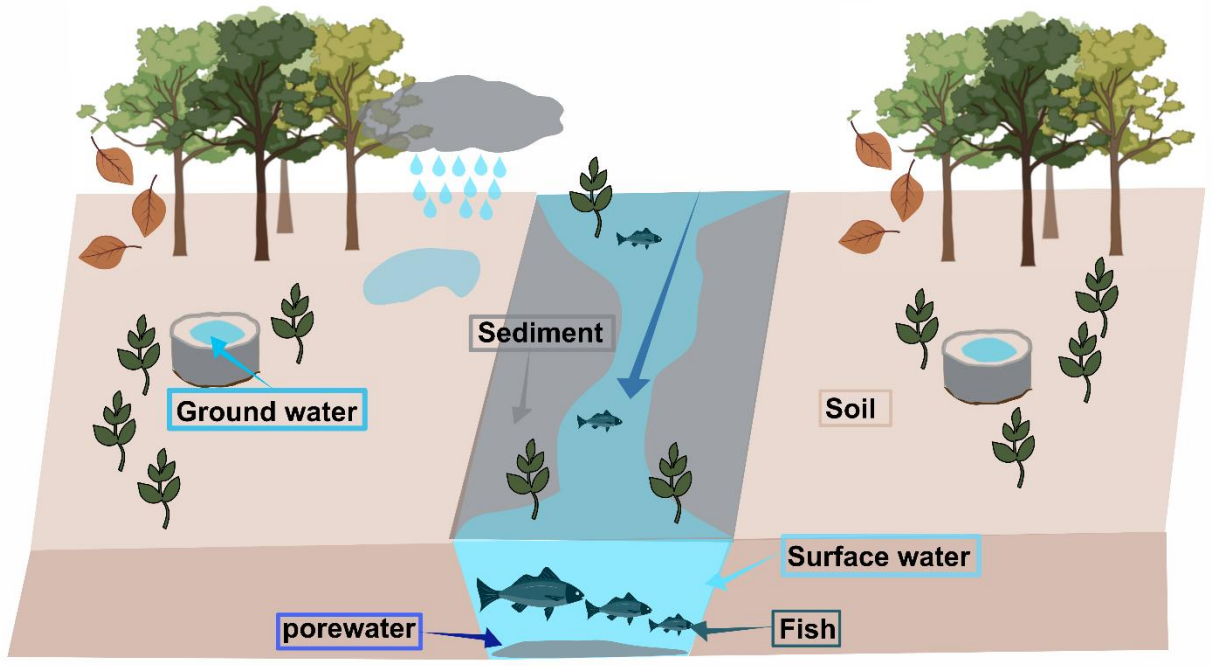


Figure I.12. *Summary of the mining environment compartments sampled during this thesis. Adopted from (Crespo-Lopez et al., 2021; Gerson et al., 2022).*

Consistently, surface soils were collected in each miners' villages, in ASGM sites and in remote pristine areas. Additionally, soil profiles were collected at mining sites using a manual auger. In Rivers, surface sediments and sediment cores were collected from upstream to downstream ASGM sites.

Finally, fish were collected from the Niger River by fishermen.

I.3.3.2.2. Geochemical characterization

As for the sampling strategy, the analytical methodology was implemented uniformly across sites so that data would be comparable between sites and across the entire mining ecosystem (mine, adjacent hydrosystem, and mining villages). The analyses include the physicochemical characterization of solutions and solids, as well as elemental chemistry, speciation, and characterization of Hg carrier phases.

With regard to elemental chemistry, all techniques are detailed in chapters II to VI. Briefly, physicochemical parameters and cyanide in water were measured in the field using a multiparameter probe Hach® and a cyanide kit. Analyses of THg, MeHg, dissolved organic carbon (DOC), major anions, major and trace elements in water were performed in the laboratory using CVAFS (cold vapour atomic fluorescence spectroscopy), NDIR (Non-Dispersive Infrared**)**, ion chromatography, inductively coupled plasma atomic emission spectroscopy (ICP-AES), and Inductively coupled plasma mass spectrometry (ICP-MS), respectively. In solids, THg, MeHg, organic carbon, as well as major and trace elements were analyzed using AAS [atomic adsorption spectroscopy (AMA 254)], GC-CVAFS (Tekran 2700), CRDS [Cavity Ring-Down Spectroscopy (Picarro)], and elemental analysis by ICP methods, respectively.

For the speciation and characterization of Hg carrier phases in solids, particular attention was paid to thermodesorption techniques and selective extractions, which appear to be simple methods to implement in West African laboratories that do not have chemical speciation equipment's. These methods are presented and discussed in the following section.

- **Techniques for Hg speciation and characterization of Hg carrier phases in solids**

Understanding the affinity of Hg for soil and sediment carrier phases is a key information for the determination of its reactivity (i.e., pH, redox, solubility…) and availability for micro-organisms (i.e., methylation, reduction…) and its potential environmental impact when these phases are subject to changes in environmental context. Amongst methodologies used for such determination, the most commonly used are chemical speciation (i.e., selective and sequential extractions) and thermodesorption methods, but other such as synchrotron-based methods are also powerful methods.

The use of thermal desorption (TD) techniques to identify the distribution and/or the speciation of Hg in contaminated soils have been widely used and discussed over the last decades (Reis et al., 2012, 2015; Rumayor et al., 2013, 2015, 2016; Meloni et al., 2024). Thermodesorption consist on the release of Hg from solid samples by increasing temperature, which varies based on bond strength. It has been highlighted as particularly effective in identifying Hg species, though the precision of the method decreases at low concentrations (Ghezzi et al., 2023). TD is a valuable method for identifying Hg species, but it faces challenges in distinguishing between Hg compounds like $HgCl_2$ and Hg bound to organic matter, which have overlapping desorption peaks. A study performed in the Almaden mining district, one of the most Hg-contaminated areas globally, have quantified Hg present as cinnabar (HgS) by TD and shown that this sulfide phase dominated the speciation in this environment. By using TD, Reis et al. (2015) were able to map out desorption temperatures for different Hg species ($HgCl_2$ between 75 and max at 180°C; HgS between 180 and max at 250°C; Hg Fe_2O_3 between 60°C and max at 180°C), contributing to a better understanding of Hg's environmental behavior. The study also shows how Hg binds strongly to various components in soil, such as iron and sulfur. Rumayor et al. (2015) have introduced a modified TD method to identify Hg species in carbon-rich materials, particularly focusing on how Hg interacts with organic matter and other soil components. TD is compared with other speciation techniques like X-ray absorption spectroscopy (EXAFS) and sequential extraction (SE), which have limitations such as high detection limits and contamination risks (Huggins et al., 2003; Bacon and Davidson, 2008). TD, however, remains highly effective for identifying Hg species in complex soil matrices, particularly in low-concentration samples where other methods may fail. These studies have revealed Hg TD gradients that enable specific species to be identified, such as elemental Hg0 desorbing between 70 and 90°C; Hg bound to humic compounds between 146 and 220°C; $HgCl_2$

between 150 and 200°C; $HgFeS_2$ between 90 and 180°C; and HgS between 100 and 300°C. This highlights the overlap between the peaks of the different Hg species, demonstrating the difficulty of accurately determining each species. The use of TD techniques for the determination of Hg speciation in solids presents advantages: low cost, not time consuming, efficient for elemental Hg desorption and organic matter or iron oxides type of carrier phases. It is a reliable and accessible method for Hg speciation, even in low-concentration samples, making it a valuable tool in pollution studies. However, it has limitations due to overlapping peaks, which means it is not specific to each species. This necessitates the use of selective or sequential extractions to determine the species of Hg in each matrix more accurately.

Selective extractions have been used for this purpose by several researchers (Kostka and Luther, 1994; Rodríguez Martín-Doimeadios et al., 2000; Bloom et al., 2003; Guedron et al., 2009; Veiga et al., 2004; Raiswell et al., 2010) to determine Hg bound to organic matter by NH_4OH extraction and Hg bound to poorly crystallized iron oxides by ascorbate extraction. The effectiveness of extracting organic matter with NH_4OH has been demonstrated in tropical Amazonian soils (Guedron et al., 2009). In addition, studies have compared ascorbate extraction and physical methods (i.e., TEM, XRD), and have demonstrated the validity of ascorbate extraction as a selective extractant of amorphous iron oxides. Through TEM and XRD observations, Raiswell et al. (2010) and Guedron et al. (2009) have shown that ascorbic acid at pH 7.5 quantitatively dissolves Fe in fresh ferrihydrite, and that this extraction has little effect on other Fe oxyhydroxide minerals. They also showed that ascorbate did not significantly affect goethite and hematite content in Amazonia soils. One cannot exclude potential dissolution to small extent of metal-SOM complexes, and Fe oxides such as little amounts of goethite and hematite (Reyes and Torrent, 1997; Rennert, 2019). The chemical characterization of selective extraction supernatants (i.e., analysis of major elements by ICP-AES) combined with Hg analyses allows to combine the quantification of Hg bound to selectively dissolved carrier phases.

It is important to note that due to the high selectivity of extractions and TD, these methods must be tested on each matrix studied and cannot be used generically on environmental matrices. These experiments were carried out on the soils and sediments collected in this study, the results have been validated and are presented and discussed in detail in Chapter II. Speciation and characterization of Hg-bearing phases using TD appear to be simple methods to implement in laboratories in the South that do not have chemical speciation equipment.

After reviewing the current state of knowledge on mercury contamination in West Africa, including its sources, forms, pathways of environmental transfer, and impacts, it is therefore important to understand the specific processes that gouvern the transfer and transformation of mercury at the local level.

Chapter II

Transfer and Transformation from Mine Soil to River Sediment: The Potential Role of Amorphous Iron Oxides in Methylation Processes in Southern "Burkina Faso".

This first chapter focuses on the speciation of mercury from artisanal gold mining and the phases carrying Hg in soil and sediments in Burkina Faso. It shows the impact of mining practices on the transfer of contaminants from soil to river sediments and highlights the potential role of amorphous iron oxides in the methylation process and the accumulation of MeHg in these sediments.

This article was published in the journal Environmental Sciences and Processes and is available at https://doi.org/10.1039/D5EM00426H

Article 1. Mercury Transfer and Transformation from Mine Soil to River Sediment: The Potential Role of Amorphous Iron Oxides in Methylation Processes in Southern "Burkina Faso"

D. Dabré*[1, 2], S. Guédron[1], Y. Maïga[2], S. Jelavic[1], S. Campillo[1], J. Fin[1], S. Sentenac[1], O. Bruneel[3, 4], O. Ouédraogo[2], and R. Mason[5].

[1] Univ. Grenoble Alpes, Univ. Savoie Mont Blanc, CNRS, IRD, IFSTTAR, ISTerre, 38000 Grenoble, France

[2] Université Joseph KI-ZERBO, 03 BP 7021 Ouagadougou 03, Laboratoire de Microbiologie et Biotechnologie Microbienne (LAMBM) ; Laboratoire de Biologie et Écologie Animale (LBEA), Burkina Faso

[3] HydroSciences Montpellier, University of Montpellier, CNRS, IRD, Montpellier, France

[4]Univ Nangui Abrogoua, Lab Biotechnol & Microbiol Aliments, 02 BP 801, Abidjan 02, Côte Ivoire

[5] University of Connecticut, 1080 Shennecossett Rd, Groton, CT 06340 USA Dept Chemistry, Dept Marine Sciences, UConn, Storrs, CT

*email: djamilatou.dabre@univ-grenoble-alpes.fr

Highlights:

- Artisanal goldmining in Burkina Faso contaminate soil with mercury (Hg).
- Once eroded into rivers, Hg bound to soil amorphous iron oxides are likely to favour Hg methylation

Environmental Significance Statement

Artisanal and small-scale gold mining (ASGM) is one of the largest contributors to mercury (Hg) pollution in terrestrial and aquatic ecosystems worldwide. The Hg used for gold amalgamation is volatilized into the atmosphere or released into terrestrial ecosystems, where it can be transformed into methylmercury (MeHg) under reducing conditions in river sediment. This toxic molecule accumulates in food webs, ultimately exposing humans. In this work, we emphasize the significance of amorphous iron oxides in the retention of Hg in mine soils of Burkina Faso, and suggest they are prone to methylation once eroded to river sediment. By linking Hg chemical and solid speciation, we demonstrate the importance of this characterization in assessing the availability of Hg for methylation.

Abstract

Since the early 2000s, artisanal and small-scale gold mining (ASGM) has rapidly expanded in Burkina Faso. Mercury (Hg) is widely used to extract gold and its release through burning amalgams has led to soil contamination near mining sites. However, the fate and speciation of Hg in soils remains poorly understood, especially the reactivity or methylation potential of soil particles eroded into rivers. In this study, Hg contamination levels and speciation was assessed in water, soil, and sediment from five ASGM districts along the Mouhoun River. Surface waters near riverside mining sites showed high levels of particulate Hg (11 - 239 ng L^{-1}), while more arid sites showed Hg contamination localised to ore-washing ponds. Mercury thermodesorption and selective extraction analysis revealed that in soils collected in the vicinity of amalgam burning sites, around 10% of total Hg (THg) was elemental (Hg0), with most remaining Hg bound in divalent state to amorphous iron oxides (~60% THg) and organic matter (~ 30% THg). In river sediment, Hg bound to amorphous iron was halved, while methyl Hg (MeHg) levels increased fivefold (0.7 ± 0.2 ng g^{-1}) suggesting that iron reduction in sediment promote MeHg production and accumulation. These results highlight the potential risks of Hg exposure for local communities and the need for regional Hg management in ASGM areas.

Keywords

(Methyl)mercury, speciation, Artisanal and Small-Scale Goldmining, Burkina Faso

II.1. Introduction

Most of artisanal and small-scale goldmining (ASGM) activities are located in the intertropical region, involving between 10 to 19 million miners across Asia, Africa and South America (Esdaile and Chalker, 2018). In comparison to Asia and South America, west Africa has experienced its most extensive gold rush during the last decades. Gold (Au) is typically recovered by crushing Au-ores, washing it to isolate heavy gold particles, and then mixing it with elemental mercury (Hg0) to form an amalgam. Burning of amalgam to extract gold releases mercury (Hg) vapor into the surrounding environment, which exposes miners and their family to Hg related risks (Tomicic et al., 2011; Black et al., 2017). Globally, it is estimated that ASGM is responsible for around 40% of global atmospheric mercury (Hg) emissions (AMAP/UNEP, 2019). Environmental Hg contamination around ASGM sites results from multiple pathways including the direct loss of liquid Hg to soils and rivers, the release of particulate-bound Hg into river, and the deposition of Hg vapor in the environment following the amalgam burning (Grimaldi et al., 2015; Niane et al., 2019b).

Previous studies in West Africa demonstrated high levels of Hg in ASGM topsoils with concentrations up to 410 µg g^{-1} in Ghana (Gyamfi et al., 2021), and 8 µg.g^{-1} in Senegal (Niane et al., 2019b; Gerson et al., 2018; Niane et al., 2014). High levels of Hg in river sediments close to ASGM sites have also been reported, reaching up to 10 µg g^{-1} in Senegal (Niane et al., 2014), 5.4 µg g^{-1} in Tanzania, 2.9 µg g^{-1} in Ghana, and 20.4 µg g^{-1} in Côte d'Ivoire(Kouadio et al., 2025), compared to the geochemical background that is between 0.005 to 0.3 µg g^{-1} (Adjorlolo-Gasokpoh et al., 2012; Donkor et al., 2006; Rajaee et al., 2015a; Van Straaten, 2000). Such elevated Hg concentration in sediment, result from important release of particulate bound Hg from ASGM sites, together with liquid Hg droplets close to the ore washing sites (Niane et al., 2019b). Consistently, elevated Hg levels in unfiltered surface water have been reported surrounding mining areas in Ghana (28.7 to 420 ng L^{-1}), Côte d'Ivoire (6.6 to 53 ng L^{-1}), Senegal (5.8 to 974 ng L^{-1}), and Burkina Faso up to 21 ng L^{-1} (Asare-Donkor and Adimado, 2016; Donkor et al., 2006; Mason et al., 2019; Niane et al., 2019b; Ouédraogo and Amyot, 2013). Once in the aquatic system, inorganic mercury can be converted by microorganisms into methylmercury (MeHg), a toxic compound that bioaccumulates and biomagnifies in the trophic chain (Mason et al., 2019; Gadd, 1993; Mason et al., 1995; Parks et al., 2013).

However, very few studies have examined MeHg levels in West Africa near ASGM sites. Amongst available studies, data indicate high MeHg accumulation in river sediment, with highest concentration of 8.0 ± 7.8 ng g^{-1} in Senegal (Niane et al., 2019b), and between 0.7 and 4.3 ng g^{-1} in Cote d'Ivoire (Mason et al., 2019). These studies indicated that MeHg levels are not related to total Hg concentration, but to sediment geochemical conditions. Consistently, highest MeHg concentrations are reported in suboxic to anoxic river sediments downstream ASGM sites, as well as in ponds and

shallow eutrophicated sites (Mason et al., 2019; Niane et al., 2019b). Hence, the release of Hg from ASGM sites into productive and stratified aquatic ecosystems, promotes the formation of MeHg (Alanoca et al., 2016). It is therefore hypothesised that Hg-rich particles eroded from ASGM sites during mining operations or during the monsoon periods, supply downstream aquatic environments, where methylation occurs.

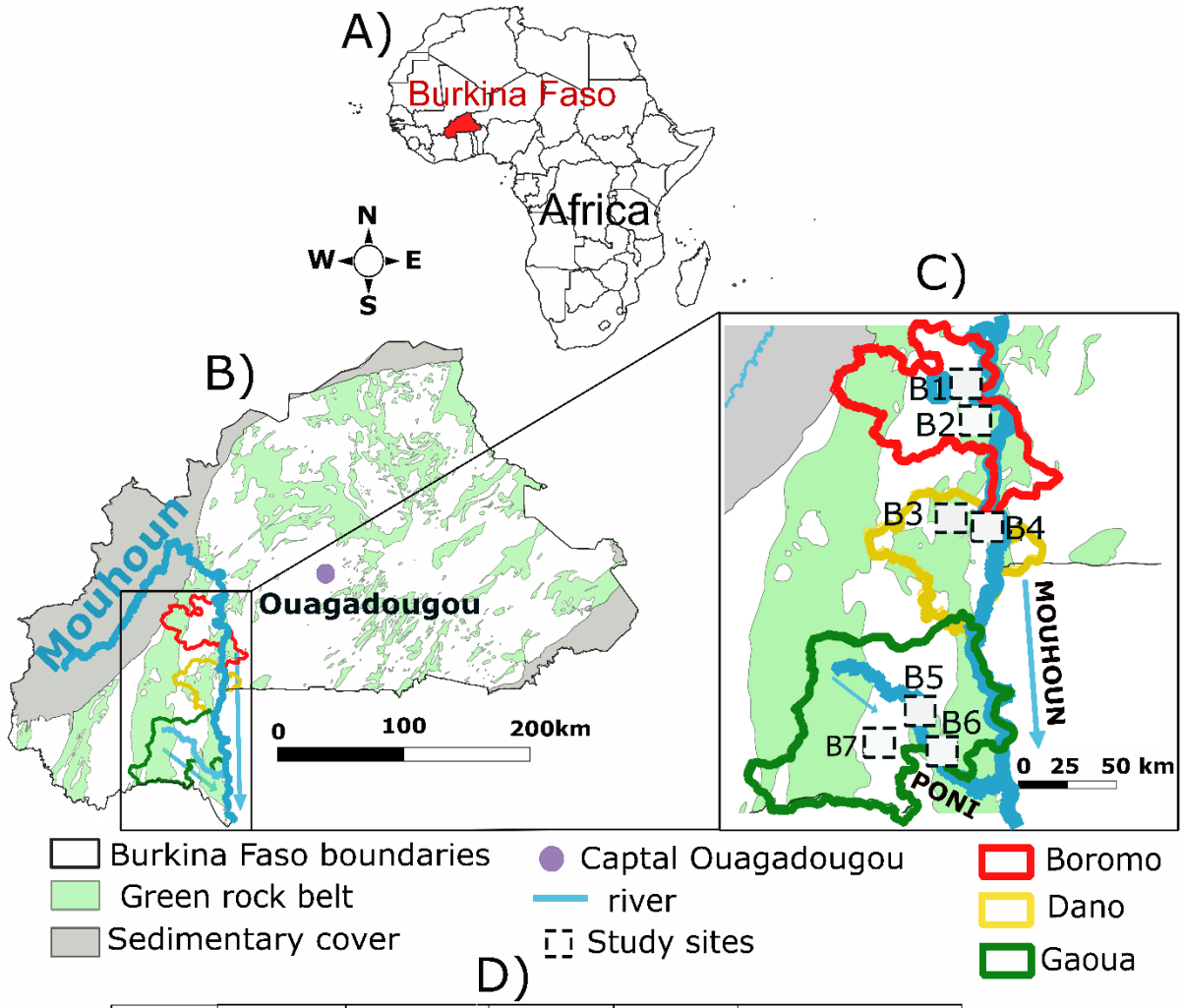
Despite a wide use of Hg in ASGM, little is known about the speciation and fate of Hg in iron-rich tropical soils, which dominate much of West Africa. Once deposited on the soil, Hg can volatilised or complexed with organic matter and minerals, such as iron oxides and clay minerals (Guedron et al., 2009). Understanding the distribution of Hg between soil components is thus key to document the reactivity of Hg carrier phases, which are prone to (bio)reduction and (bio)methylation when deposited in river sediments (Guedron et al., 2011; Guédron et al., 2020). During sediment diagenesis, organic matter degradation and Fe(III)-reduction are driven by microorganisms such as sulfate-reducing bacteria “SRB” , iron-reducing bacteria “FeRB”, and methanogens, some of which carry gene clusters putatively required for Hg methylation, *i.e. hgcA* and *hgcB* (Gilmour et al., 2013; Parks et al., 2013). Other contaminants such as Pb and As can also be mobilised through ASGM operations either from ore dust emission (Nriagu et al., 1996) or pumped groundwater (Bretzler et al., 2017).

In this study, the Hg speciation (i.e., Hg0, THg and MeHg) and distribution in soils and river sediments was analysed across five ASGM sites along the Mouhoun River in southern Burkina Faso. We used thermodesorption experiments with selective extraction, grain size characterization and elemental chemical analysis to trace Hg from mine to river environment. Comparative experiments between selective extraction and Hg thermodesorption experiments were also developed to test the reliability of thermal analysis applied to tropical soil and sediment. Finally, we document the levels of other geogenic contaminants such as As and Pb and examine the potential links between the contamination and site activity and history.

II.2. Material and methods

II.2.1. Environmental settings

Burkina Faso (BF) is located in West Africa, and bordered by Mali, Niger, Benin, Togo, Ghana and Côte d'Ivoire (**Figure II.1**A). Burkina Faso experiences a tropical climate divided into a dry season, from November to May with warmer temperatures (> 40°C) from March to May, and a rainy season from June to October (Fowe et al., 2015). The regional BF geology is dominated by Precambrian rocks, including granites, greenstone belts, and metamorphic formations of the West African Craton (Kirk Woodman et al., 2016; Robertson and Peters, 2016). The greenstone belts are especially rich in gold deposits. Most of informal or small-scale gold mining activities in the country extract ores from these belts by digging. These sites vary in age, size and the numbers of miners involved. After extraction, the ore is milled both manually and using small stone crushers. Milled ores are then washed using either groundwater or surface water, depending on availability, to separate light particles from denser gold-bearing fractions using sluices. Gold particles are then concentrated through amalgamation with liquid Hg. The resulting amalgam is then burnt on site or in nearby houses to extract the gold. While most of these sites rely solely on the Hg-based amalgamation technique, some sites also employ cyanidation using sodium cyanide. Details of the extraction processes are provided in the supplementary information (Fig. S1).



D)

Mining Sites	ASGM type	Miners (indivi-duals)	Creation year	Surface (ha)	Water use in mining process
B1	Hg	~300	2009	6	River
B2	Hg+CN	~1000	2006	24	Groundwater
B3	Hg	~300	2019	100	Groundwater
B4	Hg	~500	1997	100	Groundwater
B5	Hg	~1200	1995	100	River
B6	Hg	N.D	N.D	N.D	Groundwater
B7	Hg	N.D	N.D	N.D	Groundwater

Figure II.1. *Map of the study site with A) The location of Burkina Faso within Africa. B) Geological map of Burkina Faso showing the greenstone belt, the Mouhoun and Poni rivers, and the three studied mining districts: Boromo, Dano and Gaoua. C) Zoomed in excerpt. D) synthetic information for all studied sites about the type of ASGM extraction process (mercury and or cyanidation), the number of miners, year of set-up, surface area at the date of sampling, and source of water used in the mining process.*

II.2.2. Sample collection and conditioning

Sampling was carried out in the south-western part of Burkina Faso during two field campaigns performed in May/June 2018 (sites detailed in Table S1), and the second in November 2022 as a part of the survey led by Agence Nationale d'Encadrement des Exploitations Minières Artisanales et Semi – mécanisés (ANEEMAS). The November 2022 focused on five ASGM sites along the Mouhoun River (**Figure II.1**C) just before the access to these sites was restricted because of terrorist groups activity. The studied area encompasses three main districts: i) the rural district of Boromo, covering the mines of Siby (site B1) and Siggnonghin (B2); ii) the urban district of Dano covering the mining areas of Gnikpière (B3) and Memer (B4); and iii) the urban district of Gaoua including the mines of Djikando (B5), the Quadaradouo (B6), and the neighboring small mines of Bandediera, Banfara and Poniro (B7). To document the environmental impact of these mining activities, surface water (Poni River and a pristine intermittent river at Dano, 3km from the mining sites) and groundwater (wells and boreholes) were sampled at each site and in downstream villages in 2022 campaign. At the same time, physico-chemical parameters (pH, Eh, conductivity, turbidity) were measured using a multiparameter probe Hach® (HQ4300).

Sampling was performed following ultra-trace sampling procedure. At each sampling site, samples were collected in 250 mL FEP Teflon containers, and filtered with 0.45 µm sterivex filters (Millipore). Unfiltered (UNF) and filtered (F) samples for THg and MeHg analyses were transferred to 125mL FEP vials, and acidified with HCl (0.5% v/v, trace grade - Baker). Filtered water samples for major (Fe, Al, S, Mn and P) and trace elements (As, Pb) analyses were stored in trace-grade 15 mL polyethylene falcon tubes, acidified with HNO_3 (2% v/v, trace-grade - Baker). Additional filtered water samples for anion (sulphate, chlorine and phosphate) were stored frozen until analysis. For dissolved organic carbon (DOC) analysis, filtered water samples were collected in pre-burnt (550°C for 3 hours) 20mL amber borosilicate vials, and acidified with HCl (0.1N) following published protocols (Némery et al., 2013). All samples were packed in double bags and stored at 6°C in the dark until analysis.

To assess the Hg levels throughout the Au extraction process, samples of primary rocks, milled ores, waste piles, and solid concentrates remaining after ore washing, were collected in 2018 at the B6 and B7 mining sites. During the 2022 campaign, soils and sediments were collected at the B1 to B5 mining sites. At each site, a composite surface soil sample (0-5cm depth) was collected by pooling 5 sub-samples over ~ 12 m^2 and stored in Whirl pack® sterile bags. These samples were homogenized in the bag and kept at room temperature until returned to the laboratory. Surface river sediments (0-5 cm depth) were collected with a polyethylene shovel from riverbanks, stored in a Whirl pack® sterile bags, homogenized, and kept cool at 4°C until analysis.

II.2.3. Soil and sediment characterization

In the laboratory, soil and sediment samples were freeze-dried, and dry sieved to recover the sand (0.5mm-2mm), and clay + silt (<0.5mm) granulometric fractions. Each fraction was weighed to determine its relative proportion. An aliquot was then ground into a fine powder (<63 µm) for chemical analysis.

X-ray diffraction (XRD) was carried out on the clay + silt fraction, to determine mineral phases using the PROFEX freeware following published protocol (Doebelin and Kleeberg, 2015).

II.2.4. Chemical analyses

II.2.4.1. Elemental analysis

Total Hg concentrations in filtered (THg_F) and unfiltered (THg_{UNF}) water were determined by cold vapor atomic fluorescence spectrometry (CV-AFS) after conversion of all Hg species into Hg0 followed by detection using a Tekran® Model 2500 (Guedron et al., 2011; Guédron et al., 2020). Quality assurance, quality control (QA/QC) was ensured using the certified reference material (ORMS-5), with THg concentrations obtained for repeated analyses (27.1 ± 0.6 ng L^{-1}, N=3) always within the range of certified value (26.2 ± 1.3 ng L^{-1}). Field and analytical blank values for THg were 0.7 ± 0.3 ng L^{-1}, attesting to the absence of contamination during sampling and filtration in the field. The detection limit (DL) defined as 3 times the standard deviation of 10 blanks was 0.04 ng L^{-1}.

Total mercury analysis (THg) in solids (soil and sediment), was performed by atomic absorption spectroscopy (AAS) after pyrolysis at 550°C and gold amalgamation (AMA 254, Altec) with a relative precision of ± 5% determined from triplicates. Concentrations of THg obtained for repeated analyses of certified international reference materials ERM CC 141 [European Commission; 0.078 ± 0.003 µg g^{-1}, (N=7)] and IAEA 158 [International Atomic Energy Agency; 0.123 ± 0.002 µg g^{-1}, (N= 3)] never exceeded the certified range published (i.e., ERM CC 141= 0.083 ± 0.017 µg g^{-1}, and IAEA 158= 0.132 ± 0.014 µg g^{-1}, respectively). THg in mine waste solid samples was analysed by AAS after pyrolysis at 550°C and gold amalgamation using a Nippon DMA-3000, following published procedure (Nugraha et al., 2022). Briefly, ~1 g of sample was digested in 5 mL of *aqua regia* overnight before analysis. QA/QC was ensures using the standard reference material MESS-4 (Marine sediment SRM from NRC; 0.079 ± 0.001 µg g^{-1}), with relative standard deviation (%RSD) below 5%. For waste piles, rock and concentrate, including samples where Hg was added by miners, %RSD was <15%, given the inherent inhomogeneity of these samples.

Methylmercury concentrations in the filtered ($MeHg_F$) and unfiltered ($MeHg_{UNF}$) water samples were analyzed using an ethylation purge and trap gas-chromatograph, cold vapour atomic fluorescence spectroscopy (GC-CVAFS) analysis (Tekran®, model 2700) following published protocols (U.S. Environmental Protection Agency, 1998; Munson et al., 2014; Guédron et al., 2017). The results were

validated by duplicate analysis and quantification using the standard addition technique (Guédron et al., 2014a). Field and analytical blanks values were 0.038 ± 0.004 ng MeHg L^{-1}, attesting to the absence of contamination during field sampling, filtration and laboratory analysis. The detection limit (DL) was 0.01 ng MeHg L^{-1}. MeHg concentrations in soil were determined by the same method after acid digestion following published protocols (Hammerschmidt and Fitzgerald, 2004, 2001). Briefly, a mass of ~2 g was digested with 5 mL KBr (18%), 1 mL $CuSO_4$ 1M and 10 mL DCM (dichloromethane). The 0.5mL of DCM containing MeHg was then diluted in 30 mL milliQ water, and purged with argon for 30 minutes to remove all traces of DCM (Horvat, 1990; Liang et al., 1994). QA/QC was checked with triplicated analysis of reference material ERM CC 580 (74.8 ± 2.4 ng MeHg g^{-1}), which was within the range of certified value (74 ± 4 ng MeHg g^{-1}).

The concentration of major (Al, Ca, Fe, Mg, Mn, S, Ti) and trace (Pb, Cu, Zn, Cd, Cr, As, Se) elements were analysed in filtered water and solids using an ICP-AES (Agilent, Varian 720-ES) and ICP-MS (Agilent, 7900), respectively, after total microwave digestion for solids (ultraWAVE, Milestone) at 250°C as described by Falciani et al. (2000) and Melaku et al. (2005) (Falciani et al., 2000; Melaku et al., 2005). For filtered water, QA/QC was assessed through the analysis of the certified standards SLRS4 and SLRS6. For solids, QA/QC was assessed by the analysis of certified reference materials JSD3, IAEA-405 and BR24 for the sediment samples, and ERM CC 141 for the soils. Accuracies were always within the range of certified value range with a ± 5% margin of error.

The concentrations of major anions (Cl^-, NO_2^- , NO_3^-, PO_4^{3-}, SO_4^{2-}) were determined by ion chromatography (Dionex ICS 2000) controlled by the Chromeleon® chromatographic management system following published protocol (Rutz et al., 2017).

Dissolved organic matter (DOC) was measured using a TOC-VCSN analyzer (Shimadzu®) as described by Tisserand et al. (2022, 2024) (Tisserand et al., 2024, 2022). Precision and recovery rate were better than 5%. Total carbon (TC), total organic carbon (C_{org}) content and isotopic signatures ($\delta^{13}C_{bulk}$ and $\delta^{13}C_{org}$) was performed on the silty-clay fraction, using a Cavity Ring- Down Spectrometry (Picarro, Inc.®) coupled with Combustion Module (Costech, Inc.®) (CM-CRDS) using the analytical method describe in Guédron et al. (2019) (Guédron et al., 2019). QA/QC was performed using a reference material PACS-2 (certified value: $\delta^{13}C$ = -23.07 ± 0.6).

II.2.4.2. Mercury thermodesorption experiments

Mercury thermodesorption experiments on soil and sediment samples were performed, following published protocols (Biester and Scholz, 1997; Windmöller et al., 2017). Briefly, 50 to 100 mg of soil and sediments (depending on the initial Hg concentration) were heated successively in an oven for 48 hours at 80°C for the determination of Hg0 (Meloni et al., 2024), then at 180°C for the determination of Hg bound to organic matter (Hg_{180}), and finally by heating at 550°C for the determination of Hg

bound to refractory phases (Hg_{Res}). The concentration of Hg associated to each of these fraction was then obtained from the difference between THg in the bulk sample and the residue of pyrolysis as previously published (Guedron et al., 2009).

II.2.4.3. Selective extraction experiment

Two selective extractions were carried out on soil and sediment samples to identify and quantify the main Hg-bearing phases. The Hg bound to the organic matter (OM) was extracted by adding 4 mL of NH_4OH (1M) to 40 mg of samples (Rodríguez Martín-Doimeadios et al., 2000; Bloom et al., 2003) under stirring. Extraction of the Hg bound to poorly crystallised Fe(III) oxide minerals and ferrihydrite was carried out by adding ascorbate to approximately 40 mg of sample aliquot stirred at room temperature for 24 hours (Kostka and Luther, 1994; Raiswell et al., 2010). The entire analysis protocol is presented in previous publications (Guedron et al., 2009; Rodríguez Martín-Doimeadios et al., 2000; Veiga et al., 2004). Briefly, experiments were carried out in 15 mL trace grade vials at a solid/liquid ratio of 1:100 (Bloom et al., 2003). At the end of the extraction time, samples were centrifuged (3000 rpm for 20 min), the supernatant was analyzed for major elements, and the solid residue was freeze-dried before Hg analysis. Complementary experiments were also performed to verify that the two selective extractions effectively remove Hg0. The NH_4OH or ascorbate selective extractions were thus performed both before (before T80) and after thermo-desorption at 80°C (after T80).

II.2.5. Statistical analysis

Because geochemical data were not normally distributed, the geochemical dataset reported in this manuscript is presented as the mean, the median and the standard error of the mean (SEM), [Mean (Median) ± SEM], and the number of observations (N) (Webster, 2001). In addition, non-parametric Mann–Whitney rank sum test (U test) and Kruskal–Wallis one-way analysis of variance on ranks (H test) were used to compare two or more than two data sets, respectively. Pearson correlations were applied to compare multiple data set pairs. Correlation coefficient (R^2) and p values (p) are reported. All statistical treatment was performed with R software (R.4.4.1), Sigmaplot and Sigmastat® softwares.

II.3. Results and interpretations

II.3.1. Mercury, arsenic and lead contents in surface and groundwater

Across all studied sites, both surface water (river) and groundwater exhibited close to neutral pH, averaging 7.3 (7.4) ± 0.1 (***Table II-1***). Concentrations of phosphate, nitrate and DOC remained relatively low in river water, indicating limited influence of anthropogenic activities such as domestic wastewater

discharge or agricultural runoff. In contrast, water used for ore processing was slightly more alkaline with an average pH of 8.3 (8.3) ± 0.2 (***Table II-1***).

Groundwaters also exhibited the highest electrical conductivity values, which increased from north to south. The highest conductivity was measured at Gaoua (site B5, up to 900 µS cm^{-1} in groundwater, and 507 µS cm^{-1} in river), the oldest site in the study (active since 1995), which covers a large area (100 ha) and supports a dense mining population of around 1,200 workers. Upstream at Boromo and Dano, although conductivity is lower, high sulfate levels are found in groundwater suggesting the release of sulfate from sulphide minerals oxidation (i.e., pyrite) in groundwater *(Bigham and Nordstrom, 2000; Dos Santos et al., 2016)*.

Total mercury concentrations in filtered water (THg_F) are low, with the lowest values in groundwater (0.1 to 2 ng L^{-1}) and the highest in mining effluents (0.9 to 6.5 ng L^{-1}) and surface water (2 to 8 ng L^{-1}). Highest THg concentrations are found in surface water at Boromo (8 ng L^{-1}) and in mine water from Dano's washing tanks (6.5 ng L^{-1}). Meanwhile, methylmercury represents 11 to 20% of THg in mine water (washing tanks and mine drainage), and 11 to 35% in filtered groundwater. In filtered river water, methylmercury remains below 3% of THg, except in Gaoua, where it exceeds 10%, highlighting a localized increase in methylation processes. Total mercury concentration in unfiltered surface water (THg_{UNF} = between 11.6 and 239 ng L^{-1}) are 4 to 27 times higher than filtered concentrations (between 2.7 and 8.7 ng L^{-1}), and rise with turbidity levels, notably at Boromo (B1, THg_{UNF} = 239 ng L^{-1}, Turb = 459 NTU) and Gaoua (B5, THg_{UNF} = 37 ng L^{-1}, Turb = 152 NTU), where river water is used for ore processing. This highlights that Hg is mainly associated with suspended particles (Fig. S2). In unfiltered river and mine water, methylmercury (MeHg) represents less than 6% of THg, whereas in groundwater, it accounts for 10 to 30%, indicating different partitioning of MeHg between water and particles.

Table II-1. *Physico-chemical parameters and metal(loïdes) concentrations in filtered and unfiltered water at Boromo, Dano and Gaoua districts. * indicate pristine river collected 3 km away from mining Dano site. ° Indicate sites where river water is used for ore processing whereas the others use groundwater. The SEM only appear when there are at least two values. N.D indicate not determined.*

Filtered water									
Sample	District	Site	pH	SO_4^{2-} (mg L^{-1})	DOC (mg L^{-1})	THgF (ng L^{-1})	MeHgF (ng L^{-1})	As (µg L^{-1})	Pb (µg L^{-1})
River	Boromo	B1°	7.2	0.9	4.2	8.7	0.2	1.2	1.0
	Dano*	B3	7.5	0.9	1.4	2.7	0.03	0.4	0.06
	Gaoua	B5° (N=3)	7.2 (7.11) ±0.1	3.7 (2.1) ±1.7	2.2 (2.0) ±0.7	4.6 (2.7) ±2.0	0.6 (0.5) ±0.2	0.5 (0.4) ±0.1	0.06 (0.05) ±0.01
Ground water	Boromo	B2	6.5	3.0	0.3	2.3	0.8	0.2	0.1
	Dano	B3 (N=2)	7.8	1.3 (1.3) ±0.03	0.3 (0.3) ±0.03	1.4 (1.4) ±0.3	0.5 (0.5) ±0.3	5.1 (5.1) ±0.6	0.02
	Dano	B4	7.9	14.1	0.2	0.1	N.D	61	0.06
	Gaoua	B5°	7.4	<DL	0.5	1.2	0.3	1.4	0.03
Water used in mining process	Boromo	B2	8.0	0.8	1.5	0.9	0.1	1.6	0.1
	Dano	B4	8.5	3.0	1.5	6.5	1.3	140	0.1

Unfiltered water						
			Turb (NTU)	Cond (µS cm^{-1})	THg_{UNF} (ng L^{-1})	$MeHg_{UNF}$ (ng L^{-1})
River	Boromo	B1°	454	80	239	0.1
	Dano	B3	57	70	11.6	0.6
	Gaoua	B5° (N=3)	152 (132) ±36	540 (560) ±248	37 (23) ±18	1.2 (1.0) ±0.6
Ground wate	Boromo	B2	14.1	120	N.D	N.D
	Dano	B3 (N=2)	11.1	250	2.4 (2.4) ±0.4	0.7
	Dano	B4	10.8	320	3.0	0.4
	Gaoua	B5°	11.0	940	3.7	0.7
Water used in mining process	Boromo	B2	84	210	16.6	0.4
	Dano	B4	136	260	50.7	0.2

Finally, in ASGM locations where surface water is not available (**Figure II.1**), the pumping of water from geogenically enriched lead (Pb) and arsenic (As) substrates can lead to co-contamination of surface waters. Concentrations in As and Pb in filtered water are low at most sites (Table S2) and with both water types, with average concentrations of 1.6 (0.7) ± 0.7 µg L^{-1}. Only the site of Dano (B4) exhibit high As levels in groundwater reaching **61** µg L^{-1}, which is consistently found in the water used for ore washing (140 µg L^{-1}, Table II-1).

II.3.2. Mercury, arsenic and lead levels in soils and sediments

Total mercury levels in rocks and lateritic soils are low, i.e., from 0.001 to 0.02 µg g^{-1} (Table II-2), and in the range of the geochemical background in pristine environments in Ghana (Akoto et al., 2017). In organic matter poor topsoil (i.e., C_{org} from 0.3 to 1.4 µg g^{-1}, Table 2) with highly humidified OM (C/N = 17 ± 2, Table S5) located over 2 km from ASGM sites, THg concentration were slightly higher, averaging 0.3 (0.3) ± 0.1 µg g^{-1} (Table II-2). These value are close to those reported for pristine soils in western Africa [i.e., < 0.3 µg g^{-1} (Adewumi and Laniyan, 2020)], and fall within the range reported in South American pristine soils [0.01 to 0.49 and 0.9 µg g^{-1} (Guedron et al., 2009; Leiva G. and Morales, 2013)], but higher than the values reported for cropland soil in Burkina Faso [0.03 ± 0.01 µg.g^{-1} (Sako and Nimi, 2018)].

Table II-2. *Concentrations of metal(loïds) in crushed rock, soils, sediments, concentrate, concentrate to which mercury has been added, and waste material for sites in the districts of Boromo, Dano and Gaoua. Concentrations are given in dry weight. N.D indicates not determined, and < DL indicates below detection limits. The SEM only appear when there are at least two values. * indicate all three studied districts (Boromo, Dano and Gaoua).*

Soils, Rocks and sediments								
Type	District	C_{org} (%)	THg in clay & silt (%)	THg in sand (%)	THg ($\mu g\ g^{-1}$)	MeHg ($ng\ g^{-1}$)	As ($\mu g\ g^{-1}$)	Pb ($\mu g\ g^{-1}$)
Green belt rocks	Boromo (N=4)	N.D	N.D	N.D	0.006 (0.002) ±0.005	N.D	<DL	<DL
Soil outside mine	All* (N=3)	0.8 (0.7) ±0.1	66 (68) ±9	34 (32) ±9	0.3 (0.3) ±0.1	0.1 (0.1) ±0.08	47.2 (2.8) ±45.1	11.7 (8.4) ±5.4
Mining soils	Boromo (N=3)	0.3 (0.3) ±0.04	85 (83) ±3	15 (17) ±3	2.3 (0.2) ±2.1	0.04 (0.04) ±0.01	3.4 (1.8) ±1.8	14.8 (8.1) ±6.9
	Dano (N=4)	1.4 (1.5) ±0.2	72 (75) ±6	28 (25) ±6	4.5 (1.5) ±3.5	0.2 (0.1) ±0.1	87 (77) ±44	28 (23) ±10
	Gaoua	0.9	84	16	0.9	0.3	3	5.7
waste pile	Gaoua (N=3)	N.D	N.D	N.D	7.4 (3.1) ±5.5	N.D	N.D	N.D
concentrate	Gaoua (N=2)	N.D	N.D	N.D	2.2 (2.2) ±1.6	N.D	N.D	N.D
concentrate+Hg	Gaoua (N=4)	N.D	N.D	N.D	4147 (2056) ±2725	N.D	N.D	N.D
Sediment (upstream ASGM)	Boromo	0.4	54	46	0.17	0.9	1.9	9
	Dano (N=2)	1.7 (1.7) ±0.1	64 (64) ±20	36 (36) ±20	0.05 (0.05) ±0.01	0.08	4.6 (4.6) ±0.3	8.5 (8.5) ±0.1
	Gaoua	1.2	50	50	0.3	0.8	6.7	13.8
Sediment (ASGM ore leaching area)	Gaoua	1.4	45	55	7.8	1.5	10.6	18.8
Sediment (downstream ASGM)	Gaoua	1.2	40	60	0.1	0.2	5	10

Similarly, THg concentrations in sediments upstream of mining sites are low, between 0.05 and 0.3 $\mu g\ g^{-1}$ consistent with natural background levels. In contrast, THg levels in mining areas are 4.5 to 22 times higher, with the highest concentration found in mine waste and ores concentrates, which exhibit THg

values between 7.4 (3.1) ± 5.5 and 2.2 (2.2) ± 1.6 µg g^{-1}, respectively (Table S1). The most extreme THg concentration is observed in Hg-amalgamated ore concentrates at Gaoua, where THg levels average 4147 (2056) ± 2725 µg g^{-1}. Similarly, THg concentrations in ASGM topsoils vary between 0.9 to 4.5 µg g^{-1}, which is substantially higher compared to reference soils. In contrast, THg levels in river sediment are moderate (0.1 (0.1) ± 0.04 µg g^{-1}, Table II-2), except for the ore washing site at Gaoua, where THg concentration reach up 7.8 µg g^{-1}. The majority of THg in soils is associated to the silty-clay granulometric fraction (75 (83) ± 4% of THg). In sediments, however, the THg is equally represented in the clay+silt fraction (53 (47) ± 7%) compared to sand fraction (47 (53) ± 7%).

Methylmercury (MeHg), concentrations in soils are overall low and range from 0.04 to 0.3 ng g^{-1}, with no significant difference between reference soils and ASGM-impacted soils. MeHg constitutes <0.1% of THg, indicating limited methylation in these environments. In sediments, MeHg percentages at least five times higher compared to soils, with higher MeHg concentrations (0.7 (0.8) ± 0.2 ng g^{-1}) suggesting enhanced MeHg accumulation in sediment. In addition, sediment collected on site with low THg concentration (i.e., Dano, B3-3) had lower proportion of MeHg than those collected downstream ASGM sites.

Lead (Pb) concentrations in soils were low (17.9 (10.1) ± 4.7 µg g^{-1}), falling within the geochemical background range of 4 - 35 µg.g^{-1} as previously reported (Alloway, 1995; Salonen and Korkka-Niemi, 2007; Dos Santos and Alleoni, 2013; Alfaro et al., 2015). Arsenic (As) levels were similarly low (3.3 (2.4) ± 1.3 µg g^{-1}, Table II-2), with the exception of the Dano ASGM site, where concentrations reached up to 87 µg g^{-1}. Consistently, both As and Pb concentrations in sediments were generally low, except at Gaoua ore leaching site, where they reached 10.6 and 18.8 µg g^{-1}. These localized hotspots likely reflect contamination linked to naturally enriched ores and site-specific ore processing activities.

II.3.3. Mercury speciation and carrier phases in soils and sediments

Elemental mercury (Hg0) quantified by thermodesorption at 80°C (**Figure II.2**), averaged 10 (9) ± 3% THg in pristine soils, and increased moderately at ASGM sites (15 (7) ± 6% THg,), with higher levels at Boromo (B1-1 and B2-1) and Dano (B4-1), where Hg0 reached up to 57% THg. In river sediments, although THg concentration were lower than in soils, except at Gaoua ore washing area (B5-3), Hg0 still averaged 8 (8) ±1% THg in pristine sediments, and 12 (11) ± 2% THg for downstream of ASGM sites. To verify that the two selective extractions (NH_4OH or ascorbate) effectively remove Hg0, they were performed both before (before T80) and after thermo-desorption at 80°C (after T80). In all cases, the THg recovered before T80 equalled the sum of the THg recovered by thermodesorption at 80°C plus THg recovered after T80, confirming that both extractants also extracted Hg0 present in soils and sediments (Fig. S3). Hence, in the remainder of the manuscript, reference to NH_4OH extraction

performed after thermodesorption will be referred to as Hg_{OM}, and ascorbate extraction performed after T80 will be referred to as Hg_{amFe}.

Hg_{OM} in pristine soil corresponded to 40 (38) ± 5% of THg, while in ASGM soil it corresponded to 32 (29) ± 4% (**Figure II.2**). In contrast, Hg_{amFe} is more abundant in both cases (59 (58) ± 2%) in pristine soils and ASGM soils (57 (57)± 3%), suggesting that amorphous or weakly crystalline iron oxides such as ferrihydrite likely dominate Hg partitioning in soil (Kostka and Luther, 1994).

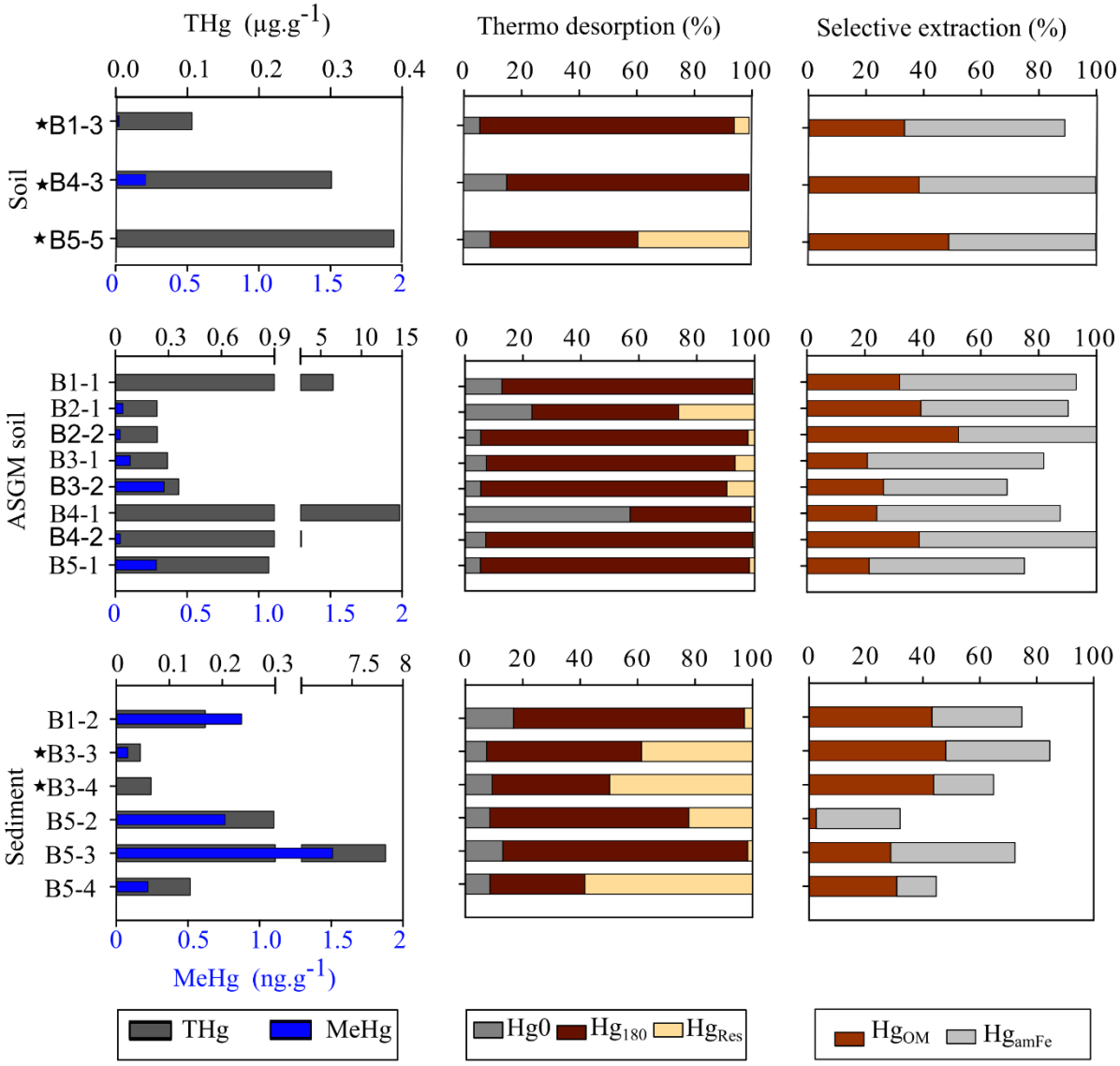


Figure II.2. *From left to right: methylmercury (MeHg) and total mercury (THg) concentrations. Proportions of THg (%) released by thermodesorption at 80°C (Hg0), 180°C (Hg_{180}) and the difference between 180 and 550°C (Hg_{Res}), NH_4OH (Hg_{OM}) or ascorbate (Hg_{amFe}) selective extraction in soil away from ASGM sites (top); ASGM-influenced soil (middle) and river sediment (bottom). Stars indicate pristine environment, i.e., soil samples at Boromo, Dano and Gaoua (Site B1-3, B4-3 and B5-5, respectively) were collected few km downstream the ASGM site, and sediment samples were collected upstream the ASGM site at Dano (sites B3-3 and B3-4). All Gaoua sediment samples (site B5) were collected downstream the ASGM site.*

In river sediment, Hg_{OM} was higher in pristine samples (46 (46) ± 2%THg) than in sediments samples collected downstream from ASGM sites (26 (30) ± 9%). However, Hg_{amFe} remained similar between pristine (29 (29) ±8%THg), and ASGM-influenced sediment (30 (31) ± 6%THg).

II.3.4. Comparison between thermodesorption and selective extractions

Thermodesorption has been used by many authors to identify Hg association with carrier phases in soils and sediments, providing an alternative to laborious sequential chemical extractions (Biester and Scholz, 1997; Guedron et al., 2009; Reis et al., 2012; Rumayor et al., 2013; Reis et al., 2015; Rumayor et al., 2015, 2016). To test its reliability in these tropical soils and sediment, we compared Hg thermo-released at 180°C (Hg_{180}), expected to represent divalent mercury bound to organic matter (Reis et al., 2015; Rumayor et al., 2015), with results from NH_4OH and ascorbate extractions. Thermodesorption at 180°C released 77 (89) ± 13% of THg from pristine and 78 (86) ± 7% THg from ASGM soils (**Figure II.3**).

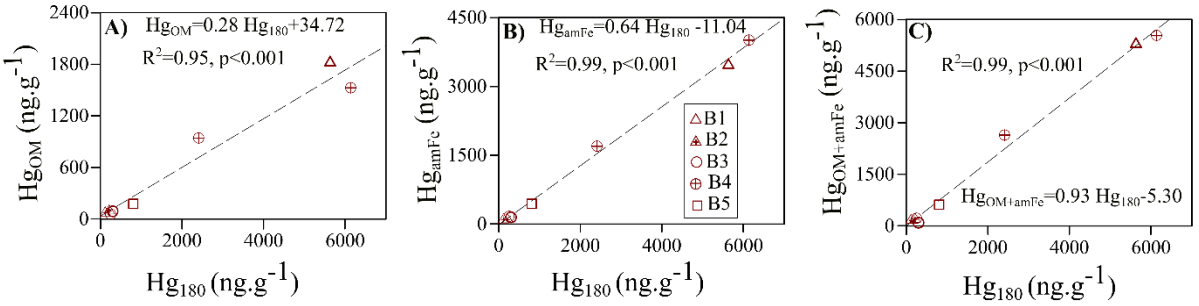


Figure II.3. *ASGM soils. Biplots between Hg released by thermal desorption at 180°C (Hg_{180}) and A) Hg_{OM} (extracted by NH_4OH; B) Hg_{amFe} (extracted by ascorbate), and C) the sum of Hg_{OM} plus Hg_{amFe} ($Hg_{OM+amFe}$).*

Hg_{180} showed a significant correlation with Hg_{OM} (R^2 = 0.95, p<0.01) but the slope of the regression curve (Hg_{OM} = 0.28 Hg_{180} + 34.72) suggests that only ~28% of Hg_{180} is Hg_{OM}, as quantified by the NH_4OH extraction (**Figure II.3**A). In contrast, Hg_{180} correlated more strongly with Hg_{amFe} (R^2 = 0.99, p<0.01, **Figure II.3**B), with a larger regression slope (Hg_{amFe} = 0.64 Hg_{180} -11.04) indicating greater thermal recovery of Fe-bound Hg. Finally, when Hg_{180} is compared to the sum of Hg_{OM} and Hg_{amFe}, the correlation remained high (R^2 = 0.99, p<0.001, **Figure II.3**C) with a near unity slope ((Hg_{OM} + Hg_{amFe}) = 0.93 Hg_{180} - 5.30), suggesting that treatment at 180°C likely captures Hg associated with both OM and amorphous or weakly crystalline Fe oxides. In river sediments, Hg_{180} was lower than in pristine soils, averaging 47 (47) ± 6% in pristine samples and 67 (75) ± 12% in ASGM-influenced ones.

The residual divalent Hg (Hg_{Res}), defined as the difference between thermodesorption at 180 °C and 550 °C, was minor in soils, typically <6%. However, Hg_{Res} increased in river sediments, averaging 44 (44) ± 6% THg in pristine sediments and 23 (16) ± 13% downstream of ASGM sites.

Finally, from an analytic perspective, low-cost thermodesorption approves a valuable tool for analysis of West African tropical soils. Thermodesorption at 80 °C reliably captures Hg0, while thermodesorption at 180 °C reflects Hg associated with both organic matter and amorphous iron oxides. However, distinguishing between those two fractions still requires selective chemical extractions.

II.4. Discussion

II.4.1. Impact of ASGM activities on mercury and arsenic contamination of surface water

Mercury concentrations in filtered groundwater and surface water (THg_F = 5.0 (2.7) ±1.5 .ng L^{-1}) across the three ASGM districts were comparable to background values reported for pristine surface water in BF (5.3±6 ng L^{-1}) (Ouédraogo and Amyot, 2013), and were lower than those reported downstream of ASGM areas in Senegal (5.6 to 34.5 ng L^{-1}) (Niane et al., 2019b). The positive correlation found between THg_F and DOC (R^2=0.74, p<0.05, Fig. S1, Table S4) suggests that dissolved and colloidal Hg is mainly bound to organic ligands (Guédron et al., 2014b, 2015). $MeHg_F$ concentration and contribution to THg_F (below 3%) aligned with observations in other surface waters of BF and Côte d'Ivoire (Mason et al., 2019; Ouédraogo and Amyot, 2013). In groundwater, THg_F and DOC do no show significant correlation (p>0.05) suggesting that Hg is not only bound to organic ligands, but potentially to other inorganic ones (Table S3).

In contrast to filtered fractions, unfiltered surface and mine waters exhibited higher THg_{UNF} concentrations (up to 240 ng L^{-1}). These values were positively correlated with turbidity (0.97, p<0.01), indicating that particulate-bound Hg is the main vector of Hg transport in aquatic systems (Niane et al., 2019b). The highest THg_{UNF} concentration was found at Boromo site (B1), the most recent ASGM site (established in 2009), which has the lowest number of miners. In contrast, THg_{UNF} levels were lower at Gaoua (B5), the oldest ASGM and most intensively mined site (**Figure II.1**), likely because of the easier access to the Poni river, which dilutes the suspended solids and associated contamination. This suggests that local hydrographic conditions, particularly the river type (intermittent/permanent), play a larger role in controlling Hg mobilisation compared to size, age and the intensity of ASGM activities. For example, during the dry season, water levels in intermittent rivers like Boromo drop, resulting in minimal direct input of contaminated waters directly into surface waters.

In sites where river is not accessible, miners rely on groundwater to wash ores. This practice supplies As-rich water to the surface, especially when geogenic As levels in groundwater are high. The green stone belt of BF contains sulfidic minerals such as pyrite and arsenopyrite, which are known sources of high concentrations of arsenic (Verma and Chaurasia, 2024). Elevated As levels in groundwater have been reported across the country, ranging from 0.2 - 140 µg L^{-1} (Bretzler et al., 2017; Somé et al., 2012; Nzihou et al., 2013). A notable case is Dano, where As concentration in wells used for drinking water

exceeded the WHO guidelines of 10 µg L^{-1} (World Health Organization, 2017), posing a potential public health risk (Naujokas et al., 2013; Nzihou et al., 2013). Groundwater samples from Dano revealed high As concentration (60 µg L^{-1}) along with high sulfate concentrations (14 mg L^{-1}), supporting that the oxidation of sulfidic minerals is the likely sources of As in this region.

II.4.2. Partitioning of mercury species onto soil carrier phases in ASGM context.

Mercury concentration in topsoils from ASGM sites (0.9 to 4.5 µg g^{-1}) were 3 to 15 times higher than those measured in non- ASGM sites (0.3 (0.3) ± 0.1 µg g^{-1}), which had similar levels to background levels reported for tropical soils in South Africa [0.075 to 0.15 µg g^{-1} (McNab et al., 1997)], West Africa [<DL to 0.19 µg g^{-1} (Rajaee et al., 2015a)], New Zealand [(0.018 to 0.339 µg g^{-1} (Martin et al., 2017)], Amazonia [0.01 to 0.9 µg g^{-1} (Guedron et al., 2009; Leiva G. and Morales, 2013)], and Australia [0.68 µg g^{-1} (MacSween and Edwards, 2021)]. Elemental mercury at (T80) in pristine topsoils (10 (9) ± 3% THg) are virtually the same as in ASGM soil (9 (7) ± 2%, without sample B4-1). This shows that all the soils collected in this study contain at least ~ 10% of Hg in the form of thermally unstable Hg reported to be represented mainly by Hg0, and small proportions of Hg chlorides (Biester and Scholz, 1997; Martínez-Cortizas et al., 1999).The high amounts of Hg0 in ASGM topsoils (**Figure II.2**), in particular at Dano, suggests its deposition after condensation near amalgam burning sites (Niane et al., 2019b). Under BF's dry and warm climate, this accumulated Hg0 might be re-emitted into the atmosphere (Gustin et al., 2003), making these topsoils long term sources of atmospheric Hg0. Unfortunately, the limited number of collected topsoil samples in Hg0 contaminated sites, such as Dano, do not allow for the modelling of Hg0 re-emissions, which will need to be quantified in future research. In parallel, the presence of elemental mercury in river sediment downstream from mining sites (~10%, **Figure II.2**), also suggests transport of Hg0 from topsoils to river during the wet season when erosion is most important.

In both pristine and ASGM soils, divalent Hg is mainly bound to amorphous or weakly crystalline Fe oxides (58 ± 3% THg), highlighting their major role in Hg retention (Avotins and Sciences, 1975; Guedron et al., 2009; Tiffreau et al., 1995). Amorphous oxides are known for their high metal sorption capacity, particularly due to the significant contribution of intraparticle diffusion, and site densities as much as 3 orders of magnitude greater for amorphous iron oxide than for goethite (Fan et al., 2005; Trivedi and Axe, 2001). This is further supported by the low proportion of Fe and Al extracted with ascorbate (<2% of total soil Fe or Al; Table S5-S6). Although ascorbate extraction has been reported to be highly selective and specific for amorphous oxides (Kostka and Luther, 1994; Raiswell et al., 2010; Reyes and Torrent, 1997), the potential dissolution to small extent of metal-SOM complexes, and Fe oxides such as little amounts of goethite and hematite cannot be excluded(Rennert, 2019; Reyes and Torrent, 1997). In contrast with Amazonian soil, where divalent Hg is mainly associated with OM (Guedron et al., 2009; Grimaldi et al., 2015), the BF soils exhibit a lower Hg-OM association (Hg_{OM} = 34

(33) ± 3%THg). Furthermore, a positive correlation between Hg_{OM} and total sulfur content in soils (R^2 = 0.74, p<0.05, **Figure II.4**A) suggests that Hg is complexed with sulfur-containing functional groups in OM, which is consistent with the observations in Amazonian soils (Guedron et al., 2009). The agreement between Hg levels measured with thermo-desorption at 180°C and the combined sum of Hg_{OM} and Hg_{amFe} likely indicates that the divalent Hg is associated with both OM and amorphous or weakly crystalline Fe oxides (Reis et al., 2015), such as organic coatings on Fe/Al oxides, which have been described in the Amazonian region (Guedron et al., 2009; Meloni et al., 2024; Rumayor et al., 2015).

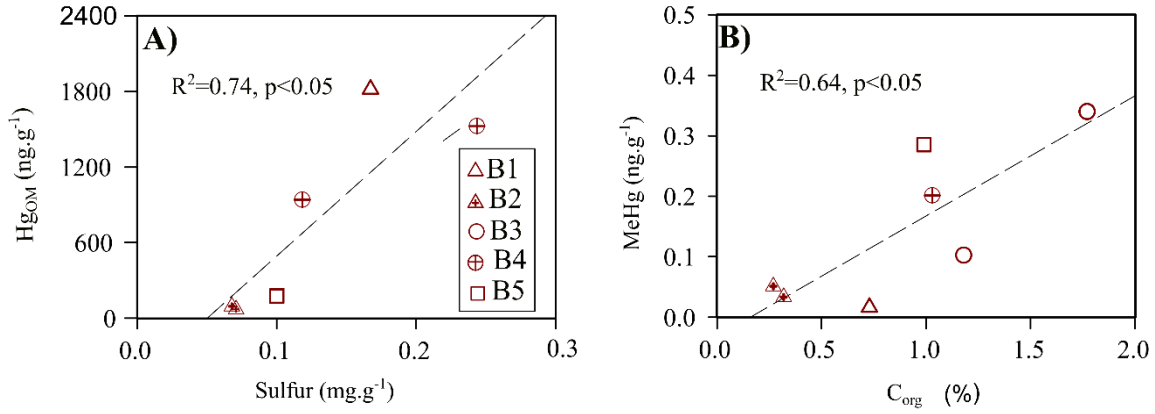


Figure II.4. *ASGM soil. Biplots between A) Hg_{OM} (extracted with NH_4OH) and total sulfur, B) MeHg concentration versus organic carbon (C_{org}).*

Although the proportion of MeHg in soil were low (<0.1% HgT), a significant correlation with organic matter (R^2=0.67; p<0.05, Fig. S4B) suggests that OM controls the MeHg accumulation in soils, consistent with earlier studies (Roulet, 2001). Yet, the data on MeHg in tropical African soils remain scarce. The concentrations found in BF soils (0.13 (0.08) ± 0.04 ng g^{-1}) fall at the lower end of the range reported for Amazonian soil and litter [<1 ng g^{-1} (Fostier et al., 2023)]. Such low MeHg levels likely reflect limited atmospheric MeHg input via throughfall and litterfall (Guedron et al., 2011; Gerson et al., 2022), or unfavorable geochemical conditions for *in-situ* methylation in arid conditions (Ikingura and Akagi, 2003).

Although crystalline Fe oxides (goethite and hematite), and kaolinite account for about a quarter (25 (24) ± 9%, Fig. S4) of the soil composition, the high proportion of Hg associated with amorphous iron oxides suggests that these crystalline iron oxides and clay minerals play a secondary role in Hg retention, in line with observations from Amazonian soils (Guedron et al., 2009). The remaining divalent Hg fraction (Hg_{Res} = THg- Hg_{180} – Hg0) correlated with Al concentrations (R^2 = 0.66, p<0.05, Fig. S2). This suggests that HgRes is likely associated with aluminosilicates consistent with the silicate-rich soils composed mainly of quartz (40–80%) and kaolinite (5–30%), with minor amounts of minerals such as goethite, hematite, mica and others (Fig. S4)

II.4.3. Fate of Hg carrier phases and implication on MeHg accumulation in river sediment

Hg in ASGM soils is primarily associated with silt and clay size particles (Table S5), and these fractions are the most susceptible to erosion and downstream transport during the rainy season. Once deposited in river sediments, amorphous and weakly-crystallized iron oxides – enriched in the clay fraction because of their small particle size, rapidly dissolve in reducing environments or get recycled by sediment microorganisms during early diagenesis (Bravo et al., 2015; Niane et al., 2019b). This transformation enhances Hg availability for methylating organisms. Consistently, the proportion of Hg bound to amorphous or weakly crystalline oxides in sediment is at least twice as low compared to soil (all detailed in Table S7). This difference is offset by a five-fold increase in Hg associated with undefined mineral phases in the residual fraction (Hg_{Res} = 30 (30) ± 9% THg vs. Hg_{Res} = 9 (3) ± 4% THg in soil). Meanwhile, Hg associated with OM in sediment (Hg_{OM} = 33 (37) ± 7% THg) remains similar to soil values (Hg_{OM} = 34 (33) ± 3% THg). Thus, the decline in Hg_{amFe} without rise in Hg_{OM}, offset by the rise in Hg_{Res} suggests Hg released from the dissolution of amorphous iron oxides in anoxic conditions has been recycled onto diagenetically neoformed minerals (Guédron et al., 2020; Muresan et al., 2008).

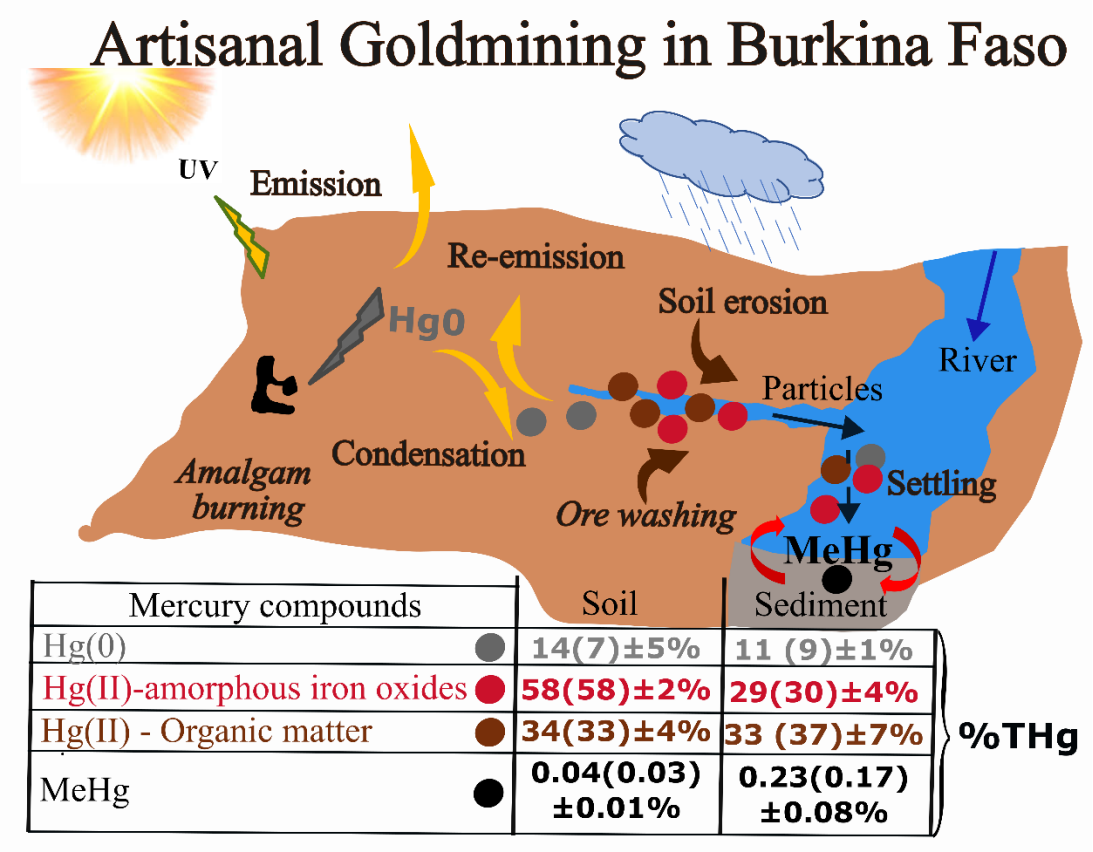


Figure II.5. Synthesis figure showing the environmental processes involved in gold mining and the percentages of different mercury compounds in soils and sediments downstream of mining sites in Burkina Faso.

The percentage of MeHg in river sediments (0.23 (0.17) ± 0.08 % THg) is at least five times higher compared to soils (0.04 (0.03) ± 0.01 % THg) suggesting enhanced MeHg production and accumulation in river sediment (Niane et al., 2019b). It is therefore likely that some Hg released during sediment amorphous Fe oxides dissolution has becomes available for methylating microorganism (Bravo et al., 2015; Hellal et al., 2015). Although the presence of Hg associated with amorphous iron oxides is known to promote methylation(Bravo et al., 2015; Jackson, 1989), (de)methylation rates in sediment are directly influenced by Hg biochemical availability, as well as by a large number of environmental variables, including biological and nutrient availability, pH, temperature, redox potential (i.e., anaerobic conditions), and the presence of inorganic and organic (e.g., inhibition due to sulphide formation) complexing agents (Ullrich et al., 2001; Benoit et al., 2001; Lambertsson and Nilsson, 2006; Bouchet et al., 2018). All these environmental factors strongly influenced metabolic activities of specific methylating microbial activity (Parks et al., 2013), such as sulfate (SRB) and iron-reducing (IRB) bacteria (Gilmour et al., 2013; Hellal et al., 2015; Yu et al., 2012; Si et al., 2015). Interestingly, MeHg percentages in sediments decreased as C_{org} increased (R^2=0.82, p<0.05, Fig. S5) suggesting that Hg associated with OM is less bioavailable to methylating organisms compared to Hg associated with reactive iron oxides (Bravo et al., 2015; Guédron et al., 2020). In parallel, no significant correlation is found between THg and MeHg concentrations in sediment indicating that MeHg accumulation is independent from the amount of THg, but rather depends on the reactivity and type of Hg carrier phases (Guedron et al., 2011; Guédron et al., 2020), the geochemical condition (e.g., redox) (Mason et al., 2019; Niane et al., 2019b), as well as the type of microorganisms (e.g., SRB and IRB) present in the system that carry gene clusters putatively required for Hg methylation (Parks et al., 2013; Gilmour et al., 2013). In addition, even at highly contaminated sites, such as Gaoua sediment downstream of the ore washing area (THg = 7.8 µg g^{-1}), MeHg remains low. This likely results from the predominance of Hg in forms such as Hg0 (Hg0 = 13% THg) which are potentially less available for microbial methylation.

II.5. Conclusion

This study highlights that the recent expansion of artisanal and small-scale gold mining (ASGM) activities in Burkina Faso has a major impact on the Hg contamination in soils, especially near amalgam burning sites. The magnitude and the extent of contamination are closely related to local mining practices and environmental context (access to river or groundwater for ore washing, and location of amalgam burning sites), rather than to the size or age of the ASGM sites and the number of miners.

River sediment contamination results from high particulate Hg release to rivers in areas where ore is processed directly on river banks. In contrast, groundwater-based ore processing limits downstream contamination, but increase the risk of arsenic mobilisation from bedrocks.

In ASGM soils, Hg0 accounts for approximately 15% of THg, and up to 57% in amalgamation areas. Divalent Hg is mostly bound to amorphous iron oxides (~60%) and organic matter (~30%). In contrast, in river sediments, amorphous iron oxides-bound Hg decreased sharply by five-fold, and methylmercury (MeHg) concentrations increase proportionally. Our findings suggest that once associated with amorphous iron oxides, Hg is likely more bioavailable to methylation in river sediment. By contrast, Hg associated with OM appears less bioavailable for methylating organisms.

Future research should focus on the fate of elemental Hg in soils, including volatilization rates, quantify exposure risks for nearby populations and miner community, and investigate microbial communities responsible for MeHg production in river sediments. Experiments using isotopically enriched Hg adsorbed onto carrier phases such as amorphous Fe oxides could determine the conditions under which Hg becomes bioavailable and methylated, and how OM enhances or impedes Hg bioavailability.

CRediT authorship contribution statement

D. Dabre: Conceptualization, Data curation, Formal analysis, Investigation, Methodology, Validation, Writing - original draft, Writing – review & editing. S. Guédron: Conceptualization, Data curation, Formal analysis, Methodology, Resources, Supervision, Validation, Writing - original draft, Writing – review & editing. Y.Maiga: Methodology, Supervision, Writing – review & editing. S. Jelavic: Data curation, Methodology, Validation, review & editing. S. Campillo: Data curation, Formal analysis & Methodology. J. Fin: Data curation, Formal analysis & Methodologie. S. Sentenac: Data curation, Formal analysis & Methodology. O. Bruneel: Methodology, Supervision, Writing – review & editing. O. Ouedraogo: Methodology, Supervision, Writing – review & editing. R. Mason: Data curation, Formal analysis, Methodology, Supervision, Writing – review & editing.

Conflicts of interest statement

There are no conflicts to declare.

Data availability

The data supporting this article have been included as part of the Supplementary Information.

Acknowledgments

This research is the product of a joint project between the University Joseph KI-ZERBO (Ouagadougou, Burkina Faso), and the French National Research Institute for Sustainable Development (IRD, France). This publication was made possible through support provided by the African centers of excellence (ACE Partner - IRD and AFD) and by a grant from LabEx
OSUG@2020 (Investissements d'avenir – ANR10 LABX56). We thank the ANEEMAS (Agence Nationale d'Encadrement des Exploitations Minières Artisanales et Semi – mécanisés) in the Burkina Faso for having authorized and supported this research, as well as the IRD Representation in Burkina Faso for their collaboration with the Project. We would like to thank Jacques Gardon of Hydrosciences Montpellier for his guidance and advice, and Bruno Lanson of the Institut des Sciences de la Terre for his help with the mineralogical analysis of our samples. Our sincere thanks go to Pr A.S.Ouattara, the recently deceased director of the host laboratory at the Université Joseph kI-ZERBO, who provided us with the space needed to condition our samples. We also thank Dr Benjamin Sawadogo from IRD Burkina, Pr Koussoubé Youssouf, Dr Cheick Omar Tidiane Compaoré and Palé Dagoro from University Joseph KI-ZERBO, who gave us moral support during sampling campaigns in recognized Jahadist danger zones.

II.6. Supplementary information



Figure. S1. *Photographs of ASGM process and artisanal mining sites in southwest Burkina Faso (Credit D. Dabre) with A) ores extraction from pits; B) ores crushing; C) ores mechanical grinding into powder; D) ore powder panning; E) gold separation from ore powder on sluices; F) gold amalgamation with Hg; G) ore powder cyanidation process in artisanal cyanidation basins; H) waste piles; I) Burkina-Faso South-west ASGM site; and J) mining pond used for ore washing at Dano site.*

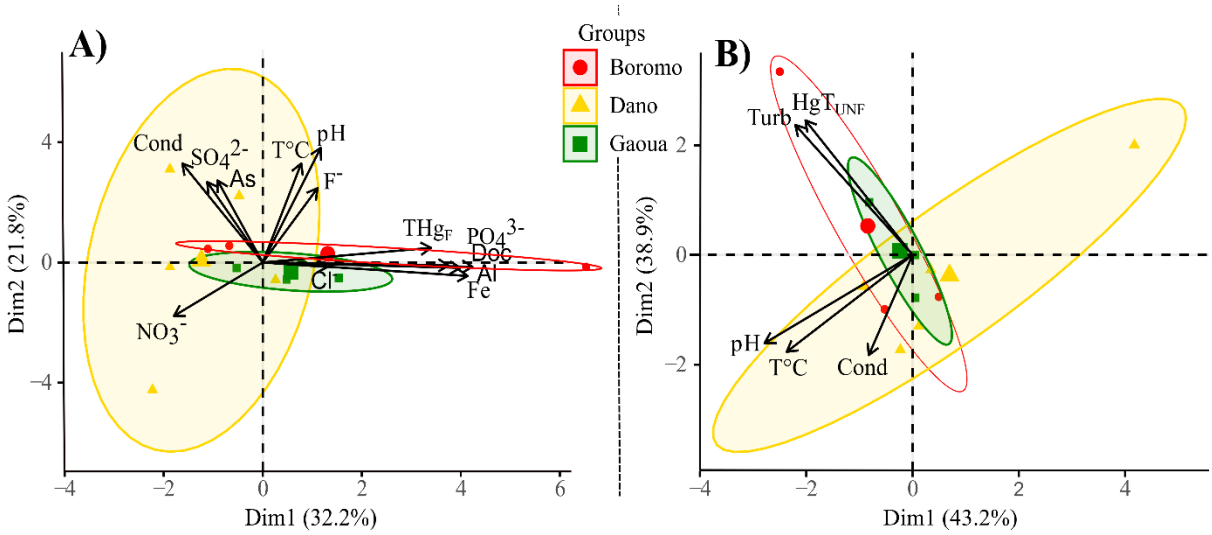


Figure. S2*. Principal component analysis (PCA) for A) filtered and B) unfiltered water. The PCA analysis for filtered surface water (A) shows that water from collected at Boromo, Dano and Gaoua share a similar distribution pattern for the studied elements although elemental concentrations are different. The first principal component (32.2%, Fig. S2A) has high positive loadings on THg_F, dissolved organic carbon (DOC), phosphates (PO_4^{3-}), aluminium (Al), and iron (Fe), which supports dissolved OM and Fe or Al colloids as the main carriers for Hg(Alanoca et al., 2016). The second principal component (21.8%) has high positive loadings on conductivity (Cond), sulphate (SO_4^{2-}), and arsenic (As), which suggest that As is likely geogenic, and originates from the dissolution of sulphides (Smith et al., 2021). The PCA analysis for unfiltered surface water (B) shows that the suspended particles in aquatic hydrosystems downstream mining sites are the main carrier for Hg. Indeed, the second principal component (38.9%) has high positive loadings on turbidity (Turb), and THg_{UNF}.*

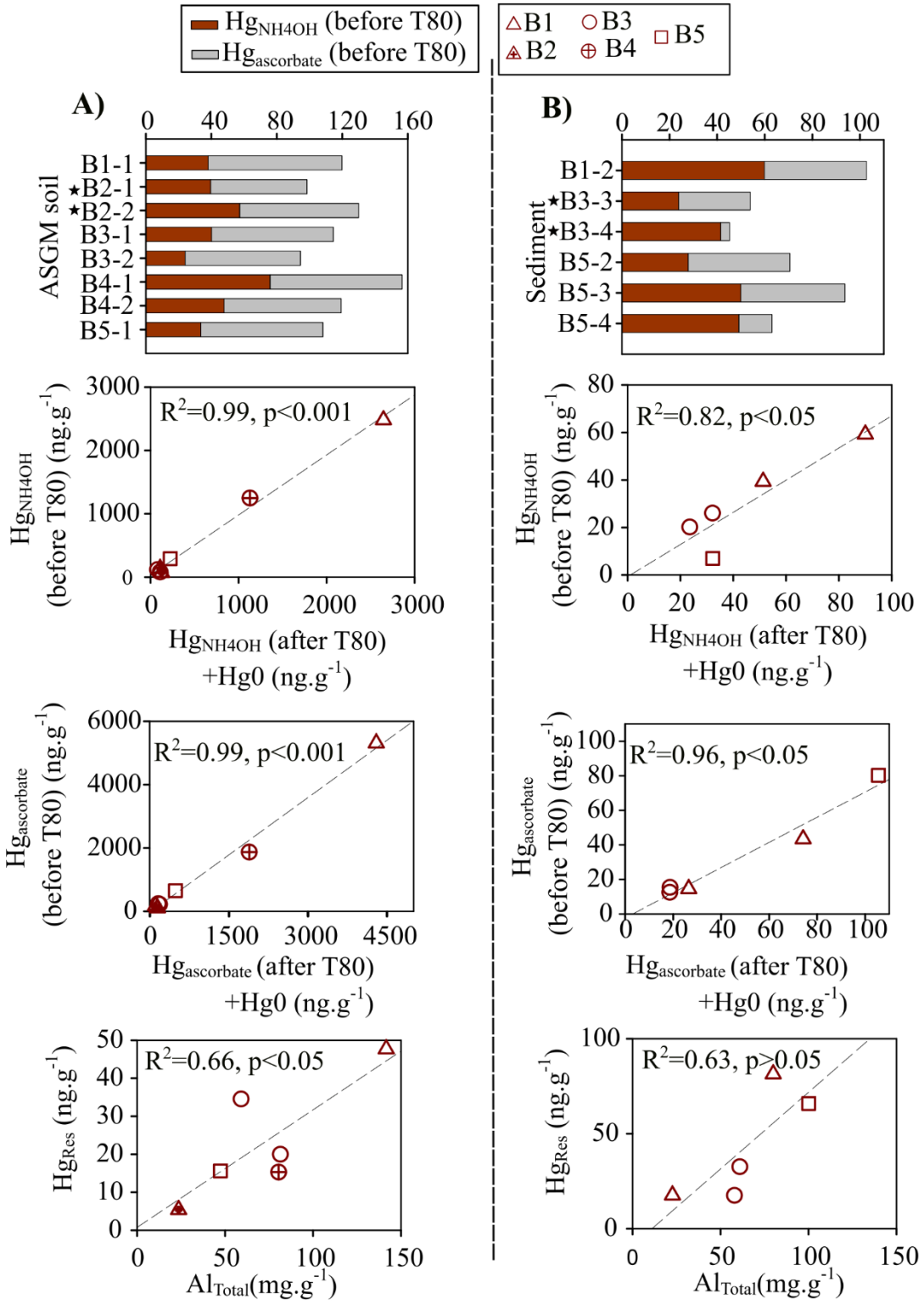


Figure.S3. *Biplots showing NH_4OH (second panels) and ascorbate (third panels) selective extractions before thermodesoption at 80°C (T80) versus the same extraction performed after T80 plus elemental mercury (Hg0) measured at T80 in a) soil (left panels) and b) sediment (right panels). The strong correlation and slope close to 1, show that both the NH_4OH and ascorbate selective extractions extract Hg0 contained in the sample. This is well illustrated by the overlap between the two extractions (Guedron et al., 2009), whose pooling before Hg0 extraction exceeds 100% (Top panels).*

Bottom panels show the biplot between residual Hg (Hg_{Res}), obtained by difference between Hg released at 550°C minus the one released at 180°C, and aluminium (Al) a) soil (left panels) and b) sediment (right panels). This correlation supports aluminosilicates (likely kaolinite) as the main carrier for residual Hg (in addition to Hg_{OM} and Hg_{amFe}).

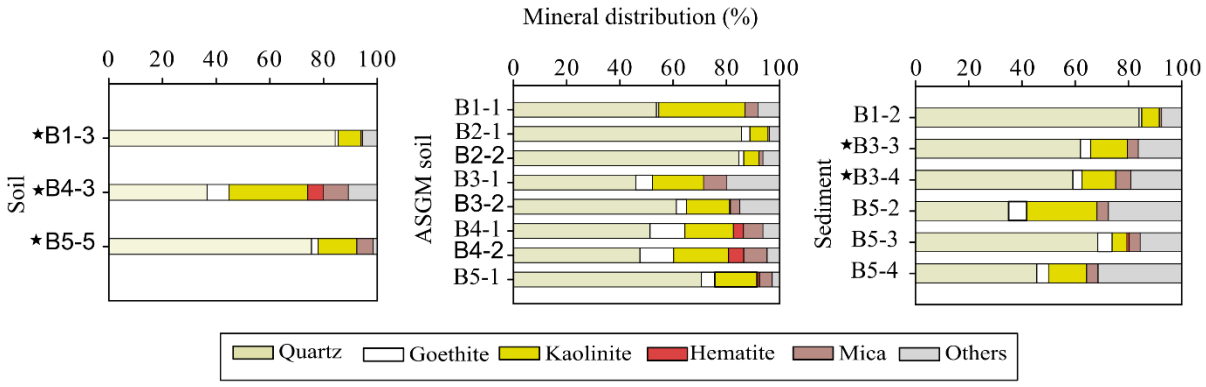


Figure.S4. *Mineralogical background. XRD analysis shows that soil mineral composition across the three regions is dominated by quartz (63 (65) ± 5%) and kaolinite (17 (16) ± 3%), with smaller amounts of goethite (5 (4) ± 1%), haematite (3 (4) ± 1%) and dioctahedral mica (likely muscovite, 5 (5) ± 1 %). Pristine river sediment, as well as sediment collected downstream of ASGM sites, have a comparable composition, with primarily quartz (61 (61) ± 1%) and kaolinite (13 (13) ± 1%), with some goethite (4 (4) ± 0.2 %) and dioctahedral mica (5 (5) ± 1 %). Other minerals such as clays are found in high quantities in sediments, demonstrating the hydrous transport of fine particles to aquatic hydrosystems.*

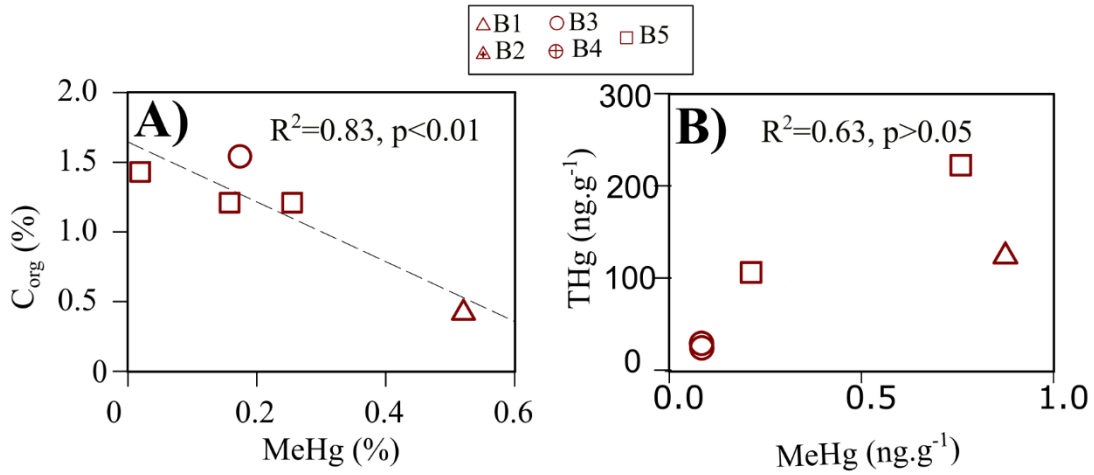


Figure. S5. *A) Biplots showing relationship between percentage MeHg (%THg) versus organic carbon (C_{org}) (R^2= 0.83, p<0.01). B) Biplots showing relationship between MeHg versus THg concentration (R^2= 0.63, p> 0.05).*

Table S1*: Concentrations of total mercury (THg) in crushed rock, concentrate, concentrate with mercury added, waste piles from mining locations (A); in sediment and suspended particulate , Water quality parameters for the water bodies (B), sampled in the study in the north and south-west of Burkina Faso in 2018.*

A) Location 1	Sample Type	THg (µg g^{-1})
Kayara	Crushed Rock	0.09
	Concentrate	2.37
	Conc.+Hg	284 ± 12
	Waste Pile	13.8 ± 1.9
Radago	Crushed Rock	0.45
	Concentrate	0.13
	Conc.+Hg	39 ± 5
	Waste Pile	0.61
	Cyanide Waste	0.77
Banfara	Crushed Rock	2.79
	Concentrate	3.79 ± 0.54
	Conc+Hg	518 ± 15
Quadara-douo	Waste Pile	18.35 ± 0.40
	Waste Pile #2	3.06 ± 0.08
	Waste Pile #3	0.94
	Conc+Hg #1	3509 ± 128
	Conc+Hg #2	12044 ± 877

B) Location 2	Sample Type	THg (µg g^{-1})	pH	DO (mg L^{-1})	Redox (mv)
Koidi Dam	Sediment	0.6± 0.3			
	Part. Hg	0.56			
	Water		7.6	3.78	229
Nakambe River	Sediment	3.9 ± 0.7			
	Part. Hg	1.3			

	Water		7.6	2.9	203
Nakambe River extension	Sediment	2.4 ± 2.3			
	Part. Hg	0.2			
	Water		7.37	3.88	221
Tibim Dam	Sediment	0.2± 0.08			
	Part. Hg	0.67			
	Water		7.18	5.54	179
Retkongla River	Sediment	1.7			
	Part. Hg	0.4			
	Water				
Bounoum Dam	sediment	1.37			
	Water		6.8	5.16	195
Poniro Dam	Sediment	0.23 ±0.02			
	Water, TSS	0.92			
	Water		7.21	3.86	213

Table S2. *Concentration Major and trace element in filtered ground and surface water. Results are presented as mean plus or minus standard deviation (Mean ± SD). SD is only presented when there are at least 2 values. <DL indicate below detection limit.*

	Goundwater				**Surface water**			
Elements	Boromo	Dano	± SD	Gaoua	Boromo	Dano	Gaoua	± SD
Al (mg L^{-1})	0.002	0.001	0.0002	0.1	1.4	0.1	0.04	0.03
P (mg L^{-1})	3.2	0.3	0.01	1.3	0.2	0.03	0.14	0.05
Ca (mg L^{-1})	12.7	47.1	10.8	62.8	4.9	5.9	13.8	15.5
Fe (mg L^{-1})	0.003	0.0002	0.0001	0.06	1.2	0.5	0.34	0.22
K (mg L^{-1})	3.7	1.8	1.7	0.3	5.7	1.4	2.9	3.0
Mg (mg L^{-1})	2.9	12.8	0.6	27.8	1.4	2.1	4.9	5.9
Mn (mg L^{-1})	0.0	0.0009	0.0008	0.1	0.2	0.01	0.34	0.28
Na (mg L^{-1})	12.1	42.2	40.8	12.0	7.1	4.3	17.8	23.1
S (mg L^{-1})	0.4	1.9	1.0	1.9	<DL	< DL	0.91	0.77
Si (mg L^{-1})	83.6	35.0	12.7	58.5	6.3	5.4	8.0	1.3
Sr (mg L^{-1})	0.3	0.5	0.3	0.1	0.1	0.04	0.10	0.08
Zn (mg L^{-1})	0.002	0.0011	0.0003	0.5	0.004	0.001	0.010	0.008
PO_4^{2-} (mg L^{-1})	<DL	<DL	<DL	<DL	0.39	<DL	0.24	n=1
THg (ng L^{-1})	2.3	1.0	0.8	1.2	8.7	2.7	4.6	3.5
MeHg (ng L^{-1})	0.8	0.5	0.4	0.3	0.2	0.03	0.6	0.4
B (µg L^{-1})	2.3	13.5	7.6	3.5	8.0	2.8	4.2	3.2
Ti (µg L^{-1})	1.0	0.6	0.2	2.6	20.1	0.7	0.4	0.2
Cr (µg L^{-1})	0.3	0.14	0.04	0.2	1.1	0.3	0.2	0.1
Co (µg L^{-1})	0.03	0.02	0.01	0.08	1.2	0.1	1.2	0.5
Ni (µg L^{-1})	0.6	0.06	0.02	0.4	1.2	0.5	0.8	0.2
Cu (µg L^{-1})	0.22	0.50	0.44	0.20	1.6	1.2	0.7	0.1
As (µg L^{-1})	0.2	23.6	32.1	1.4	1.2	0.4	0.5	0.2
Se (µg L^{-1})	0.04	0.5	0.4	0.04	0.08	0.04	0.04	0.01
Mo (µg L^{-1})	6.9	1.3	1.1	0.1	0.08	0.31	2.6	3.6
Cd (µg L^{-1})	0.01	0.005	0.001	0.01	0.004	0.001	0.002	0.001
Tl (µg L^{-1})	0.004	0.002		<DL	0.03	<DL	0.007	0.002
Pb (µg L^{-1})	0.08	0.04	0.03	0.03	1.05	0.06	0.06	0.03
Th (µg L^{-1})	0.001	0.001		0.001	0.20	0.01	0.007	0.006
U (µg L^{-1})	0.4	0.7	1.00	0.1	0.17	0.01	0.06	0.08

Table S3. *Inorganic ions and dissolved organic carbon (DOC) concentrations (mg L^{-1}) in surface and ground water. * indicate pristine river collected 3 km away from mining Dano site; <DL indicate below detection limit. Br^- and NO_2^- were below the detection limit for all samples and are not shown in this table.*

Sample	Districts	F^-	Cl^-	NO_3^-	PO_4^{3-}	SO_4^{2-}	DOC
River	Boromo	0.2	3.0	0.7	0.4	0.9	4.2
	Dano*	0.2	1.3	0.7	<DL	0.9	1.4
	Gaoua	0.2	0.7	0.9	<DL	2.1	2.0
	Gaoua	0.2	26.6	0.8	<DL	1.9	3.5
	Gaoua	0.2	1.4	3.6	0.2	7.0	1.3
Ground water	Boromo	0.2	0.3	1.0	<DL	3.0	0.3
	Dano	0.2	0.5	3.6	<DL	1.4	0.2
	Dano	0.2	0.6	3.8	<DL	1.3	0.3
	Dano	0.2	1.4	1.3	<DL	14.1	0.2
	Gaoua	0.2	0.7	<DL	<DL	<DL	0.5
Water used in mining process	Boromo	0.2	5.6	2.4	<DL	0.8	1.5
	Dano	0.2	2.7	1.0	<DL	3.0	1.5

***Table S4**. Pearson correlation matrix (correlation coefficient (CC), p value(p), and number of samples (N) with T°C (temperature), cond (conductivity), physico-chemical and multi-elementary parameters for filtered waters.*

parameters	*Statistics*	*pH*	*Cond*	*T°C*	*THg_F*	*Doc*	*F^-*	*Cl^-*	*NO_3^-*	*PO_4^{3-}*	*SO_4^{2-}*	*Al*	*Fe*	*As*	*Pb*
pH	CC	**1.00**													
	p	**0.00**													
	N	11													
Cond	CC	**0.43**	**1.00**												
	p	0.70	**0.00**												
	N	11	11												
T°C	CC	**0.90**	0.18	**1.00**											
	p	**0.29**	0.03	**0.00**											
	N	11	11	11											
THg_F	CC	0.24	-0.07	0.02	**1.00**										
	P	0.92	0.87	0.92	**0.00**										
	N	11	11	11	12										
Doc	CC	0.24	**-0.40**	0.17	**0.74**	**1.00**									
	P	0.12	0.42	0.05	**0.00**	**0.00**									
	N	11	11	11	12	12									
F^-	CC	0.26	0.35	0.24	-0.04	0.14	**1.00**								
	p	0.00	0.64	0.02	0.00	0.00	**0.00**								
	N	11	11	11	12	12	12								
							-								
Cl^-	CC	0.14	-0.21	0.12	**0.63**	**0.47**	0.26	**1.00**							
	P	0.49	0.72	0.18	**0.00**	0.00	0.00	**0.00**							
	N	11	11	11	12	12	12	12							
		-				-		-							
NO_3^-	CC	**0.47**	0.09	**-0.52**	**-0.42**	0.24	0.02	0.20	**1.00**						
	P	0.81	0.78	**0.92**	0.00	0.00	0.00	0.00	**0.00**						
	N	11	11	11	12	12	12	12	12						
								-							
PO_4^{3-}	CC	0.06	-0.23	-0.02	**0.40**	**0.70**	**0.55**	0.08	0.06	**1.00**					
	P	0.39	0.63	0.42	0.00	**0.00**	**0.00**	0.00	0.00	**0.00**					
	N	11	11	11	12	12	12	12	12	12					
						-		-							
SO_4^{2-}	CC	0.17	**0.45**	0.16	-0.24	0.19	**0.59**	0.11	0.11	0.03	**1.00**				
	P	0.00	0.56	0.00	0.00	0.00	**0.00**	0.00	0.00	0.00	**0.00**				
	N	11	11	11	12	12	12	12	12	12	12				
								-	-						
Al	CC	0.06	-0.13	-0.07	**0.56**	**0.63**	0.34	0.06	0.26	**0.84**	-0.20	**1.00**			
	P	0.54	0.26	0.62	**0.00**	**0.00**	0.00	0.00	0.00	**0.00**	0.00	**0.00**			
	N	11	11	11	12	12	12	12	12	12	12	12			
								-	-						
Fe	CC	0.12	-0.34	0.03	**0.47**	**0.77**	0.22	0.08	0.27	**0.80**	-0.20	**0.87**	**1.00**		
				<											
	P	0.00	0.64	0.0001	0.00	**0.00**	0.00	0.00	0.00	**0.00**	0.00	**0.00**	**0.00**		
	N	11	11	11	12	12	12	12	12	12	12	12	12		
						-		-	-			-	-		
As	CC	0.26	0.61	0.05	0.26	0.15	0.12	0.09	0.15	-0.19	0.35	0.15	0.26	**1.00**	
	P	0.00	0.42	0.00	0.00	0.00	0.00	0.00	0.00	0.00	0.00	0.00	0.00	**0.00**	
	N	11	11	11	12	12	12	12	12	12	12	12	12	12	
								-	-					-	
Pb	CC	0.11	-0.03	-0.03	**0.58**	**0.64**	**0.41**	0.03	0.26	**0.82**	-0.16	**0.99**	**0.84**	0.09	**1.00**
	P	0.42	0.00	0.79	**0.00**	**0.00**	0.00	0.00	0.00	**0.00**	0.00	**0.00**	**0.00**	0.00	**0.00**
	N	11	11	11	12	12	12	12	12	12	12	12	12	12	12.00

***Table S5**. Soil and sediment granulometry, carbon, nitrogen, major (Al, Ca, Fe, Mg, Mn, S and Ti), trace elements (Pb, Cu, Zn, Cd, As and Se) and percentage of Al and Fe obtained by NH_4OH and ascorbate selective extractions. Major and trace elements were obtained by total digestion. N.D = not determined; <DL = below detection limit. (X) indicates ASGM samples and (*) indicates pristine samples. Asc=ascorbate*

																						NH_4OH		**Ascorbate**	
Locality	Type	site	clay + silt	Sand	C_{org}	N	$\delta^{13}C$	THg	MeHg	Al	Ca	Fe	Mg	Mn	S	Ti	Pb	Cu	Zn	Cd	As	Se	Al_{NH4OH}	Fe_{NH4OH}	Al_{asc}	Fe_{asc}
			%	%	%	%	‰	µg g^{-1}	ng g^{-1}	mg g^{-1}							µg g^{-1}						%			
Soil																									
Boromo	X	B1	83.1	16.9	0.49	0.04	-21.7	6.5	**N.D**	141.5	3.1	29.6	2.0	0.4	0.17	8.5	28.6	20.6	40.2	0.9	7.0	0.2	0.8	0.8	0.3	1.3
Boromo	X	B2	90.0	10.0	0.47	0.02	-20.7	0.2	0.05	20.6	<DL	21.3	<DL	<DL	0.07	2.5	8.1	8.2	40.2	0.5	1.8	0.04	0.8	0.2	0.6	1.1
Boromo	X	B2	81.8	18.2	0.36	0.04	-18.4	0.2	0.03	23.6	<DL	10.2	<DL	0.3	0.07	3.2	7.8	10.5	18.9	0.6	1.5	0.1	1.0	0.4	0.8	2.1
Dano	X	B3	72.8	27.2	1.20	0.07	-17.2	0.3	0.10	81.4	2.5	54.8	2.7	1.0	0.26	4.0	11.7	24.2	50.4	0.4	11.3	0.3	0.2	0.1	0.4	1.0
Dano	X	B3	53.6	46.4	1.85	0.11	-20.6	0.4	0.34	59.1	3.4	34.4	1.6	0.8	0.37	4.9	10.1	26.1	30.6	0.3	11.9	0.2	0.3	0.1	0.8	1.9
Dano	X	B4	78.1	21.9	1.73	0.09	-23.4	14.7	**N.D**	69.3	9.5	106.3	2.4	0.9	0.24	3.6	54.1	57.6	467.6	0.4	181.4	0.8	0.1	0.03	0.4	0.4
Dano	X	B4	81.7	18.3	1.24	0.08	-19.7	2.6	0.03	80.4	4.7	110.6	1.9	0.4	0.12	4.4	35.1	51.5	86.2	0.4	141.8	0.7	0.2	0.06	0.4	0.3
Gaoua	X	B5	84.3	15.7	1.08	0.06	-20.4	0.9	0.29	47.3	1.2	35.9	0.7	0.5	0.10	4.3	5.8	28.9	35.0	0.3	3.0	0.9	0.9	0.5	0.6	1.4
Boromo	*	B1	68	32	0.73	-	-22.1	0.1	N.D	23.8	<DL	8.1	<DL	0.1	0.10	4.3	8.4	5.2	15.2	0.5	1.5	<DL	2.4	1.4	0.8	2.1
Dano	*	B5	81	19	1.03	0.06	-23.1	0.3	0.02	106.5	<DL	118.4	2.0	0.2	0.12	5.7	22.2	47.8	42.8	0.5	137.3	0.5	0.6	0.2	0.3	0.3
Gaoua	*	B5	49	51	0.68	0.03	-22.1	0.4	0.20	47.4	<DL	24.7	0.6	0.3	0.08	3.4	4.5	27.0	12.9	0.3	2.8	0.5	2.6	2.3	0.7	1.8
sediments																									
Boromo	**x**	B1	54.2	45.8	0.42	0.03	-23.6	168.01	0.87	22.7	<DL	7.6	<DL	<DL	0.07	2.8	9.0	5.1	21.2	0.4	1.9	0.2	2.7	1.7	0.8	7.5
Dano	*	B3	84.1	15.8	1.54	0.10	-25.7	45.4	0.08	57.9	2.1	37.4	1.4	0.5	0.10	5.4	8.5	35.2	46.1	0.3	4.8	0.2	2.7	1.9	1.5	8.1
Dano	*	B3	43.3	56.7	1.76	0.11	-24.9	65.59	**N.D**	61.00	1.9	34.2	1.5	0.4	0.17	5.5	8.6	34.8	40.2	0.5	4.3	0.2	2.2	1.5	1.7	10.9
Gaoua	x	B5	50.2	49.8	1.21	0.09	-21.9	297.5	0.76	100.1	8.4	83.6	3.2	1.9	0.09	7.5	13.8	60.7	65.5	0.6	6.7	0.4	1.2	0.5	1.8	7.3
Gaoua	x	B5	44.6	55.6	1.43	0.10	-23.6	7828.5	1.51	36.8	3.2	45.2	1.4	0.9	0.12	3.4	18.8	41.6	269.6	0.5	10.6	0.5	0.2	0.1	0.7	2.8
Gaoua	x	B5	39.9	60.1	1.21	0.09	-24.0	139.5	0.22	79.9	20.1	75.9	3.3	1.6	0.15	4.9	10.1	57.0	44.5	0.2	5.3	0.4	0.9	0.5	2.2	5.9

Table S6. *Majors elements (Al, Ca, Fe, Mg, Mn and Ti) and trace elements (As, Cu, Pb, Sn and Se) by selective extractions (NH_4OH and ascorbate). <DL= below detection limit. (X) indicates ASGM samples and (*) indicates pristine samples. Since As, Pb, and Se are below the detection limit for NH_4OH and ascorbate, and the values for Cu and S are below the detection limit for NH_4OH and ascorbate, respectively, at all sites, they are not shown in the table.*

				NH_4OH extraction							Ascorbate extraction						
Locality	Type	ASGM/ pristine	Site	Al	Ca	Fe	Mg	Mn	S	Ti	Al	Ca	Cu	Fe	Mg	Mn	Ti
				$\mu g\ g^{-1}$							$\mu g\ g^{-1}$						
Boromo	Soil	X	B1	1071	<DL	236	30.2	1.3	46.6	7.4	492	852	<DL	394	117	80.2	4.0
Boromo		X	B2	163	<DL	36.3	<DL	0.8	0.0	1.8	116	<DL	<DL	224	<DL	53.6	2.0
Boromo		X	B2	238	<DL	45.2	4.7	2.6	0.0	1.8	188	<DL	<DL	216	<DL	76.7	2.0
Dano		X	B3	171	<DL	69.1	5.8	1.5	91.9	2.3	342	927	<DL	523	125	280	3.9
Dano		X	B3	166	<DL	40.2	6.0	1.3	53.9	1.7	451	1104	<DL	652	126	183	4.0
Dano		X	B4	95.4	214	27.9	4.3	0.5	41.5	0.9	267	1464	<DL	408	111	257	4.0
Dano		X	B4	171	268	71.4	6.6	0.6	32.1	3.0	306	1183	<DL	363	76	232	5.9
Gaoua		X	B5	433	<DL	160	9.1	3.1	31.8	4.2	283	528	<DL	505	54.6	144	4.0
Boromo		*	B1	567	<DL	111	11.2	3.7	30.5	5.2	190	<DL	<DL	172	<DL	33.8	2.0
Dano		*	B4	680	<DL	192	9.2	0.9	<DL	2.8	328	370	<DL	328	85.3	40.4	1.9
Gaoua		*	B5	1252	<DL	567	25.8	4.1	30.8	7.9	349	<DL	<DL	445	<DL	72.7	4.0
Boromo	Sediments	x	B1	620	<DL	131	7.7	1.2	<DL	4.5	186	<DL	<DL	571	<DL	21.6	2.0
Dano		*	B3	1543	<DL	693	35.3	5.2	23.4	12.7	842	562	2.0	3011	111	147	6.0
Dano		*	B3	1354	<DL	524	30.3	4.9	24.6	9.3	1014	551	2.0	3745	108	152	8.0
Gaoua		x	B5	1228	<DL	420	23.9	7.4	27.3	12.1	1835	807	3.9	6144	196	582	27.3
Gaoua		x	B5	87.8	<DL	37	3.2	0.9	29.1	1.2	257	790	2.1	1273	79.1	328	4.1
Gaoua		x	B5	741	<DL	339	21.6	3.6	25.7	8.5	1726	867	4.0	4454	226	555	24.0

Table S7. *Mercury species concentration (ng. g^{-1}) extracted by thermodesorption (Hg0 at 80°C and Hg_{Res} between 180°C and 550°C) and selective extraction (Hg_{OM} by NH_4OH and Hg_{amFe} by ascorbate) in soils and sediments. Selective extractions have been performed after removing Hg0 (after T80). Results are presented as minimum (min), maximum (max) and average. (-) indicates no data.*

Sampling sites	Amont	THg		Hg0		Hg_{OM}		HgamFe		Hg_{Res}	
		Soil	Sed	Soil	Sed	Soil	Sed	Soil	Sed	soil	sed
Boromo	Min	105	-	6.0	-	33.2	-	55.5	-	5.4	-
	Max	6508	168	829	30.7	1817	59.3	3463	43.4	61.9	17.6
	Average	1771	-	225.5	-	504	-	927	-	30.1	-
Dano	Min	295	45.4	19.2	3.8	57.1	20.2	144	12.5	8.0	17.5
	Max	14707	65.6	8382	6.1	1525	26.1	4008	15.3	188	32.6
	Average	3655	55.5	1732	4.7	544	23.1	1238	13.9	53.2	25.1
Gaoua	Min	387	139	35.8	11.9	171	6.9	204	14.5	15.6	65.8
	Max	869	7828	45.9	1022	176	1954	441	3420	150	131
	Average	628	2755	40.9	353	174	666	323	1171	83.2	92.8

After examining the processes governing the transfer and transformation of mercury from mining soils to river sediments in southern Burkina Faso, it is important to extend the analysis to areas potentially affected by human activity. Mercury first accumulates in soils before reaching aquatic environments; however, it is not yet clear whether this accumulation occurs in areas where people live or work. It is therefore essential to study local practices to understand the potential exposure of these populations.

Chapter III

Transfer of mercury contamination from mine to village in Guinea: the case of artisanal and small-scale goldmining.

This second chapter focuses on the role of mining practices in the transfer of mercury contamination from mines to gold mining villages in the Republic of Guinea. It highlights the potential chronic exposure of the populations of these villages to elemental mercury inhalation during the burning of amalgams, as well as from re-emissions from contaminated soils.

The article will be submitted to the journal Science of the Total Environment.

Transfer of mercury contamination from mine to village in Guinea: the case of artisanal and small-scale goldmining

D. Dabré*[1,2], S. Guédron[1], Y. Maïga[2], O. Bruneel[3], A. A Konaté[4], I.K. Doumbouya[4], J. Gardon[3], S. Campillo[1], S. Sentenac[1], O. Ouédraogo[2], and E. Resongles[3]

[1] Univ. Grenoble Alpes, Univ. Savoie Mont Blanc, CNRS, IRD, IFSTTAR, ISTerre, 38000 Grenoble, France

[2] Université Joseph KI-ZERBO, 03 BP 7021 Ouagadougou 03, Laboratoire de Microbiologie et Biotechnologie Microbienne (LAMBM), Burkina Faso

[3] HydroSciences Montpellier, University of Montpellier, CNRS, IRD, Montpellier, France

[4] Laboratoire de Recherche Appliquée en Géosciences et Environnement, Institut Supérieur des Mines et Géologies de Boké, BP 84, Baralandé, Boké, Republic of Guinea

Highlights:

- Goldmining is a source of environmental mercury (Hg) contamination
- In Guinea, Hg amalgamation is performed in miners' villages
- Hg levels in village topsoils reached up to 10 µg g^{-1}
- Elemental Hg in soil reach up to 75%THg
- This indicates potential risks of chronic exposure for local populations

Abstract

Artisanal and small-scale gold mining (ASGM) is a widespread activity in Guinea. Gold ore is traditionally extracted mainly by men at mining sites, and then transported to villages where women predominantly recover gold through mercury (Hg) amalgamation.

In this study, Hg speciation [total Hg (THg), methylmercury (MeHg), and elemental Hg (Hg0)] was investigated in soils from two ASGM sites and miner's villages. Results show that Hg is primarily found in topsoil with higher levels in villages center (up to 10 μg g^{-1} THg and 7.5 μg g^{-1} Hg0) compared to mining sites (up to 0.6 μg g^{-1} THg and 0.2 μg g^{-1} Hg0). High THg concentrations (up to 7.5 ng L^{-1} THg) were also found in water from village wells, supporting well contamination through the spreading of soil particles.

Estimated annual Hg deposition in the two villages topsoil during the period of ASGM activities were 36 (29) ±12 mg m^{-2} yr^{-1}, ~ 84 (84) ±53 mg m^{-2} yr^{-1} [mean (median) ±SEM (standard error of the mean)], with Hg0 making up 62-75% of THg.

This study highlights that ASGM practices in Guinea leads to significant environmental contamination beyond the mining sites themselves. The direct burning of Hg amalgams in households and possible Hg0 re-emission from village topsoil highlight the potential risks of chronic exposure for local populations. This underscores the urgent need of raising awareness among mining communities about the impacts of their traditional Hg-based practices.

Keywords: Mercury speciation; Artisanal and Small-Scale Gold mining; village; Guinea Republic.

III.1. Introduction

Gold mining is a major economic activity in Africa, with underground gold reserves positioning several countries as major global producers. Guinea is estimated to be the fifth-largest gold producer on the continent (Chevrillon-Guibert and Magrin, 2018), and has witnessed a surge in artisanal and small-scale gold mining (ASGM) activities since the early 2000s (Schön-Blume et al., 2021). Although economically vital for local populations, ASGM practices, pose serious environmental and public health risks due to the widespread use of mercury (Hg) for gold extraction (Verbrugge and Geenen, 2020).

The gold extraction process in ASGM sites typically involves crushing and grinding the ore, followed by Hg amalgamation, and sometimes, cyanidation of Hg-rich tailings (Velásquez-López et al., 2011). These practices result in significant Hg emissions, both through liquid spills and gaseous elemental Hg (Hg0) emission during the burning of amalgams (Keita, 2001). Gaseous Hg0 can then condense and re-deposit onto surrounding soils (Grimaldi et al., 2008). This results in elevated Hg levels in ASGM soils, with reported concentrations of 9.1 to 410 $\mu g \cdot g^{-1}$ in Ghana (Gyamfi et al., 2021), 0.27 to 0.85 $\mu g\ g^{-1}$ in Niger (Adewumi and Laniyan, 2020), and between 3.9 to 130 $\mu g\ g^{-1}$ in Senegal (Gerson et al., 2018; Niane et al., 2019b). Furthermore, cyanidation of tailings enhances Hg mobility and bioavailability by forming soluble Hg–CN complexes (Brugger et al., 2018; Tulasi et al., 2021).

Despite gold mining being a longstanding tradition in Guinea, dating back to the 9th century (Mbodj, 2009), data on environmental Hg contamination remain scarce. More than 200 ASGM sites have been identified in eastern Guinea, with reports of intense deforestation and significant dust inhalation risks for local population in the northern Siguiri area (Bah et al., 2016; Cissé, 2019; Doumbouya et al., 2024; Mbodj, 2009).

Mining practices in Guinea differ from those observed in alluvial goldmining regions such as the Amazon, where gold is processed by amalgamation with Hg directly on site (Lechler, 2000; De Oliveira et al., 2001; Brabo et al., 2003; Guédron et al., 2018). In contrast, Guinean ores are extracted from mining pits mainly by men, sometimes assisted by women. The collected gold ores are then transported to the villages, where men crush them while women handle washing, amalgamation and burning. This practice leads to Hg contamination of inhabited areas, and exposure of both burner and bystanders to Hg vapour, which may exceed the Permissible Exposure Limit (PEL) of 100 mg m^{-3}, and to a minor extent to levels considered to be Immediately Dangerous to Life and Health (IDLH) of 10,000 mg m^{-3}, as reported in Burkina Faso's ASGM sites (Black et al., 2017). In addition, waste tailings are frequently dumped untreated near houses, increasing environmental Hg dissemination (Ikingura et al., 2006; Leiva G. and Morales, 2013). During the wet season, Hg can be washed out and contaminate surface and groundwater (Amalric et al., 2003), as reported in South Africa [0.05–2.44 $\mu g\ L^{-1}$; (Nevondo et al., 2019)] and Kenya [100–760 $\mu g\ L^{-1}$; (Omondi et al., 2023)]. Moreover, the use of groundwater for

both ore processing and drinking raises concerns about co-contamination by other toxic elements, such as arsenic (As) and lead (Pb). Recent findings suggest that As concentrations can exceed WHO guideline values (>10 µg L^{-1}) in certain aquifers (Konaté et al., 2022, 2025b; Dabré et al., 2025), compounding health risks for local populations.

Once released into the aquatic environment, Hg undergoes complex transformations. Under reducing conditions, specific microbial communities can methylate inorganic Hg into methylmercury (MeHg), a highly toxic and bioaccumulative compound (Gilmour et al., 2013; Parks et al., 2013; Ma et al., 2018; Zhang et al., 2024). Understanding Hg speciation and transformation pathways is therefore essential to assessing the long-term environmental and health risks associated with ASGM.

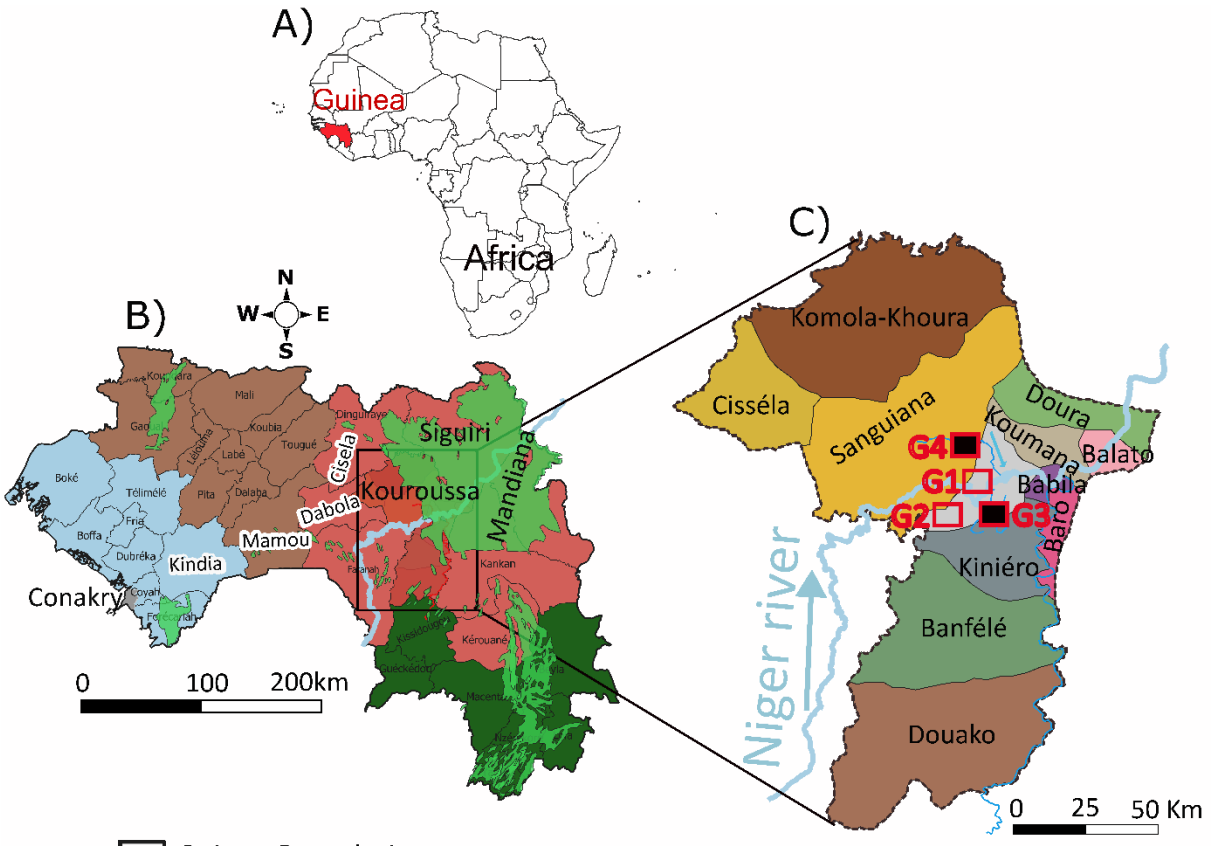
In this study, we report for the first time the levels and stocks of Hg species in soils and groundwater from ASGM sites and miner's villages, in order to assess the impact of these mining practices on the spreading of Hg contamination. To this end, we conducted a comprehensive field study in the Kouroussa ASGM district (Upper Guinea), and documented Hg speciation, including total (THg), elemental (Hg0), and methyl- (MeHg) mercury in soil and groundwater samples. Additional parameters, including lead (Pb), arsenic (As), anions, organic carbon, and physico-chemical parameters, were also analysed. We finally discuss the potential implications of such Hg contamination on the environment and human health.

III.2. Material and methods

III.2.1. Environmental settings and sampling strategy

Guinea, is located in West Africa, and bordered by six neighboring countries Guinea-Bissau, Senegal, Mali, Côte d'Ivoire, Liberia, and Sierra Leone (**Figure III.1**A). The main alluvial gold deposits are localized in Upper Guinea, where the landscape consist of wooded savannah. Upper Guinea is characterized by a warm, and dry tropical climate, with two alternating seasons; a dry season from November to May, strongly influenced by the desert wind called harmattan, and a rainy season from June to October (Dessertine, 2021). The Siguiri and Mandiana areas located in northeast Guinea are the two main mining areas (**Figure III.1**B), which concentrate 100,000 miners out of a total population of 180,000 (Veiga et al., 2006). Other alluvial gold deposits, which have been intensely exploited for about 20 years, are located in the northwest of the Kouroussa region (Sidam-Minorex, 1998).

Four sites were sampled in the Kouroussa region (**Figure III.1**.C) during two field campaigns performed between March and April in 2023 and 2024 (detailed sites in **Figure III.1**.D). During the first campaign in 2023, a regional sampling strategy was carried out at four mining sites (more precisely, the villages located on these sites), revealing that the entire extraction process took place in the villages (full details in Fig.S1).



D)

Mining Sites	Locality	ASGM type	Miners Number	Creation year	Surface (ha)	Water use in mining process
G1	Bankan	Hg	~1500	2021	1	Groundwater
G2	Djaragbela	Hg	~300	2021	0.05	Groundwater
G3	Saman	Hg+CN	~500	1983	3	River
G4	Dionko	Hg	~500	1993	2	Groundwater

Figure III.1. *Map of study area showing A) Guinea in Africa; B) study region location; C) study sites locations and D) sites characteristics.*

The sampled mining sites include Bankan (G1), a 1 ha site with the largest number of miner (~1500); Djaragbela (G2), a 0.05 ha site with the lowest number of miner (~300); Saman (G3), a 3 ha site employing the ~500 miners where both Hg amalgamation and cyanidation are combined for Au extraction; and Dionko (G4), a 2ha site with the ~500 miners (**Figure III.1**C and **Figure III.1**D). Sampling in 2024 focused on the mining site and miners' villages of the two most impacted sites; namely G3 (Saman) located on the river banks (sampling at the), and G4 (Dionko) located far from the River Niger (G3 and G4 sites are shown in black square filled in red, **Figure III.1**.C).

III.2.2. Soil collection and conditioning

Topsoils samples (0 – 5 cm) were collected at all sites during the 2023 campaign, while soil profiles were sampled in 2024 at sites G3 and G4. In addition, four topsoil samples, considered unaffected by ASGM activities, were collected at least 67 kilometers away from Conakry along the road to Kouroussa, including Kiandia, Mamou, Cisela, and Dabola (**Figure III.1**B). At each site, a composite topsoil sample (0-5 cm depth) was obtained by pooling five sub-samples over approximately 12 m^2, and stored in sterile Whirl pack® bags. Soil profiles were sampled every 10 to 20 cm at sites G3 (Saman, 10 profiles) and G4 (Dionko, 7 profiles), to a maximum depth of 60 cm and 55 cm, respectively (Fig.S1). Soil profiles were sampled along a transect extending from the mining area, where gold is extraction occurs, toward the village and its outskirts. Control soil profiles were also collected outside the Kouroussa village, where no mining activity is taking place. Each profile was sampled at different horizons depending on lithology and soil color change, using an auger, and collected in sterile Whirl pack® bags. In the laboratory, soils were freeze-dried, and sieved to 2 mm. The fraction below 2mm was then ground to obtain a powder <63 µm for chemical analysis.

III.2.3. Groundwater sampling and conditioning

Groundwater was collected from village wells used for drinking water and mine water (pumped from the mining holes), in the villages and at some mining sites in Saman and Dionko. At the same time, physico-chemical parameters (pH, Eh, conductivity, ORP) were measured using a Hach® multiparameter probe (HQ4300). Sampling was performed following the ultra-trace technique ((Cossa and Gobeil, 2000; Dabré et al., 2025) . At each sampling site, bulk water was collected in 250 mL FEP Teflon containers, and filtered with 0.45 µm sterivex filters (Millipore). Both unfiltered (UNF) and filtered (F) water samples were collected in 125mL FEP vials, and acidified with HCl (0.5% v/v, trace grade - Baker). Filtered water samples for the analysis of major (Fe, Al, S, Mn and P) and trace elements (As, Pb) were collected in trace-grade 15 mL polyethylene falcon tubes (Fisherbrand™), acidified with HNO_3 (2% v/v, trace-grade - Baker). Additional filtered water samples for anion (sulphate, chlorine and phosphate) analysis were stored frozen until analysis. Samples for dissolved organic carbon (DOC) analysis were filtered in pre-burnt (550°C for 3 hours) 20mL amber borosilicate vials, and acidified with HCl (0.1N) following published protocols (Némery et al., 2013). All samples double bagged and stored at 6°C in the dark until analysis.

III.2.4. Samples characterization and chemical analysis

In the laboratory, soil grain size distribution, i.e., clay (<2µm), silt (2-63µm) and sand (>63µm), was performed on freeze-dried samples (fraction below 2mm) using a laser granulometer (Malver, Mastersizer 2000) equipped with a Hydro 2000G unit, following dispersion during 7 min by sonication

in deionized water (Fisher et al., 2017). Topsoil total carbon (C) and nitrogen (N) contents were measured using a Flash Smart elemental analyser (ThermoFisher Scientific).

Total mercury (THg) analysis in soil was performed by atomic adsorption spectroscopy (AAS) after pyrolysis at 550°C and gold amalgamation with an AMA 254, Altec (Guedron et al., 2009). Methylmercury (MeHg) concentrations in soil were determined by an ethylation purge and trap gas-chromatograph, cold vapour atomic fluorescence spectroscopy (GC-CVAFS) analysis (Tekran®, model 2700) after acid digestion following published protocols (Hammerschmidt and Fitzgerald, 2001, 2004). For all these analyses, the precision of ± 5% was determined from triplicates. A relative standard deviation (RSD) always lower than 5% was obtained by determining the quality assurance, quality control (QA/QC) with concentrations obtained for repeated analyses from certified international reference materials ERM CC 141 [European Commission; 0.078 ± 0.003 µg g^{-1}, (N=7)] and IAEA 158 [International Atomic Energy Agency; 0.123 ± 0.002 µg g^{-1}, (N= 3)] for THg and from MESS-4 reference materials (Marine sediment SRM from NRC; 0.079 ± 0.001 µg g-1) for MeHg. Mercury thermodesorption experiments on soil samples were performed, following published protocols (Biester and Scholz, 1997; Windmöller et al., 2017). The elemental mercury (Hg0) was determined by heating approximately 100 mg of sample at 80°C (Meloni et al., 2024). Hg bound to organic matter plus non-crystalline iron oxide (Hg_{OM}+$Hg_{ascorbate}$) was determined by heating samples at 180°C (Dabre et al., 2025). Finally, the refractory phases (Hg_{Res}), was determined as the difference between THg measured at 550 °C (THg) and the Hg released at 180 °C following published protocol (Guédron et al., 2009). To control the reliability of the thermodesorption at 180 °C, two selective extractions, i.e., NH_4OH (Hg_{OM}) and ascorbate ($Hg_{ascorbate}$) were carried out on a selection of samples (Dabre et al., 2025), including at least one surface soils per site (N=6), according to published protocols (Kostka and Luther, 1994; Rodríguez Martín-Doimeadios et al., 2000; Bloom et al., 2003; Raiswell et al., 2010). Total concentration was measured, after microwave digestion (ultraWAVE, Milestone) of approximately 100 mg of sample at 250°C as described by Falciani et al. (2000) and Melaku et al. (2005). The concentration of major (Al, Ca, Fe, Mg, Mn, S, Ti) and trace (Pb, Cu, Zn, Cd, Cr, As, Se) elements in soil extraction digestates (total and selective) were analysed using a ICP OES (Agilent 7800 VDV) and ICP MS (Agilent 7900), respectively. QA/QC was assessed by the analysis of certified reference materials ERM-CC-141 and the accuracies were always within the certified value range with a ± 5% margin of error.

Total Hg concentrations in filtered (THg_F) and unfiltered (THg_{UNF}) water samples were determined by cold vapor atomic fluorescence spectrometry (CV-AFS) after conversion of all Hg species into Hg0 followed by detection using a Tekran® Model 2500 as described by (Guédron et al., 2011; Guédron et al., 2020). Methylmercury concentrations in the filtered ($MeHg_F$) and unfiltered ($MeHg_{UNF}$) water samples were analyzed using the same analyser as for soil following published protocols (U.S. Environmental Protection Agency, 1998; Munson et al., 2014; Guédron et al., 2017). Field and

analytical blank values were 0.7 ± 0.3 ng L^{-1} for THg and 0.038 ± 0.004 ng L^{-1} for MeHg attesting to the absence of contamination during sampling and filtration in the field and were all subtracted from the sample measurements. QA/QC was ensured using the certified reference material (ORMS-5), with THg concentrations obtained for repeated analyses (27.1 ± 0.6 ng L^{-1}, N=3) that were within the range of the certified value (26.2 ± 1.3 ng L^{-1}). MeHg results were validated in duplicate analysis and quantification using the standard addition technique for MeHg (Guédron et al., 2014b), and the recovery rate was always within the 100 ± 5% range. Major (Al, Ca, Fe, Mg, Mn, S, Ti) and trace (Pb, Cu, Zn, Cd, Cr, As, Se) elements concentration in filtered water were analyzed using the same equipment as for digested soil, and the QA/QC was assessed through the analysis of the certified standards SLRS4 and SLRS6. Accuracies were always within the range of certified value range with a ± 5% margin of error.

The anion concentrations (Cl^-, NO_3^-, PO_4^{3-}, SO_4^{2-}) and dissolved organic carbon (DOC) in filtered water were determined respectively by ion chromatography (Dionex ICS 2000) and the TOC-VCSN analyzer (Shimadzu®), following published protocols (Rutz et al., 2017; Tisserand et al., 2022, 2024). Precisions and recovery rates were below 5%.

III.2.5. Statistical analysis, mapping, and calculation

Data was assessed for normal distribution using a Shapiro-Wilk test and for homoscedasticity. As some geochemical data were normally distributed and some were not (Webster, 2001), the geochemical dataset reported in this manuscript is presented as the mean (median) ± SEM (standard error of the mean) and also as mean ± SD (standard deviation). All statistical treatments were performed using R software (R.4.4.1), sigmaplot and sigmastat® software. Linear regressions were performed and Pearson correlation coefficient (R^2) are reported when p-values are below 0.05. Mercury concentration maps were produced using Qgis and the inverse distance weighting (IDW) interpolation method published elsewhere (Saha et al., 2023). The Hg stock was estimated using the following formula (Turetsky et al., 2006):

$$Hg\ stock\ (kg) = \frac{\text{Area}\ (\text{m}^2)\ \times\ \text{Depth}\ (\text{m})\ \times\ \text{Soil density}\ (\text{t/m}^3)\ \times\ \text{Hg concentration}\ (\text{mg/kg})}{1000000}$$

III.3. Results and interpretations

III.3.1. Hg distribution in soil profiles: evidence for topsoil contamination

Total mercury (THg) concentrations in pristine sites (0.14 ± 0.04 µg g^{-1}, **Figure III.2**) were homogeneous throughout the profiles. Spatially, the lowest THg concentrations [63 (50) ±14 ng g^{-1}), Tables S1 and S2] were found in reference sites such as in Kindia (46.7 ng g^{-1}), Dabola (49.3 ng g^{-1}), Cisela (51.13 ng g^{-1}), and Mamou (105 ng g^{-1}, Table S1).

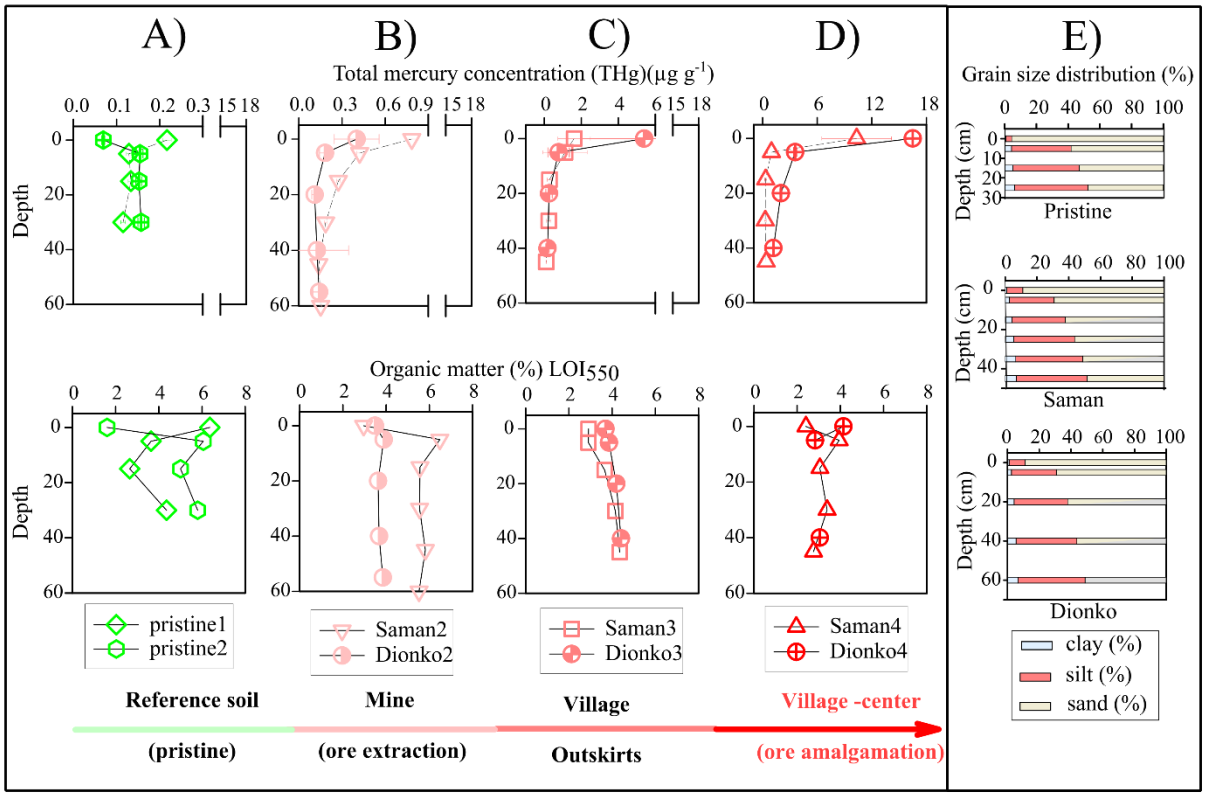


Figure III.2. *Mercury (top) and organic matter (bottom) in soil profile in A) pristine; B) Mine sites where ore is extracted; C) Village at the periphery and D) Village where amalgamation occurs and E) Grain size distribution in pristine soils (top), Saman (middle) and Dionko (bottom).*

These values are within the range of concentrations reported for pristine soils worldwide [0.02 to 0.25 µg g^{-1} (Adriano, 2001; Ndzana et al., 2023)], including soils from South America [0.01 to 0.9 µg g^{-1} (Guedron et al., 2009; Leiva G. and Morales, 2013)]. These concentrations are also in the range of reported values in West African pristine soils, such as those from Nigeria [i.e., < 0.3 µg g^{-1} (Adewumi and Laniyan, 2020)], Burkina Faso [0.3 ± 0.1 µg g^{-1} (Dabre et al,.2025)], and Senegal [5 to 60 ng g^{-1} (Niane et al., 2019b)].

In contrast, mine topsoil THg concentrations (0.3 to 0.9 µg g^{-1}) were 2 to 4-times higher than those in control sites. In ASGM soil profiles, THg concentrations decreased rapidly with depth to reach values in the range of reference soils bellow 10 cm depth at all sites (**Figure III.2**). At ASGM sites, where Hg is used directly to assess gold content, these values are in the lower to mid-range of levels reported in ASGM soils in Senegal [0.13 to 3.9 µg g^{-1} (Niane et al., 2019b; Thiombane et al., 2023)], in Ghana [0.1

to 40 µg g^{-1} (Rajaee et al., 2015b)], in South Africa [0.046 -2.58 µg g^{-1} (Lusilao-Makiese et al., 2014; Kamunda et al., 2016; Malehase et al., 2016; Shapi et al., 2020)], and other ASGM-impacted regions globally [0.6 -1.96 µg g^{-1} Zhang et al., 2022)].

Topsoil THg concentration at the village outskirts ranged from 0.6 to 1.3 µg g^{-1} and 0.3 to 3 µg g^{-1} at Saman and Dionko, respectively, and were 10 to 27 times higher than in control topsoils. The highest THg values were found in the middle of the village, averaging [5.6 (4.6) ±2.0 to 10.0 (10.0) ±6.5 µg g^{-1}], with values reaching 12 to 18 µg g^{-1} in sites where amalgamation and amalgam burning are carried out, being 40 to 72 times higher than the pristine sites of Saman and Dionko, respectively. Consistent with the ASGM soil profiles, THg concentrations decreased with depth, but remained 10 to 100-fold higher than reference sites in depth (**Figure III.2**), averaging 0.3±0.05 and 1.6±0.6 µg g^{-1} below 10cm at Saman and Dionko respectively. These values are in the range of concentrations reported in residential areas near an ASGM sites in Peru [1.1 to 32.3 µg g^{-1} (Quispe Aquino et al., 2024)], and soils of an ASGM village in Sumatra, Indonesia [5.6 to 19 µg g^{-1} (Arrazy et al., 2023)].

In both Saman and Dionko villages, grain size distribution in soil profiles was dominated by sand (63±5%), followed by silt (33±13%), with a small clay fraction (4±2%). The silt fraction increased with depth from 3 to 9% in surface up to 46% between 35 to 50 cm in all sites. THg was found positively correlated with sand (R^2 = 0.67, p<0.001) but negatively correlated with silts (R^2 = 0.69, p<0.001) and clay (R^2=0.47, p<0.005, Fig. S2). In addition, no significant correlation (p> 0.05) was found between THg and total organic carbon (TOC) in soil profiles, indicating that organic matter is probably not the main and unique carrier phase for Hg in Saman and Dionko soils.

III.3.2. Hg carrier phases in ASGM and village topsoil: elemental Hg contamination

Because Hg contamination affects mainly topsoils, Hg speciation experiment were performed specifically on these samples. Elemental mercury (Hg0) quantified by thermodesorption at 80°C (**Figure III.3**B) averaged 9.4 (9.3) ± 0.11 % THg in pristine topsoils with the exception of the Dabola site, which reached 28% THg. A significant increase was found on ASGM sites reaching 36.1 (40.2) ± 4.5% THg at Bankan, 40.1 (40.1) ± 5.0% THg at Djaraguela, 42.2 (44.9) ± 4.3% THg at Saman, and up to 50.8 (53.9) ± 3.9% THg at Dionko. Such proportions of Hg0 in ASGM soil (averaging 40 to 50%THg) is higher than those found on surface mining soils in Burkina Faso (15 (7) ± 6%), and close to the Gaoua site in Burkina Faso, where it reached 57% THg (Dabre et al., 2025).

The comparison between thermodesorption at 180°C and selective extractions (i.e., NH_4OH and ascorbate, Fig. S3), which extract respectively Hg bound to OM (Hg_{OM}) and non-crystalline iron oxides ($Hg_{ascorbate}$), confirms observations made in soil of Burkina Faso (Dabre et al., 2025). Mercury bound to organic matter (Hg_{OM}) and non-crystalline iron oxides ($Hg_{ascorbate}$) represents respectively 30 ± 12% and 10 ± 6% of THg. This indicates that thermodesorption at 180°C extracts about 58% of Hg_{OM} and about

22% of $Hg_{ascorbate}$. The positive correlation found between Hg_{OM} and TOC (R^2=0.70, p<0.05, Fig. S3) shows that Hg binds preferentially to OM. In addition, the positive correlation between Hg_{OM} and sulfur (R^2=0.63, p<0.05, Fig. S3) in topsoil confirms the strong affinity of Hg for sulfur-bearing groups of OM, consistently with observations made in Amazonian and Chinese tropical soils (Guédron et al., 2009; Yin et al., 2013). The remainder refractory fraction is found minority in mining soils (5-10%), whereas it is important in reference soils (30-40%, **Figure III.3**).

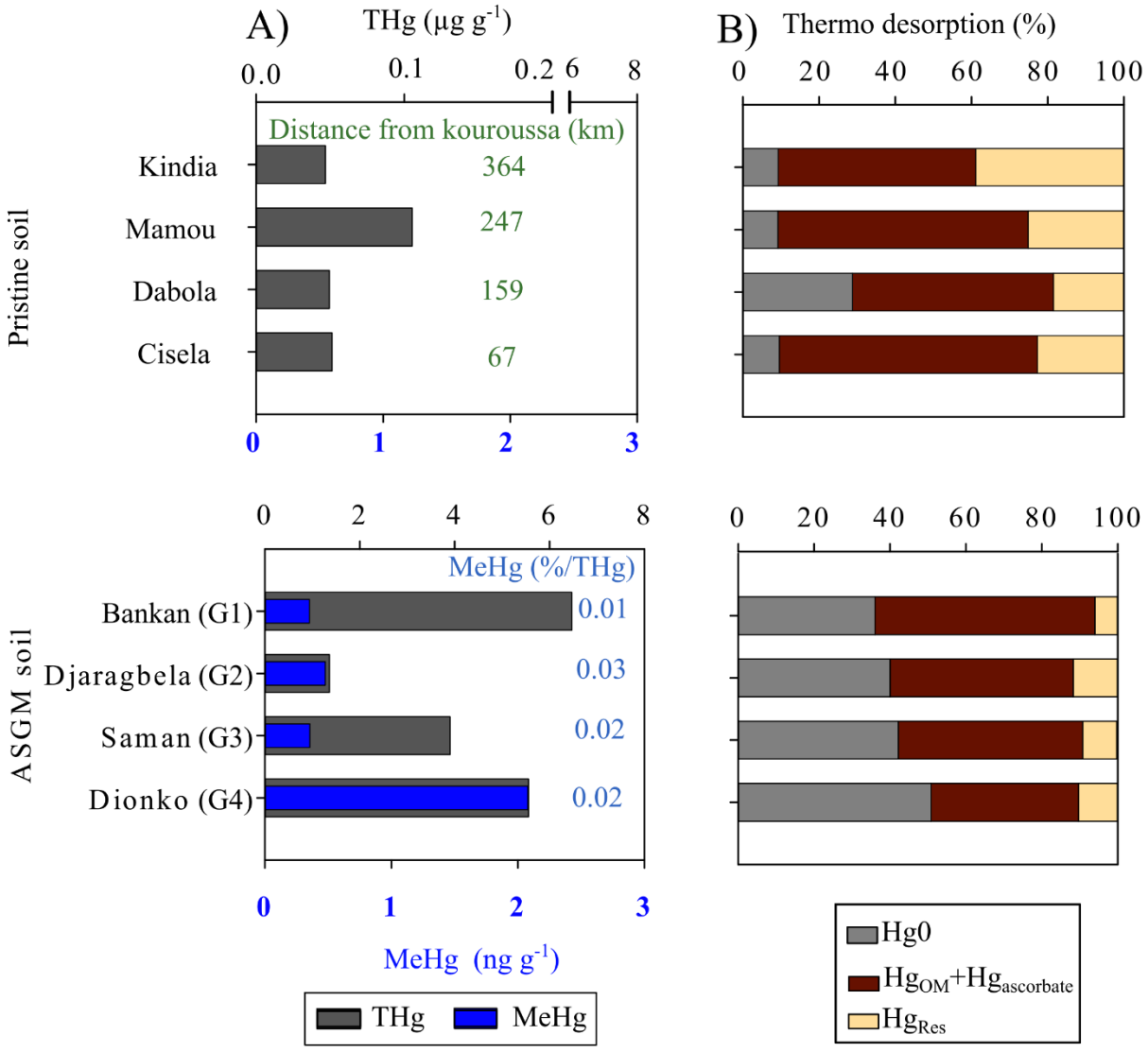


Figure III.3. *From left to right: A) Methylmercury (MeHg) and Total mercury (THg) concentration, with the distances of pristine sites from Kouroussa in green (top) and the proportion of MeHg in THg shown in light blue (bottom), on the right side of the figure. B) Proportion of Hg0 released by thermodesorption at 80°C (Hg0), 180°C (Hg_{OM}+ $Hg_{ascorbate}$) and the difference between 180 and 550°C (Hg_{Res}).*

Methylmercury (MeHg) concentrations in ASGM soils were generally low, ranging from 0.3 to 0.5 ng g^{-1}, except at Dionko where values reached 2.01 (1.7) ± 0.5 ng g^{-1}. These concentrations are comparable to those found in Amazonian soils [0.1 to 1.0 ng g^{-1} (Fostier et al., 2023)], but lower than those reported

for African soil in Senegal [0.13 to 19 ng g^{-1} (Gerson et al., 2018)]. In contrast, no significant differences in the proportion of MeHg (0.01 to 0.03% THg) were observed between reference and ASGM impacted sites, such as Saman and Dionko.

Lead (Pb) concentration in ASGM topsoil averaged 20.1 (14.6) ± 3.7 µg g^{-1} (Fig. S4; Table S3), which stands within the regional geochemical background range [0.1-35 µg g^{-1}; Table S4 (Alloway, 1995; Alfaro et al., 2015)], and fall within the lower range reported in southwest Burkina Faso [3 to 49 µg g^{-1} (Kagambega et al., 2014)]. In contrast, arsenic (As) levels were moderately high, averaging 65.6 (19.6) ± 24.1 µg g^{-1}, with the exception of Saman samples, where concentrations reach up to 151.9 (101.6) ± 33.9 µg g^{-1} (Fig. S4; Table S3). These relatively high As concentration likely reflects a naturally high geochemical background or contamination by enriched residues from ASGM processed ores.

III.3.3. Hg levels and speciation in ground water

Total filtered Hg (THg_F) concentrations were low in groundwater of the four mining villages (0.1 to 2 ng L^{-1}), except for samples collected from wells in Saman and Dionko villages which reached 3 to 7.5 ng L^{-1} (**Figure III.4**.A), with the highest values found in Saman (up to 7.5 ng L^{-1}). THg_F showed a significant positive correlation with dissolved organic carbon (DOC), particularly at the Dionko (R^2=0.86; p<0.01) and Saman (R^2=0.88; p<0.01) sites (Fig. S6). Total unfiltered Hg (THg_{UNF}) concentrations in all groundwater (50 (21) ±13 ng L^{-1}) were much higher than those of filtered Hg (THg_F,1.4 (0.2) ±1.2 ng L^{-1}), with values reaching up to 223 and 350 ng L^{-1} in the Dionko and Saman mining villages, respectively (**Figure III.4**C; Table S5). These concentrations are 47 to 70 times higher than the average THg_F concentrations in villages. The ratio between THg_{UNF} and THg_F concentrations in groundwater (93±8%) shows that THg was predominantly associated with suspended particles, which remained below the maximum permissible concentration of 6 µg L^{-1} for drinking water according to the WHO standard guideline for inorganic mercury (World Health Organization, 2017), with dissolved Hg accounting for less than 10%. These THg_{UNF} values are lower than those reported in groundwater of northern Burkina Faso [530 to 4,920 ng L^{-1} (Somé et al., 2016)], in Kenya [1,010 to 3,300 ng L^{-1} (Lusilao-Makiese et al., 2014)], in Nigeria [1,000 to 9,000 ng L^{-1} (Aliyu Haruna Sani et al., 2023)], and within the lower range of groundwater from Ghana (0 to 6 µg L^{-1}), and well below (10-7160 µg L^{-1}) in the southwest of Ghana (Rajaee et al., 2015b).

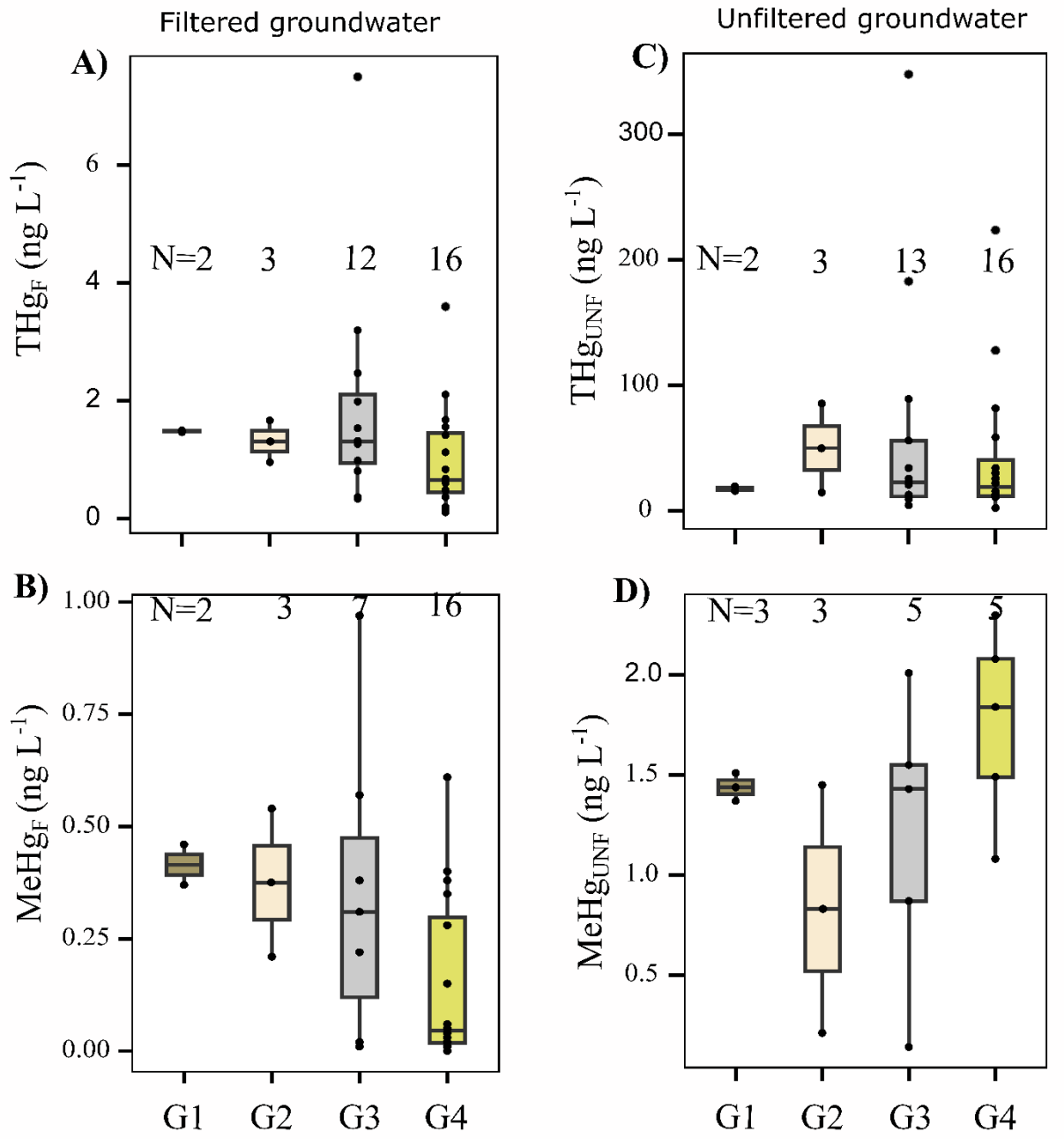


Figure III.4. *Boxplot of mercury levels and speciation in filtered water on the left with A) THg_F and B) $MeHg_F$, and unfiltered water on the right with C) THg_{UNF} and D) $MeHg_{UNF}$. Upper and lower end of the box show the 25th and 75th percentile, full lines indicate the mean, minimum and maximum of each data set (N is the number of samples).*

In groundwater, filtered MeHg ($MeHg_F$) account for 12 to 30% of THg, whereas it represents less than 10% in unfiltered groundwater ($MeHg_{UNF}$), except at Saman, where the percentage of $MeHg_{UNF}$ reaches 16% THg. These values are comparable to those reported in Burkina Faso, where $MeHg_F$ values ranged from 10 to 30% of THg_F, while $MeHg_{UNF}$ represented less than 6% of THg_{UNF} (Dabre et al., 2025). Groundwater pumping for mining activities in areas where surface water is unavailable may contribute to co-contamination of surface waters with geogenic lead (Pb) and arsenic (As). Consistent with topsoil

data, Pb concentration in all groundwater samples were low, ranging from 0.01 to 0.17 µg L^{-1} (Fig. S4; Table S6), and below the value reported in central Burkina Faso [0.6 to 9.2 µg L^{-1} (Sako et al., 2016)]. Arsenic concentrations were also low, ranging from 0.85 to 8 µg L^{-1}, except for one groundwater sample in Saman (13 µg $L^{-1,}$ Fig. S4), where it exceeds the WHO guideline of 10 µg L^{-1}. These concentrations are within the lower range of As concentrations measured in groundwater from in Mexico City [<5 to 450 µg L^{-1}; Table S7(Guédron et al., 2014a; Wurl et al., 2014)].

III.4. Discussion

III.4.1. Transfer of mercury contamination from mine to village: a mass balance

A total Hg distribution map (**Figure III.5**) was drawn up for the two villages of i) Dionko, located more than 5 km from the mining area and the Niger river, and ii) Saman, located close to the mining sites and the Niger River. Guinean artisanal gold miners move between sites throughout the year depending on where they find gold (Berriane et al., 2021; Dessertine, 2013; Grätz, 2004; Migration data portal, 2020; Petit-Roulet, 2025). Consequently, mining villages were established following the discovery of the first gold deposits, and are currently located at varying distances from the mining sites in operation. The Dionko mine topsoil's THg concentrations [~0.3 (0.3) ±0.05 µg g^{-1}, **Figure III.2**B] are slightly lower than those at Saman (0.6 (0.6) ±0.2 µg g^{-1}). This could be attributed to the proximity and downwind location of the Saman village, which may supply atmospheric Hg to the mining area (Davies and Notcutt, 1996; Pirrone et al., 1996).

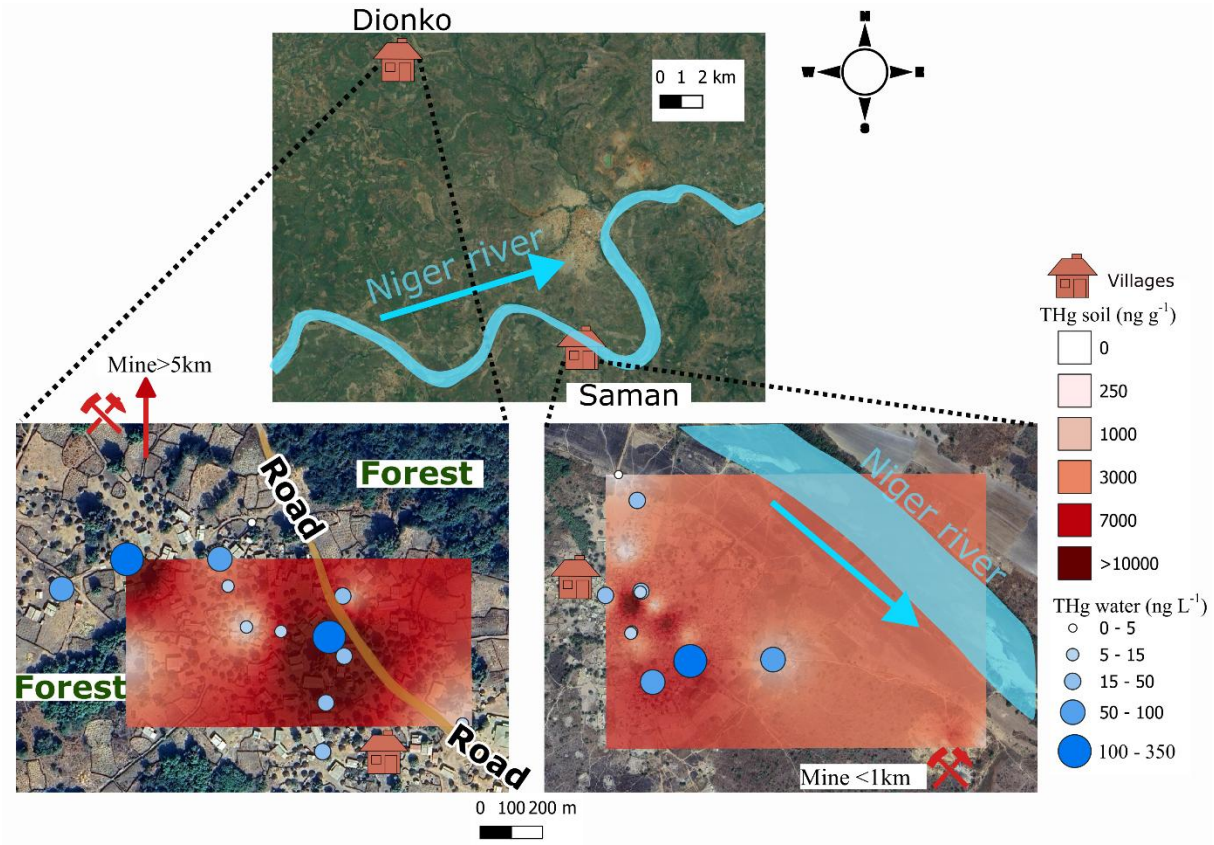


Figure III.5. *IDW (Inverse Distance Weighted) interpolated map of mercury concentrations in surface soils at Dionko and Saman. Top: map showing the location of the two villages in relation to the Niger River. Bottom left: interpolated soil map of Dionko village in the background, with unfiltered water superimposed in blue. Bottom right: interpolated soil map of the village and Saman mine with unfiltered water superimposed in blue.*

Higher Hg concentrations in the center of both villages are on average 17-times higher than those measured at the mining sites, clearly showing the transfer of mining practices from the mines to the villages, which become the hotspot of Hg contamination. Thermodesorption experiments indicate that the high THg concentrations measured in the village center, where amalgams are burned in houses and tents, consist mainly of Hg0 resulting either from direct loss during amalgamation, or from the condensation of Hg0 emitted during amalgam burning (Grimaldi et al., 2015; Niane et al., 2014, 2019b). The highest THg concentrations are found in the village of Saman, reaching up to more than 10 µg g^{-1} (**Figure III.2**). Although lower in the village of Dionko, the high THg concentrations found in the forest topsoil (up to 1 µg g^{-1}, **Figure III.5**) located outside the village center, suggest that vegetation acts as an atmospheric Hg sink for soils through litterfall deposition, as reported in other regions worldwide (Fu et al., 2010; Tomiyasu et al., 2013, 2012; Yu et al., 2014; Feinberg et al., 2022).

Total Hg is predominantly stored within the upper 10 cm of topsoil compared to deeper horizons (Figs. 2 and 3), with Hg0 as the dominant form in both villages, indicating recent contamination by atmospheric Hg deposition (Tomiyasu et al., 2012). To assess the amount of Hg deposited over village

and mining sites during the past decades, Hg stocks per surface unit were calculated for both study sites using the average soil bulk density (2.65 t m^{-3}) published for tropical soil (Brady, 1984; Adekiya et al., 2021; Avornyo et al., 2023; Padonou et al., 2025) and correcting for geochemical background values (0.14 µg g^{-1} for THg and 0.018 µg g^{-1} for Hg0). The surface area of each village was defined as the area covered by houses (i.e., 0.12 and 1.05 km^2 for Dionko and Saman, respectively), while mining site area was defined as those covered by ore extraction holes (i.e., 0.02 and 0.19 km^2 for Dionko and Saman, respectively).

Table III-1*. Total and elemental mercury stock per surface unit at the two mining sites and villages in Saman (1.05km^2) and Dionko (0.12 km^2).*

Sites	Surface (km^2)	THg (µg g^{-1})	THg stock (kg)	THg stock (g m^{-2})	Hg0 (µg g^{-1})	Hg0 stock (kg)	Hg0 stock (g m^{-2})
Saman mine	0.19	0.6 (0.6) ±0.2	31.1 (31.1) ±9.3	0.16 (0.16) ±0.05	0.2 (0.2) ±0.01	10.1 (10.1) 0.5	0.05 (0.05) ±0.003
Saman village	1.05	5.7 (4.6) ±2.0	1581.1 (1283.8) ±554.5	1.5 (1.2) ±0.5	3.5 (3.4) ±1.0	985.2 (944.3) ±285.2	0.93 (0.89) ±0.27
Dionko mine	0.02	0.3 (0.2) ±0.05	1.5 (1.3) ±0.3	0.08 (0.06) ±0.01	0.2 (0.2) ±0.03	1.1 (1.3) ±0.2	0.06 (0.06) ±0.01
Dionko village	0.12	10.0 (10.0) ±6.5	306.5 (306.5) ±197.5	2.7 (2.7) ±1.7	7.5 (7.5) ±0.3	229.2 (229.2) ±8.4	2.0 (2.0) ±0.07

At Saman village, Hg level per surface unit (1.5 (1.2) ±0.5 g Hg m^{-2}) was 9-fold higher than in mined soils (0.16 (0.16) ±0.05 g m^{-2}, **Table III-1**). The calculated stock of THg deposited in the village topsoil was estimated at 1581 (1284) ±554 kg, corresponding to an annual Hg deposition of approximately 38 kg over the past 42 years of ASGM activities in the area. It is worth mentioning that this estimate does

not take into account the possible dumping or recycling of mining residues in the village, or the potential loss of Hg through remobilization (erosion) and gaseous reemissions. The same calculation at Dionko village, yields a Hg level per surface unit of 2.7 (2.7) ±1.7 g m^{-2}, which is 33-times higher than the mined soils (i.e., 0.08 (0.06) ±0.01 g m^{-2}, **Table III-1**), and a stock of 306 (306) ±197 kg of Hg deposited in the village topsoil over the last 32 years of ASGM activities. This correspond to an annual Hg deposition of approximately 10 kg in the village, which is more than three-times lower than at Saman, despite a similar miner population but a tenfold smaller inhabited surface area. These findings highlight that Hg accumulation is more closely related to the intensity of ASGM activities, particularly the use of Hg0 for gold amalgamation, rather than the duration and proximity to mining operations. When normalized Hg fluxes to the age of the sites, the miner's village would have accumulated approximately 36 (29) ±12 mg m^{-2} yr^{-1} for Saman, and 84 (84) ± 53 mg m^{-2} yr^{-1} at Dionko, which is an order of magnitude higher than the values reported for ASGM impacted soils (0.65 to 420 $\mu g \cdot m^{-2} \cdot yr^{-1}$) in Venezuela and Amazonia (García-Sánchez et al., 2006; Gerson et al., 2022).

As the Hg stocks in the village' soil are high and composed of 69 ± 7% Hg0, the Hg0 re-emission to the atmosphere is expected to be high in Guinea's arid and warm conditions [average annual temperature of 27.2 ±2.7°C (Eludoyin et al., 2014; Loua et al., 2019)]. Previous studies have shown that under comparable meteorological conditions, such as solar radiation, soil temperature, and moisture, the soil Hg content controls the Hg volatilization into the atmosphere (Wang et al., 2005; Lin et al., 2010; Song and Vanheyst, 2005). Under relatively similar weather conditions, reported Hg0 emission rates in soil measured above ground using a flux chamber, display highly variable values, ranging from 0.045 up to 2.0 $\mu g\ m^{-2}\ h^{-1}$ (THg: 2.7 to 101 $\mu g\ g^{-1}$) in an open-pit gold mine in the USA (Gustin et al., 2003), 2.3 ± 2.4 $\mu g\ m^{-2}\ h^{-1}$ (THg: 170 to 614 $\mu g\ g^{-}1$) in a Chinese tropical surface soil impacted by ASGM (Wang et al., 2005), from 0.1 to10 $\mu g\ m^{-2}\ h^{-1}$ (THg: 15 to 494 $\mu g\ g^{-}1$) in areas disturbed by mining in the New Indria (USA) district (Gustin et al., 2000; Coolbaugh et al., 2002), between 0.03 and 27.6 $\mu g\ m^{-2}\ h^{-1}$ (THg: 0.4 to 9060 $\mu g\ g^{-}1$) in the silver cloud mine (USA) where soil THg levels range between 0.5 to 9060 μg Hg g^{-1} of (Engle et al., 2001); and up to 100 $\mu g\ m^{-2}\ h^{-1}$ (THg: 5 to 500 $\mu g\ g^{-}1$) in a highly contaminated industrial goldmining site in USA (Zhang and Lindberg, 1999). Based on the concentration levels in the two villages studied, and similar levels provided in the literature, a reasonable estimate range for re-emission would be between 0.05 and 3 $\mu g\ m^{-2}\ h^{-1}$ (reference herein). Hence, the theoretical time required to deplete the Hg0 stock present in the topsoils of the two villages would be between 35 (34) ± 10 to 2143 (1032) ± 616 years, and 76 (76) ± 3 to 4566 (4566) ± 160 years in Saman and Dionko, respectively. The soils of the mining villages therefore appear to be long-term atmospheric sources of Hg0, which will disperse to local and regional areas, including probable redeposition, gradually contaminating the surrounding environment, with possible exposure risk for local populations.

III.4.2. Potential health risk of Hg exposure in miner's villages

High Hg0 levels in village topsoil, indicate that ASGM practices potentially expose village residents to Hg0 via inhalation, dermal contact (mainly miners), or contamination of food (Tomicic et al., 2011; Nelson, 2013; Noble et al., 2016; Black et al., 2017). The reference atmospheric concentration of 0.3 µg m^{-3} Hg0 (USEPA, 1997), which are levels that might cause adverse health effects in people most sensitive to such chemical due to inhalation of Hg0, is likely greatly exceeded at amalgam burning sites for the two mining communities of Saman and Dionko. Similarly, a study conducted in Burkina Faso has reported an average concentration of 1,735 µg m^{-3} Hg in the air of a semi-enclosed amalgam burning hut with measured levels as high as 14.9 µg m^{-3} (Black et al., 2017). This study also reports that spectators inside and outside the hut were exposed to levels ranging from 100 and 1,000 µg m^{-3}, while those downwind of the open-air burning sites were exposed to levels exceeding the immediately dangerous to life and health (IDLH) threshold of 10,000 µg m^{-3}. Even at 10 to 12 meters away from the combustion site, Hg levels exceeded the permissible exposure limit (PEL) of 100 µg m^{-3} (ATSDR, 2014; Black et al., 2017). Similar observations are reported for ASGM communities in Columbia, where outdoor Hg concentrations ranging from 0.3 to 10 µg m^{-3} were reported around the gold store, with indoor levels reaching up to 1,000 µg m^{-3} , indicating persistent atmospheric contamination (Cordy et al., 2011). Although atmospheric Hg levels were not measured in the two villages, the high concentrations measured in the soil likely reflect significant Hg emissions during gold refining processes, and acute or chronic exposures during amalgam burning activities and in enclosed environments, respectively.

High Hg levels in well water may also represent another exposure pathway for local populations. To identify the source of well contamination, the spatial distribution of THg_{UNF} in wells was compared with that of topsoils. A spatial overlap is observed between Hg-rich topsoils and THg_{UNF} hotspots in groundwater (**Figure III.5**), suggesting that Hg originates from contaminated topsoil particles eroded by wind erosion or surface runoff, and potentially from direct Hg0 depositions. Well type also appears to influence the contamination level, as only open match the values in the surrounding soil, unlike closed wells do not, which are protected from atmospheric inputs. The highest THg_{UNF} concentration up to **350 ng L^{-1}** in groundwater found at the Saman ASGM site (**Figure III.4**) exceeds background Hg levels in pristine groundwater (<0.04 ng L^{-1} to 10 ng L^{-1}) reported in West Africa and Europe (Bollen et al., 2008; Charlet et al., 2017; Kowalski et al., 2018; Maha et al., 2024), but remain well below levels reported near ASGM sites in West Africa [1000 to 9000 ng L^{-1} (Lusilao-Makiese et al., 2014; Somé et al., 2016; Aliyu Haruna Sani et al., 2023)]. This maximum concentration is well below the WHO guideline value of 6000 ng L^{-1} for THg in drinking water (World Health Organization, 2011, 2017), and below the sub-guideline levels (600 to 2000 ng L^{-1}) of chronic exposure, which can lead to neurological symptoms such as tremors, fatigue, and impaired renal function in pregnant women (Arisawa et al.,

2000; Zhang et al., 2020). In contrast to THg, $MeHg_{UNF}$ levels (< 2 ng L^{-1}) are low, and represent less than 10 % THg_{UNF}. Considering an average daily consumption of 2 L of drinking water for an adult with a body weight of 70kg, and an average $MeHg_{UNF}$ concentration of 1.4 ng L^{-1}, the daily MeHg intake would be of 2.8 ng day^{-1} and 0.04 ng kg^{-1} day^{-1}, which is in the upper range of the estimated average daily intake of 0.0007 ng kg^{-1} day^{-1} to 0.05 ng kg^{-1} day^{-1} for an adult in the USA (USEPA, 2001; Holmes et al., 2009). Hence, although villager rely daily on these unfiltered water source, yet, no epidemiological data are available and the potential **risk** of **chronic exposure of** this population via drinking water cannot be assessed.

III.5. Conclusion

This study demonstrates that artisanal and small-scale gold mining (ASGM) practices in Guinea result in moderate Hg concentration in topsoil, but severe Hg contamination in miner villages, where ores are transported and amalgamated by artisanal miners directly within residential areas. This Hg accumulates primarily in the top 10 cm of soil, and remains highly prone to environmental dispersion through wind, runoff, and volatilization. Such high Hg levels in the topsoil, contribute to the contamination of wells, the main source of drinking water for local populations.

The high Hg concentrations in topsoils of these village include up to 75% of Hg0. This highlights a potential risk of exposure to Hg0 vapor, mainly during the burning of amalgams, for population living in these mining villages. Epidemiological studies should be conducted to assess the current health status of local communities. This would provide critical insights for risk assessment and guide future outreach strategies to inform and protect local populations. This work underscores not only the environmental burden of ASGM-related Hg pollution but also its potentially profound and long-lasting implications for human health in mining communities. Sustainable mining practices (including Hg recycling), regulation of its use, and community education are essential steps to mitigate ongoing contamination and protect vulnerable populations and soil biodiversity in Guinea.

CRediT authorship contribution statement

D. Dabre: Conceptualization, Data curation, Formal analysis, Investigation, Methodology, Validation, Writing - original draft, Writing – review & editing. S. Guédron: Conceptualization, Data curation, Formal analysis, Methodology, Resources, Supervision, Validation, Writing - original draft, Writing – review & editing. Y.Maiga: Methodology, Supervision, Writing – review & editing. A.A. Konaté: Methodology, Supervision, Writing – review & editing. I.K Doumbouya: Data curation, Writing – review & editing. J.Gardon: Methodology, Supervision, Writing – review & editing. S. Campillo: Data curation, Formal analysis & Methodology. S. Sentenac: Data curation, Formal analysis & Methodology. O. Bruneel: Methodology, Supervision, Writing – review & editing. O. Ouedraogo: Methodology, Supervision, Writing – review & editing. E. Resongles: Data curation, Formal analysis, Methodology, Writing – review & editing.

Conflicts of interest statement

There are no conflicts to declare.

Data availability

The data supporting this article have been included as part of the Supplementary Information.

Acknowledgments

This research is the product of a joint project between the University Joseph KI-ZERBO (Ouagadougou, Burkina Faso), and the French National Research Institute for Sustainable Development (IRD, France). This publication was made possible through support provided by the African centers of excellence (ACE Partner - IRD and AFD) and by a grant from LabEx
OSUG@2020 (Investissements d'avenir – ANR10 LABX56). We thank the IRD Representation in Burkina Faso for their collaboration with the Project. We would like to thank the Prefecture of Guinea, the Prefect, and the Deputy Prefect for their hospitality and assistance in facilitating our work in the mining villages. Our sincere thanks also go to Mr. Condé Moussa, a brother who facilitated our work on the sites and in the mining villages. We would also like to personally thank Mr. Kataka Mawelamba, Mr. Patrick Ouiminga, Ms. Sylvie Kabré, and Ms. Françoise Nikiéma from IRD, who helped me prepare for the mission, send samples from Guinea to France, and purchase consumables. Our thanks also go to Simona Denti, formerly recruited at Isterre, for her help in purchasing equipment and robust field devices. We would like to thank Robert Mason from the University of Connecticut in the USA, who trained us and provided us with the equipment needed to analyze methylmercury in our soils and sediments. We thank also Delphine Tisserand from the Isterre laboratory, who trained us for DOC analysis. We would like to thank Naomi Nitschke for her advices during the paper writing. Our sincere

thanks go to Pr A.S.Ouattara, the recently deceased director of the host laboratory at the Université Joseph kI-ZERBO, who provided us with the space needed to condition our samples. We also thank Mr Kataka Mawelemba from IRD Burkina, Dr Cheick Omar Tidiane Compaoré and Palé Dagoro from University Joseph KI-ZERBO, who welcomed me warmly to the LAMBM laboratory and encouraged me during my fieldwork in the remote and potentially dangerous gold mining areas of Guinea.

III.6. Supplementary information



Figure S1*: Photographs (credit D. Dabre) of artisanal and small-scale gold mining (ASGM) process and sites in Kouroussa, Upper Guinea. Photographs of Dionko site (A to E), with A) ASGM site; B) gold bearing ore extraction from pits; C) ores crushing on ASGM site; D) ores grinding in a mortar on ASGM site; E) ores washing & amalgamation on ASGM site to assess for gold abundance. Photographs of Saman site (F to L), with F) ores crushing in the miner's village; G) ores mechanical grinding by men in the miner's village; H) ores washing by women in the miner's village; I) ore amalgamation and burning by women in open air in the miner's village; J) ore burning by women in a miner's village house; K) counter for the burning of amalgam and the repurchase of gold by the Djatis (person in charge of a counter where he burns amalgam and buy gold); L) liquid mercury used by Djatis; and M) counter of the Djatis in the miner's village. N) open well in the Dionko miner's village; O) closed-well equipped with a pump in the Saman miner's village.*

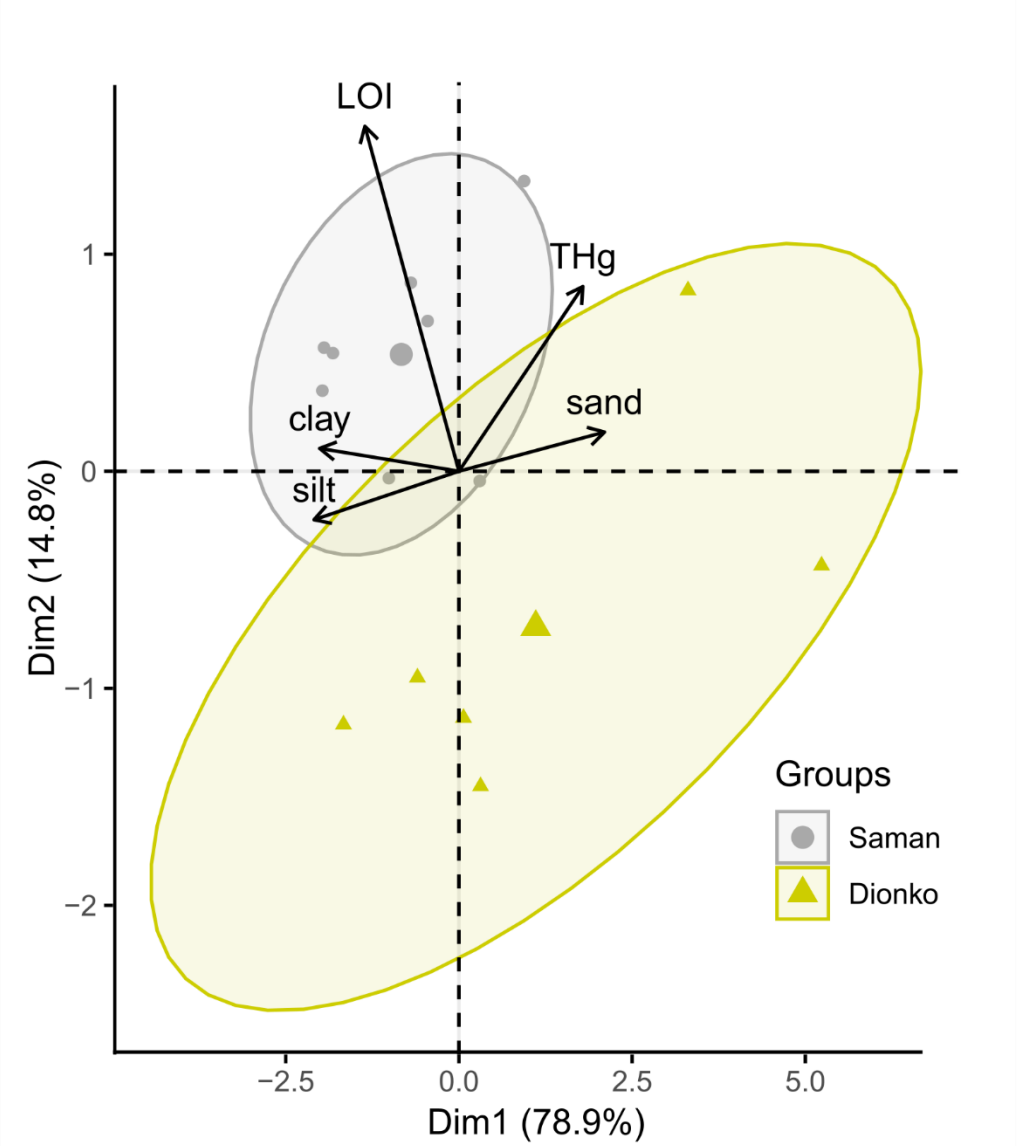


Figure S2. *Principal component analysis (PCA) for soil profiles in Saman (gry circles) and Dionko (dark yellow triangles). The first principal component (78.9%) has high positive loading on total mercury (THg) and sand, and negative loading on clay and silt. The second principal component (14.8%) has high positive loading on LOI and THg.*

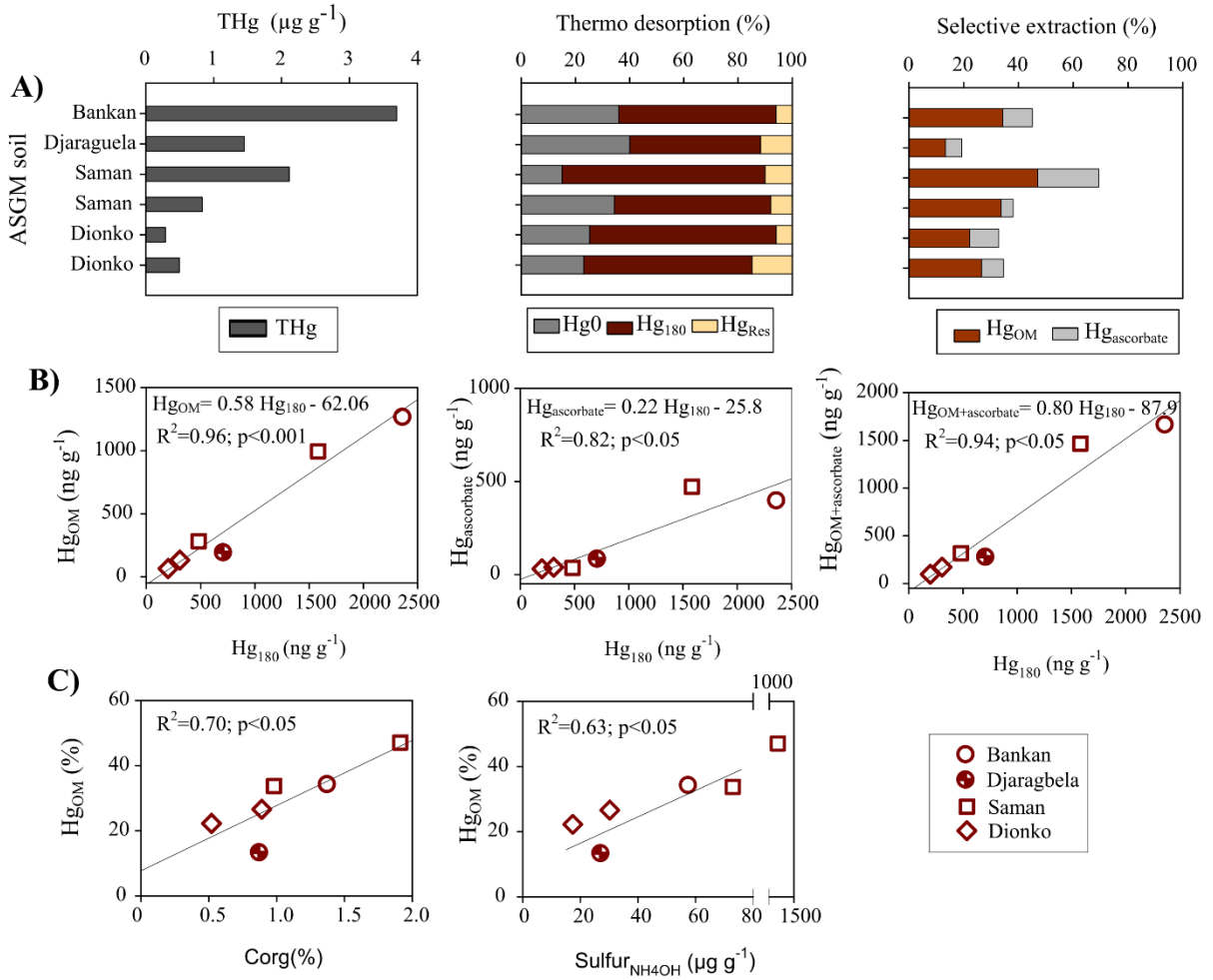


Figure S3. *From left to right: A) Total mercury concentration (THg) (left panel), thermodesorption (middle panel) showing Hg0 released at 80°C, Hg_{180} released at 180°C, Hg_{Res} obtained by difference between Hg released at 550°C minus the one released at 180°C, and Hg associated to organic matter (Hg_{OM}) and non-crystalline Fe oxides ($Hg_{ascorbate}$) recovered after NH_4OH and ascorbate selective extraction, respectively, both performed after removing the elemental Hg (Hg0) at 80°C. B). Biplot between Hg_{OM} and Hg_{180} (left panel); $Hg_{ascorbate}$ and Hg_{180} (middle panel) and $Hg_{OM+ascorbate}$ and Hg_{180}. The positive correlation (R^2 =0.94, p<0.05) between Hg_{OM}+$Hg_{ascorbate}$ and Hg_{180} with the near unity slope ($Hg_{OM+ascorbate}$ = 0.80*Hg_{180} - 87.9), confirms that thermodesorption at 180°C extract both Hg bind to organic matter and non-crystalline Fe oxide, consistently with observation made for Burkina Faso soil (Dabre et al., 2025). C) Biplot between Hg_{OM} and C_{org} (left panel); Hg_{OM} and sulfur extracted by NH_4OH (middle panel). The positive correlation between Hg_{OM} and C_{org} (R^2=0.7, p<0.05) confirms that Hg extracted by NH_4OH is mainly associated with carbon functional group of organic matter and the positive correlation between Hg_{OM} and sulfur extracted by NH_4OH (R^2=0.63, p<0.05) suggests that Hg is complexed with sulfur-containing functional groups in OM, consistently with observations made for Amazonian soils(Guedron et al., 2009).*

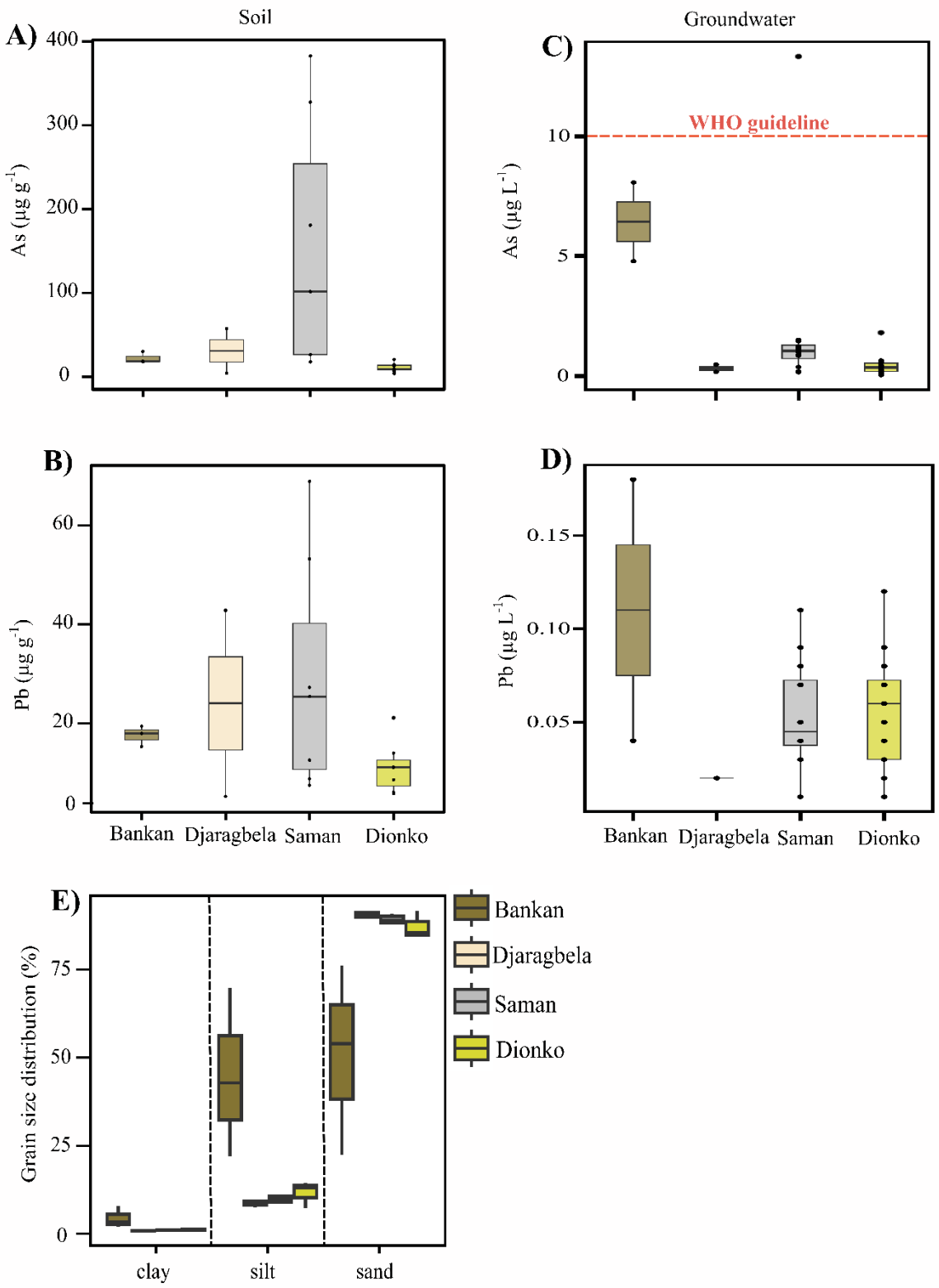
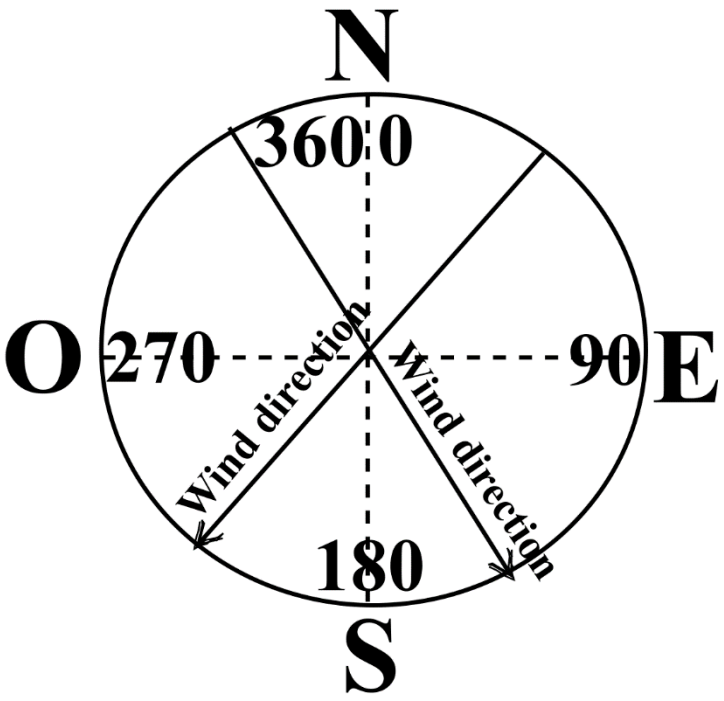


Figure S4. *Boxplot presentation of A) arsenic (As), and B) lead (Pb) concentrations in soils, and C) arsenic (As), and D) lead (Pb) concentrations in groundwater, and E) grain size distribution in soils for the Bankan, Djaragbela, Saman and Dionko ASGM sites. Pb and As concentrations in groundwater are low in all site, and above the WHO guideline of 10 µg L^{-1} for drinking water, excepted for one groundwater at Saman. This latter value is consistent with the As content in Saman ASGM soil, which exceed 300 µg g^{-1}, showing that mined soils are geogenically enriched in As, possibly resulting from contamination by ore residues.*



classes (degree)	Wind direction	event number	Mean wind direction (degree)
0 -90	N-E	2809	40.07
90 -180	E-S	3985	140.5
180 - 270	S-O	4198	221
270 - 360	N-O	1586	319.5

Figure S5. *Wind direction from January to December 2024 (sources: https://content.meteoblue.com/fr/recherche-education/specifications/variables-meteo/vent), indicating that dominant winds are from North-East and North-West at that time.*

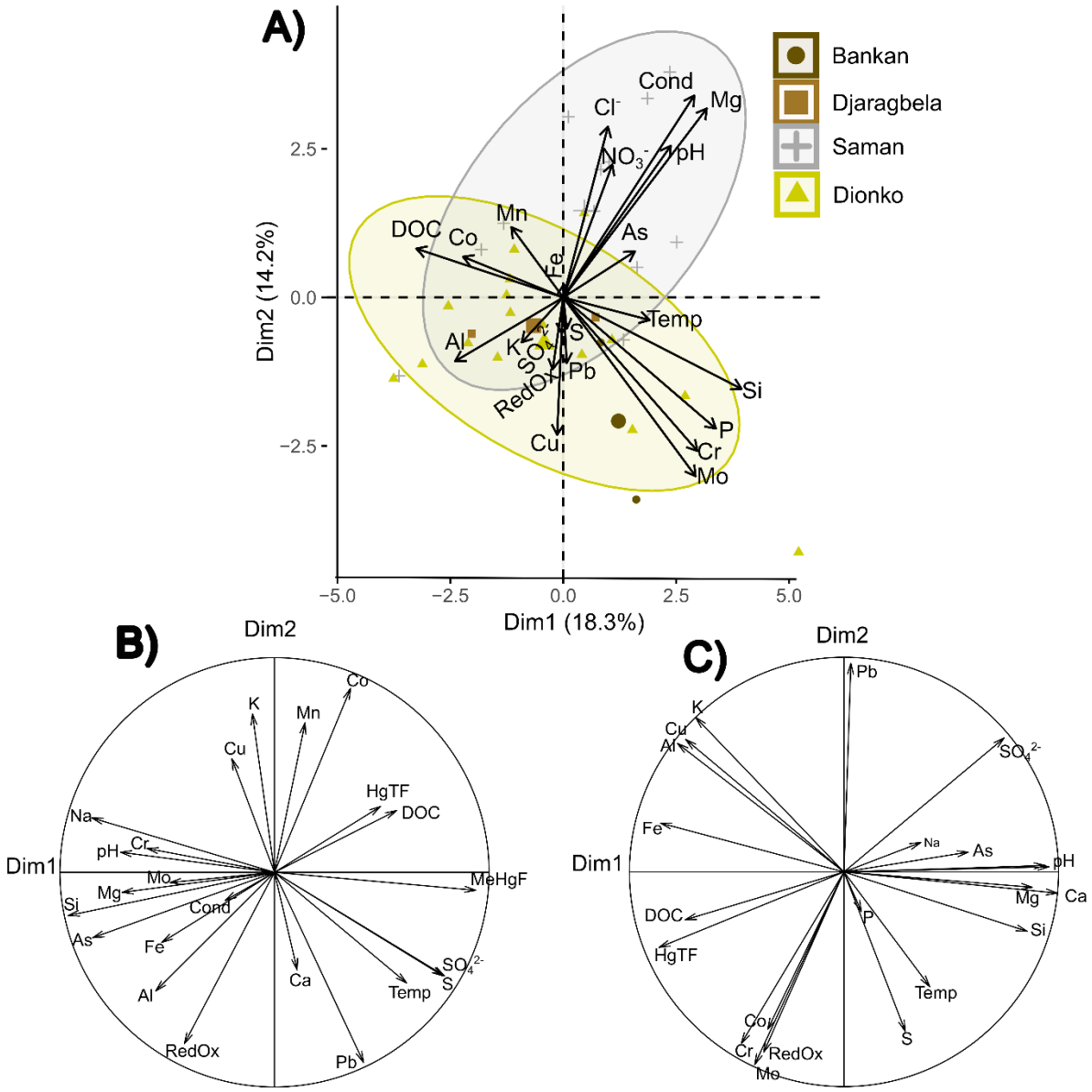


Figure S6. *Principal Component Analysis (PCA) for filtered groundwater showing in A) the physico-chemical parameters and water chemical composition for the Bankan, Djaragbela, Saman and Dionko ASGM sites. B) PCA for filtered groundwater showing physico-chemical parameter and chemistry for groundwater collected at Dionko. C) PCA) for filtered groundwater showing physico-chemical parameter and water chemical composition for groundwater collected at Saman. The first principal component has high positive loading on total THg_F and dissolved organic carbon (DOC) for both Saman and Dionko groundwater, which supports that DOC is the most likely ligand for mercury in Saman and Dionko waters. A high positive loading is also found on total sulfur (S), sulfate (SO_4^{2-}) and methylmercury (MeHg) for both Saman and Dionko sites, suggesting sulfate reducing bacteria as possible main Hg methylators.*

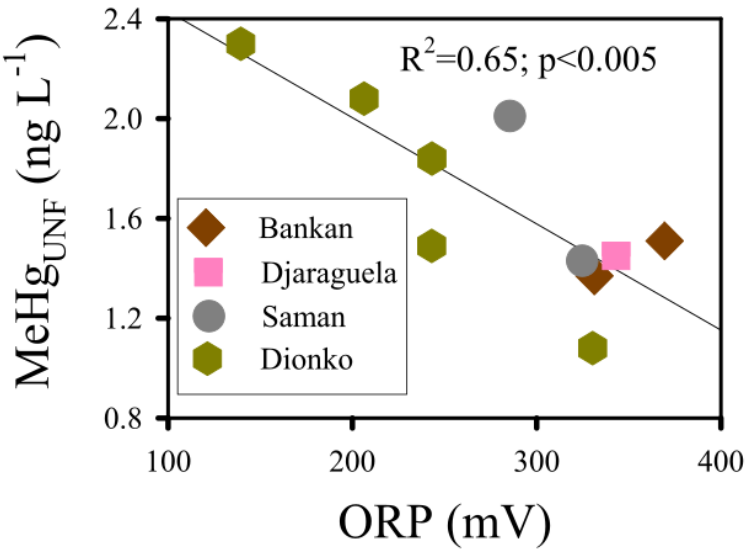


Figure S7. *Biplot between unfiltered methylmercury ($MeHg_{UNF}$) and oxido-reduction potential (ORP) in unfiltered groundwater collected in village's wells. This supports that (bio)methylation or MeHg accumulation is favoured in more reductive conditions.*

Table.S.1. *Background mercury level and speciation in Guinea pristine soil (Kindia, Mamou, Dabol, and Cisela) obtained by thermodesorption (i.e., Hg0 released at 80°C, Hg_{180} (~ $Hg_{OM+ascorbate}$) released at 180°C after removing the elemental Hg (Hg0) at 80°C, and Hg_{Res} obtained by difference between Hg released at 550°C minus the one released at 180°C), granulometry of soils and organic matter content obtained by loss on ignition (LOI_{550}) at 550°C.*

Location	Distance to the ASGM site (km)	THg (ng g^{-1})	Hg0 (%)	Hg_{180} (%)	Hg_{Res} (%)	clay (%)	Silt (%)	sand (%)	LOI_{550} (%OM)
Kindia	364.2	46.7	9.3	51.8	38.9	6.5	35.8	57.7	11.3
Mamou	247.3	105.3	9.3	65.7	25.1	5.9	40.6	53.6	24.2
Dabola	159.7	49.3	28.7	52.8	18.5	8.5	46.2	45.3	10.2
Cisela	67.2	51.1	9.6	67.7	22.7	9.8	56.1	34.1	12.1
Mean	Over 67km	63.1	14.2	59.4	26.5	6.6	41.2	52.3	13
(Med)		(50.2)	(9.4)	(59.3)	(23.9)	(6.3)	(40.8)	(53.2)	(11.5)
SEM		14.1	4.8	3.4	4.2	1.2	4.8	6.0	2.8

Table S2. *Average, median (between comas) and standard error (SD) concentration of organic carbon (C_{org}), granulometric fractions (sand, clay and silts), total mercury (THg), methylmercury (MeHg), arsenic (As), and lead (Pb) in pristine and contaminated soils collected at Bankan, Djaragbela, Saman and Dionko ASGM sites. N.D. indicates not determined.*

sites	C_{org}	Clay	silt	sand	THg (ng g^{-1})	MeHg (ng g^{-1})	As (µg g^{-1})	Pb (µg g^{-1})
pristine (N=4)	N.D	6.6 (6.3) ±1.2	41.4 (40.8) ±3.9	52.3 (53.2) ±4.9	63.1 (50.2) ±14.1	N.D	N.D	N.D
Bankan (N=4)	3.4 (3.3) ±0.7	4.4 (3.3) ±1.5	44.8 (42.8) ±11.9	50.8 (53.9) ±13.5	6467 (5132) ±1813	0.35	27.5 (24.4) ±6.0	17.9 (18.5) ±0.9
Djaraguela (N=2)	0.7 (0.7) ±0.02	0.8 (0.8) ±0.1	8.6 (8.6) ±1.1	90.5 (90.5) ±1.2	1360 (1360) ±90.4	0.48	30.9 (30.9) ±26.7	24.1 (24.1) ±18.8
Saman (N=20)	1.0 (1.1) ±0.1	1.91 (1.03) ±0.54	15.5 (9.9) ±4.0	82.6 (89.0) ±4.6	3902.5 (2331) ±926	0.35 (0.39) ±0.04	152 (102) ±33.8	29.1 (25.4) ±5.3
Dionko (N=14)	1.1 (1.1) ±0.1	1.2 (1.3) ±0.1	11.7 (13.1) ±1.0	87.2 (85.5) ±1.08	5555 (2054) ±1685	2.07 (1.67) ±0.53	11.1 (9.4) ±1.5	11.1 (11.1) ±1.4

Table S3. *Majors (Al, Ca, Fe, Mg, Mn, S and Ti), traces elements (Pb, Cu, Zn, Cd, Cr, As, and Se) obtain by complete acid digestion and by selective extractions (i.e., NH_4OH and ascorbate) in topsoil. <DL indicates below detection limit; (Med) indicates median; (SEM) indicates standard error of the mean. Med and SEM appear only if there are at least 2 values.*

		Major (mg g^{-1})							**Traces (µg g-1)**							**NH_4OH (mg g^{-1})**		**Ascorbate (mg g^{-1})**	
Site		Al	Ca	Fe	Mg	Mn	S	Ti	Pb	Cu	Zn	Cd	Cr	As	Se	Al	Fe	Al	Fe
Bankan	Mean	66.9	5.0	64.5	1.6	0.7	0.3	5.3	17.9	42.9	141.6	0.6	154.3	27.5	0.3	0.7	0.1	1.1	0.7
	Med	57.8	3.5	56.0	1.6	0.7	0.3	5.8	18.5	44.1	153.9	0.6	145.7	24.4	0.3	0.	0.05	0.3	0.4
	SEM	16.1	2.3	14.1	0.3	0.1	0.0	1.0	0.9	10.6	45.2	0.1	29.9	6.0	0.1	0.6	0.1	0.7	0.4
Djaraguela	Mean	18.9	2.6	22.6	0.4	1.3	0.2	4.0	24.1	16.4	35.3	0.5	79.6	31.0	0.1	0.3	0.05	0.2	0.3
	Med	18.9	2.6	22.6	0.4	1.3	0.2	4.0	24.1	16.4	35.3	0.5	79.6	31.0	0.1	0.3	0.05	0.2	0.3
	SEM	1.5	2.0	7.5	0.1	1.2		2.0	18.8	9.9	13.7	0.2	15.9	26.7		0.06	0.01	0.04	0.2
Saman	Mean	43.6	3.7	51.0	2.8	0.7	0.6	3.7	29.1	91.5	152.9	0.7	162.7	152.0	0.4	0.3	0.1	0.4	0.5
	Med	29.2	3.6	43.1	2.5	0.7	0.2	3.2	25.4	45.8	99.4	0.5	165.0	101.6	0.3	0.1	0.07	0.3	0.4
	SEM	7.8	0.4	8.0	0.5	0.1	0.2	0.4	5.3	18.9	33.3	0.1	15.9	33.8	0.1	0.1	0.03	0.07	0.05
Dionko	Mean	30.1	2.3	30.8	1.0	0.3	0.2	3.4	11.1	13.8	84.9	0.5	126.6	11.1	0.2	0.5	0.2	0.4	0.3
	Med	20.0	2.7	20.2	1.0	0.3	0.2	3.1	11.1	12.8	55.0	0.6	57.0	9.4	0.1	0.1	0.2	0.2	0.2
	SEM	7.3	0.2	8.0	0.1	0.1	0.0	0.5	1.4	1.6	23.2	0.0	39.4	1.5	0.1	0.2	0.04	0.1	0.04

Table S4. *Mercury, methylmercury, arsenic and lead in surface topsoil from studies in Africa and other part of the world. (-) indicates no data available.*

soil Type	Location	THg (µg g^{-1})	MeHg (ng g^{-1})	As (µg g^{-1})	Pb (µg g^{-1})	Reference
pristine topsoil	Worldwide	0.02–0.25	-	0.1–35	-	Alloway (1995); Alfaro et al. (2015).
	South America	0.01–0.9	0.12±0.02 -		-	Guedron et al. (2009); Leiva G. and Morales (2013).
	Nigeria	<0.3	-		-	Adewumi and Laniyan (2020).
	Burkina Faso	0.3 ± 0.1	0.1±0.08		-	Dabré et al. (2025).
	Senegal	0.05–0.6	-		-	Niane et al. (2019).
	Guinea	0.14± 0.04	-		-	This study
ASGM topsoil	Guinea	0.3–0.9	0.3–0.5	65.6± 24.1	20.1±3.7	This study.
	Senegal	0.13–3.9	0.13–19		-	Thiombane et al. (2023); Niane et al. (2019); Gerson et al. (2018).
	Ghana	0.1 –40	-		-	Rajaee et al. (2015).
	South Africa	0.046–2.58	-		-	Lusilao-Makiese et al. (2014); Kamunda et al. (2016); Malehase et al. (2016); Shapi et al. (2020).
	South America	0.1–1.0	0.6±0.06		-	Fostier et al. (2023).
	Burkina Faso	2.4±1.4	0.1±0.04	46 ±21	18 ±5 3–49	Kagambega et al. (2014); Dabré et al. (2025).
Inhabitant zone topsoil	Guinea	12–18	-		-	This study
	Peru	1.1–32.3	-		-	Quispe Aquino et al. (2024).
	Indonesia	5.6–19	-		-	Arrazy et al. (2023).
	South America	0.005-0.04	0.2±0.09	-	-	(Guédron et al., 2025)

Table S5. *Physico-chemical parameters [pH, redox potential (Eh) and conductivity (cond.)], filtered total mercury (THg) and methylmercury (MeHg), arsenic (As), lead (Pb, sulfate (SO_4^{2-}) and dissolve organic carbon (DOC) concentration in filtered water, and THg and MeHg concentrations in unfiltered water collected in wells at Bankan, Djaragbela, Saman and Dionko ASGM sites, in the Niger River surface water, and in water used in mining process at Saman and Dionko ASGM sites. ° Indicate sites where river water is used for ore processing whereas the others use groundwater. CN indicates cyanidation*

					Filtered water						**Unfiltered water**	
Sample	Site	pH	Eh (mV)	Cond. (µS cm^{-1})	THg_F (ng L^{-1})	MeHgF (ng L^{-1})	As (µg L^{-1})	Pb (µg L^{-1})	SO_4^{2-} (mg L^{-1})	DOC (mg L^{-1})	THg_{UNF} (ng L^{-1})	$MeHg_{UNF}$ (ng L^{-1})
Ground water	Bankan (N=2)	6.4 (6.4) ±0.03	350.4 (350.4) ± 19.0	191.5 (191.5) ± 20.5	1.5 (1.5) ±0.02	0.4 (0.4) ±0.04	6.4 (6.4) ±1.6	0.1 (0.1) ±0.07	0.9 (0.9) ±0.06	0.2 (0.2) ±0.04	17.5 (17.5) ±1.84	1.4 (1.4) ±0.07
	Djaraguela (N=3)	6.3 (6.3) ±0.1	309.9 (309.9) ±27.1	110.6 (110.6) ±24.3	1.3 (1.3) ±0.29	0.4 (0.4) ±0.1	0.3 (0.3) ±0.1	0.02	0.9 (0.9) ±0.09	1.8 (1.8) ±0.7	49.8 (49.8) ±28.9	0.8 (0.8) ± 0.5
	Saman (N=13)	6.7 (6.7) ±0.1	258.4 (259.4) ±11.6	339.3 (352) ±43.5	1.9 (1.3) ±0.5	0.4 (0.3) ±0.09	1.9 (1.1) ±1.0	0.05 (0.05) ±0.01	1.2 (0.9) ±0.3	1.8 (0.9) ±0.5	38.4 (21.6) ±14.41	1.47 (1.49) ±0.13
	Dionko (N=18)	6.3 (6.33) ± 0.08	246.6 (255.9) ±16.5	188.0 (172.5) ±33.8	1.06 (0.68) ±0.22	0.16 (0.05) ±0.04	0.98 (0.36) ±0.54	0.06 (0.06) ±0.01	11.11 (1.36) ±5.44	2.6 (0.6) ±1.3	41.8 (21.8) ±13.4	1.8 (1.8) ±0.1
Surface water	Niger (N=3)	8.7 (8.4) ±0.5	275.8 (270.7) ±18.5	70.3 (76.3) ±13.9	1.7 (1.4) ±0.5	0.08 (0.06) ±0.04	0.2 (0.1) ±0.01	0.03 (0.03) ±0.01	0.02	2.3 (1.9) ±0.3	77.5 (56.7) ±42.3	0.6
	Niger CN (N=2)	7.1 (7.1) ±0.6	244.3 (244.3) ±105.7	56.1 (56.1) ±10.4	1.5 (1.5) ±0.4	0.3 (0.3) ±0.1	0.2 (0.2) ±0.02	0.04 (0.04) ±0.02	1.05 (1.05) ±0.1	0.9 (0.9) ±0.02	202.2 (202.2) ±185.9	0.6

Water use in mining process	Saman° (N=1)	6.9	239.2	145	3.9	0.50	2.32	0.01	1.26	2.21	114.9	0.5
	Dionko (N=2)	6.3 (6.3) ±0.001	75.6 (75.6) ±10.4	3912 (392) ±207	2.0 (2.0) ±0.01	1.16 (1.16) ±0.81	9.2 (9.2) ±0.6	0.04 (0.04) ±0.02	<DL	18.4 (18.4) ±4.5	94.8 (94.8) ±63.6	0.9

Table S6. *Majors (Al, Ca, Fe, Mg, Mn, S and Ti), traces elements (Pb, Cu, Zn, Cd, Cr, As, and Se) elements and anions (Cl^-, NO_3^-, PO_4^{3-}, and, SO_4^{2}) concentrations in filtered ground water. (<DL) indicates below detection limit; (Med) indicates median; (SEM) indicates standard error of the mean. Med and SEM appear only if there are at least 2 values.*

		Majors (mg L^{-1})							**Traces (µg L^{-1})**							**Anions (mg L^{-1})**			
Site		Al	Ca	Fe	Mg	Mn	S	Ti	Pb	Cu	Zn	Cd	Cr	As	Se	Cl^-	NO_3^-	PO_4^{3-}	SO_4^{2-}
Bankan	Mean	0.01	31.9	0.02	6.7	<DL	1.4	0.7	0.11	1.8	0.01	0.005	8.8	6.4	0.03	0.6	1.6	N.D	0.9
	Med	0.01	31.9	0.02	6.7	<DL	1.4	0.7	0.11	1.8		0.005	8.8	6.4	0.03	0.6	1.6	N.D	0.9
	SEM	0.004	0.16	0.01	0.6	<DL	0.2	0.1	0.07	1.3		0.003	5.9	1.6	0.02	0.1	0.7	N.D	0.1
Djaraguela	Mean	0.004	14.7	0.06	5.9	0.09	1.1	0.5	0.02	0.6	0.01	0.01	2.9	0.3	0.06	0.9	2.9	0.41	0.9
	Med	0.004	14.7	-	5.9	0.09	1.1	0.5	0.02	0.6	0.01	0.01	2.9	0.3	0.06	0.9	2.9	-	0.9
	SEM	0.001	2.8	-	3.7		0.1	0.04	0.001	0.3		0.01	0.9	0.1	0.05	0.4	0.8	-	0.1
Saman	Mean	0.02	42.0	0.02	13.3	0.10	1.0	1.2	0.05	0.4	0.04	5.6	4.3	1.9	0.04	10.8	45.9	0.5	1.2
	Med	0.01	45.1	0.01	12.6	0.03	0.9	1.0	0.05	0.2	0.03	8.2	3.9	1.0	0.03	6.5	44.3	0.5	0.9
	SEM	0.01	5.2	0.01	1.8	0.04	0.1	0.3	0.01	0.1	0.01	1.2	1.1	1.0	0.004	3.2	14.1	0.05	0.3
Dionko	Mean	0.02	15.3	0.15	4.8	0.03	9.9	1.0	0.06	0.4	0.04	4.3	5.5	0.4	0.03	2.4	21.6	0.7	11.1
	Med	0.01	16.1	0.05	4.5	0.02	10.4	0.9	0.06	0.4	0.02	6.0	0.8	0.4	0.02	1.7	4.8	0.8	1.4
	SEM	0.01	2.6	0.08	0.8	0.01	0.9	0.1	0.01	0.1	0.01	0.8	2.9	0.1	0.01	0.7	15.8	0.1	5.4

Table S7. *Mercury, methylmercury, arsenic and lead in groundwater from studies in Africa and other part of the world. (-) indicates no data available.*

water Type	Location	THg ($ng\ L^{-1}$)	MeHg ($ng\ L^{-1}$)	As ($\mu g\ L^{-1}$)	Pb ($\mu g\ L^{-1}$)	Reference
Filtered	Guinea	1.4 ±1.2 up to 7.5	0.2 ± 0.2		0.01–0.17	This study
	Burkina Faso	1.3 ±0.4	0.5 ± 0.1	14 ±11	0.05±0.01	Dabré et al. (2025).
	Burkina Faso	-	-		0.6–9.2	Sako et al. (2016).
	Mexico	-	-	<6–8 105–450	-	Wurl et al. (2014).
	South America	1.5±1.8	0.06±0.03	-	-	(Guédron et al., 2025)
Unfiltered		50±13, up to 350	1.4 ±0.6			This study
	Burkina Faso	530–4920		-	-	Somé et al. (2016).
	Burkina Faso	2.5 ±0.5	0.6 ±0.1	-	-	Dabré et al. (2025).
	Kenya	1010–3300	-	-	-	Lusilao-Makiese et al. (2014).
	Nigeria	1000–9000	-	-	-	Aliyu Haruna Sani et al. (2023).
	Ghana	6–7160	-	-	-	Rajaee et al. (2015).

Given current knowledge about the transfer of mercury from mining sites to populated areas, and given the significant accumulation of mercury in the soil, concerns naturally arise about its migration into surface waters. It is therefore essential to study how this contamination spreads through aquatic ecosystems in Guinea.

Chapter IV

Impact of artisanal and small-scale goldmining on (methyl)mercury contamination of the Niger River in Guinea Republic: insights from sediment and fish bioaccumulation.

This fourth chapter focuses on the impact of gold mining activities on the contamination of the Niger River and its tributaries, as well as on fishery resources in the Republic of Guinea. It highlights the role of mercury (Hg) particulate emissions in the spread of contamination. The relatively high levels of mercury and methylmercury in the fish collected in this study suggest a health risk for communities dependent on fishing.

The article will be submitted to the journal Environmental Pollution.

Impact of artisanal and small-scale goldmining on (methyl)mercury contamination of the Niger River in Guinea Republic: insights from sediment and fish bioaccumulation.

D. Dabre[*1,2,4], S. Guédron[1], I.K. Doumbouya[4], C.O.T. Compaoré[2], Y. Maïga[2], O. Bruneel[3], J. Gardon[3], J. Fin[1], E. Resongles[3], A. A Konaté[4], S. Campillo[1], S. Sentenac[1], O. Ouédraogo[2], and R. Mason[5].

[1] Univ. Grenoble Alpes, Univ. Savoie Mont Blanc, CNRS, IRD, UGE, ISTerre, 38000 Grenoble, France

[2] Université Joseph KI-ZERBO, 03 BP 7021 Ouagadougou 03, Laboratoire de Microbiologie et Biotechnologie Microbienne (LAMBM), Burkina Faso

[3] HydroSciences Montpellier, University of Montpellier, CNRS, IRD, Montpellier, France

[4] Laboratoire de Recherche Appliquée en Géosciences et Environnement, Institut Supérieur des Mines et Géologies de Boké, BP 84, Baralandé, Boké, Republic of Guinea

Highlights:

- In Guinea, goldmining creates hotspots of mercury contamination in the sediments of the Niger River.
- Hg is mainly bound to organic matter and amorphous iron oxides present in the sediments.
- Elemental mercury dominates in downstream mining areas, limiting the production of methylmercury in these sediments.
- methylmercury levels in fish exceed health standards, posing risks to fishing communities.

Abstract

Artisanal and small-scale gold mining (ASGM) is the largest source of mercury (Hg) pollution on Earth. The recent boom of ASGM in West Africa gives rise to concerns about Hg contamination of aquatic environment, which is a key resource for local populations who consume fish. In this study Hg speciation and carrier phases were assessed in sediment, water, and fish of the Niger River and its tributaries in Guinea to document their levels and potential human exposure. Results show that downstream of ASGM activities, THg concentrations in the Niger River sediments reach hotspots exceeding 700 ng g^{-1}, with contamination primarily resulting from the discharge and sedimentation of Hg-rich particles. Thermodesorption experiments indicate that Hg in sediment is mainly bound to organic matter and non-crystalline iron oxides, two carrier phases known to favour Hg availability for methylating microorganisms. Methylmercury (MeHg) concentrations in surface sediment are generally low (<3 ng g^{-1}). Downstream mining areas, percentages of MeHg in THg in surface sediment decrease with rising proportions of elemental Hg (up to 78%THg), suggesting lower availability of Hg for methylating organisms. In contrast high MeHg concentration in fish (median 294 ng g^{-1}, wet weight), exceeded USEPA standards for human health protection, suggesting a health risk of MeHg exposure for communities dependent on fishing. More data is needed on MeHg levels in fish species of the Niger River. If these levels are confirmed, prevention campaigns must be implemented to inform and raise awareness among local populations whose diet is heavily reliant on fish consumption.

Keywords: (Methyl)mercury; Artisanal and Small-Scale Goldmining; water; Sediment

IV.1. Introduction

Artisanal and small-scale gold mining (ASGM) is currently one of the primary causes of aquatic habitat deterioration in tropical regions (Macdonald et al., 2014; Sissoko, 2019; Lino et al., 2019; Maiga et al., 2022; Ngom et al., 2023). Both terrestrial (alluvial) and riverine (dredging) ASGM activities degrade landscapes and waterways at scales from elemental to large river basins through deforestation, soil reworking, and erosion (Grimaldi et al., 2015; Dossou Etui et al., 2024). Aquatic biodiversity and ecosystem productivity are therefore impacted by these physical disturbances, including changes in the morphology of riverbeds, increase in river turbidity, and water quality degradation (Macdonald et al., 2020, 2015; Darko et al., 2023). Additionally, ASGM is responsible for environmental mercury (Hg) contamination, as elemental mercury (Hg0) is used in the gold amalgamation process (Grimaldi et al., 2015; Niane et al., 2019b). On a global scale, anthropogenic Hg emissions have increased by more than 300% between 1960 and 2021, with a relative decrease in emissions from northern countries, offset by a marked increase in several southern regions, particularly Africa and the Amazon where ASGM is booming (Brocza et al., 2024; Qiu et al., 2025). As a pervasive and volatile pollutant, Hg can travel significant distances in the atmosphere, ultimately contaminating terrestrial and aquatic ecosystems (Kumar et al., 2024). The Minamata Convention adopted in 2013, attempts to lower Hg emissions and phase-out the use of Hg in industrial processes and ASGM (UNEP, 2023).

Once released or deposited in aquatic ecosystems, Hg can be converted to methylmercury (MeHg), the most toxic Hg form that accumulates and biomagnifies in trophic chains (Gadd, 1993; Parks et al., 2013; Mason et al., 2019). Sulfate- and iron-reducing bacteria like *Desulfovibrio* and *Geobacter* can convert Hg^{2+} into MeHg by expressing the *hgcA* and *hgcB* genes, which are primarily responsible for methylation mainly in reducing aquatic environments (Parks et al., 2013; Gilmour et al., 2013; Martins et al., 2025). The methylation process depends on environmental factors, including the availability of sulfate and iron, pH, organic matter and dissolved oxygen content, as well as the microbial composition of sediments (Baptista-Salazar et al., 2021). Once produced, MeHg can bioaccumulate and biomagnify, leading to high concentrations of MeHg in fish at the top of the food chain (Ouédraogo et al., 2015). This can finally expose population whose diet rely on fish consumption, especially organisms at the end of the food chain, such as predatory species (Chain (CONTAM), 2012; Sunderland et al., 2018). MeHg has major neurotoxic effects, including cardiovascular impacts in adults and cognitive and motor development impairments in children, after passing through the placental and blood-brain barriers (Chan et al., 2003; Grandjean et al., 2010; Holmes et al., 2009). International authorities have established food safety standards, with a MeHg concentration limit of 0.5 $\mu g\ g^{-1}$ for the majority of fish (The European Commission, 2023), and a tolerated weekly intake (PTWI) of 1.6 µg of MeHg per kilogram of body weight (World Health Organization/FAO, 2007).

Sediments act as both a sink and a secondary source of Hg, where the Hg can be converted to MeHg under anaerobic conditions (Maurice-Bourgoin, 2000; Gray et al., 2002). (Methyl)mercury contamination in large river basins affected by ASGM is well documented. Total (THg) and methylmercury (MeHg) concentration in sediments of large tropical rivers range widely, from 9 - 95.3 ng g^{-1} THg up to 155 ng g^{-1} in the Madre de Dios and Tapajos rivers in the Amazon region (Diringer et al., 2015; Lino et al., 2019). Similar THg and MeHg concentrations were found in the Comoé and Etholié rivers in Côte d'Ivoire [18.7 – 97.8 ng g^{-1} THg and 0.7 – 4.3 ng g^{-1} MeHg; (Mason et al., 2019)], in the upper Volta basin in Ghana [11.9 to 70.3 ng g^{-1} THg, (Kwaansa-Ansah et al., 2011)]. Higher levels have been reported in west Africa Gambia River in Senegal [2 – 10 µg g^{-1} THg and 8 ± 7.8 ng g^{-1} MeHg (Niane et al., 2014, 2019a, 2019b)] and up to 20.4 µg g^{-1} THg in the Kokumbo River in Côte d'Ivoire (Kouadio et al., 2025). Fish from these large rivers have high concentrations in wet weight between 6 to 230 ng g^{-1} THg up to 500 ng g^{-1} THg and 6 - 185 ng g^{-1} MeHg up to 300 ng g^{-1} MeHg in the Comoe River in Cote d'Ivoire, the Loumbila reservoir and Nakambe River in Burkina Faso (Ouédraogo and Amyot, 2013; Ouédraogo et al., 2015; Mason et al., 2019, 2022). Similar concentrations of 3.3 – 980 ng g^{-1} THg; 1.1-69.5 ng g^{-1} MeHg were found in the Pra River and the upper Volta basin in Ghana (Donkor et al., 2006; Oppong et al., 2010; Kwaansa-Ansah et al., 2011). Thus, fish, particularly predatory and long-lived species whose Hg concentrations reflect long-term exposure and ecosystem contamination levels, are widely used as bioindicators for Hg contamination (De Paula Gutiérrez and Agudelo, 2020). More specifically, together, sediment and fish analyses provide complementary indicators for assessing the extent and ecological risks of Hg pollution in large tropical river systems (UNEP, 2023).

The Niger River, the primary waterway of West Africa, flows through multiple countries and is supplied by various tributaries, many of which are affected by ASGM. Today, no reliable data is available on Hg and MeHg levels in sediments and fish in the Niger River and its tributaries. This data deficiency hinders accurate risk assessments for communities reliant on fish from the Niger River. In order to fill these gaps for the first time in the Niger River and its tributaries at Kouroussa region in upper Guinea, this study will focus on three aspects. i) Firstly, quantifying Hg and MeHg in sediments, surface water, porewater, and fish in the Niger River and its tributaries at Kouroussa, Guinea. ii) Secondly, identifying the mineral and organic phases that act as carriers of Hg and assessing their involvement in methylation. iii) Finally Assessing the potential risk to human health in relation to health thresholds (USEPA, EU, WHO).

IV.2. Materials and Methods

IV.2.1. Environmental settings and sampling sites

The Republic of Guinea is located in West Africa and divided into four regions, including the Atlantic coastal area in the west (lower Guinea), a savanna area in the North-East (upper Guinea), the central mountainous region (medium Guinea), and a forested area in the South-East (Forest Guinea, **Figure IV.1**). The climate is tropical and divided into a dry season (from November to April) and a rainy season (May to October), which duration varies between regions (MMG, 2010; Konaté et al., 2022).

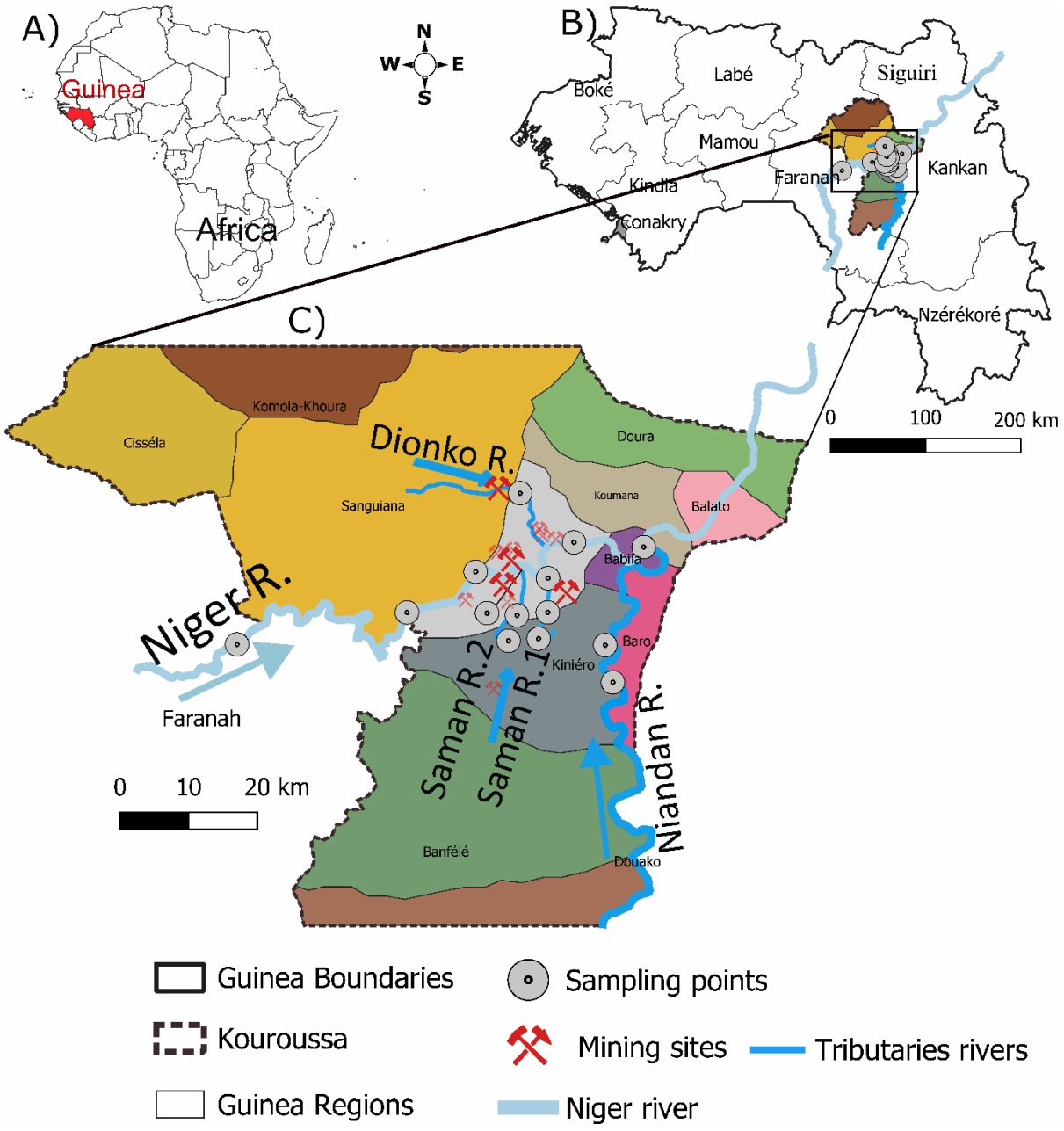


Figure IV.1. *Map of study area showing A) Guinea in Africa; B) the study region Kouroussa location in Guinea and C) Sampling sites along the main studied rivers.*

The Niger River is sources in the southern Loma Mountains (800m a.s.l.) and then flows north-east through the upper Guinea, where the climate in drier. In this study, the Niger River was sampled in the Kouroussa region in Upper Guinea. Gold deposits are numerous in the northwest of Kouroussa, including those of Siguiri and Sankarani in the Nzérékoré region (**Figure IV.1**B). These sites are mined since ca. 1932, and today include 27 mining sites in Kouroussa, and 260 in Siguiri (MEEF, 2021; PROJEG, 2018; Sidam-Minorex, 1998). Gold is mainly extracted from pits performed through soil to reach the ore deposit bellow the ferralitic soils, which are mainly composed of kaolinites and iron oxides (Maignien, 1958).

The samples were collected between March and April 2024 in the Niger River and its tributaries, including two permanent tributaries (Niandan and Saman rivers), and an intermittent tributary (Dionko river), which was dry at the time of the study (**Figure IV.1**C). Sample collection along the Niger stream was performed from an upstream location (Faranah, site Fa) to sites located downstream the Kourousa mining area, which includes at least 12 mining sites (**Figure IV.1**C), including four main mining sites namely Saman, Diaraguela, Bankan and Dionko (large dark red symbol in **Figure IV.1**C), and other smaller mining sites (small pale red symbols in **Figure IV.1**C).

IV.2.2. Sample collection and conditioning

At each sampling site, surface water, suspended solids, sediment porewater and cores were collected to document the impact of mining operations on the Niger River ecosystem.

Surface water physico-chemical parameters (pH, Eh, conductivity, and ORP) were simultaneously monitored using a Hach® multiparameter probe (HQ4300). Surface water samples were collected following ultra-trace protocols by Cossa and Gobeil (2000). Briefly, unfiltered water (UNF) samples were collected at each sampling location in acid washed 250 mL FEP containers. Filtered (F) samples analysis were collected after filtration through 0.45 µm PVDF (sterivex filters, Millipore) and collected into i) FEP vial for Hg speciation analysis, ii) 15 mL polyethylene (trace-grade, falcon) tubes for cation and anion analysis, and iii) 20 mL pre-burned (550°C) amber borosilicate vials for dissolved organic carbon (DOC) analysis. Filtered samples for Hg speciation analysis were acidified with HCl (0.5%, v/v, trace grade – Baker). Samples for cation analysis were acidified with HNO_3 (2%, v/v, trace grade – Baker), and samples for DOC with 0.1 N HCl (trace grade – Baker) (Némery et al., 2013). All samples were kept in the dark at 6°C in double bags, until analysis. Samples for anions (nitrate, chlorine, and sulfate) were kept frozen (-20°C) until analysis.

Suspended solid were collected through filtration onto 0.45 µm PVDF (47mm diameter filters, Merck Millipore Ltd). In the laboratory, filters were air-dried in a laminar flow hood for 48 h, and weighed to determine the amount of particle.

Sediment porewater were collected on site using microporous polymer tube samplers (rhizon® SMS, Rhizosphere Research Products) inserted vertically into the sediment at 5 cm depth (Guédron et al., 2012) and collected as for filtered surface waters.

Surface sediments (0 to 5 cm depth) were collected by merging four subsamples covering an area of about 12 m² on river's shores, and stored in sterile bags (Whirlpack®). Sediment cores (12 to 25 cm deep) were collected manually with a 66 mm-diameter PVC tubes from the banks of the rivers, below a 0.2 to 0.5-meter-deep water column (Fig. S1A). Cores were then sliced on site every 2-cm. The sediment in contact with the coring tube was removed to avoid contamination, and each slice was stored in sterile plastic bags (Fig. S1C). All samples were kept in a fridge at 4°C in the field, and subsequently frozen, freeze-dried, sieved at 1.25 mm and crushed to obtain a powder (<63 µm) for chemical analysis in the laboratory. For each sample, an aliquot was kept to determine the grain size distribution.

Eleven fish samples were procured from local fishermen along the Niger River and its tributaries. Each fish was photographed, measured, and weighed, then identified at the genus level (Table S1; Fig. S1). For each individual, a ~ 5 g muscle tissue sample was collected for Hg speciation analysis. Samples were dried on site in aluminium bags at 50°C for transportation, and subsequently freeze-dried, and ground into a fine powder in the laboratory.

IV.2.3. Analytical methods

IV.2.3.1. Mercury speciation in water, sediment and fish

Total Hg contents in filtered (THg_F) and unfiltered (THg_{UNF}) water (surface and porewater) were measured using cold vapor atomic fluorescence spectrometry (CV-AFS, Model Tekran® 2500) after converting all Hg species to Hg0 (Guedron et al., 2011; Guédron et al., 2020). Methylmercury (MeHg) in filtered ($MeHg_F$), unfiltered ($MeHg_{UNF}$) water and PVDF digestate samples was measured using an ethylation purge and trap gas-chromatograph, cold vapour atomic fluorescence spectroscopy (GC-CVAFS) analysis (Tekran®, model 2700) following established procedure (U.S. Environmental Protection Agency, 1998; Munson et al., 2014; Guédron et al., 2017). Field and analytical blank values never exceeded 0.4 ng L^{-1} for THg and 0.05 ng L^{-1} for MeHg.

Total mercury (THg) in sediment and fish samples was measured by atomic absorption spectrophotometry (AAS) using automated mercury analysers [AMA 254 (Altec), and DMA 80 (Milestone Inc.)] following catalytic decomposition and gold amalgamation (Guedron et al., 2009). Repeated analysis of the certified international reference material (CRM) ERM CC 141 (European Commission; 0.078 ± 0.003 µg g^{-1}, *N*=7; certified value: 83 ±17 ng g^{-1}) yielded the measurement accuracy for sediment. The certified reference materials DORM-4 (Dogfish muscle, National Research Council, Canada, certified value: 0.410 ±0.055 µg g^{-1}) and TORT-3 (lobster hepatopancreas, National

Research Council, Canada, certified value: 0.292 ±0.022 µg g^{-1}) were employed for fish QA/QC, and the recoveries were respectively 100 ± 10% (*N*=3) and 100 ± 7% (*N*=3).

Methylmercury (MeHg) in sediment and fish samples was measured after digestion in KBr (18%), 1M $CuSO_4$ and 6N HNO_3 (trace – Baker) respectively, and ethylation with $NaBET_4$ (sodium tetraethylborate) following published protocols for sediment (Hammerschmidt and Fitzgerald, 2001, 2004) and fish (Mason et al. (2019, 2022). The QA/QC was performed using ERM CC 580 (estuarine sediment, National Research Concil; 0.075 ± 0.003 µg g^{-1} *N*=3; certified value: 0.074 ±0.004 µg g^{-1}) with the recovery range of 100 ±5% for sediments and the TORT-3 (0.137 ± 0.012 µg g^{-1}, N=2) and DORM-2 (4.47± 0.32 µg g^{-1}, N=2) with the recovery range of 100 ±5% for fish.

Elemental mercury (Hg0) in sediment was analysed through thermodesorption, by heating ca. 100 mg of sample at 80°C followed AAS analysis. The Hg associated to organic matter and non-crystalline iron oxides (Hg_{180}) was determined after heating ca. 100 mg of sample at 180°C, following established procedures (Biester and Scholz, 1997; Meloni et al., 2024; Dabré et al., 2025). Finally, Hg bonded to refractory phases was calculated as the difference between THg and Hg_{180}.

IV.2.3.2. Cyanide analysis in water

Free cyanide (CN^-) and cyanide complexes in water that can be broken down by chlorine were measured *in situ* using QUANTOFIX® cyanide test strips for concentrations between 0 and 30 mg L^{-1}. Measured amounts of Cyanide 1 and drops of Cyanide 2 were added to the sample, and the test strip was then immersed in the solution. The result was read after 10 seconds, and the color of the strip was compared to the color scale.

IV.2.3.3. Elemental analysis in water and sediment

Analyses of major (Al, Ca, Fe, Mg, Mn, S, Ti) and trace (Pb, Cu, Zn, Cd, Cr, As, Se) elements concentrations in filtered water (surface and porewater) and solids were performed using an ICP-AES (Agilent, Varian 720-ES) and ICP-MS (Agilent, 7900), respectively, after total microwave digestion for solids (ultraWAVE, Milestone) at 250 °C following published protocols (Falciani et al., 2000; Melaku et al., 2005). The certified standards SLRS4 and SLRS6 were used for filtered water and the certified reference materials JSD3, IAEA-405 and BR24 for sediment to evaluate the QA/QC with accuracies always within the range of certified values with ±5% margin error.

Ion chromatography (Dionex ICS 2000) and the TOC-VCSN analyzer (Shimadzu®) were used to measure the concentration of major anion (Cl^-, NO_2^-, NO_3^-, PO_4^{3-}, and SO_4^{2-}) and dissolved organic matter (DOC) in filtered water, respectively, in accordance with established protocols (Rutz et al., 2017; Tisserand et al., 2022, 2024).

Total carbon (TC), total organic carbon (C_{org}) content, isotopic signatures ($\delta^{13}C$ and $\delta^{13}C_{org}$) and total nitrogen (TN) was determined on the <2mm fraction, using Cavity Ring-Down Spectrometry (Picarro,

Inc.®) coupled with a Combustion Module (Costech, Inc.®) (CM-CRDS) for TC following published protocol (Guédron et al., 2019) and the Flash Smart elemental analyzer (ThermoFisher Scientific) for TN. The QA/QC was performed using a reference material, PACS-2 for TC and the aspartic acid for TN with the recovery range of 100 ±5%. The organic matter content (OM) was estimated using the loss on ignition (LOI) method by heating sediment to 550 °C for three (3) hours following published protocol (Heiri et al., 2001).

IV.2.3.4. Sediment grain size analysis

Grain size distribution was analyzed after dispersion for seven minutes using sonication in deionized water with a laser granulometer diffraction sizer (Malvern, model Mastersizer 2000) equipped with a Hydro 2000G (Fisher et al., 2017).

IV.2.3.5. Data analysis

A Shapiro-Wilk test was used to evaluate the data for homoscedasticity and normal distribution. The geochemical dataset given in this publication is presented as the mean ± SD and also as mean (median) and SEM (standard error of the median). R (R.4.4.1), sigmaplot, and sigmastat® softwares were used for all statistical treatments. The Pearson correlation coefficient (R^2) and p-values are presented based on linear regressions.

Maps for Hg distributions were created using Qgis 3.42.2.

IV.3. Results and interpretation

IV.3.1. Spatial distribution of mercury species and cyanide in surface water

The lowest THg concentrations in filtered (THg_F = avg. ± SD= 0.6 ± 0.2 ng L^{-1}) and unfiltered water (THg_{UNF}=13.6 ±5.4 ng L^{-1}) were found in the upstream parts of the Niger (i.e., site FA), and the Saman Rivers, and the entire Niandan River (**Figure IV.2**A & B). These values are in the range of baseline concentrations for in Amazonian pristine freshwater systems [THg_F = 0.5 - 5 ng L^{-1} (Guedron et al., 2011; Lacerda et al., 2012; Hellal et al., 2020)]. Consistently, THg_{UNF} values are in the range of baseline values reported for African pristine rivers [5– 20 ng L^{-1} (Meili, 1997; Niane et al., 2019b)]. This highlights that upstream sites and the Niandan River are weakly or unaffected by ASGM activities.

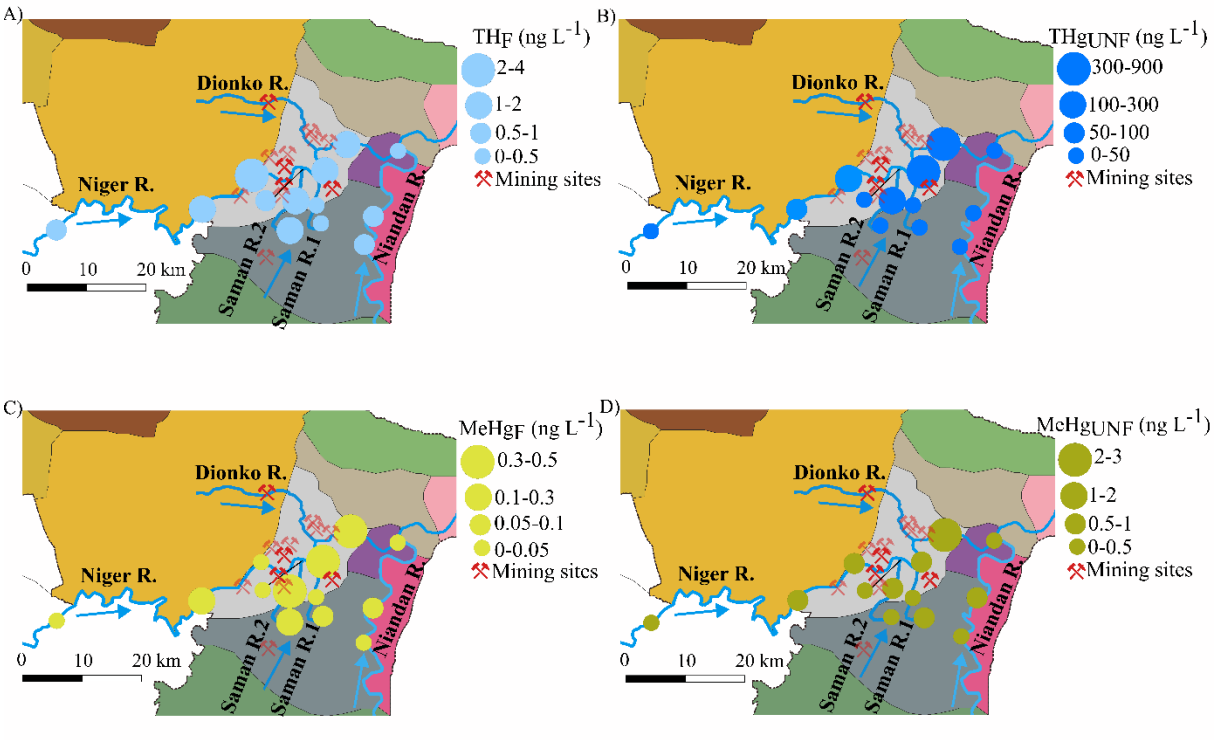


Figure IV.2. *Spatial distribution of total mercury concentration in A) filtered (THg_F) and unfiltered (THg_{UNF}) surface water; and metylmercury in C) filtered ($MeHg_F$) and D) unfiltered ($MeHg_{UNF}$) surface water.*

Downstream ASGM sites, THg_F concentrations (1.4 ± 0.9 ng L^{-1}) rise by a factor 2 to 4, with the highest concentrations found in the Saman R.1 and R.2, reaching up to 3.2 ng L^{-1} (Table S2). These values remain however lower than concentrations reported in African rivers affected by ASGM, such as the Gambia River in Senegal [32 - 34 ng L^{-1} (Niane et al., 2019b)], the Malagarasi River in Tanzania [10 -70 ng L^{-1} (Taylor et al., 2005)], and the Inkomati rivers in South Africa [16.6 ±0.3 ng L^{-1} (Williams et al., 2010)]. In contrast to THg_F, THg_{UNF} (Mean (med) ± SEM= 222 (113) ± 106 ng L^{-1}) shows a sharp increase downstream mining area in the Niger river, and the Saman tributaries, with concentration from 11 up to 902 ng L^{-1}. These values are in average 16 times higher than the baseline levels, and are within or above the concentrations range reported in ASGM impacted surface waters in Ghana [29 to 420 ng L^{-1} (Donkor et al., 2006)], in Côte d'Ivoire [6.6 to 53 ng L^{-1} (Mason et al., 2019)], in Burkina Faso [up to 21 ng L^{-1} (Ouédraogo and Amyot, 2013)], and in Senegal [86 to 974 ng L^{-1} (Niane et al., 2019b)]. When compared with the filtered fraction, THg associated with suspended particles represents up to 98% of THg in water, and this percentage increases downstream. This highlights that Hg contamination from ASGM activities mainly results from the discharge of Hg-rich particles.

As for THg, the baseline levels of MeHg concentrations in filtered ($MeHg_F$= 0.06±0.04 up to 0.5 ng L^{-1}, **Figure IV.2**C) and unfiltered water ($MeHg_{UNF}$= 0.4±0.3 up to 0.8 ng L^{-1}, **Figure IV.2**D) are found in upstream sites. These concentration are in the upper range of the concentrations reported in pristine surface water ($MeHg_F$= 0.006 – 0.2 ng L^{-1}; $MeHg_{UNF}$= 0.2 ng L^{-1}) in Africa and Amazonia (Guedron et al.,

2011; Niane et al., 2019b), but higher than those found in surface waters of reservoirs in Burkina Faso [$MeHg_F$=0.03±0.02 (Ouédraogo and Amyot, 2013)]. Downstream mining sites, $MeHg_F$ (0.2 ±0.2 ng L^{-1}) and $MeHg_{UNF}$ (1.0 ±0.6 ng L^{-1}) are 2 to 4 times higher, respectively, than the baseline levels. These values are in the lower range reported for water impacted by ASGM activities in the Gambia river in Senegal [$MeHg_F$=0.1 - 4.6 ng L^{-1}; $MeHg_{UNF}$=2.0 – 10.0 ng L^{-1} (Niane et al., 2019b)]; by coal-fired power plants in South African Olifants and Upper Vaals rivers [$MeHg_F$=0.02 - 0.89 ng L^{-1} (Williams et al., 2010)], but higher than those found in surface waters of Napoleon Gulf in lake Victoria impacted by fish processing plant and tannery in East Africa [$MeHg_{UNF}$=0.1±0.03 (Ramlal et al., 2003)]. Filtered and unfiltered MeHg concentrations represent 16±9%THg_F and below 1%THg_{UNF}, respectively.

Cyanide in surface water was always bellow de detection limits of the method, except at one point on the Niger River located between Fa+63 and Fa+75 km (Table S3) where a minimal level of 1 µg L^{-1} was detected. This shows that although amalgamation sludge residues are treated for cyanidation to recover the remaining gold (Velásquez-López et al., 2011; Bansah et al., 2018; Lanzano and Arnaldi Di Balme, 2021), cyanide contamination is negligible in this part of the Niger River. Furthermore, concentrations of As and Pb in filtered water were low at all sites (Table S3), with average concentrations of 0.51±0.43 and 0.04 ±0.02 µg L^{-1}, respectively, in the Niger River and its tributaries. These values are similar to the concentrations reported in Burkina Faso (0.5-1.2 µg L^{-1} As; 0.06–1.0 µg L^{-1} Pb) and in Amazonian Bolivia [0.62–1.9 µg L^{-1} As; 0.08-1.8 µg L^{-1} Pb (Avigliano et al., 2025; Dabré et al., 2025)], indicating that local geogenic levels of As and Pb are relatively low, and that ASGM activities do not export these elements from groundwater pumping (As) or ore extraction (Pb) (Dabré et al., 2025).

IV.3.2. Spatial distribution of mercury species in river sediments

THg concentration in surface sediment range between 18 and 833 ng g^{-1} (Table S4), and increase progressively downstream toward ASGM areas, showing evidence of contamination gradients (**Figure IV.3**A). In accordance with THg_{UNF} concentrations, lowest THg levels in sediments are observed in the Niandan River (18 to 72 ng g^{-1}) and the upstream parts of the Niger River and tributaries, indicating little impact of ASGM activities. In contrast, downstream ASGM sites in the Saman and Niger Rivers, average concentrations [193 (111) ± 58.2, **Figure IV.3**] rise up to 833 ng g^{-1} in the Niger River. These values are higher than those reported in rivers impacted by ASGM, such as the Etholié River in Cote d'Ivoire [97.8±2.9 ng g^{-1} (Mason et al., 2019)], but within the lower range of those found in the Bantako River in Senegal [1162 ± 799 ng g^{-1} (Niane et al., 2019b)].

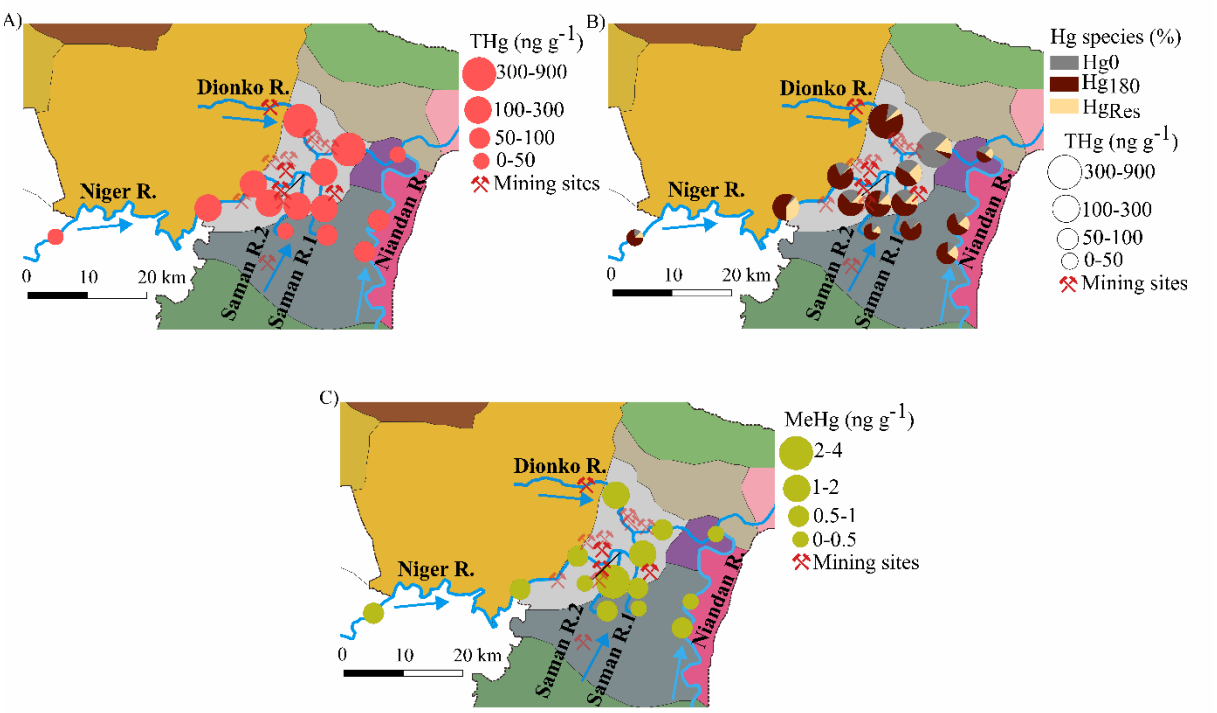


Figure IV.3. *Concentration and speciation of mercury (Hg) in surface sediment with A) total mercury; B) elemental Hg, and Hg associated to organic matter and non-crystalline Fe oxides, and Hg bound to refractory minerals, and C) methylmercury.*

Mercury carrier phases and speciation (**Figure IV.3**B and C) exhibit major spatial changes along the Niger River and between its tributaries (Fig. S3). In upstream sediments, Hg is found mainly associated with OM and weakly-crystalline Fe oxides (Hg_{180} = 72 ± 5 %THg), with less than 20% of elemental mercury (Hg0). It is worth mentioning that such proportions of Hg0 in sediments with low THg concentrations might be overestimated due to an analytical artifact (Leermakers et al., 2005). In contrast, downstream ASGM sites, the proportion of Hg_{180} is offset by larger amounts of Hg0 (47±26%THg), reaching up to 78%THg in Niger river, against Hg_{180} (40±24%THg). Such proportions of Hg0 are higher than those reported in ASGM impacted river sediment in southwestern Burkina Faso, where a percentages of Hg0 never exceeded 25%THg downstream ASGM sites (Dabré et al., 2025). MeHg concentrations in sediments are generally low, and increase downstream from 0.5±0.3 ng g^{-1} to 1.9±0.9 ng g^{-1}. Percentages of MeHg in THg are similar between upstream (1.2±0.9% THg) and downstream (1.5±0.8% THg) in the Niger River and its tributaries. These values are in the range of MeHg concentrations reported in the Samekouta (2.3±2.2 ng g^{-1}) and Mako rivers (8.0±7.8 ng g^{-1}) in Senegal (Niane et al. 2019), with similar percentages of 0.7 and 2.1% THg, respectively.

Depth THg concentrations in sediment profiles collected across non-impacted zones (upstream ASGM sites), show relatively homogeneous values (70.3±21.8 ng g^{-1}, **Figure IV.4**). The predominance of silts and sands and the low clay content may partly explain the limited variability of THg concentrations observed with depth in non-impacted zones (Fig. S2). Consistently with surface sediment values, THg

concentrations in sediment profiles increase downstream ASGM areas to 128.5 ± 31.4 and 130.2 ± 57.0 ng g^{-1} in the Niger and Saman Rivers, respectively (**Figure IV.4**). Although these values are almost doubled compared to the non-impacted upstream sites, they are 28 to 66 times lower than reported values in the Tinkoto, Sabodala, and Bantako Rivers in Senegal [THg 4 250 to 9 930 ng g^{-1} (Niane et al. (2014)]. Mercury enrichment in sediment cores is mainly observed in surface layers across all cores located downstream ASGM areas (THg=109.6 to 214.5 ng g^{-1}; **Figure IV.4**; Table S5), supporting recent Hg inputs from mining activities. Although no chronological model is available, episodic depositional peaks are observed in addition to the recent Hg enrichment, with concentrations that are multiplied by 2 to 3 times at 7, 13 and 17 cm depth in a Niger core (Fa+63km, **Figure IV.4**A).

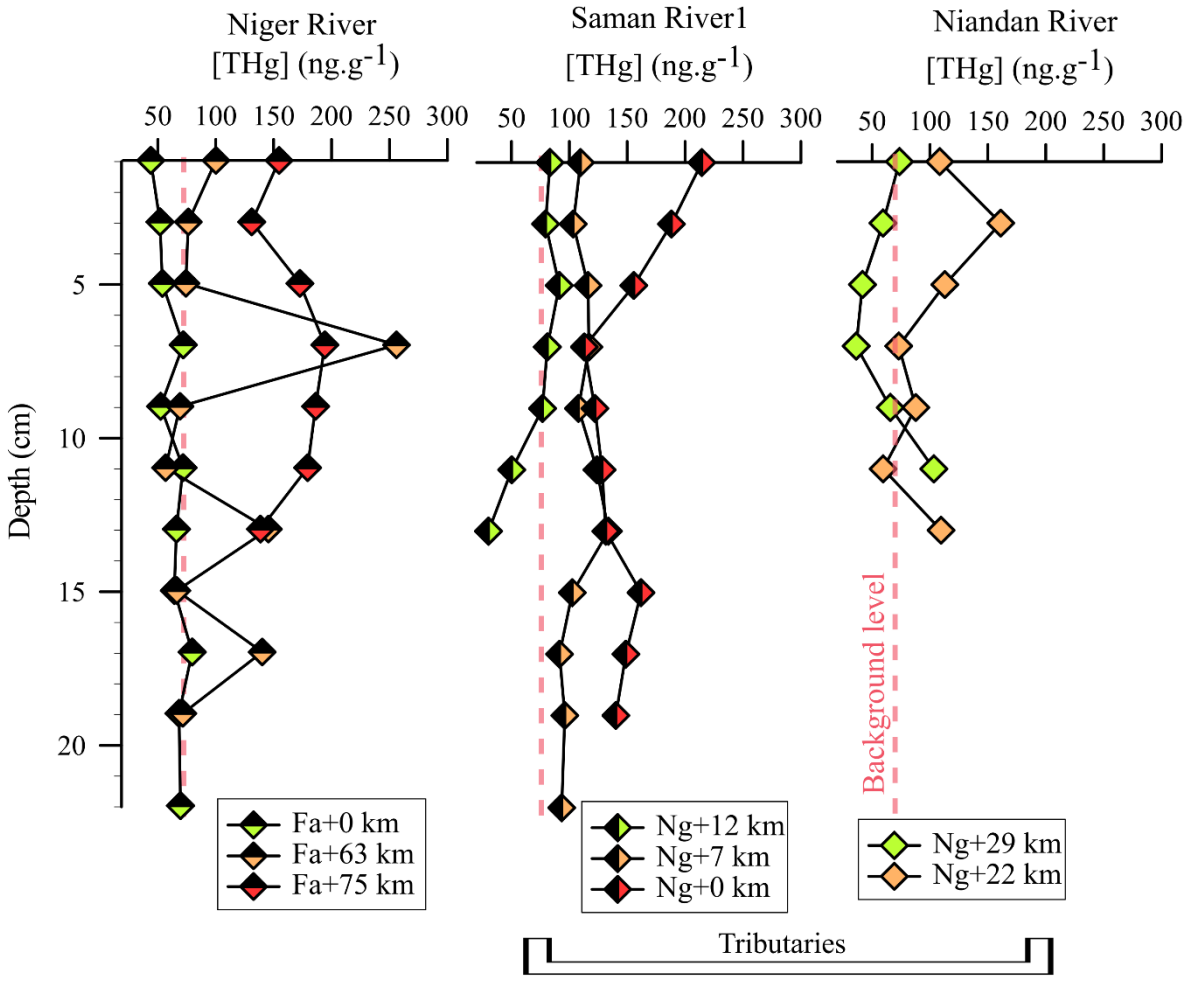


Figure IV.4. *Depth profiles of mercury concentrations in sediment cores collected in the Niger River (left), the Saman River1 (middle), and the Niandan River (right). For the Niger river caption, Fa + Km represents the distance from Faranah (Fa) along the Niger River, and for the Saman and Niandan tributaries Ng+ Km represents the distance to the confluence with Niger River (Ng).*

THg concentrations in sediment porewaters (PW) show a downstream increase from 2.6 ±1.3 ng L^{-1} to 13.9±12.0 ng L^{-1}, with the highest THg concentrations up to 35.8 ng L^{-1} found in the Saman R.1 downstream ASMG sites (**Figure IV.5**A). These values are in the ranges of reported concentrations in

Amazonian flooded soil [2.3±1.7 ng L^{-1} (Guedron et al., 2011)], the Parnaiba River Delta porewater in Brazil [1.1-3.9 ng L^{-1} (Rodrigues et al., 2025)], and the Minamata Bay porewater in Japan [6.64 ±4.93 ng L^{-1} (Matsuyama et al., 2018)].

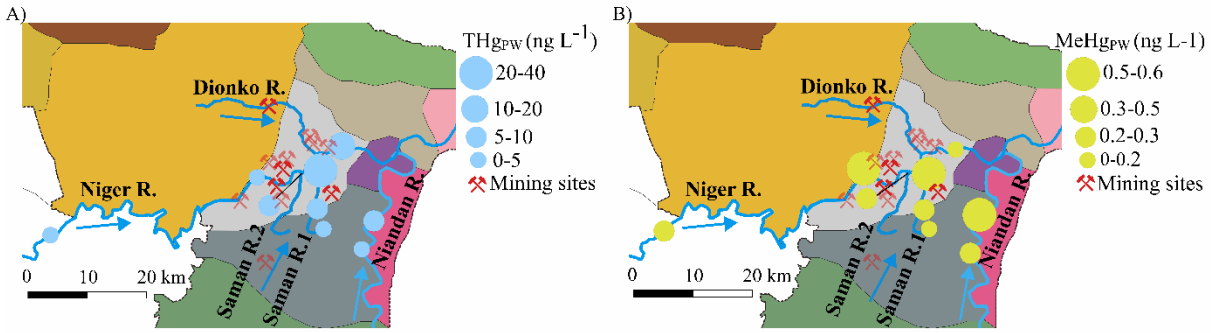


***Figure IV.5**. Mercury (A) and methylmercury (B) concentrations in sediment porewater*

Methylmercury concentrations in PW are in the same range in both upstream (0.3±0.05 ng L^{-1}) and downstream (0.4±0.2 ng L^{-1}) sediment. These values are similar to values reported [0.16±0.05 ng L^{-1} (Guedron et al., 2011; Guédron et al., 2017)] in Amazonia flooded soils, but higher than those reported in Parnaiba River Delta porewater in Brazil [0.01±0.004 ng L^{-1} (Rodrigues et al., 2025)] and lower than those found in Minamata Bay porewater in Japan [2.69 ±2.07 ng L^{-1} (Matsuyama et al., 2018)]. However, the proportions of MeHg in THg are different between sites, with the highest proportions in the upstream river sediment of Niandan (4.5% THg) and Saman R.1 (17.5% THg), and the lowest in downstream ASGM sites (i.e., between 1.6 and 5.2% THg). In contrast, the downstream Niger River site located 63km from Fa, shows MeHg level of 21% THg, whereas downstream at 75km from Fa this value decreases to 1.1%THg.

IV.3.3. Mercury and methylmercury levels in fish

Total mercury and methylmercury concentrations in fish collected from the Niger River are approximately ten-fold higher in piscivorous (THg=339±42.1 ng g^{-1}; MeHg= 295±54.2 ng g^{-1}, wet weight, *N*=3) than in omnivores (THg=37.5±14.0 ng g^{-1}; MeHg= 31.02±12.2 ng g^{-1}, wet weight (w.w), *N*=8).

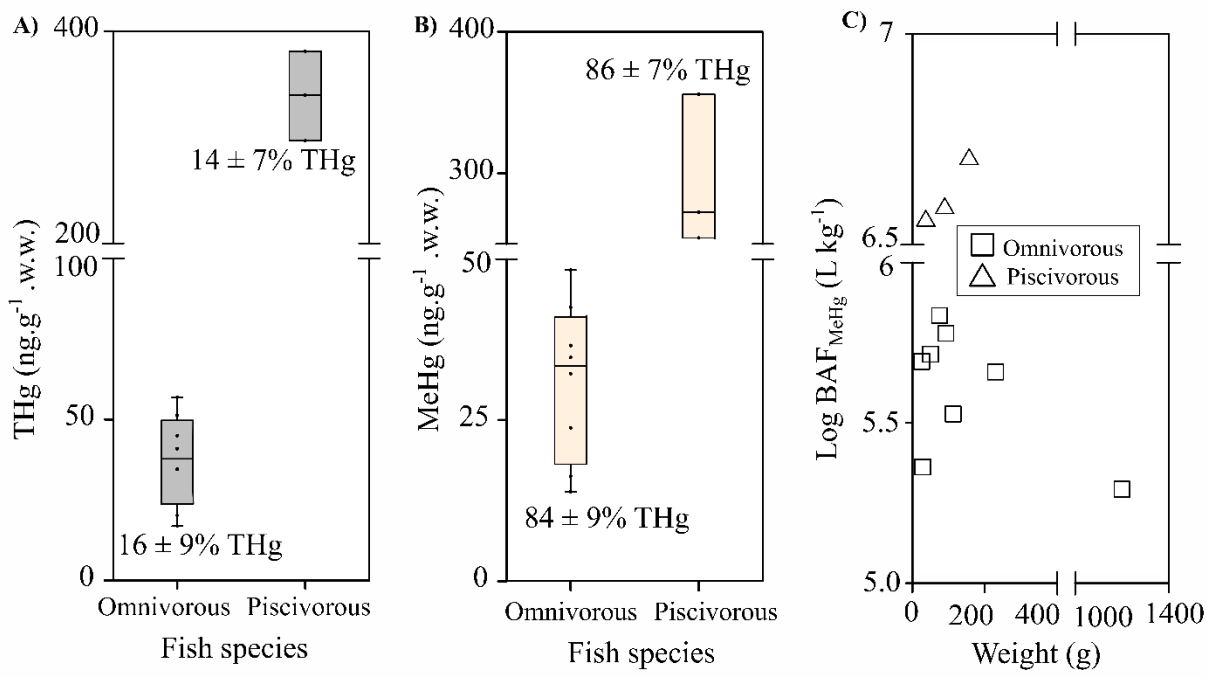


Figure IV.6. *Biplots of A) total mercury and B) methylmercury concentrations in fish species sampled in the Niger river. C) Bioaccumulation factor (BAF) vs fish weight.*

These values are similar to reported concentrations in fish from a reservoir in Burkina Faso and from the Comoé River in Côte d'Ivoire, with concentration up to 500 ng g^{-1} THg and 300 ng g^{-1} MeHg in piscivorous, and from 6 up to 45 ng g^{-1} THg and 40 ng g^{-1} MeHg in omnivorous fish (Ouédraogo and Amyot, 2013; Mason et al., 2019; Ouédraogo et al., 2015). However, these values are in the lower ranges of THg (16-900 ng g^{-1}) and MeHg (1.4 to 69.5 ng g^{-1}) concentrations found in fish from the Pra River in Ghana (Donkor et al., 2006; Oppong et al., 2010; Kwaansa-Ansah et al., 2011).

In both trophic groups, methylmercury constitutes the dominant Hg species representing 84 to 86% THg in omnivorous and piscivorous, respectively. The higher MeHg fraction in piscivorous fish indicates higher bioaccumulation in piscivorous fish, consistent with their higher trophic level position (**Figure IV.6**C). However, no trend was observed between (Me)Hg concentration and size, length or weight (Table S1; **Figure IV.6**C) for omnivorous fish species, consistent with other studies in tropical regions (Ouédraogo and Amyot, 2013; Mason et al., 2019, 2022), and temperate regions (Tadiso et al., 2011).

IV.4. Discussion

IV.4.1. Particulate transport drive mercury contamination from ASGM in the Niger River

The mapping of Hg concentrations in the compartments of the Niger River and tributaries (**Figure IV.2** and **Figure IV.3**) shows that ASGM activities affect this riverine ecosystem mainly through particulate emissions (Fig. S3). In surface water, THg is encountered almost entirely in the unfiltered fraction (THg_{UNF}>>THg_F) highlighting the dominance of particulate phases in Hg transport (Benoit et al., 2001; Dias Filho and Do Carmo, 2006; Dabré et al., 2025). Similar pattern of THg enrichment in surface river sediment (i.e., THg_{UNF} vs $THg_{sediment}$, R^2= 0.74; $p < 0.05$; Fig. S4A) indicates rapid sedimentation of Hg-rich particles downstream active ASGM areas, likely favored by low water levels during the dry season. In the sediment cores collected in the upstream part of the Niger, Saman, and Niandan Rivers, the positive correlation found between THg in sediment and the abundance of silt-clay particles (R^2=0.56; $p<0.001$; Fig. S4C) or C_{org} (R^2=0.52; $p<0.001$; Fig. S4B), supports the deposition of fine and OM rich particles enriched in Hg, known to have high sorption capacity for Hg (Soto-Jiménez and Páez-Osuna, 2001; Dias Filho and Do Carmo, 2006; Grimaldi et al., 2008). In contrast, the negative correlation between THg in sediment and sand (R^2=0.56; $p<0.001$; Fig. S4D) indicates the dilution of fine Hg rich particles with sands. In downstream cores impacted by ASGM activities, high THg concentrations are also found associated with high abundances of silty-clay particles and elevated C_{org} contents. However, the absence of correlation between THg and silty-clay or C_{org} are likely attributed to the presence of elemental Hg (micro)droplets and/or amalgamated with residual Au particles into the THg, as found in the ASGM districts of French Guiana (Guedron et al., 2009). This is consistent with observation made in surface sediment, where Hg is found mainly associated with OM and weakly crystalline Fe oxides (Hg_{180}), whereas downstream ASGM sites Hg0 becomes the majority reaching up to 78%. This highlights that ASGM activities affects both the Hg concentrations and speciation in river sediments along the stream. Hence, the resuspension of contaminated sediments during the flood, likely in the wet season, might contribute to spreading of this contamination further downstream, consistent with previous studies conducted in tropical river systems affected by gold mining (Guédron et al., 2017; Armijos et al., 2020).

Although cyanidation is used in some of the ASGM sites together with Hg amalgamation, the absence of detectable levels of CN in surface water are likely due to the mainly oxic condition in surface water, which likely favors its rapid oxidation (Kuyucak and Akcil, 2013). Additionally, low levels of As and Pb in surface water supports low geogenic levels in this region, in contrast with reported hotspots of As and Pb in several ASGM sites in the neighbouring Burkina Faso.

IV.4.2. Link between Hg carrier phases and MeHg levels in the river

In surface water, THg_F and $MeHg_F$ concentrations downstream mining sites are positively correlated (R^2= 0.76; p=0.002; Fig. S4E) suggesting that THg and MeHg originate from the same source. Although the percentage of MeHg is low, the partitioning of MeHg between the filtered fraction and suspended solids (log Kd_{MeHg}=2.5±0.5) is lower than for inorganic Hg (log Kd_{Hg}=3.7±0.6), indicating that MeHg has a greater affinity for the dissolved or colloidal fraction than inorganic Hg (Guédron et al., 2015) in the Niger River surface water. Although no correlation was found between Hg or MeHg and DOC, the significant correlation found between $MeHg_F$ and total sulphur concentration (R^2= 0.60; p<0.01) but not with THg, indicates that $MeHg_F$ and inorganic Hg are likely carried by different (in)organic ligands (Mangal et al., 2022).

The most likely major source of MeHg for surface water is the river sediment, where produced MeHg might be released to surface water through diffusion or shear stress during floods (Chen et al., 1996; Heyes et al., 2004; Guédron et al., 2012; Dai et al., 2021). In the Niger and Niandan Rivers, THg concentrations in surface sediments are found positively correlated with organic matter (R^2=0.52; p<0.001; Table S6). A positive correlation is also found between Hg_{180} and the OM (R^2=0.84; p=0.004; Fig. S4F) for pristine sites confirming that Hg is mainly bound to OM and to non-crystalline iron oxides. In addition, the proportion of MeHg in THg (%MeHg) is also significantly correlated with C_{org} (R^2=0.69; p<0.05, Table S7) and Hg_{180} (R^2=0.72; p=0.03; Fig. S4G) in the upstream pristine sediments, supporting that Hg bound to organic carbon and to reactive carrier phases, such as non-crystalline Fe oxides, is available for methylating microorganisms and likely favor MeHg production and accumulation in surface sediment (Benoit et al., 1999; Ikingura and Akagi, 2003; Ouédraogo and Amyot, 2013b; Dabré et al., 2025; Balcom et al. 2015). In contrast, the absence of correlation between OM and THg in surface sediment of downstream mining areas is attributed to rising proportions of Hg0 up to 79%THg, consistently with observation made in freshwater sediments in Côte d'Ivoire (Mason et al. 2019). In addition, the negative correlation between Hg0 and percentage MeHg support lower availability of Hg0 for methylation (Ullrich et al., 2001; Hu et al., 2013).

The spatial distribution of THg concentrations in sediments and porewater shows a similar gradient along the stream (i.e., THg_{PW} vs THg_{Sed}, R^2=0.56; p<0.05, excluding the high value found at Saman R.1; Fig. S4H), which suggests an equilibrium of Hg partitioning between sediment and porewater Hg. However, the wide range in %MeHg from up to 21%THg upstream to only 1.1% THg downstream in PW, indicates that MeHg accumulation in sediment PW is not proportionally linked to the THg content in pore-waters, but rather to the available forms of inorganic Hg for methylating microorganism and to the sediment geochemical conditions including diagenetic processes (Ullrich et al., 2001; Guédron et al., 2020). The lack of a significant correlation between MeHg concentrations in pore water and surface water further indicates that the transfer to SW of MeHg produced in sediment PW is likely

regulated by sediment texture and composition, which may drive MeHg diffusion, degradation (demethylation) or scavenging (adsorption) at the water-sediment interface (Pak and Bartha, 1998; Holmes and Lean, 2006; Chen et al., 2008; Feyte et al., 2010).

Overall, Hg speciation and carrier phases in sediment control both its mobility and availability for methylating micro-organisms. Produced dissolved and particulate MeHg in the sediment is then expected to be resuspended into the water column during flood events in the wet season.

IV.4.3. Hg levels in fish and potential health risks for local population

Amongst the 11 collected fishes, 27% exceeded the world quality criterion (WQC) of 100 ng Hg g^{-1} for the protection of aquatic fauna, suggesting possible issues on fish reproduction (Crump and Trudeau, 2009; Penglase et al., 2014). The absence of relationship between the BAF (bioaccumulation factor) and fish weight or length (**Figure IV.6**C) could be attributed to food diversification and the seasonal availability of food resources among different fish species in the region (Maurice-Bourgoin, 2000; Ouédraogo and Amyot, 2013; Mason et al., 2022).

From the perspective of human exposure, 18% of the 11 fish (representing 67% of collected piscivorous fishes), exceeded the fish quality criterion of MeHg (300 ng g^{-1} w.w.) for the protection of human health (USEPA, 2001). These reference values (500 ng THg g^{-1} d.w) was established by the World Health Organization (OMS and ONU, 2016), based on an average of one meal per week for a woman weighing 70 kg, to protect groups vulnerable to Hg toxicity. In Guinea, local fish is generally cheaper than meat, and large part of the population relies on fishing from the Niger River for their livelihood (Diallo, 1996; Le Fur et al., 2011), as major source of protein. Average fish consumption per person in Guinea is not available in the literature. Thus, we estimated a weekly intake of 54.8 µg to 85.5 µg MeHg $week^{-1}$ assuming that local population eats equally piscivorous and omnivorous, with similar weekly fish consumption as reported in Côte d'Ivoire and Ghana, averaging 337g to 523g fish per week (FOA, 2025; FAO, 2025). During the field survey in 2022 and 2023, a dozen of people interviewed at the sampling sites mentioned consuming fish five times a week and twice a day. In this case, considering a dietary habit of two fish meals per day, and applying the USEPA's estimate of one portion of fish of 113 g, a 70 kg person in Guinea would ingest between 1.3 µg kg^{-1} $week^{-1}$ body weight (b.w) up to 2.6 µg kg^{-1} $week^{-1}$ b.w. These levels are 1.6 to 2 times higher than the tolerable weekly intake (TWI) of 1.6 µg kg b.w and 1.3 µg kg b.w of JECFA (Joint FAO/WHO Expert Committee on Food Additives) and EFSA (European Food Safety Authority) respectively (Chain (CONTAM), 2012). Recently, Mason et al. (2022) proposed to reconsider the average body weight to 60 kg for a women in Côte d'Ivoire, reducing the reference value to 100 ng g^{-1} MeHg per week instead of 300 ng g^{-1}. Applying this reference to Guinea, and considering a 10 fish meals per week, a person weighing 60 kg would ingest a minimum of 37.6 µg MeHg per week, which is almost equal to the USEPA reference dose of 33.9 µg MeHg $week^{-1}$. Although

only a restricted sample of fish individual was collected in this study, results suggest an elevated health risk of MeHg exposure for local populations that depend on fishing, especially for pregnant women, which may expose their child to nervous system issues (Clarkson and Magos, 2006).

IV.5. Conclusion

The mapping of Hg speciation and carrier phases in the compartments of the Niger River and its tributaries shows Hg contamination from artisanal and small-scale gold mining (ASGM) activities mainly results from the discharge of Hg-rich particles, with high elemental mercury (Hg0) proportions. Once deposited in the riverbed, THg bound to organic matter and non-crystalline iron oxides are likely prone to undergo biomethylation. The absence of relationship between THg and MeHg in sediments and porewater, suggests that methylation is governed by the availability of reactive Hg forms and geochemical conditions, rather than total Hg amount.

From a limited number of fish species, high Hg bioaccumulation and biomagnification was found, with MeHg representing the dominant fraction of total Hg (>85%). Piscivorous fish showed MeHg and THg concentrations an order of magnitude higher than omnivorous species. Approximately 18% of the sampled fish surpassed the USEPA standards for human health protection, demonstrating an elevated potential health risk of MeHg exposure for communities reliant on fishing.

More data is needed on MeHg levels in fish species of the Niger River to confirm these observations. Future studies should include epidemiological investigation assessing health risks in population that regularly consume local fish compared to control groups. Finally, prevention campaigns must be implemented to inform and raise awareness among local populations whose diet is heavily reliant on fish consumption.

CRediT authorship contribution statement

D. Dabre: Conceptualization, Data curation, Formal analysis, Investigation, Methodology, Validation, Writing - original draft, Writing – review & editing. S. Guédron: Conceptualization, Data curation, Formal analysis, Methodology, Resources, Supervision, Validation, Writing - original draft, Writing – review & editing. I.K. Doumbouya: Data curation, Writing – review & editing. C.O.T. Compaoré: Writing – review & editing. Y.Maiga: Methodology, Supervision, Writing – review & editing. O. Bruneel: Methodology, Supervision, Writing – review & editing. J. Gardon: Methodology, Supervision, Writing – review & editing. J. Fin: Data curation, Formal analysis & Methodology. E. Resongle: Data curation, Formal analysis, Methodology, Writing – review & editing. A.A. Konaté: Methodology, Supervision, Writing – review & editing. S. Campillo: Data curation, Formal analysis & Methodology. S. Sentenac: Data curation, Formal analysis & Methodology. O. Ouedraogo: Methodology, Supervision, Writing – review & editing. R.Mason: Methodology, Supervision, Writing – review & editing.

Conflicts of interest statement

There are no conflicts to declare.

Data availability

The data supporting this article have been included as part of the Supplementary Information.

Acknowledgments

This research is the product of a joint project between the University Joseph KI-ZERBO (Ouagadougou, Burkina Faso), and the French National Research Institute for Sustainable Development (IRD, France). This publication was made possible through support provided by the African centers of excellence (ACE Partner - IRD and AFD) and by a grant from LabEx OSUG@2020 (Investissements d'avenir – ANR10 LABX56). We thank the IRD Representation in Burkina Faso for their collaboration with the Project. We would like to thank the Prefecture of Guinea, the Prefect, and the Deputy Prefect for their hospitality and assistance in facilitating our work in the mining villages. Our sincere thanks also go to Mr. Condé Moussa, a brother who facilitated our work on the sites and in the mining villages. Our sincere thanks go to Pr A.S.Ouattara, the recently deceased director of the host laboratory at the Université Joseph kI-ZERBO, who provided us with the space needed to condition our samples. We would particularly like to thank the Aquaculture and Aquatic Biodiversity Research Unit (URA-Baq) for their expertise in identifying fish species. Many thanks to Professor Toguyéni and Dr. Sissao Rokiatou for all their help during my research work. We also thank Palé Dagoro from University Joseph KI-ZERBO, who welcomed me warmly to the LAMBM laboratory and encouraged me during my fieldwork in the remote and potentially dangerous gold mining areas of Guinea.

IV.6. Supplementary information



Figure S1. *Photographs of artisanal and small-scale gold mining (ASGM) impacted rivers with, pore water, surface water, and fish samples from the Niger River and its tributaries (credit D. Dabre). A) 66 mm PVC core sampler. B) Sampling point at the confluence of the Niandan River and the Niger River. C) Banks of the Niandan River. D) Sediment core cut into 2 cm slices. E) Confluence of the Niandan River and the Niger River. F) Porous water sampling in the Niger River. G) Surface water filtration devices on PVDF membranes. H) Direct analysis of cyanide in water from a settling basin 50 meters from the Niger River. I) Results of the rapid cyanide test. J) Confluence of the Saman River and the Niger River. K) 1.2 kg trout-like fish caught in the Niger River. L) Weighing the fish; M) Measuring an omnivorous fish. N) Measuring a omnivorous fish of the Clarias species. 0) Confluence of the Saman2 River and the Niger River.*

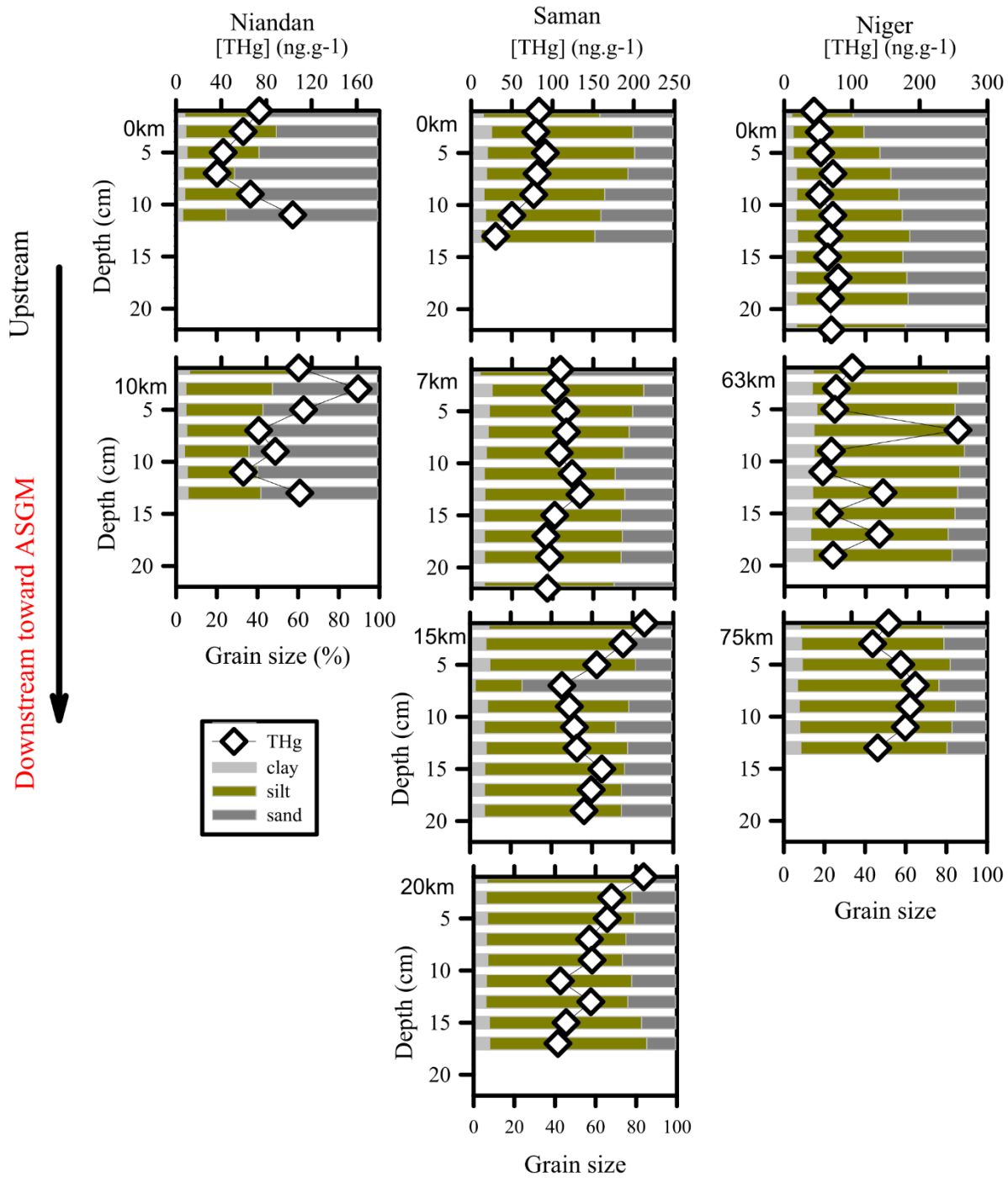


Figure S2. *Mercury distribution in sediments core with grain size distribution in background.*

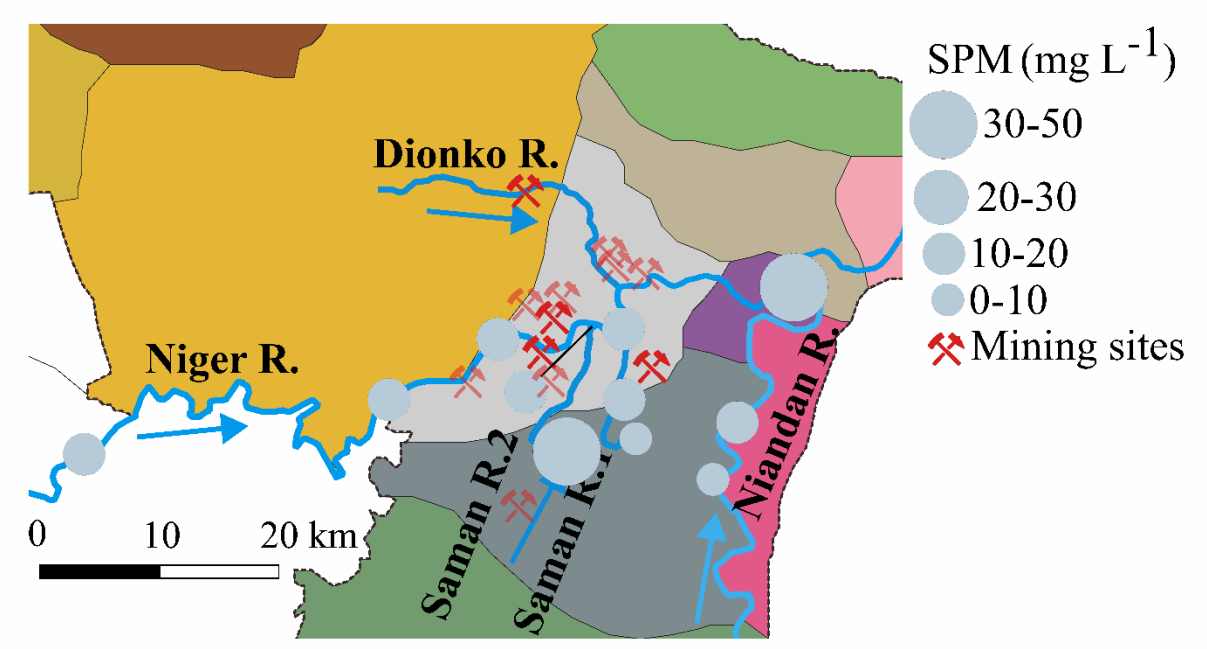


Figure S3. *Suspended particulate matter (SPM) concentrations in surface water.*

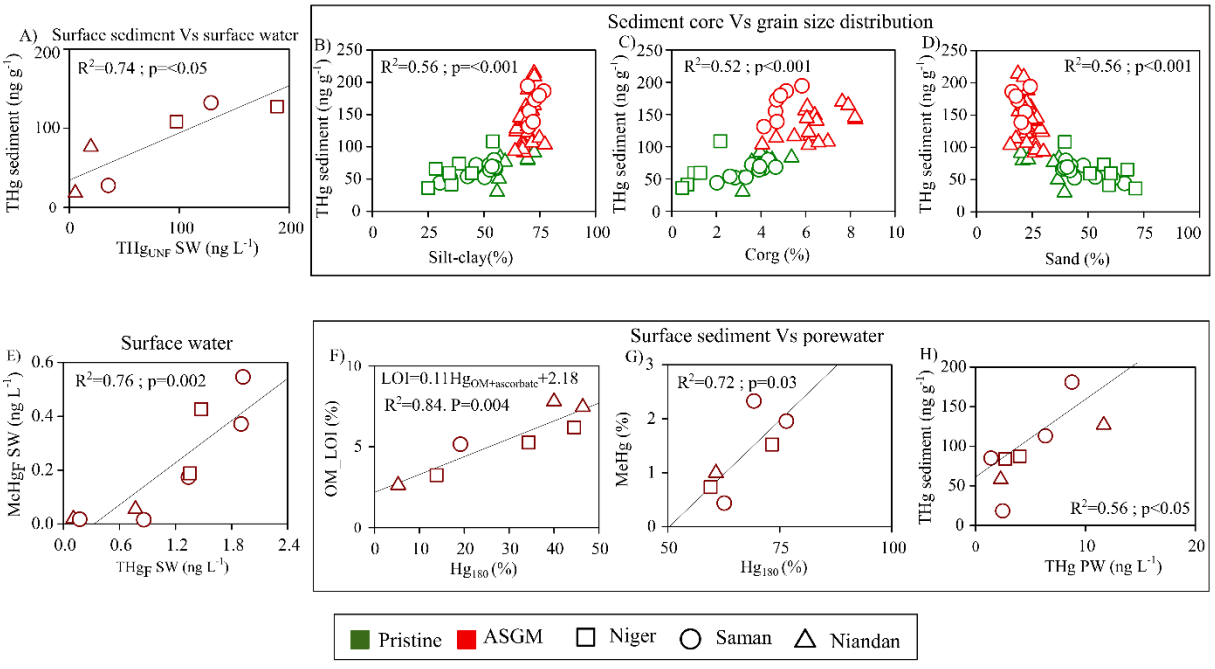


Figure S4. *Biplot of total mercury in sediments versus A) unfiltered THg in surface water. Biplot of THg between sediment core versus B) Silt+Clay granulometric fraction, C) organic carbon, and D) Sand. Biplot of filtered MeHg versus E) THgF in surface water. Biplot of Hg_{180} in surface sediment versus F) OM and G) %MeHg. Biplot of THg in surface sediment versus H) THg in porewater.*

Table S1. *Information on the species, trophic position, size and weight characteristics of the fish*

Fish species	Trophic position	Length (cm)	weight(g)
Lates niloticus	piscivorous	13.5	37.09
Silurus glanis	piscivorous	24.5	89.2
Bagrus bajad	piscivorous	29.5	156.69
squalius cephalus	omnivorous	42	1200
Oreochromis niloticus	omnivorous	11.4	75.05
Ochenoglanis occidentalis	omnivorous	19.3	50.09
Oreochromis niloticus	omnivorous	21.2	92.44
Claris gariepinus	omnivorous	22	112.55
Heterobranchus longifilis	omnivorous	31.3	229.74
Ochenoglanis occidentalis	omnivorous	12	28.36
Ochenoglanis occidentalis	omnivorous	23	25.88

Table S2. *Mercury species concentrations, percentages and partitioning in surface water. Fa=Faranah; Ng=Niger; N.D indicates not determined; (-) indicates not available.*

Sites	Distance	Filtered (ng L-1)		Unfiltered (ng L-1)		Filtered (%)		Unfiltered (%)		Log kd		Other parameters			
Rivers	Sampling point (km)	THg_F	$MeHg_F$	THg_{UNF}	$MeHg_{UNF}$	THg	MeHg	THg	MeHg	THg	MeHg	pH	Eh (mV)	SO42- (mg L^{-1})	DOC (mg L^{-1})
Niger	Fa+0	0.6	0.04	14.0	0.2	93.3	6.7	98.7	1.3	3.29	2.48	7.7	260	0.5	2.1
	Fa+48	1.4	0.2	97.4	0.6	86.1	13.9	99.4	0.6	3.65	2.07	8.4	324	-	1.9
	Fa+63	3.2	0.02	189	0.6	99.5	0.5	99.7	0.3	3.67	3.35	8.5	281	-	2.0
	Fa+75	1.5	0.4	902	2.1	71.1	28.9	99.8	0.2	4.88	2.74	7.0	108	0.8	1.1
Saman1	Ng+12	0.4	0.1	11.8	0.6	75.0	25.0	94.9	5.1	3.59	2.83	6.6	177	0.1	2.0
	Ng+7	0.2	0.02	24.8	0.2	90.1	9.9	99.4	0.6	4.03	2.78	7.3	236		6.2
	Ng+0	1.9	0.4	388	0.6	80.5	19.5	99.9	0.1	4.89	2.16	7.7	350	1.2	1.0
Saman2	Ng+16	1.3	0.2	35.5	0.4	87.0	13.0	98.8	1.2	2.79	1.45	8.0	214	0.2	8.1
	Ng+10	1.9	0.5	129	0.7	71.6	28.4	99.5	0.5	-	-	8.0	240	-	2.1
	Ng+0	0.9	0.02	11.0	0.05	98.2	1.8	99.6	0.4	3.60	2.69	7.5	253	-	2.0
Niandan	Ng+29	0.8	0.04	17.0	0.1	95.3	4.7	99.6	0.4	3.30	1.88	9.0	236	0.1	1.4
	Ng+22	0.8	0.1	19.6	0.8	92.9	7.1	95.7	4.3	3.51	3.00	8.5	210	0.0	4.0
	Ng+0	0.1	0.02	5.4	0.2	81.5	18.5	95.7	4.3	3.23	2.53	9.2	246	0.1	8.4

***Table S3**. Physoco-chemical parameters, traces and major elements concentrations in surface water.*

Site							Major (mg L^{-1})							Traces (µg L^{-1})					
		pH	Eh (mV)	Cond (µS/cm)	Temp (°C)	CN- (mg L^{-1})	Al	Ca	Fe	Mg	Mn	S	Ti	Pb	Cu	Zn	Cd	Cr	As
Niger (N=4)	Mean	8.5	238	63.8	29.8	<DL	0.01	3.74	0.16	1.81	0.09	0.40	0.35	0.02	0.44	0.01	4.20	2.97	0.30
	Med	8.4	259	63.3	31.0	<DL	0.01	3.23	0.09	1.65	0.03	0.38	0.35	0.01	0.42		2.80	2.45	0.16
	SEM	0.6	46.9	15.3	1.7	<DL	0.00	0.70	0.10	0.32	0.07	0.19	0.08	0.01	0.04		2.68	1.28	0.15
Niger CN (N=2)	Mean	7.1	244	56.1	28.1	0.001	0.01	3.10	0.53	0.99	1.07	0.68	0.45	0.04	0.35	0.01	3.10	1.29	0.19
	Med	7.1	244	56.1	28.1		0.01	3.10	0.53	0.99		0.68		0.04	0.35		3.10	1.29	0.19
	SEM	0.6	106	10.4	0.2		0.00	0.07	0.49	0.10		0.02		0.02	0.02		3.10	0.79	0.02
Saman1 (N=3)	Mean	6.9	210	123	27.7	<DL	0.01	5.24	0.88	2.29	1.37	0.12	0.28	0.03	0.29	0.02	6.01	2.21	1.05
	Med	6.8	236	84.1	26.1	<DL	0.01	5.63	0.39	2.21	1.88	0.12	0.28	0.04	0.37	0.02	6.09	2.00	1.15
	SEM	0.2	53.1	53.2	1.7	<DL	0.01	1.34	0.67	0.53	0.66	0.01	0.02	0.01	0.12	0.01	0.11	1.01	0.50
Saman2 (N=3)	Mean	7.9	236	64.9	28.2	<DL	0.02	3.05	0.15	1.38	0.14	0.34	1.54	0.07	0.86	<DL	5.09	3.02	0.89
	Med	8.0	240	54.9	28.4	<DL	0.02	3.13	0.13	1.46	0.08	0.25	0.36	0.06	0.40	<DL	6.68	2.47	0.66
	SEM	0.2	11.5	21.1	2.9	<DL	0.00	0.35	0.06	0.15	0.10	0.18	1.21	0.04	0.54	<DL	2.60	1.05	0.51
Niandan (N=3)	Mean	8.9	231	104	32.0	<DL	2.3	5.31	0.50	2.44	0.02	0.24	0.79	0.04	0.55	0.10	4.70	0.91	0.13
	Med	9.0	235	110	33.2	<DL	2.6	5.36	0.08	2.44	0.02	0.24	0.66	0.04	0.61	0.10	4.62	1.23	0.12
	SEM	0.2	10.6	8.1	1.3	<DL	1.2	0.10	0.43	0.03	0.01	0.06	0.19	0.01	0.08	0.04	0.16	0.35	0.01

Table S4. *(Methl)mercury concentration and Hg carrier phases proportion in surface sediment.*

Rivers sediments	sampling point	distance (km)	THg (ng g-1)	MeHg (ng g-1)	THg (%)	MeHg (%)	Hg0 (%)	$Hg_{OM+ascorbate}$ (%)	Hg_{Res} (%)
Niger	1	Fa+0	46.8	0.7	98.5	1.5	13.6	73.3	13.2
	2	Fa+48	109	0.8	99.3	0.7	3.5	59.5	36.9
	3	Fa+63	127	0.8	99.4	0.6	18.7	79.8	1.5
	4	Fa+75	833	0.9	99.9	0.1	78.6	5.3	16.0
Saman1	1	Ng+12	83.2	0.1	99.9	0.1	21.5	77.4	1.0
	2	Ng+7	111	0.6	97.7	2.3	23.7	61.1	15.2
	3	Ng+0	215	3.3	98.5	1.5	28.9	44.9	26.2
Saman2	1	Ng+16	27.7	0.6	97.7	2.3	14.0	72.23	13.77
	2	Ng+10	132	2.6	98.0	2.0	9.0	76.5	14.5
	3	Ng+0	109	0.5	99.6	0.4	24.1	62.6	13.3
Dionko	1	Ng+7	329	2.0	99.4	0.6	9.9	84.9	5.2
Niandan	1	Ng+29	61.2	0.7	99.1	0.9	12.3	65.3	22.3
	2	Ng+22	76.4	0.5	99.0	1.0	17.8	60.7	21.5
	3	Ng+0	18.3	0.5	97.1	2.9	30.5	47.2	22.3

Table S5. *chemical parameter in sediment core*

		THg (ng g^{-1})		Clay (%)		Silt (%)		Sand (%)		N (%)		Corg (%)	
Rivers	Average depth	Mean	SD	Mean	SD	Mean	SD	Mean	SD	Mean	SD	Mean	SD
Niger	Background level	63.1	10.9	5.1	0.9	48.0	8.6	46.9	9.4	0.3	0.04	3.6	0.8
	1	99.6	55.4	8.2	5.2	55.7	22.2	36.0	26.3	0.2	0.1	2.8	1.6
	3	86.4	40.5	8.5	4.7	58.8	20.7	32.7	24.9	0.2	0.1	2.9	1.2
	5	100	63.5	9.4	5.7	61.2	16.2	29.5	20.7	0.2	0.1	2.9	1.7
	7	174	93.7	8.7	4.7	62.7	14.1	28.6	17.5	0.2	0.2	3.6	2.2
	9	103	72.9	9.0	4.5	67.0	14.5	24.0	17.4	0.2	0.2	3.2	1.9
	11	103	66.9	9.1	4.7	66.2	12.1	24.7	15.3	0.2	0.1	3.6	1.6
	13	117	44.0	9.1	3.8	66.2	9.5	24.7	12.4	0.2	0.1	3.5	1.6
	15	65.3	1.6	9.2	5.4	61.6	12.6	29.3	18.0	0.2	0.1	2.8	1.6
	17	110	42.7	8.9	5.0	61.1	9.3	30.0	14.3	0.2	0.2	2.9	2.0
	19	69.9	2.3	9.6	5.6	61.6	9.5	28.8	20.6	0.2	0.2	3.0	2.4
	22	69.5		5.7		53.6		40.8		0.3		3.9	
Saman1	Background level	70.3	21.9	6.8	1.6	63.0	7.2	30.2	8.5	0.2	0.02	4.0	0.8
	1	136	69.4	6.2	2.5	57.7	14.6	36.1	17.1	0.3	0.1	5.4	0.3
	3	124	57.2	9.1	1.3	71.3	2.9	19.7	3.8	0.2	0.0	4.5	0.1
	5	121	32.5	8.6	0.9	71.5	1.0	19.9	1.0	0.3	0.1	5.1	1.1
	7	104	19.7	5.9	3.1	54.0	26.9	40.2	29.9	0.3	0.1	5.2	1.4
	9	102	23.1	7.1	1.2	65.5	5.3	27.4	6.4	0.3	0.1	5.6	1.8
	11	101	43.9	6.5	0.4	62.0	4.5	31.6	4.3	0.3	0.2	5.9	3.9
	13	98.4	59.2	6.2	1.5	64.8	7.7	29.0	9.1	0.2		3.2	
	15	132	42.0	6.5	0.7	68.1	0.9	25.4	1.5	0.4	0.0	6.1	0.0
	17	120	40.6	6.4	0.5	67.6	0.3	25.9	0.2	0.4		6.4	

	19	118	31.1	6.5	0.5	67.3	0.1	26.2	0.5	0.4		6.5	
	22	93.4		6.1		63.9		30.0		0.4		7.2	
	1	209		6.3		72.5		21.2		0.5		7.8	
	3	170		6.0		71.6		22.4		0.5		7.6	
	5	164		6.5		72.5		21.1		0.5		7.9	
	7	142		6.0		68.6		25.4		0.5		8.2	
Saman2	9	146		6.7		66.2		27.1		0.5		8.2	
	11	107		6.0		71.5		22.5		0.4		6.6	
	13	144		5.7		69.8		24.5		0.4		6.0	
	15	114		7.5		74.8		17.7		0.3		4.7	
	17	104		7.6		77.3		15.1		0.3		4.1	
	Background level	63.5	23.7	4.8	0.9	37.2	9.8	58.0	10.5	0.1	0.04	1.1	0.7
	1	91.0	24.6	4.7	1.6	46.4	10.7	48.4	12.3	0.2	0.1	1.6	0.8
	3	110	71.9	5.1	0.0	43.6	1.4	51.8	1.4	0.1	0.0	1.3	0.4
Niandan	5	77.3	50.3	5.3	0.4	36.7	1.8	58.4	1.4	0.1	0.0	1.2	0.7
	7	59.6	20.2	30.6	30.8	23.7	8.4	57.0	18.5	5.8	9.8	0.6	0.4
	9	70.2	15.8	37.7	38.9	21.0	15.8	50.5	26.8	1.3	2.1	0.6	0.5
	11	65.1	35.7	37.3	38.9	18.9	16.9	51.9	28.7	0.4	0.5	0.7	0.5
	13	110		5.6		35.9		58.5		0.1		1.1	

***Table S6**. Pearson correlation (correlation coefficient (CC), p value (p), and number of samples (N)) with total mercury (THg), and methylmercury (MeHg) in sediments core.*

Parameters	Statistics	THg (ng g^{-1})	clay (%)	silt (%)	sand (%)	N (%)	C_{org} (%)
THg (ng g^{-1})	CC	1					
	p	0.00					
	N	59					
Clay (%)	CC	0.60	1				
	p	<0.001	0.00				
	N	59	61				
silt (%)	CC	0.74	0.80	1			
	p	<0.001	<0.001	0.00			
	N	59	61	61			
Sand (%)	CC	-0.74	-0.83	-0.99	1		
	p	<0.001	<0.001	<0.001	0.00		
	N	59	54	48	48		
N (%)	CC	0.74	0.43	0.76	-0.74	1	
	p	<0.001	<0.001	<0.001	<0.001	0.00	
	N	53	48	54	54	48	
C_{org} (%)	CC	0.72	0.44	0.74	-0.72	0.96	1
	p	<0.001	0.002	<0.001	<0.001	<0.001	0.00
	N	47	61	48	54	48	47

***Table S7**. Pearson correlation (correlation coefficient (CC), p value (p), and number of samples (N)) with total mercury (THg), and methylmercury (MeHg) in surface sediments.*

Parameters	Statistics	THg (ng g^{-1})	MeHg (ng g^{-1})	clay (%)	silt (%)	sand (%)	N (%)	C_{org} (%)
THg	CC	1						
	p	0.00						
	N	6						
MeHg	CC	0.59	1					
	p	0.2	0.00					
	N	6	6					
Clay	CC	0.34	-0.09	1				
	p	0.40	0.86	0.00				
	N	8	6	8				
silt	CC	0.34	-0.005	0.85	1			
	p	0.40	0.99	0.007	0.00			
	N	8	6	8	8			
sand	CC	-0.34	0.01	-0.88	-0.99	1		
	p	40.00	0.98	0.004	<0.001	0.00		
	N	8.00	6	8	8	8		
C_{org}	CC	0.85	0.83	0.04	0.09	-0.09	1	
	p	8	0.04	0.93	0.82	0.83	0.00	
	N	0.01	6	8	8	8	8	
N	CC	0.84	0.56	0.16	0.41	-0.39	0.83	1
	p	0.01	0.24	0.69	0.31	0.33	0.01	0.00
	N	8	6	8	8	8	8	8

Chapter V

Summary of the main results and presentation of new research questions and perspectives

General conclusion and outlook

V.1. Summary of key results

The main objective of this study was to document environmental contamination linked to the use of Hg in ASGM activities in west Africa and its potential health impacts on populations in Burkina Faso and Guinea. Through this doctoral thesis, I tried to answer the following scientific questions:

I. What are the baseline concentrations and levels of contamination of Hg, arsenic, cyanide, and lead in west African ecosystems impacted by ASGM activities, and how do they evolve downstream ASGM sites?

II. What is the behaviour and fate of Hg species when transferred into aquatic compartments, and what are the main carrier phases that carry Hg?

III. What are the main species implied and the potential main route of human exposure?

The first part of this thesis focussed on the understanding of Hg speciation and distribution in soils and sediments with a special emphasis on carrier phases that might favor availability of Hg for methylating microorganisms once transferred into rivers. This study conducted in mining districts in Burkina Faso and Guinea revealed that Hg dissemination in aquatic ecosystem downstream ASGM sites mainly originates from emissions of Hg-rich particles. In the terrestrial environment, high Hg levels in soils result from direct deposition or condensation of Hg following amalgamation and burning of the amalgams. Thermodesorption analysis and selective extractions showed that Hg was mainly found as elemental Hg, or bound to organic matter and non-crystalline iron oxides. In Burkina Faso, Hg0 represented a minority fraction (~10% THg), and Hg was found mainly bound to non-crystalline iron oxides (~60% THg) and to organic matter (~30% THg) in ASGM soil. Once deposited in River sediments, Hg bound to non-crystalline iron oxides was reduced by half, coinciding with an increase in MeHg levels, suggesting that non-crystalline iron oxides are preferentially reduced in sediment, promoting the production and accumulation of MeHg.

In contrast to Burkina Faso, Hg0 reached up to 75% in Guinean miner's villages topsoils, where the burning of the amalgams is traditionally performed. In the Niger River, THg and Hg0 concentrations increased in sediment downstream ASGM sites, whereas MeHg proportions decreased from 21% to 1.1% THg. This non-proportionality of Hg concentration and MeHg proportion indicates that MeHg accumulation in sediments depends on the available forms of inorganic Hg for biomethylation and on the geochemical conditions of sediments.

The second part of this study focused on the study of specific gold mining practices by Guinean and Burkina Faso communities, and their impact on the transfer of the Hg contamination from mine to miner's villages. In Guinea, specific gold mining practices lead to the transfer of Hg from the mines to

miners' villages, where men crush the ores and women handle washing, amalgamation and burning of amalgams within their households exposing their community and their families to Hg0 vapors. In the miner's villages, high levels of Hg up to 10 µg g^{-1} were found to be present in topsoils collected in the center of the village. In addition, thermodesorption experiments have shown that elemental Hg represented between 40 and 69% of THg in these soils, indicating Hg0 loss during amalgamation or redeposition of Hg0 from the burning of the amalgam. This also highlighted a risk of human exposure through Hg0 inhalation for local populations. In Burkina Faso, mining is often performed directly on riverbanks or within the village, with Hg release and tailings remaining close to the community.

The third part of this study focussed on the impact of this ASGM on the contamination of aquatic fauna and the related risk of exposure for Guinean populations living along the Niger River. High levels of (Me)Hg were found in carnivore fish collected in the Niger Rivers, highlighting Hg bioaccumulation in fish. Approximately 18% of fish collected from the Niger River were found to be contaminated with Hg and MeHg at levels exceeding USEPA standards for human health protection. This finding raises concerns regarding potential health risks associated with MeHg exposure among fishing-dependent communities. The study revealed that these populations relied heavily on fish as a primary protein source, consuming fish at least five times per week and, in many cases, twice daily, thereby potentially increasing their cumulative exposure to methylmercury**.**

V.2. Scope and level of response to the research questions

Overall, the results obtained in this doctoral thesis provide a new dataset, which documents the Hg contamination of west-African environment impacted by ASGM and helps understanding the dissemination and processes implied in Hg methylation and transfer into trophic chains. Unfortunately, health aspects were only addressed indirectly, through the identification of exposure routes and potential risks. Due to the field complexity and to cultural constraints (impossibility of collecting hair, urine and blood samples), the epidemiological study initially planned could not be carried out.

With regard to environmental contamination, this thesis provides a detailed quantification of Hg, CN, As, and Pb concentrations in soils, sediments, water, and aquatic biota at several ASGM sites in Burkina Faso and Guinea. The spatial approach, combined with speciation analyses, has clearly identified ASGM as a major anthropogenic source of mercury contamination and characterized its transport, transformation, and accumulation in hydrological systems. In this regard, the objectives related to the quantification and characterization of metal contamination in West African ecosystems have been fully achieved. However, certain key aspects of contamination linked to ASGM could not be addressed in greater detail within the scope of this work. These include the precise attribution of mercury sources (anthropogenic vs natural), the quantification of atmospheric Hg levels and (re)emissions and the

associated exposure through inhalation, and a more comprehensive assessment of dietary risks through multi-metal analyses in fish.

With regard to health impacts, this research identifies the main routes of human exposure to mercury, including inhalation of elemental mercury during ore amalgamation, re-emission of mercury stored in the soil in mining villages, and consumption of contaminated fish. However, although these routes of exposure are clearly documented, the direct assessment of impacts on human health remains incomplete, as it is based on environmental indicators and dietary surveys rather than epidemiological data or human biomarkers. Consequently, the health dimension of ASGM-related contamination is addressed partially from the perspective of exposure and potential risk rather than through direct measurement of health effects. These limitations do not call into question the environmental conclusions of this thesis, but rather define clear priorities for future research, which are detailed in the following (5.4.) section on prospects.

V.3. Practical recommendations

To reduce miners and local population exposure to Hg, it is recommended to train gold miners in a moderate use of Hg as well as raising awareness of the dangers of chemicals (Hg, CN, and acids) in gold extraction practices. It is clear that nothing can stop miners from using Hg, given that there are virtually no other environmentally clean friendly and profitable techniques available. Existing techniques, such as centrifugal concentration gravimetry, magnetic methods, and Hg-free flotation, are cost and time-consuming. In the case of Burkina Faso, at one of the ANEEMAS sites (Gnikpière, site B3), the implementation of PlanetGold's Hg-free gravimetric system has reduced Hg use by 0.065 tons between 2022 and 2023 over a period of ~18 months. All this was made possible thanks to the support of ANEEMAS and the supervision and training of gold miners (PlanetGOLD, 2023). In light of this achievement, the use of borax for smelting instead of Hg could be adopted by gold miners, if they are trained to use it, as it would be cheaper, yield higher gold returns, and pose less environmental risks compared to Hg. Training in Hg recovery and condensation techniques that are suitable and accessible to miners, through recycling and burning the amalgam in pressure cookers, is necessary to reduce the environmental impact of Hg. Gold miners also need training in cyanidation techniques, which they currently perform blindly, without using lime during leaching, leading to the dissemination of cyanide in the environment. Finally, ASGM needs to be formalized and regularly monitored to prevent mining practices from being transferred to villages within local communities, exposing the entire population to harmful Hg0 vapors.

V.4. Perspectives

During this doctoral thesis, we answered almost entirely the main scientific questions mentioned above. However, others questions deserve further investigation and refinement. These include the apportionment of anthropogenic sources of mercury, characterizing atmospheric mercury emissions from ASGM activities and associated inhalation exposure, expanding Hg analyses in fish to better assess dietary risks, and evaluating human exposure. These questions, as well as the methods and tools to answer them, are developed in the following paragraphs:

1. How can the origin of Hg in ASGM-impacted ecosystems be more accurately differentiated between anthropogenic and natural sources? The strategies and tools we propose to answer this question would be a study of isotopic tracers using multi-collector ICPMS to determine the stable isotopes of Hg [MDF (mass-dependent fractionation): δ^{202}Hg; MIF (mass-independent fractionation): Δ^{199}Hg and Δ^{201}Hg]. This technique, coupled to a mixing model can make it possible to identify and apportion natural and anthropogenic sources of Hg, if their isotopic compositions are distinct. This will make this study more robust by complementing the geochemistry of total Hg determined in the samples. Another complementary approach to geochemistry would be to link sources and receptors using remote sensing/GIS through spatial-cartographic analysis. This tool will make it possible to identify areas of anthropogenic impact by interpolation [Inverse distance weighting (IDW) and Kriging], establish impact gradients (amalgamation areas, washing areas, dispersion paths, spatial analysis, etc.), and then target relevant isotopic analyses in the area in order to spatialize the anthropogenic contribution of gold mining in the area.

2. What is the amount of atmospheric Hg in the ambient air of these mining environments, and to what extent do they contribute to human exposure through inhalation? Answering this question is essential to understanding the dynamics of Hg in the environment affected by ASGM, as atmospheric emissions and re-emissions represent a major pathway of human exposure (Chapter 3). In order to assess the Hg-related risks and identify its actual sources, an analysis of gaseous Hg0 in ambient air using automatic atomic fluorescence analysis, the use of passive Hg0 sensors (i.e., MerPas), and the use of an atmospheric deposition collector will be useful for quantifying Hg fluxes. These atmospheric measurements can be combined with Hg isotopes and mapping to develop a model of anthropogenic Hg transport and deposition.

3. What is the methylation potential of Hg in the soils studied? Answering this question is also very important in determining the microorganisms involved and the methylation/demethylation rates in river sediment. A molecular and atomic approach is therefore proposed, involving DNA extraction from the microorganisms present in the samples, starting with PCR to quantify the genes involved in sequencing and metagenomics combined with 16S rRNA to identify the methylator groups. This will

provide insight into the different microorganisms implied in the production or degradation of MeHg found in the different compartments of the environment impacted by mining activities. In addition, determining the rate of demethylation through enriched Hg isotopes incubation will be essential to understanding the methylation/demethylation rates in the aquatic environments of Burkina Faso and Guinea.

In this study, DNA extractions were performed on filters obteained after water filtration, as well as on soil, and sediment samples in Burkina Faso and Guinea, but the sequencing results could not be analyzed or processed, explaining the absence of this part in the thesis document. These results will be analyzed and published in the near future.

It is also necessary to expand the fish database through the analysis of a larger number of fish necessary to draw a definitive conclusion regarding the human risk of exposure. In addition, an epidemiological study analyzing biomarkers in urine and hair would be interesting in mining communities in Burkina Faso and Guinea, compared to a control community, in order to study more precisely the impact of gold mining on the health of populations.

At the same time, it would be interesting to develop a remediation system by setting up a pilot system for treating mining effluents in order to limit Hg flows into aquatic ecosystems. Blagodatsky et al. (2020) have shown that phytoremediation combined with arbuscular mycorrhizal fungi is a very promising alternative for the restoration of mining sites. Another alternative would be phytostabilization of contaminants by terrestrial plants present on mining sites by planting trees to scavenge contaminants in the soil matrix, preventing them from ending up in surface water systems during periods of flooding.

Finally, the perspectives presented highlight the need for a deeper understanding of the origin of Hg, its speciation, its bioavailability and bioaccumulation, and its effects on human health, in a context where growing demand for gold is fuelling illegal gold mining in West Africa, with 435 tons of gold exported illegally in 2022 (Ummel and Schulz, 2024). In view of this growing demand for gold for jewellery, electronics, and other uses, which is fuelling the boom in gold mining in West Africa (Buy Gold Africa, 2025), the proposed outlook is a crucial need for government authorities throughout West Africa. Il calls for the implementation of a sustainable management strategy that can reconcile societal needs with the preservation of ecosystems, leading to the protection of human health.

References

Adekiya, A.O., Aremu, C., Agbede, T.M., Olayanju, A., Ejue, W.S., Adegbite, K.A., Olayiwola, I.E., Ajiboye, B., Oni, A.T., 2021. Soil productivity improvement under different fallow types on Alfisol of a derived savanna ecology of Nigeria. Heliyon 7, e06759. https://doi.org/10.1016/j.heliyon.2021.e06759

Adeotan, Y.S.O., Vouillamoz, J.-M., Lawson, F.M.A., Koita, M., Zorom, M., Traore, Y.S., Sanou, R., Hector, B., Balima, M., 2025. Beyond lineaments: Exploring the influence of weathered layers on borehole productivity in basement rocks of Burkina Faso, West Africa. Hydrogeol. J. 33, 411–424. https://doi.org/10.1007/s10040-025-02876-5

Adewumi, A.J., Laniyan, T.A., 2020. Contamination, sources and risk assessments of metals in media from Anka artisanal gold mining area, Northwest Nigeria. Sci. Total Environ. 718, 137235. https://doi.org/10.1016/j.scitotenv.2020.137235

Adjorlolo-Gasokpoh, A., Golow, A.A., Kambo-Dorsa, J., 2012. Mercury in the Surface Soil and Cassava, Manihot esculenta (Flesh, Leaves and Peel) Near Goldmines at Bogoso and Prestea, Ghana. Bull. Environ. Contam. Toxicol. 89, 1106–1110. https://doi.org/10.1007/s00128-012-0849-7

Adriano, D.C., 2001. Trace Elements in Terrestrial Environments, in: Trace Elements in Terrestrial Environments. Springer New York, New York, NY, pp. 411–458. https://doi.org/10.1007/978-0-387-21510-5_11

Afrifa, J., Ogbordjor, W.D., Duku-Takyi, R., 2018. Variation in thyroid hormone levels is associated with elevated blood mercury levels among artisanal small-scale miners in Ghana. PLOS ONE 13, e0203335. https://doi.org/10.1371/journal.pone.0203335

AFRODAD, 2020. Assessment of Guinea's Domestication of The African Mining Vision.

Ahiamadjie, H., Serfor-Armah, Y., Tandoh, J.B., Gyampo, O., Ofosu, F.G., Dampare, S.B., Adotey, D.K., Nyarko, B.J.B., 2011. Evaluation of trace elements contents in staple foodstuffs from the gold mining areas in southwestern part of Ghana using neutron activation analysis. J. Radioanal. Nucl. Chem. 288, 653–661. https://doi.org/10.1007/s10967-011-0979-0

Airault, P., 2012. Burkina Faso : la soif de l'or – Jeune Afrique [WWW Document]. JeuneAfrique.com. URL https://www.jeuneafrique.com/142610/archives-thematique/burkina-faso-la-soif-de-l-or/ (accessed 10.25.22).

Akanchise, T., Boakye, S., Borquaye, L.S., Dodd, M., Darko, G., 2020. Distribution of heavy metals in soils from abandoned dump sites in Kumasi, Ghana. Sci. Afr. 10, e00614. https://doi.org/10.1016/j.sciaf.2020.e00614

Akoto, O., Bortey-Sam, N., Ikenaka, Y., Nakayama, S.M.M., Baidoo, E., Yohannes, Y.B., Ishizuka, M., 2017. Contamination Levels and Sources of Heavy Metals and a Metalloid in Surface Soils in the Kumasi Metropolis, Ghana. J. Health Pollut. 7, 28–39. https://doi.org/10.5696/2156-9614-7.15.28

Alanoca, L., Guédron, S., Amouroux, D., Audry, S., Monperrus, M., Tessier, E., Goix, S., Acha, D., Seyler, P., Point, D., 2016. Synergistic effects of mining and urban effluents on the level and distribution of methylmercury in a shallow aquatic ecosystem of the Bolivian Altiplano. Environ. Sci. Process. Impacts 18, 1550–1560. https://doi.org/10.1039/C6EM00547K

Aleksander-Kwaterczak, U., Ciszewski, D., 2016. Pollutant dispersal in groundwater and sediments of gaining and losing river reaches affected by metal mining. Environ. Earth Sci. 75, 95. https://doi.org/10.1007/s12665-015-4859-8

Aleku, D.L., Biester, H., Pichler, T., 2025. Elevated mercury (Hg) in groundwater caused by oil and gas production. Appl. Geochem. 179, 106259. https://doi.org/10.1016/j.apgeochem.2024.106259

Aleku, D.L., Lazareva, O., Pichler, T., 2024. Mercury in groundwater – Source, transport and remediation. Appl. Geochem. 170, 106060. https://doi.org/10.1016/j.apgeochem.2024.106060

Alfaro, M.R., Montero, A., Ugarte, O.M., Do Nascimento, C.W.A., De Aguiar Accioly, A.M., Biondi, C.M., Da Silva, Y.J.A.B., 2015. Background concentrations and reference values for heavy metals in soils of Cuba. Environ. Monit. Assess. 187, 4198. https://doi.org/10.1007/s10661-014-4198-3

Aliyu Haruna Sani, Amanabo Musa, Musa Dickson Achimugu, 2023. Assessment of heavy metal pollution of drinking water sources and staple food cultivars around artisanal mining site in Igade-Mashegu, Niger State, Nigeria. World J. Biol. Pharm. Health Sci. 14, 306–319. https://doi.org/10.30574/wjbphs.2023.14.2.0162

Alloway, B.J., 1995. Heavy metals in soils, 2nd ed. ed. Blackie academic & professional, London Glasgow Weinheim [etc.].

Amalric, L., Baran, N., Jeannot, R., Martin, J.C., Mouve, C., 2003. Les mécanismes de transfert des ' produits phytosanitaires du sol vers les I nappes et les méthodes d'analyse des produits phytosanitaires dans les eaux.

AMAP/UNEP, 2019. Technical background report for the global mercury assessment 2018, Arctic Monitoring and Assessment Programme, Oslo, Norway / UN Environment Programe, Geneva, Switzerland.

Amponsah, L.O., Sørensen, P.B., Nkansah, M.A., Vorkamp, K., Yevugah, L.L., Darko, G., 2023. Mercury contamination of two e-waste recycling sites in Ghana: an investigation into mercury pollution at Dagomba Line (Kumasi) and Agbogbloshie (Accra). Environ. Geochem. Health 45, 1723–1737. https://doi.org/10.1007/s10653-022-01295-9

AMR, A. pour une M. responsable, 2021. Diagnostic genre dans le secteur de la mine artisanale et à petite échelle (MAPE) au Burkina Fasoet prospection de recommandation d'actions ciblées.

Antonini, S., Nguyen, P.T., Arnold, U., Eichert, T., Clemens, J., 2012. Solar thermal evaporation of human urine for nitrogen and phosphorus recovery in Vietnam. Sci. Total Environ. 414, 592–599. https://doi.org/10.1016/j.scitotenv.2011.11.055

Arisawa, K., Takahashi, T., Nakano, A., Liu, X.J., Saito, H., Takizawa, Y., Koba, T., 2000. [Potential exposure to inorganic mercury in people living near a sewage sludge dumping site: urinary excretion of mercury, subjective symptoms and renal function]. Nihon Koshu Eisei Zasshi Jpn. J. Public Health 47, 134–144.

Ariya, P.A., Amyot, M., Dastoor, A., Deeds, D., Feinberg, A., Kos, G., Poulain, A., Ryjkov, A., Semeniuk, K., Subir, M., Toyota, K., 2015. Mercury Physicochemical and Biogeochemical Transformation in the Atmosphere and at Atmospheric Interfaces: A Review and Future Directions. Chem. Rev. 115, 3760–3802. https://doi.org/10.1021/cr500667e

Armijos, E., Crave, A., Espinoza, J.C., Filizola, N., Espinoza-Villar, R., Ayes, Fonseca, P., Fraizy, P., Gutierrez, O., Vauchel, P., Camenen, B., Martiınez, J.M., Dos Santos, A., Santini, W., Cochonneau, G., Guyot, J.L., 2020. Rainfall control on Amazon sediment flux: synthesis from 20 years of monitoring. Environ. Res. Commun. 2, 051008. https://doi.org/10.1088/2515-7620/ab9003

Arrazy, S., Addai-Arhin, S., Jeong, H., Novirsa, R., Wispriyono, B., Agusa, T., Ishibashi, Y., Kobayashi, J., 2023. Spatial distribution and human health risks of mercury in the gold mining area of Mandailing Natal District, Indonesia. Environ. Monit. Contam. Res. 3, 33–42. https://doi.org/10.5985/emcr.20230003

Asare-Donkor, N.K., Adimado, A.A., 2016. Influence of mining related activities on levels of mercury in water, sediment and fish from the Ankobra and Tano River basins in South Western Ghana. Environ. Syst. Res. 5, 5. https://doi.org/10.1186/s40068-016-0055-4

ASFF, A.S.F.F., 2022. Droits de l'Homme et industries extractives en Guinée : cartographie des acteurs, cadres juridiques applicables, dispositifs et enjeux de protection.

ATI, A.T.I., 2025. Flux d'or illicites et évasion fiscale dans huits pays partenaires de l'ATI. Cas de Madagascar, Tanzanie, Ghana, Liberia, Nigeria, Burkina Faso, Malawi et Éthiopie.

ATSDR, 2014. Medical Management Guidelines for Mercury.

Avigliano, E., Resongles, E., Moreno, E., Marie, M., Jaldín, M., Pouilly, M., 2025. Transboundary mining pollution? Metal(oid) concentrations in water, sediments, and risk assessment for fish

consumption in a lower Andean-to-Chaco sediment-choked basin. Environ. Sci. Pollut. Res. 32, 15258–15273. https://doi.org/10.1007/s11356-025-36563-5

Avornyo, V.K., Zakariah, M., Amo, B.O., 2023. CHARACTERIZATION AND CLASSIFICATION OF A TYPICAL IRON PAN SOIL FORMED OVER VOLTAIAN SHALE. UDS Int. J. Dev. 10, 1–8. https://doi.org/10.47740/768.UDSIJD6i

Avotins, P., Sciences, S.U.D. of A.E., 1975. Adsorption and Coprecipitation Studies of Mercury on Hydrous Iron Oxide. Stanford University.

Bacon, J.R., Davidson, C.M., 2008. Is there a future for sequential chemical extraction? The Analyst 133, 25–46. https://doi.org/10.1039/B711896A

Bah, A.L., OUEDA, A., BARRY, A., KABBRE, G., 2016. Diagnostics des Sources Potentielles de Pollution du Fleuve Niger a Faranah (GUINEE).

Bah, M.O., Jean, B., 1996. Forêts, politiqueforestière et gestion des ressources naturelles en Guinée.

Balcom, P.H., Schartup, A.T., Mason, R.P., Chen, C.Y., 2015. Sources of water column methylmercury across multiple estuaries in the Northeast U.S. Mar. Chem. 177, 721–730. https://doi.org/10.1016/j.marchem.2015.10.012

Balma, S., Aka, I., 2016. Cartographie des sites d'orpaillage de l'espace de competence de l'Agence de l'Eau du Mouhoun.

Banchirigah, S.M., 2008. Challenges with eradicating illegal mining in Ghana: A perspective from the grassroots. Resour. Policy 33, 29–38. https://doi.org/10.1016/j.resourpol.2007.11.001

Bansah, K.J., Dumakor-Dupey, N.K., Stemn, E., Galecki, G., 2018. Mutualism, commensalism or parasitism? Perspectives on tailings trade between large-scale and artisanal and small-scale gold mining in Ghana. Resour. Policy 57, 246–254. https://doi.org/10.1016/j.resourpol.2018.03.010

Bantenga, M., 1995. L'Or des Regions de Poura et de Gaoua: Les Vicissitudes de l'Exploitation Coloniale, 1925-1960. Int. J. Afr. Hist. Stud. 28, 563. https://doi.org/10.2307/221174

Baptista-Salazar, C., R. Quadra, G., Sobek, A., Jonsson, S., 2021. Insights into the factors influencing mercury concentrations in tropical reservoir sediments. Environ. Sci. Process. Impacts 23, 1542–1553. https://doi.org/10.1039/D1EM00156F

Barbé, L.L., Lebel, T., Tapsoba, D., 2002. Rainfall Variability in West Africa during the Years 1950–90. J. Clim. 15, 187–202. https://doi.org/10.1175/1520-0442(2002)015<0187:RVIWAD>2.0.CO;2

Barbieri, F.L., Gardon, J., 2009. Hair mercury levels in Amazonian populations: spatial distribution and trends. Int. J. Health Geogr. 8, 71. https://doi.org/10.1186/1476-072X-8-71

BARRO-TRAORE, F., TIENDREBEOGO, S.R.M., LALLOGO, S., TIENDREBEOGO, S., DABAL, M., OUEDRAOGO, H., 2005. Manifestations cutanées de l'arsenicisme au Burkina Faso: aspects épidémiologiques et cliniques. Vol 28 No 1 2 2005 Janvier-Déc. Vol. 28.

Basu, N., Bastiansz, A., Dórea, J.G., Fujimura, M., Horvat, M., Shroff, E., Weihe, P., Zastenskaya, I., 2023. Our evolved understanding of the human health risks of mercury. Ambio 52, 877–896. https://doi.org/10.1007/s13280-023-01831-6

Benkadi, 2021. Cartographie des mines artisanales, des artisants miniers, et du niveau d'utilisation de produits chimiques interdites (en partciculier le mercure et le cyanure) / Dégradation des terres dans les régions des Cascades et du Centre-Est.

Benoit, Janina.M., Cynthia, C., Gilmour, C.C., Mason, R.P., Heyes, A., 1999. Sulfide Controls on Mercury Speciation and Bioavailability to Methylating Bacteria in Sediment Pore Waters. Environ. Sci. Technol. 33, 951–957.

Benoit, J.M., Gilmour, C.C., Mason, R.P., 2001. The Influence of Sulfide on Solid-Phase Mercury Bioavailability for Methylation by Pure Cultures of *Desulfobulbus propionicus* (1pr3). Environ. Sci. Technol. 35, 127–132. https://doi.org/10.1021/es001415n

Berriane, Y., Derks, A., Kreil, A., Lüddeckens, D. (Eds.), 2021. Methodological Approaches to Societies in Transformation: How to Make Sense of Change. Springer International Publishing, Cham. https://doi.org/10.1007/978-3-030-65067-4

Béziat, D., Dubois, M., Debat, P., Nikiéma, S., Salvi, S., Tollon, F., 2008. Gold metallogeny in the Birimian craton of Burkina Faso (West Africa). J. Afr. Earth Sci. 50, 215–233. https://doi.org/10.1016/j.jafrearsci.2007.09.017

Bianchi, M., Palamakumbura, R.N., MacDonald, A.M., Macdonald, D.M.J., 2023. Assessing regional variation in yield from weathered basement aquifers in West Africa and modelling their future groundwater development and sustainability. Hydrogeol. J. 31, 257–274. https://doi.org/10.1007/s10040-023-02594-w

Biester, H., Müller, G., Schöler, H.F., 2002. Binding and mobility of mercury in soils contaminated by emissions from chlor-alkali plants. Sci. Total Environ. 284, 191–203. https://doi.org/10.1016/S0048-9697(01)00885-3

Biester, H., Scholz, C., 1997. Determination of Mercury Binding Forms in Contaminated Soils: Mercury Pyrolysis versus Sequential Extractions. Environ. Sci. Technol. 31, 233–239. https://doi.org/10.1021/es960369h

Bigham, J.M., Nordstrom, D.K., 2000. Iron and Aluminum Hydroxysulfates from Acid Sulfate Waters. Rev. Mineral. Geochem. 40, 351–403. https://doi.org/10.2138/rmg.2000.40.7

Black, F.J., Paytan, A., Knee, K.L., De Sieyes, N.R., Ganguli, P.M., Gray, E., Flegal, A.R., 2009. Submarine Groundwater Discharge of Total Mercury and Monomethylmercury to Central California Coastal Waters. Environ. Sci. Technol. 43, 5652–5659. https://doi.org/10.1021/es900539c

Black, P., Richard, M., Rossin, R., Telmer, K., 2017. Assessing occupational mercury exposures and behaviours of artisanal and small-scale gold miners in Burkina Faso using passive mercury vapour badges. Environ. Res. 152, 462–469. https://doi.org/10.1016/j.envres.2016.06.004

Blagodatsky, S., Ehret, M., Rasche, F., Hutter, I., Birner, R., Dzomeku, B., Neya, O., Cadisch, G., Wünsche, J., 2020. Myco-phytoremediation of mercury polluted soils in Ghana and Burkina Faso. Presented at the EGU General Assembly Conference Abstracts, p. 19583. https://doi.org/10.5194/egusphere-egu2020-19583

Block, S., Ganne, J., Baratoux, L., Zeh, A., Parra-Avila, L.A., Jessell, M., Ailleres, L., Siebenaller, L., 2015. Petrological and geochronological constraints on lower crust exhumation during Paleoproterozoic (Eburnean) orogeny, NW Ghana, West African Craton. J. Metamorph. Geol. 33, 463–494. https://doi.org/10.1111/jmg.12129

Bloom, N.S., Preus, E., Katon, J., Hiltner, M., 2003. Selective extractions to assess the biogeochemically relevant fractionation of inorganic mercury in sediments and soils. Anal. Chim. Acta 479, 233–248. https://doi.org/10.1016/S0003-2670(02)01550-7

Bohbot, J., 2017. L'orpaillage au Burkina Faso : une aubaine économique pour les populations, aux conséquences sociales et environnementales mal maîtrisées. EchoGéo. https://doi.org/10.4000/echogeo.15150

Boischio, A.A.P., Henshel, D., 2000. Fish Consumption, Fish Lore, and Mercury Pollution—Risk Communication for the Madeira River People. Environ. Res. 84, 108–126. https://doi.org/10.1006/enrs.2000.4035

Bokar, H., Traoré, A.Z., Mariko, A., Diallo, T., Traoré, A., Sy, A., Soumaré, O., Dolo, A., Bamba, F., Sacko, M., Touré, O., 2020. Geogenic influence and impact of mining activities on water soil and plants in surrounding areas of Morila Mine, Mali. J. Geochem. Explor. 209, 106429. https://doi.org/10.1016/j.gexplo.2019.106429

Bolay, M., 2016. «Il faut être là où l'or sort !»: De l'itinérance temporaire au maintien d'un mode de vie mobile chez les orpailleurs de Haute Guinée. 542443 b. https://doi.org/10.25365/PHAIDRA.266_06

Bollen, A., Wenke, A., Biester, H., 2008. Mercury speciation analyses in HgCl2-contaminated soils and groundwater—Implications for risk assessment and remediation strategies. Water Res. 42, 91–100. https://doi.org/10.1016/j.watres.2007.07.011

Bonzongo, J.-C.J., Donkor, A.K., Nartey, V.K., Lacerda, L.D., 2004. Mercury Pollution in Ghana: A Case Study of Environmental Impacts of Artisanal Gold Mining in Sub-Saharan Africa, in: Drude De Lacerda, L., Santelli, R.E., Duursma, E.K., Abrão, J.J. (Eds.), Environmental Geochemistry in

Tropical and Subtropical Environments. Springer Berlin Heidelberg, Berlin, Heidelberg, pp. 135–156. https://doi.org/10.1007/978-3-662-07060-4_12

Bortey-Sam, N., Nakayama, S.M.M., Ikenaka, Y., Akoto, O., Baidoo, E., Yohannes, Y.B., Mizukawa, H., Ishizuka, M., 2015. Human health risks from metals and metalloid via consumption of food animals near gold mines in Tarkwa, Ghana: Estimation of the daily intakes and target hazard quotients (THQs). Ecotoxicol. Environ. Saf. 111, 160–167. https://doi.org/10.1016/j.ecoenv.2014.09.008

Bortnikov, N.S., Boeva, N.M., Volkov, A.V., Galyamov, A.L., Makarova, M.A., 2024. The wealth of the subsoil of the Republic of Guinea. *In memory of Vladimir Ibrahimovic Mamedov*. Вестник Российской Академии Наук 94, 540–549. https://doi.org/10.31857/S0869587324060042

Bose-O'Reilly, S., Lettmeier, B., Matteucci Gothe, R., Beinhoff, C., Siebert, U., Drasch, G., 2008. Mercury as a serious health hazard for children in gold mining areas. Environ. Res. 107, 89–97. https://doi.org/10.1016/j.envres.2008.01.009

Bouchet, S., Goñi-Urriza, M., Monperrus, M., Guyoneaud, R., Fernandez, P., Heredia, C., Tessier, E., Gassie, C., Point, D., Guédron, S., Achá, D., Amouroux, D., 2018. Linking Microbial Activities and Low-Molecular-Weight Thiols to Hg Methylation in Biofilms and Periphyton from High-Altitude Tropical Lakes in the Bolivian Altiplano. Environ. Sci. Technol. 52, 9758–9767. https://doi.org/10.1021/acs.est.8b01885

Boudou, A., Dominique, Y., Cordier, S., Frery, N., 2006. Les chercheurs d'or et la pollution par le mercure en Guyane française : conséquences environnementales et sanitaires. Envionnement Risque Santé 5, 167–179.

Brabo, E.S., Angélica, R.S., Silva, A.P., Faial, K.R.F., Mascarenhas, A.F.S., Santos, E.C.O., Jesus, I.M., Loureiro, E.C.B., 2003. Assessment of Mercury Levels in Soils, Waters, Bottom Sediments and Fishes of Acre State in Brazilian Amazon. Water. Air. Soil Pollut. 147, 61–77. https://doi.org/10.1023/A:1024510312250

Brady, N.C., 1984. The nature and properties of soils, 9. ed. ed. Macmillan u.a, New York.

Bravo, A.G., Bouchet, S., Guédron, S., Amouroux, D., Dominik, J., Zopfi, J., 2015. High methylmercury production under ferruginous conditions in sediments impacted by sewage treatment plant discharges. Water Res. 80, 245–255. https://doi.org/10.1016/j.watres.2015.04.039

Bravo, A.G., Peura, S., Buck, M., Ahmed, O., Mateos-Rivera, A., Herrero Ortega, S., Schaefer, J.K., Bouchet, S., Tolu, J., Björn, E., Bertilsson, S., 2018. Methanogens and Iron-Reducing Bacteria: the Overlooked Members of Mercury-Methylating Microbial Communities in Boreal Lakes. Appl. Environ. Microbiol. 84, e01774-18. https://doi.org/10.1128/AEM.01774-18

Bretzler, A., Lalanne, F., Nikiema, J., Podgorski, J., Pfenninger, N., Berg, M., Schirmer, M., 2017. Groundwater arsenic contamination in Burkina Faso, West Africa: Predicting and verifying regions at risk. Sci. Total Environ. 584–585, 958–970. https://doi.org/10.1016/j.scitotenv.2017.01.147

Bretzler, A., Stolze, L., Nikiema, J., Lalanne, F., Ghadiri, E., Brennwald, M.S., Rolle, M., Schirmer, M., 2019. Hydrogeochemical and multi-tracer investigations of arsenic-affected aquifers in semi-arid West Africa. Geosci. Front. 10, 1685–1699. https://doi.org/10.1016/j.gsf.2018.06.004

BRGM, 2024. Guide polluants et comportement des polluants dans le milieu souterrain (Version 3 du 2 décembre 2024 No. RP-74064-FR). Republique Française.

Brocza, F.M., Rafaj, P., Sander, R., Wagner, F., Jones, J.M., 2024. Global scenarios of anthropogenic mercury emissions. Atmospheric Chem. Phys. 24, 7385–7404. https://doi.org/10.5194/acp-24-7385-2024

Brugger, F., Müller, S., Zanetti, J., Winkler, M., Knoblauch, A., Wehrli, B., 2018. Small-scale gold mining in Burkina Faso: Health effects, environmental burden and socio-economic interactions with agriculture: Project Report. ETH Zurich. https://doi.org/10.3929/ETHZ-B-000282708

Budtz-Jørgensen, E., Grandjean, P., Jørgensen, P.J., Weihe, P., Keiding, N., 2004. Association between mercury concentrations in blood and hair in methylmercury-exposed subjects at different ages. Environ. Res. 95, 385–393. https://doi.org/10.1016/j.envres.2003.11.001

Buy Gold Africa, G.A., 2025. How Much Gold Does Africa Produce? – BUY GOLD AFRICA. URL https://buygold.africa/how-much-gold-does-africa-produce/ (accessed 12.10.25).

Castaño, A., Cutanda, F., Esteban, M., Pärt, P., Navarro, C., Gómez, S., Rosado, M., López, A., López, E., Exley, K., Schindler, B.K., Govarts, E., Casteleyn, L., Kolossa-Gehring, M., Fiddicke, U., Koch, H., Angerer, J., Hond, E.D., Schoeters, G., Sepai, O., Horvat, M., Knudsen, L.E., Aerts, D., Joas, A., Biot, P., Joas, R., Jiménez-Guerrero, J.A., Diaz, G., Pirard, C., Katsonouri, A., Cerna, M., Gutleb, A.C., Ligocka, D., Reis, F.M., Berglund, M., Lupsa, I.-R., Halzlová, K., Charlier, C., Cullen, E., Hadjipanayis, A., Krsková, A., Jensen, J.F., Nielsen, J.K., Schwedler, G., Wilhelm, M., Rudnai, P., Középesy, S., Davidson, F., Fischer, M.E., Janasik, B., Namorado, S., Gurzau, A.E., Jajcaj, M., Mazej, D., Tratnik, J.S., Larsson, K., Lehmann, A., Crettaz, P., Lavranos, G., Posada, M., 2015. Fish consumption patterns and hair mercury levels in children and their mothers in 17 EU countries. Environ. Res. 141, 58–68. https://doi.org/10.1016/j.envres.2014.10.029

Cerqueira, U.M.F.M., Alves, J.P.S., Santos, W.N.L., Da Silva Pita, B., Novaes, C.G., Araújo, S.A., Bezerra, M.A., 2024. Recent applications of tetramethylammonium hydroxide (TMAH) in the sample preparation for elemental analysis by spectroanalytical techniques. Adv. Sample Prep. 9, 100104. https://doi.org/10.1016/j.sampre.2024.100104

Chain (CONTAM), E.P. on C. in the F., 2012. Scientific Opinion on the risk for public health related to the presence of mercury and methylmercury in food. EFSA J. 10, 2985. https://doi.org/10.2903/j.efsa.2012.2985

Chan, H.M., Scheuhammer, A.M., Ferran, A., Loupelle, C., Holloway, J., Weech, S., 2003. Impacts of Mercury on Freshwater Fish-Eating Wildlife and Humans. Hum. Ecol. Risk Assess. Int. J. 9, 867–883. https://doi.org/10.1080/713610013

Charlet, L., Blancho, F., Bonnet, T., Garambois, S., Boivin, P., Ferber, T., Tisserand, D., Guedron, S., 2017. Industrial Mercury Pollution in a Mountain Valley: A Combined Geophysical and Geochemical Study. Procedia Earth Planet. Sci. 17, 77–80. https://doi.org/10.1016/j.proeps.2016.12.040

Chen, C., Amirbahman, A., Fisher, N., Harding, G., Lamborg, C., Nacci, D., Taylor, D., 2008. Methylmercury in Marine Ecosystems: Spatial Patterns and Processes of Production, Bioaccumulation, and Biomagnification. EcoHealth 5, 399–408. https://doi.org/10.1007/s10393-008-0201-1

Chen, Y., Bonzongo, J.C., Miller, G.C., 1996. Levels of methylmercury and controlling factors in surface sediments of the Carson River system, Nevada. Environ. Pollut. 92, 281–287. https://doi.org/10.1016/0269-7491(95)00112-3

Chevrillon-Guibert, R., Magrin, G., 2018. Ruées vers l'or au Soudan, au Tchad et au Sahel : logiques étatiques, mobilités et contrôle territorial. Bull. Assoc. Géographes Fr. 95, 272–289. https://doi.org/10.4000/bagf.3272

Choquet, C., 2018. Orpaillage « artisanal » et mutations locales 3.

Cissé, F.B., 2019. ÉTUDE DES IMPACTS DE L' EXPLOITATION ARTISANALE DE L' OR EN RÉPUBLIQUE DE GUINÉE (CAS DE LA PRÉFECTURE DE SIGUIRI).

Claon, S.J., Kouassi, S.K., Ahouéfa, N.L., Seri, L.K., Seka, A.M., Djaman, J.A., Kouadio, L.K., 2024. Mercury Levels Assessment in the Population of Aby and Frambo Villages in the Vinicity of Aby Lagoon in Côte d'Ivoire (West Africa). J. Water Resour. Prot. 16, 219–232. https://doi.org/10.4236/jwarp.2024.163013

Clarkson, T.W., Magos, L., 2006. The Toxicology of Mercury and Its Chemical Compounds. Crit. Rev. Toxicol. 36, 609–662. https://doi.org/10.1080/10408440600845619

Compaore, W.F., Dumoulin, A., Rousseau, D.P.L., 2020. Metals and metalloid in gold mine pit lakes and fish intake risk assessment, Burkina Faso. Environ. Geochem. Health 42, 563–577. https://doi.org/10.1007/s10653-019-00390-8

Compaore, W.F., Dumoulin, A., Rousseau, D.P.L., 2019. Gold Mine Impact on Soil Quality, Youga, Southern Burkina Faso, West Africa. Water. Air. Soil Pollut. 230, 207. https://doi.org/10.1007/s11270-019-4257-z

Conseil des Organisations internationales des, Sciences médicales (CIOMS), en collaboration avec, l'Organisation mondiale de la Santé (OMS), 2016. Lignes directrices internationales d'éthique pour la recherche en matière de santé impliquant des participants humains.

Coolbaugh, M.F., Gustin, M.S., Rytuba, J.J., 2002. Annual emissions of mercury to the atmosphere from natural sources in Nevada and California. Environ. Geol. 42, 338–349. https://doi.org/10.1007/s00254-002-0557-4

Cordy, P., Veiga, M.M., Salih, I., Al-Saadi, S., Console, S., Garcia, O., Mesa, L.A., Velásquez-López, P.C., Roeser, M., 2011. Mercury contamination from artisanal gold mining in Antioquia, Colombia: The world's highest per capita mercury pollution. Sci. Total Environ. 410–411, 154–160. https://doi.org/10.1016/j.scitotenv.2011.09.006

Cossa, D., Gobeil, C., 2000. Mercury speciation in the Lower St. Lawrence Estuary. Can. J. Fish. Aquat. Sci. 57, 138–147. https://doi.org/10.1139/f99-237

Côte, M., 2013. What's in a Right? The liberalisation of gold mining and decentralisation in Burkina Faso.

Côte, M., Korf, B., 2018. Making Concessions: Extractive Enclaves, Entangled Capitalism and Regulative Pluralism at the Gold Mining Frontier in Burkina Faso. World Dev. 101, 466–476. https://doi.org/10.1016/j.worlddev.2016.11.002

Courtois, N., Lachassagne, P., Wyns, R., Blanchin, R., Bougaïré, F.D., Somé, S., Tapsoba, A., 2010. Large-Scale Mapping of Hard-Rock Aquifer Properties Applied to Burkina Faso. Groundwater 48, 269–283. https://doi.org/10.1111/j.1745-6584.2009.00620.x

Crespo-Lopez, M.E., Augusto-Oliveira, M., Lopes-Araújo, A., Santos-Sacramento, L., Yuki Takeda, P., Macchi, B.D.M., Do Nascimento, J.L.M., Maia, C.S.F., Lima, R.R., Arrifano, G.P., 2021. Mercury: What can we learn from the Amazon? Environ. Int. 146, 106223. https://doi.org/10.1016/j.envint.2020.106223

Crump, K.L., Trudeau, V.L., 2009. Mercury-induced reproductive impairment in fish. Environ. Toxicol. Chem. 28, 895–907. https://doi.org/10.1897/08-151.1

Dabré, D., Guédron, S., Maïga, Y., Jelavic, S., Campillo, S., Fin, J., Sentenac, S., Bruneel, O., Ouédraogo, O., Mason, R., 2025. Mercury transfer and transformation from mine soil to river sediments: the potential role of amorphous iron oxides in methylation processes in southern Burkina Faso. Environ. Sci. Process. Impacts 27, 3246–3260. https://doi.org/10.1039/D5EM00426H

Dai, S.-S., Yang, Z., Tong, Y., Chen, L., Liu, S.-Y., Pan, R., Li, Y., Zhang, C.-J., Liu, Y.-R., Huang, Q., 2021. Global distribution and environmental drivers of methylmercury production in sediments. J. Hazard. Mater. 407, 124700. https://doi.org/10.1016/j.jhazmat.2020.124700

Darko, H.F., Karikari, A.Y., Duah, A.A., Akurugu, B.A., Mante, V., Teye, F.O., 2023. Effect of small-scale illegal mining on surface water and sediment quality in Ghana. Int. J. River Basin Manag. 21, 375–386. https://doi.org/10.1080/15715124.2021.2002345

Davies, F., Notcutt, G., 1996. Biomonitoring of atmospheric mercury in the vicinity of Kilauea, Hawaii. Water. Air. Soil Pollut. 86, 275–281. https://doi.org/10.1007/bf00279162

De Oliveira, S.M.B., Melfi, A.J., Fostier, A.H., Forti, M.C., Fávaro, D.I.T., Boulet, R., 2001. Soils as an Important Sink for Mercury in the Amazon. Water. Air. Soil Pollut. 126, 321–337. https://doi.org/10.1023/A:1005239627632

De Paula Gutiérrez, B.F., Agudelo, C.A.R., 2020. Fish as bioindicators: coal and mercury pollution in Colombia's ecosystems. Environ. Sci. Pollut. Res. 27, 27541–27562. https://doi.org/10.1007/s11356-020-09159-4

Dessertine, A., 2021. Spatializing Social Change: Artisanal and Small-Scale Gold Mining in Upper Guinea, in: Berriane, Y., Derks, A., Kreil, A., Lüddeckens, D. (Eds.), Methodological Approaches to Societies in Transformation. Springer International Publishing, Cham, pp. 213–235. https://doi.org/10.1007/978-3-030-65067-4_9

Dessertine, A., 2013. Le lu ne meurt jamais : mobilités des individus et pérennité de la résidence dans un village malinké de Guinée. Géocarrefour 88, 131–138. https://doi.org/10.4000/geocarrefour.9058

Dessertine, A., Chevrillon-Guibert, R., Gagnol, L., Betabelet, J., Malal Diallo, M., Petit-Roulet, R., Sawadogo, E., Zongo, T., Magrin, G., 2022. Orpaillage et développement des territoires en Afrique : une équation difficile ? pp. 163–181.

DIALLO, Samba.T., 1996. Status of the Guinean fishery resources. INTERGOVERNMENTAL OCEANOGRAPHIC COMMISSION (of UNESCO).

Dias Filho, N.L., Do Carmo, D.R., 2006. Study of an organically modified clay: Selective adsorption of heavy metal ions and voltammetric determination of mercury(II). Talanta 68, 919–927. https://doi.org/10.1016/j.talanta.2005.06.028

Diringer, S.E., Feingold, B.J., Ortiz, E.J., Gallis, J.A., Araújo-Flores, J.M., Berky, A., Pan, W.K.Y., Hsu-Kim, H., 2015. River transport of mercury from artisanal and small-scale gold mining and risks for dietary mercury exposure in Madre de Dios, Peru. Environ. Sci. Process. Impacts 17, 478–487. https://doi.org/10.1039/C4EM00567H

Doebelin, N., Kleeberg, R., 2015. *Profex*: a graphical user interface for the Rietveld refinement program*BGMN*. J. Appl. Crystallogr. 48, 1573–1580. https://doi.org/10.1107/s1600576715014685

Dokua Sasu, D., 2025. Gold production in Africa [WWW Document]. Statista. URL https://www.statista.com/statistics/508145/african-gold-mine-production/ (accessed 10.14.25).

Donkor, A.K., Bonzongo, J.C., Nartey, V.K., Adotey, D.K., 2006. Mercury in different environmental compartments of the Pra River Basin, Ghana. Sci. Total Environ. 368, 164–176. https://doi.org/10.1016/j.scitotenv.2005.09.046

Dos Santos, E.C., De Mendonça Silva, J.C., Duarte, H.A., 2016. Pyrite Oxidation Mechanism by Oxygen in Aqueous Medium. J. Phys. Chem. C 120, 2760–2768. https://doi.org/10.1021/acs.jpcc.5b10949

Dos Santos, S.N., Alleoni, L.R.F., 2013. Reference values for heavy metals in soils of the Brazilian agricultural frontier in Southwestern Amazônia. Environ. Monit. Assess. 185, 5737–5748. https://doi.org/10.1007/s10661-012-2980-7

Dossou Etui, I.M., Stylo, M., Davis, K., Evers, D.C., Slaveykova, V.I., Wood, C., Burton, M.E.H., 2024. Artisanal and small-scale gold mining and biodiversity: a global literature review. Ecotoxicology 33, 484–504. https://doi.org/10.1007/s10646-024-02748-w

Doumbouya, I.K., Dessertine, A., Vinches, M., Cerceau, J., 2024. Mechanization of artisanal and small-scale gold mining in Guinea: Socio-technical trajectory of a rural mining site in Upper Guinea. J. Rural Stud. 112, 103445. https://doi.org/10.1016/j.jrurstud.2024.103445

Drace, K., Kiefer, A.M., Veiga, M.M., 2016. Cyanidation of Mercury-Contaminated Tailings: Potential Health Effects and Environmental Justice. Curr. Environ. Health Rep. 3, 443–449. https://doi.org/10.1007/s40572-016-0113-0

Eagles-Smith, C.A., Wiener, J.G., Eckley, C.S., Willacker, J.J., Evers, D.C., Marvin-DiPasquale, M., Obrist, D., Fleck, J.A., Aiken, G.R., Lepak, J.M., Jackson, A.K., Webster, J.P., Stewart, A.R., Davis, J.A., Alpers, C.N., Ackerman, J.T., 2016. Mercury in western North America: A synthesis of environmental contamination, fluxes, bioaccumulation, and risk to fish and wildlife. Sci. Total Environ. 568, 1213–1226. https://doi.org/10.1016/j.scitotenv.2016.05.094

Eawag-EPFL, 2019. Mercury in the environment.

Egler, S.G., Rodrigues-Filho, S., Villas-Bôas, R.C., Beinhoff, C., 2006. Evaluation of mercury pollution in cultivated and wild plants from two small communities of the Tapajós gold mining reserve, Pará State, Brazil. Sci. Total Environ. 368, 424–433. https://doi.org/10.1016/j.scitotenv.2005.09.037

Eludoyin, O.M., Adelekan, I.O., Webster, R., Eludoyin, A.O., 2014. Air temperature, relative humidity, climate regionalization and thermal comfort of Nigeria. Int. J. Climatol. 34, 2000–2018. https://doi.org/10.1002/joc.3817

Engle, M.A., Gustin, M.S., Zhang, H., 2001. Quantifying natural source mercury emissions from the Ivanhoe Mining District, north-central Nevada, USA. Atmos. Environ. 35, 3987–3997. https://doi.org/10.1016/S1352-2310(01)00184-4

ENZO, 2017. Enquête Nationale sur le Secteur de l'Orpaillage (ENZO). Principaux résultats.
Esdaile, L.J., Chalker, J.M., 2018. The Mercury Problem in Artisanal and Small-Scale Gold Mining. Chem. – Eur. J. 24, 6905–6916. https://doi.org/10.1002/chem.201704840
European Environment Agency, 2028. Le mercure: une menace persistante pour l'environnement et la santé des citoyen (Article de journal).
Falciani, R., Novaro, E., Marchesini, M., Gucciardi, M., 2000. Multi-element analysis of soil and sediment by ICP-MS after a microwave assisted digestion method. J. Anal. At. Spectrom. 15, 561–565. https://doi.org/10.1039/b000742k
Fan, M., Boonfueng, T., Xu, Y., Axe, L., Tyson, T.A., 2005. Modeling Pb sorption to microporous amorphous oxides as discrete particles and coatings. J. Colloid Interface Sci. 281, 39–48. https://doi.org/10.1016/j.jcis.2004.08.050
FAO, 2025. Ghana - National Aquaculture Sector Overview [WWW Document]. URL https://www.fao.org/fishery/en/countrysector/gh/en?lang=en (accessed 10.30.25).
FAO, ONU, O. des Na.U. pour l'alimentation et l'agriculture, 2005. Profil de Pays – Guinée (AQUASTAT report).
Feinberg, A., Dlamini, T., Jiskra, M., Shah, V., Selin, N.E., 2022. Evaluating atmospheric mercury (Hg) uptake by vegetation in a chemistry-transport model. Environ. Sci. Process. Impacts 24, 1303–1318. https://doi.org/10.1039/D2EM00032F
Feyte, S., Tessier, A., Gobeil, C., Cossa, D., 2010. In situ adsorption of mercury, methylmercury and other elements by iron oxyhydroxides and organic matter in lake sediments. Appl. Geochem. 25, 984–995. https://doi.org/10.1016/j.apgeochem.2010.04.005
Figueiredo, B.R., De Campos, A.B., Da Silva, R., Hoffman, N.C., 2018. Mercury sink in Amazon rainforest: soil geochemical data from the Tapajos National Forest, Brazil. Environ. Earth Sci. 77, 296. https://doi.org/10.1007/s12665-018-7471-x
Fisher, P., Aumann, C., Chia, K., O'Halloran, N., Chandra, S., 2017. Adequacy of laser diffraction for soil particle size analysis. PLOS ONE 12, e0176510. https://doi.org/10.1371/journal.pone.0176510
FMI, F.M.I., 2021. Consultations de 2021 au titre de l'article IV. Recettes minières en Guinée (Consultations de 2021 au titre de l'article IV No. 21/147). Fonds Monaitaire International.
FOA, 2025. Côte d'Ivoire - National Aquaculture Sector Overview [WWW Document]. URL https://www.fao.org/fishery/en/countrysector/ci/fr?lang=fr (accessed 10.30.25).
Fonds monétaire international, F., 2021. CONSULTATIONS DE 2021 AU TITRE DE L'ARTICLE IV EN GUINEE.
Fontaine, A., Eglinger, A., Ada, K., André-Mayer, A.-S., Reisberg, L., Siebenaller, L., Le Mignot, E., Ganne, J., Poujol, M., 2017. Geology of the world-class Kiaka polyphase gold deposit, West African Craton, Burkina Faso. J. Afr. Earth Sci. 126, 96–122. https://doi.org/10.1016/j.jafrearsci.2016.11.017
Fostier, A.H., Amouroux, D., Tessier, E., Viana, J.L.M., Richter, L., 2023. Methylmercury content in soil and litter from the Amazonian rainforest and its potential fate during forest fires. Front. Environ. Chem. 4, 1242915. https://doi.org/10.3389/fenvc.2023.1242915
Fowe, T., Karambiri, H., Paturel, J.-E., Poussin, J.-C., Cecchi, P., 2015. Water balance of small reservoirs in the Volta basin: A case study of Boura reservoir in Burkina Faso. Agric. Water Manag. 152, 99–109. https://doi.org/10.1016/j.agwat.2015.01.006
Fréèze, R.A., Cherry, J., 1979. Chapter 9: Groundwater Contamination | Freeze and Cherry Groundwater Book. URL https://fc79.gw-project.org/english/chapter-9/ (accessed 11.20.25).
Fu, X., Feng, X., Zhu, W., Rothenberg, S., Yao, H., Zhang, H., 2010. Elevated atmospheric deposition and dynamics of mercury in a remote upland forest of southwestern China. Environ. Pollut. 158, 2324–2333. https://doi.org/10.1016/j.envpol.2010.01.032
Gadd, G.M., 1993. Microbial formation and transformation of organometallic and organometalloid compounds. FEMS Microbiol. Rev. 11, 297–316. https://doi.org/10.1111/j.1574-6976.1993.tb00003.x

García-Sánchez, A., Contreras, F., Adams, M., Santos, F., 2006. Atmospheric mercury emissions from polluted gold mining areas (Venezuela). Environ. Geochem. Health 28, 529–540. https://doi.org/10.1007/s10653-006-9049-x

Gerardeaux, E., Kourouma, M., 1998. La culture cotonnière en Haute-Guinée (No. 17).

Gerson, J.R., Driscoll, C.T., Hsu-Kim, H., Bernhardt, E.S., 2018. Senegalese artisanal gold mining leads to elevated total mercury and methylmercury concentrations in soils, sediments, and rivers. Elem. Sci. Anthr. 6, 11. https://doi.org/10.1525/elementa.274

Gerson, J.R., Szponar, N., Zambrano, A.A., Bergquist, B., Broadbent, E., Driscoll, C.T., Erkenswick, G., Evers, D.C., Fernandez, L.E., Hsu-Kim, H., Inga, G., Lansdale, K.N., Marchese, M.J., Martinez, A., Moore, C., Pan, W.K., Purizaca, R.P., Sánchez, V., Silman, M., Ury, E.A., Vega, C., Watsa, M., Bernhardt, E.S., 2022. Amazon forests capture high levels of atmospheric mercury pollution from artisanal gold mining. Nat. Commun. 13, 559. https://doi.org/10.1038/s41467-022-27997-3

Ghezzi, L., Valerio, M., Petrini, R., 2023. Novel Determination of Elemental Mercury in Silicate Rock by Thermal Desorption. Anal. Lett. 56, 1270–1278. https://doi.org/10.1080/00032719.2022.2125984

Gilmour, C.C., Podar, M., Bullock, A.L., Graham, A.M., Brown, S.D., Somenahally, A.C., Johs, A., Hurt, R.A., Bailey, K.L., Elias, D.A., 2013. Mercury Methylation by Novel Microorganisms from New Environments. Environ. Sci. Technol. 47, 11810–11820. https://doi.org/10.1021/es403075t

Gnazou, M.D.-T., Sabi, E.B., Tairou, S.M., Akakpo, W., Agouda, K., Upton, K., Ó Dochartaigh, B., Bellwood-Howard, I., 2018. Hydrogeology of Togo - MediaWiki [WWW Document]. URL https://earthwise.bgs.ac.uk/index.php/Hydrogeology_of_Togo (accessed 11.19.25).

Goix, S., Maurice, L., Laffont, L., Rinaldo, R., Lagane, C., Chmeleff, J., Menges, J., Heimbürger, L.-E., Maury-Brachet, R., Sonke, J.E., 2019. Quantifying the impacts of artisanal gold mining on a tropical river system using mercury isotopes. Chemosphere 219, 684–694. https://doi.org/10.1016/j.chemosphere.2018.12.036

Grandjean, P., Satoh, H., Murata, K., Eto, K., 2010. Adverse Effects of Methylmercury: Environmental Health Research Implications. Environ. Health Perspect. 118, 1137–1145. https://doi.org/10.1289/ehp.0901757

Grandjean, P., Weihe, P., White, R.F., Debes, F., Araki, S., Yokoyama, K., Murata, K., Sørensen, N., Dahl, R., Jørgensen, P.J., 1997. Cognitive Deficit in 7-Year-Old Children with Prenatal Exposure to Methylmercury. Neurotoxicol. Teratol. 19, 417–428. https://doi.org/10.1016/S0892-0362(97)00097-4

Grätz, T., 2004. Les frontières de l'orpaillage en Afrique occidentale: Autrepart n° 30, 135–150. https://doi.org/10.3917/autr.030.0135

Gray, J.E., Labson, V.F., Weaver, J.N., Krabbenhoft, D.P., 2002. Mercury and methylmercury contamination related to artisanal gold mining, Suriname. Geophys. Res. Lett. 29. https://doi.org/10.1029/2002GL015575

Grigal, D.F., 2002. Inputs and outputs of mercury from terrestrial watersheds: a review. Environ. Rev. 10, 1–39. https://doi.org/10.1139/a01-013

Grimaldi, C., Grimaldi, M., Guedron, S., 2008. Mercury distribution in tropical soil profiles related to origin of mercury and soil processes. Sci. Total Environ. 401, 121–129. https://doi.org/10.1016/j.scitotenv.2008.04.001

Grimaldi, M., Gaudet, J., Grimaldi, C., Melieres, M.A., Spadini, L., 2001. "Programme de recheche Le Mercure en Guyane Française Rapport final, partie I : la région de St Elie et le réservoir de Petit Saut." CNRS-PEVS. (Rapport finale). CNRS-PEVS.

Grimaldi, M., Guédron, S., Grimaldi, C., 2015. Impact of gold mining on mercury contamination and soil degradation in Amazonian ecosystems of French Guiana., in: Brearley, F.Q., Thomas, A.D. (Eds.), Land-Use Change Impacts on Soil Processes: Tropical and Savannah Ecosystems. CABI, UK, pp. 95–107. https://doi.org/10.1079/9781780642109.0095

G.Sidam-Minorex, 1988. Orpaillage en Guinée.

Guédron, S., Amouroux, D., Tessier, E., Grimaldi, C., Barre, J., Berail, S., Perrot, V., Grimaldi, M., 2018. Mercury Isotopic Fractionation during Pedogenesis in a Tropical Forest Soil Catena (French Guiana): Deciphering the Impact of Historical Gold Mining. Environ. Sci. Technol. acs.est.8b02186. https://doi.org/10.1021/acs.est.8b02186

Guédron, S., Audry, S., Acha, D., Bouchet, S., Point, D., Condom, T., Heredia, C., Campillo, S., Baya, P.A., Groleau, A., Amice, E., Amouroux, D., 2020. Diagenetic production, accumulation and sediment-water exchanges of methylmercury in contrasted sediment facies of Lake Titicaca (Bolivia). Sci. Total Environ. 723, 138088. https://doi.org/10.1016/j.scitotenv.2020.138088

Guédron, S., Dabre, D., Duwig, C., Amouroux, D., Fin, J., Campillo, S., Biron, R., Guyard, H., Tessier, E., Moreno, I., Yupanqui, J., Uzu, G., Acha, D., 2025. From mine to lake: Source, fate and budget of mercury species in the high-altitude watershed of a fast-developing Andean city (El Alto, Bolivia). Sci. Total Environ. 998, 180239. https://doi.org/10.1016/j.scitotenv.2025.180239

Guédron, S., Devin, S., Vignati, D.A.L., 2015. Total and methylmercury partitioning between colloids and true solution: From case studies in sediment overlying and porewaters to a generalized model. Environ. Toxicol. Chem. 35, 330–339. https://doi.org/10.1002/etc.3190

Guédron, S., Duwig, C., Prado, B.L., Point, D., Flores, M.G., Siebe, C., 2014a. (Methyl)Mercury, Arsenic, and Lead Contamination of the World's Largest Wastewater Irrigation System: the Mezquital Valley (Hidalgo State—Mexico). Water. Air. Soil Pollut. 225. https://doi.org/10.1007/s11270-014-2045-3

Guedron, S., Grangeon, S., Lanson, B., Grimaldi, M., 2009. Mercury speciation in a tropical soil association; Consequence of gold mining on Hg distribution in French Guiana. Geoderma 153, 331–346. https://doi.org/10.1016/j.geoderma.2009.08.017

Guedron, S., Grimaldi, M., Grimaldi, C., Cossa, D., Tisserand, D., Charlet, L., 2011. Amazonian former gold mined soils as a source of methylmercury: Evidence from a small scale watershed in French Guiana. Water Res. 45, 2659–2669. https://doi.org/10.1016/j.watres.2011.02.022

Guédron, S., Huguet, L., Vignati, D.A.L., Liu, B., Gimbert, F., Ferrari, B.J.D., Zonta, R., Dominik, J., 2012. Tidal cycling of mercury and methylmercury between sediments and water column in the Venice Lagoon (Italy). Mar. Chem. 130–131, 1–11. https://doi.org/10.1016/j.marchem.2011.12.003

Guédron, S., Point, D., Acha, D., Bouchet, S., Baya, P.A., Tessier, E., Monperrus, M., Molina, C.I., Groleau, A., Chauvaud, L., Thebault, J., Amice, E., Alanoca, L., Duwig, C., Uzu, G., Lazzaro, X., Bertrand, A., Bertrand, S., Barbraud, C., Delord, K., Gibon, F.M., Ibanez, C., Flores, M., Fernandez Saavedra, P., Ezpinoza, M.E., Heredia, C., Rocha, F., Zepita, C., Amouroux, D., 2017. Mercury contamination level and speciation inventory in Lakes Titicaca & Uru-Uru (Bolivia): Current status and future trends. Environ. Pollut. 231, 262–270. https://doi.org/10.1016/j.envpol.2017.08.009

Guédron, S., Tisserand, D., Garambois, S., Spadini, L., Molton, F., Bounvilay, B., Charlet, L., Polya, D.A., 2014b. Baseline investigation of (methyl)mercury in waters, soils, sediments and key foodstuffs in the Lower Mekong Basin: The rapidly developing city of Vientiane (Lao PDR). J. Geochem. Explor. 143, 96–102. https://doi.org/10.1016/j.gexplo.2014.03.020

Guédron, S., Tolu, J., Brisset, E., Sabatier, P., Perrot, V., Bouchet, S., Develle, A.L., Bindler, R., Cossa, D., Fritz, S.C., Baker, P.A., 2019. Late Holocene volcanic and anthropogenic mercury deposition in the western Central Andes (Lake Chungará, Chile). Sci. Total Environ. 662, 903–914. https://doi.org/10.1016/j.scitotenv.2019.01.294

Gustin, M.S., Lindberg, S.E., Austin, K., Coolbaugh, M., Vette, A., Zhang, H., 2000. Assessing the contribution of natural sources to regional atmospheric mercury budgets. Sci. Total Environ. 259, 61–71. https://doi.org/10.1016/S0048-9697(00)00556-8

Gustin, S.M., Coolbaugh, M., Engle, M., Fitzgerald, B., Keislar, R., Lindberg, S., Nacht, D., Quashnick, J., Rytuba, J., Sladek, C., Zhang, H., Zehner, R., 2003. Atmospheric mercury emissions from mine wastes and surrounding geologically enriched terrains. Environ. Geol. 43, 339–351. https://doi.org/10.1007/s00254-002-0630-z

Gyamfi, O., Sørensen, P.B., Darko, G., Ansah, E., Vorkamp, K., Bak, J.L., 2021. Contamination, exposure and risk assessment of mercury in the soils of an artisanal gold mining community in Ghana. Chemosphere 267, 128910. https://doi.org/10.1016/j.chemosphere.2020.128910

Hammerschmidt, C.R., Fitzgerald, W.F., 2004. Geochemical Controls on the Production and Distribution of Methylmercury in Near-Shore Marine Sediments. Environ. Sci. Technol. 38, 1487–1495. https://doi.org/10.1021/es034528q

Hammerschmidt, C.R., Fitzgerald, W.F., 2001. Formation of Artifact Methylmercury during Extraction from a Sediment Reference Material. Anal. Chem. 73, 5930–5936. https://doi.org/10.1021/ac010721w

Hauptmann, A., Klein, S., 2009. Bronze Age gold in Southern Georgia. ArchéoSciences 33, 75–82. https://doi.org/10.4000/archeosciences.2037

Heiri, O., Lotter, A.F., Lemcke, G., 2001. Loss on ignition as a method for estimating organic and carbonate content in sediments: reproducibility and comparability of results. J. Paleolimnol. 25, 101–110. https://doi.org/10.1023/A:1008119611481

Hellal, J., Guédron, S., Huguet, L., Schäfer, J., Laperche, V., Joulian, C., Lanceleur, L., Burnol, A., Ghestem, J.-P., Garrido, F., Battaglia-Brunet, F., 2015. Mercury mobilization and speciation linked to bacterial iron oxide and sulfate reduction: A column study to mimic reactive transfer in an anoxic aquifer. J. Contam. Hydrol. 180, 56–68. https://doi.org/10.1016/j.jconhyd.2015.08.001

Hellal, J., Schäfer, J., Vigouroux, R., Lanceleur, L., Laperche, V., 2020. Impact of Old and Recent Gold Mining Sites on Mercury Fluxes in Suspended Particulate Matter, Water and Sediment in French Guiana. Appl. Sci. 10, 7829. https://doi.org/10.3390/app10217829

Hentschel, T., Hruschka, F., Priester, M., 2003. Artisanal and small-scale mining: challenges and opportunities. IIED : WBCSD, London.

Heyes, A., Miller, C., Mason, R.P., 2004. Mercury and methylmercury in Hudson River sediment: impact of tidal resuspension on partitioning and methylation. Mar. Chem. 90, 75–89. https://doi.org/10.1016/j.marchem.2004.03.011

Hill, D., 2016. Leaked map reveals chronic mercury epidemic in Peru. The Guardian.

Hilson, G., 2002. The environmental impact of small-scale gold mining in Ghana: identifying problems and possible solutions. Geogr. J. 168, 57–72. https://doi.org/10.1111/1475-4959.00038

Hilson, G., Hilson, A., Maconachie, R., 2018. Opportunity or necessity? Conceptualizing entrepreneurship at African small-scale mines. Technol. Forecast. Soc. Change 131, 286–302. https://doi.org/10.1016/j.techfore.2017.12.008

Hilson, G., Hilson, C.J., Pardie, S., 2007. Improving awareness of mercury pollution in small-scale gold mining communities: Challenges and ways forward in rural Ghana. Environ. Res. 103, 275–287. https://doi.org/10.1016/j.envres.2006.09.010

Hilson, G., Pardie, S., 2006. Mercury: An agent of poverty in Ghana's small-scale gold-mining sector? Resour. Policy 31, 106–116. https://doi.org/10.1016/j.resourpol.2006.09.001

Hilson, G., Potter, C., 2005. Structural Adjustment and Subsistence Industry: Artisanal Gold Mining in Ghana. Dev. Change 36, 103–131. https://doi.org/10.1111/j.0012-155X.2005.00404.x

Hilson, G., Potter, C., 2003. Why Is Illegal Gold Mining Activity so Ubiquitous in Rural Ghana? Afr. Dev. Rev. 15, 237–270. https://doi.org/10.1111/j.1467-8268.2003.00073.x

Holmes, J., Lean, D., 2006. Factors that influence methylmercury flux rates from wetland sediments. Sci. Total Environ. 368, 306–319. https://doi.org/10.1016/j.scitotenv.2005.11.027

Holmes, P., James, K.A.F., Levy, L.S., 2009. Is low-level environmental mercury exposure of concern to human health? Sci. Total Environ. 408, 171–182. https://doi.org/10.1016/j.scitotenv.2009.09.043

Horvat, M., 1990. A modified method for the determination of methylmercury by gas chromatography. Talanta 37, 207–212. https://doi.org/10.1016/0039-9140(90)80024-A

Hu, H., Lin, H., Zheng, W., Tomanicek, S.J., Johs, A., Feng, X., Elias, D.A., Liang, L., Gu, B., 2013. Oxidation and methylation of dissolved elemental mercury by anaerobic bacteria. Nat. Geosci. 6, 751–754. https://doi.org/10.1038/ngeo1894

Hug, S.J., Winkel, L.H.E., Voegelin, A., Berg, M., Johnson, A.C., 2020. Arsenic and Other Geogenic Contaminants in Groundwater – A Global Challenge. CHIMIA 74, 524. https://doi.org/10.2533/chimia.2020.524

Huggins, F.E., Yap, N., Huffman, G.P., Senior, C.L., 2003. XAFS characterization of mercury captured from combustion gases on sorbents at low temperatures. Fuel Process. Technol. 82, 167–196. https://doi.org/10.1016/S0378-3820(03)00068-7

IGF, 2022. Illicit Financial Flows and Conflict in Artisanal and Small-Scale Gold Mining: Burkina Faso, Mali, and Niger.

Ikingura, J.R., Akagi, H., 2003. Total mercury and methylmercury levels in fish from hydroelectric reservoirs in Tanzania. Sci. Total Environ. 304, 355–368. https://doi.org/10.1016/S0048-9697(02)00581-8

Ikingura, J.R., Akagi, H., Mujumba, J., Messo, C., 2006. Environmental assessment of mercury dispersion, transformation and bioavailability in the Lake Victoria Goldfields, Tanzania. J. Environ. Manage. 81, 167–173. https://doi.org/10.1016/j.jenvman.2005.09.026

INERIS, 2018. Revue synthétique des bonnes pratiques relatives à l'utilisation du cyanure pour le traitement de l'or dans le contexte guyanais (Rapport No. DRS-18-177174-08150B). Direction des Risques du Sol et du Sous-sol.

INS, I.N. de la S., 2021. Annuaire des statistiques de l'environnement 2020.

Insd-RGPH, C.I.N. de la S. et de la D., 2022. Cinquième Recensement Général de la Population et de l'Habitation du Burkina Faso. Synthèse des résultats définitifs.

ITIE, 2022. Initiative pour la Transparence dans les Industries Extractives de la République de Guinée.

ITIE, C. de pilotage, 2020. Initiative pour la Transparence dans les Industries Extractives en Republique de Guinée: Rapport assoupli 2019-2020.

ITIE-BDO, 2018. Initiative pour la Transparence dans les Industries Extractives de la République de Guinée.

Jackson, T.A., 1989. The influence of clay minerals, oxides, and humic matter on the methylation and demethylation of mercury by micro-organisms in freshwater sediments. Appl. Organomet. Chem. 3, 1–30. https://doi.org/10.1002/aoc.590030103

Jiskra, M., Wiederhold, J.G., Skyllberg, U., Kronberg, R.-M., Hajdas, I., Kretzschmar, R., 2015. Mercury Deposition and Re-emission Pathways in Boreal Forest Soils Investigated with Hg Isotope Signatures. Environ. Sci. Technol. 49, 7188–7196. https://doi.org/10.1021/acs.est.5b00742

Kaboré, E., 2023. #SAMAO2023: Focus on Burkina Faso's mining potential | Mines Actu Burkina. URL https://minesactu.info/en/2023/09/29/samao2023-focus-on-burkina-fasos-mining-potential/ (accessed 10.14.25).

Kagambega, N., Sawadogo, S., Bamba, O., Zombre, P., Galvez, R., 2014. Acid mine drainage and heavy metals contamination of surface water and soil in southwest Burkina Faso-West Africa.

Kamunda, C., Mathuthu, M., Madhuku, M., 2016. Health Risk Assessment of Heavy Metals in Soils from Witwatersrand Gold Mining Basin, South Africa. Int. J. Environ. Res. Public. Health 13, 663. https://doi.org/10.3390/ijerph13070663

Keita, S., 2019. Enjeux environnementaux liés à la mine artisanale en Afrique de l'Ouest: La mine artisanale en Afrique de l'Ouest francophone. N Tychsen J Charles N Eds 125–138.

Keita, S., 2001. Etude sur les Mines Artisanales et Les Exploitations Minières à Petite Echelle au Mali.

KI, F.A.L., 2009. Etude d'Impact Environnemental de la Culture du Jatropha Curcas Dans la commune de Dano.

Kiethega, J.B., Mauny, R., 1985. L'or de la Haute Volta. Archéologie et histoire de l'exploitation (Région de Poura, Haute-Volta) (Revue Française No. 266). Revue Française d'histoire d'outre-mer.

Kim, C.S., Bloom, N.S., Rytuba, J.J., Brown, G.E., 2003. Mercury Speciation by X-ray Absorption Fine Structure Spectroscopy and Sequential Chemical Extractions: A Comparison of Speciation Methods. Environ. Sci. Technol. 37, 5102–5108. https://doi.org/10.1021/es0341485

Kirk Woodman, K., Baratoux, L., Somda, A., Siebenaller, L., 2016. The Youga gold deposit, Burkina Faso. Ore Geol. Rev. 78, 631–638. https://doi.org/10.1016/j.oregeorev.2015.11.015

Knoblauch, A.M., Farnham, A., Ouoba, J., Zanetti, J., Müller, S., Jean-Richard, V., Utzinger, J., Wehrli, B., Brugger, F., Diagbouga, S., Winkler, M.S., 2020. Potential health effects of cyanide use in artisanal and small-scale gold mining in Burkina Faso. J. Clean. Prod. 252, 119689. https://doi.org/10.1016/j.jclepro.2019.119689

Kohio, E.N., Karoui, H., Sossou, S.K., Yacouba, H., 2024. Review of pollution trends and impacts in artisanal and small-scale gold mining in Sub-Saharan Africa: Advancing towards sustainable practices through equitable redistribution of gold spin-offs. J. Clean. Prod. 476, 143754. https://doi.org/10.1016/j.jclepro.2024.143754

Kohio, E.N., Sossou, S.K., Karoui, H., Yacouba, H., 2025. Environmental Cyanide Pollution from Artisanal Gold Mining in Burkina Faso: Human Exposure Risk Analysis Based on a Conceptual Site Model. Int. J. Environ. Res. Public. Health 22, 1125. https://doi.org/10.3390/ijerph22071125

Konaté, A.A., Kaba, F., Hébélamou, J., Traoré, F., 2025a. Evaluation of the geo-environmental, socio-economic, and health impacts of artisanal gold mining in the sub-prefecture of Kounsitel, Gaoual. Discov. Appl. Sci. 7, 740. https://doi.org/10.1007/s42452-025-07352-z

Konaté, A.A., Konaté, S.F., Zaheer, M., Kwame, A.G., Oularé, F., 2022. Geostatistical analysis of hydrogeological data of the Baraka gold zone, prefecture of Siguiri, Republic of Guinea. Environ. Earth Sci. 81, 232. https://doi.org/10.1007/s12665-022-10340-w

Konaté, A.A., Koné, A., Vincent, A.T., Loua, S., Cissé, M., Gemail, K.S., 2025b. Groundwater vulnerability to artisanal gold mining pollution: a modified DRASTIC-GIS framework for Siguiri, Republic of Guinea. Earth 37, 1–30. https://doi.org/10.1080/27669645.2025.2546251

Konate, A.A., Sangare, D.B., N'diaye, B.F., Dembele, N.D.J., 2025. Community perception on environmental impacts of artisanal gold mining: Case study from the commune of Fourou, Republic of Mali. J. Min. Environ. 16, 1221–1236. https://doi.org/10.22044/jme.2025.15169.2900

Koné, F.R., 2021. Going for gold in western Mali threatens human security [WWW Document]. ISS Afr. URL https://issafrica.org/iss-today/going-for-gold-in-western-mali-threatens-human-security (accessed 11.22.25).

Kostka, J.E., Luther, G.W., 1994. Partitioning and speciation of solid phase iron in saltmarsh sediments. Geochim. Cosmochim. Acta 58, 1701–1710. https://doi.org/10.1016/0016-7037(94)90531-2

Kouadio, K.B., Resongles, E., Ahoussi, K.E., Ouattara, Z., Konaté, I., Fayol, N., Borschneck, D., Baratoux, D., Delpoux, S., Domeau, A., Marie, M., Yao, K.A., Bruneel, O., 2025. Environmental contamination by metals, metalloids, and cyanides in the historic and active ASGM area of Kokumbo in Côte d'Ivoire. Environ. Sci. Pollut. Res. https://doi.org/10.1007/s11356-025-36403-6

Kouadio, K.F., 2016. Risques environementaux et sanitaires liés à l'utilisation des produits chimiques dans l'orpaillage: cas du cyanure et du mercure sur les sites de Galgouli.

Koussoubé, Y., Upton, K., Ó Dochartaigh, B., Bellwood-Howard, I., 2018. Hydrogeology of Burkina Faso [WWW Document]. URL https://earthwise.bgs.ac.uk/index.php/Hydrogeology_of_Burkina_Faso

Kowalski, A., Siepak, M,, Boszke, L., 2007. Mercury contamination of surface and ground waters of Poznań, Poland. Pol J Environ Stud, 16(1), 67-74. Pol. J Env. Stud Vol. 16, 67–74.

Kowalski, A., Zioła-Frankowska, A., Frankowski, M., 2018. Effect on reclamation on mercury concentration in groundwater: a case study of Luboń Chemical Plant (Poznań, Poland). Environ. Earth Sci. 77. https://doi.org/10.1007/s12665-018-7865-9

Krabbenhoft, D.P., Babiarz, C.L., 1992. The role of groundwater transport in aquatic mercury cycling. Water Resour. Res. 28, 3119–3128. https://doi.org/10.1029/92WR01766

Kumar, A., Kumar, V., Bakshi, P., Parihar, R.D., Radziemska, M., Kumar, R., 2024. Mercury in the natural environment: Biogeochemical cycles and associated health risks. J. Geochem. Explor. 267, 107594. https://doi.org/10.1016/j.gexplo.2024.107594

Kuyucak, N., Akcil, A., 2013. Cyanide and removal options from effluents in gold mining and metallurgical processes. Miner. Eng. 50–51, 13–29. https://doi.org/10.1016/j.mineng.2013.05.027

Kwaansa-Ansah, E.E., Agorku, S.E., Nriagu, J.O., 2011. Levels of Total Mercury in Different Fish Species and Sediments from the Upper Volta Basin at Yeji in Ghana. Bull. Environ. Contam. Toxicol. 86, 406–409. https://doi.org/10.1007/s00128-011-0214-2

Lacerda, L.D., Bastos, W.R., Almeida, M.D., 2012. The impacts of land use changes in the mercury flux in the Madeira River, Western Amazon. An. Acad. Bras. Ciênc. 84, 69–78. https://doi.org/10.1590/S0001-37652012000100007

Lafore, J. -P., Flamant, C., Giraud, V., Guichard, F., Knippertz, P., Mahfouf, J. -F., Mascart, P., Williams, E.R., 2010. Introduction to the AMMA Special Issue on 'Advances in understanding atmospheric processes over West Africa through the AMMA field campaign.' Q. J. R. Meteorol. Soc. 136, 2–7. https://doi.org/10.1002/qj.583

Lambertsson, L., Nilsson, M., 2006. Organic Material: The Primary Control on Mercury Methylation and Ambient Methyl Mercury Concentrations in Estuarine Sediments. Environ. Sci. Technol. 40, 1822–1829. https://doi.org/10.1021/es051785h

Lanzano, C., Arnaldi Di Balme, L., 2021. Who owns the mud? Valuable leftovers, sociotechnical innovation and changing relations of production in artisanal gold mining (Burkina Faso). J. Agrar. Change 21, 433–458. https://doi.org/10.1111/joac.12412

Lanzano, C., Arnaldi Di Balme, L., 2018. Des « puits burkinabè » en Haute Guinée : processus et enjeux de la circulation de savoirs techniques dans le secteur minier artisanal: Autrepart N° 82, 87–108. https://doi.org/10.3917/autr.082.0087

Lapworth, D.J., Nkhuwa, D.C.W., Okotto-Okotto, J., Pedley, S., Stuart, M.E., Tijani, M.N., Wright, J., 2017. Urban groundwater quality in sub-Saharan Africa: current status and implications for water security and public health. Hydrogeol. J. 25, 1093–1116. https://doi.org/10.1007/s10040-016-1516-6

Laur, N., Kaiser, L., Deigner, H.-P., Kinscherf, R., 2021. Sequential Analysis of Trace Elements in a Micro Volume Urine Sample Using Inductively Coupled Plasma Mass Spectrometry. Appl. Sci. 11, 3740. https://doi.org/10.3390/app11093740

Le Fur, J., Guilavogui, A., Teitelbaum, A., 2011. Contribution of local fishermen to improving knowledge of the marine ecosystem and resources in the Republic of Guinea, West Africa. Can. J. Fish. Aquat. Sci. 68, 1454–1469. https://doi.org/10.1139/f2011-061

Lechler, P., 2000. Elevated mercury concentrations in soils, sediments, water, and fish of the Madeira River basin, Brazilian Amazon: a function of natural enrichments? Sci. Total Environ. 260, 87–96. https://doi.org/10.1016/S0048-9697(00)00543-X

Leermakers, M., Baeyens, W., Quevauviller, P., Horvat, M., 2005. Mercury in environmental samples: Speciation, artifacts and validation. TrAC Trends Anal. Chem. 24, 383–393. https://doi.org/10.1016/j.trac.2004.01.001

Leiva G., M.A., Morales, S., 2013. Environmental assessment of mercury pollution in urban tailings from gold mining. Ecotoxicol. Environ. Saf. 90, 167–173. https://doi.org/10.1016/j.ecoenv.2012.12.026

Lemoalle, J., De Condappa, D., 2009. Challenge Program Water and Food. Water Atlas of the Volta Basin.

Lennett, D., Gutierrez, R., 2014. Convention de Minamata sur le mercure : texte et annexes. Nairobi : Programme des Nations Unies pour l'environnement.

Levin Sources, 2017. Diagnostic de l'exploitation artisanale de l'or en Republique de Guinée: Rapport final du Projet d'Appui à la Gouvernance dans le Secteur Minier (PAGSEM), non publié disponible sur demande sur le site http://www.levinsources.com. 166p. Les Ministères des Mines et Géologie.

Liang, L., Bloom, N.S., Horvat, M., 1994. Simultaneous determination of mercury speciation in biological materials by GC/CVAFS after ethylation and room-temperature precollection. Clin. Chem. 40, 602–607.

Lignes directrices d'éthique pour la recherche en matière de santé impliquant des participants humains, quatrième édition. Genève : Conseil des Organisations internationales des Sciences médicales et Organisation mondiale de la Santé, 2016.

Lin, C.-J., Gustin, M.S., Singhasuk, P., Eckley, C., Miller, M., 2010. Empirical Models for Estimating Mercury Flux from Soils. Environ. Sci. Technol. 44, 8522–8528. https://doi.org/10.1021/es1021735

Lin, C.-J., Pongprueksa, P., Lindberg, S.E., Pehkonen, S.O., Byun, D., Jang, C., 2006. Scientific uncertainties in atmospheric mercury models I: Model science evaluation. Atmos. Environ. 40, 2911–2928. https://doi.org/10.1016/j.atmosenv.2006.01.009

Lindqvist, O., Johansson, K., Bringmark, L., Timm, B., Aastrup, M., Andersson, A., Hovsenius, G., Hakanson, L., Iverfeldt, Ak., Meili, M., 1991. Mercury in the Swedish environment ? Recent research on causes, consequences and corrective methods. Water. Air. Soil Pollut. 55, xi–261. https://doi.org/10.1007/BF00542429

Lino, A.S., Kasper, D., Guida, Y.S., Thomaz, J.R., Malm, O., 2019. Total and methyl mercury distribution in water, sediment, plankton and fish along the Tapajós River basin in the Brazilian Amazon. Chemosphere 235, 690–700. https://doi.org/10.1016/j.chemosphere.2019.06.212

Liu, G., Cai, Y., O'Driscoll, N., 2011. Environmental Chemistry and Toxicology of Mercury. John Wiley & Sons.

Liu, Z., Wimberly, M., Dwomoh, F., 2016. Vegetation Dynamics in the Upper Guinean Forest Region of West Africa from 2001 to 2015. Remote Sens. 9, 5. https://doi.org/10.3390/rs9010005

Lombi, E., Wenzel, W.W., Adriano, D.C., 2000. Arsenic contaminated soils : II. Remedial action, chap 33, in Remediation engineering of contaminated soils, D.L. Wise, D.J. Trantolo, E.J. Cichon, H.I. Inyang and U. Stottmeister editors, Dekker, New York, in: Remediation Engineering of Contaminated Soils. D.L. Wise, D.J. Trantolo, E.J. Cichon, H.I. Inyang and U., pp. 739-758.

Loua, R.T., Bencherif, H., Mbatha, N., Bègue, N., Hauchecorne, A., Bamba, Z., Sivakumar, V., 2019. Study on Temporal Variations of Surface Temperature and Rainfall at Conakry Airport, Guinea: 1960–2016. Climate 7, 93. https://doi.org/10.3390/cli7070093

Lusilao-Makiese, J.G., Tessier, E., Amouroux, D., Tutu, H., Chimuka, L., Weiersbye, I., Cukrowska, E.M., 2014. Seasonal distribution and speciation of mercury in a gold mining area, north-west province, South Africa. Toxicol. Environ. Chem. 96, 387–402. https://doi.org/10.1080/02772248.2014.947987

Lyman, S.N., Gustin, M.S., Prestbo, E.M., Kilner, P.I., Edgerton, E., Hartsell, B., 2009. Testing and Application of Surrogate Surfaces for Understanding Potential Gaseous Oxidized Mercury Dry Deposition. Environ. Sci. Technol. 43, 6235–6241. https://doi.org/10.1021/es901192e

Ma, M., Du, H., Wang, D., Sun, T., 2018. Mercury methylation in the soils and sediments of Three Gorges Reservoir Region. J. Soils Sediments 18, 1100–1109. https://doi.org/10.1007/s11368-017-1827-9

Macdonald, K., Lund, M., Blanchette, M., 2015. Impacts of Artisanal Small-Scale Gold Mining on Water Quality of a Tropical River (Surow River, Ghana). Mine Water Environ. Res. Cent. Ed. Cowan Univ. Aust.

Macdonald, K., Lund, M., Blanchette, M., Mccullough, C., 2014. Regulation of artisanal small scale gold mining (ASGM) in Ghana and Indonesia as currently implemented fails to adequately protect aquatic ecosystems. Res. Outputs 2014 2021.

Macdonald, K., Lund, M., vanEtten, E., 2020. Riverine biota as environmental indicators of artisanal small-scale and large-scale gold mining impacts on riverine ecosystems in Brong Ahafo Region, Ghana. IOP Conf. Ser. Earth Environ. Sci. 413, 012014. https://doi.org/10.1088/1755-1315/413/1/012014

MacSween, K., Edwards, G.C., 2021. The role of precipitation and soil moisture in enhancing mercury air-surface exchange at a background site in south-eastern Australia. Atmos. Environ. 255, 118445. https://doi.org/10.1016/j.atmosenv.2021.118445

Maha, M.M., Matsuyama, A., Arima, T., Sainoki, A., 2024. Assessment of Total Mercury Levels Emitted from ASGM into Soil and Groundwater in Chami Town, Mauritania. Sustainability 16, 7992. https://doi.org/10.3390/su16187992

Maiga, F., Touré, A.O., Diya, A., Ouattara, I., Doumbia, S., 2022. Les effets de l'orpaillage par drague sur la biodiversité aquatique de l'affluent Baoulé dans la commune rurale de Kémékafo, région de Dioila. Rev. Afr. Sci. Soc. Santé Publique 4, 38–47.

Maignien, R., 1958. Le cuirassement des sols en Guinée. Afrique Occidentale. Sci. Géologiques Bull. Mém. 16, 0–0.

Malehase, T., Daso, A.P., Okonkwo, J.O., 2016. Determination of mercury and its fractionation products in samples from legacy use of mercury amalgam in gold processing in Randfontein, South Africa. Emerg. Contam. 2, 157–165. https://doi.org/10.1016/j.emcon.2016.07.003

Mamedov, V.I., Bouféév, Y.V., Nikitine, Y.A., 2010. Géologie de la Republique de Guinée. TomI. Volume I.

Mangal, V., Lam, W.Y., Huang, H., Emilson, E.J.S., Mackereth, R.W., Mitchell, C.P.J., 2022. Molecular correlations of dissolved organic matter with inorganic mercury and methylmercury in Canadian boreal streams. Biogeochemistry 160, 127–144. https://doi.org/10.1007/s10533-022-00944-6

MARAH, M. de l'Agriculture et des R.A. et H., 2023. Projet d'Appui à la Résilience et à la competitivité (PRECEL) au Burkina Faso.

Marshall, B.G., Veiga, M.M., Kaplan, R.J., Adler Miserendino, R., Schudel, G., Bergquist, B.A., Guimarães, J.R.D., Sobral, L.G.S., Gonzalez-Mueller, C., 2018. Evidence of transboundary mercury and other pollutants in the Puyango-Tumbes River basin, Ecuador–Peru. Environ. Sci. Process. Impacts 20, 632–641. https://doi.org/10.1039/C7EM00504K

Martin, A.P., Turnbull, R.E., Rissmann, C.W., Rieger, P., 2017. Heavy metal and metalloid concentrations in soils under pasture of southern New Zealand. Geoderma Reg. 11, 18–27. https://doi.org/10.1016/j.geodrs.2017.08.005

Martins, B.M., Gambardella, N., Folhas, D., Hintelmann, H., Pilote, M., Costa, J., Christensen, T.R., Magalhães, C., Canário, J., 2025. Mercury Transformation in Greenland's Thermokarst Lakes: A Combined Geochemical and Microbial Perspective. https://doi.org/10.22541/essoar.175881396.64877557/v1

Martínez-Cortizas, A., Pontevedra-Pombal, X., García-Rodeja, E., Nóvoa-Muñoz, J.C., Shotyk, W., 1999. Mercury in a Spanish Peat Bog: Archive of Climate Change and Atmospheric Metal Deposition. Science 284, 939–942. https://doi.org/10.1126/science.284.5416.939

Mason, R.P., Baumann, Z., Hansen, G., Yao, K.M., Coulibaly, M., Coulibaly, S., 2019. An assessment of the impact of artisanal and commercial gold mining on mercury and methylmercury levels in the environment and fish in Cote d'Ivoire. Sci. Total Environ. 665, 1158–1167. https://doi.org/10.1016/j.scitotenv.2019.01.393

Mason, R.P., Coulibaly, M., Hansen, G., Inman, H., Myer, P.K., Yao, K.M., 2022. An examination of mercury levels in the coastal environment and fish of Cote d'Ivoire. Chemosphere 300, 134609. https://doi.org/10.1016/j.chemosphere.2022.134609

Mason, R.P., Fitzgerald, W.F., Morel, F.M.M., 1994. The biogeochemical cycling of elemental mercury: Anthropogenic influences. Geochim. Cosmochim. Acta 58, 3191–3198. https://doi.org/10.1016/0016-7037(94)90046-9

Mason, R.P., Reinfelder, J.R., Morel, F.M.M., 1995. Bioaccumulation of mercury and methylmercury. Water. Air. Soil Pollut. 80, 915–921. https://doi.org/10.1007/BF01189744

Matsuyama, A., Yano, S., Taninaka, T., Kindaichi, M., Sonoda, I., Tada, A., Akagi, H., 2018. Chemical characteristics of dissolved mercury in the pore water of Minamata Bay sediments. Mar. Pollut. Bull. 129, 503–511. https://doi.org/10.1016/j.marpolbul.2017.10.021

Maurice-Bourgoin, L., 2000. Mercury distribution in waters and fishes of the upper Madeira rivers and mercury exposure in riparian Amazonian populations. Sci. Total Environ. 260, 73–86. https://doi.org/10.1016/S0048-9697(00)00542-8

Maury-Brachet, R., Gentes, S., Dassié, E.P., Feurtet-Mazel, A., Vigouroux, R., Laperche, V., Gonzalez, P., Hanquiez, V., Mesmer-Dudons, N., Durrieu, G., Legeay, A., 2020. Mercury contamination levels in the bioindicator piscivorous fish Hoplias aïmara in French Guiana rivers: mapping for risk

assessment. Environ. Sci. Pollut. Res. 27, 3624–3636. https://doi.org/10.1007/s11356-018-3983-x

Mbodj, F.B., 2011. Boom aurifère à l'est du Sénégal, l'ouest du Mali et au nord-est de la Guinée : mutations socio-économiques et spatiales d'anciennes marges géographiques et économiques.

Mbodj, F.B., 2009. Boom aurifère et dynamiques économiques entre Sénégal, Mali et Guinée. EchoGéo. https://doi.org/10.4000/echogeo.11034

McNab, N.J., Hughes, J.C., Howard, J.R., 1997. Pollution effects of wastewater sludge application to sandy soils with particular reference to the behaviour of mercury. Appl. Geochem. 12, 321–325. https://doi.org/10.1016/S0883-2927(97)00002-4

MEEF, 2018. Plan d'Action National pour l'extraction minière artisanale et à petite échelle de l'or (EMAPE).

MEEF, M. de l'Environnement et des E. et F., 2021. Plan d'action national pour l'extraction minière artisanale et à petite echelle de l'or (EMAPE).

MEEF, M. de l'Environnement et des E. et F., DNE, D.N. de l'Environnement, 2018. Convention de Minamata sur le mercure: Evaluation initiale de la Guinée.

MEEF, M. de l'Environnement et des E. et F., PAN, 2018. Plan d'action national pour l'extraction minière artisanale et à petite echelle de l'or (EMAPE).

Meili, M., 1997. Mercury in Lakes and Rivers. In: Metal Ions in Biological Systems. Mercury and its Effect on Environment and Biology. A. Sigel and H. Sigel, Eds., Marcel Dekker Inc., New York, 1997, chp. 2, 21-51., in: Mercury and Its Effect on Environment and Biology. Institute of Earth Sciences , Uppsala university, p. chp. 2, 21-51.

Melaku, S., Dams, R., Moens, L., 2005. Determination of trace elements in agricultural soil samples by inductively coupled plasma-mass spectrometry: Microwave acid digestion versus aqua regia extraction. Anal. Chim. Acta 543, 117–123. https://doi.org/10.1016/j.aca.2005.04.055

Meloni, F., Higueras, P.L., Cabassi, J., Nisi, B., Rappuoli, D., Vaselli, O., 2024. Thermal desorption technique to speciate mercury in carbonate, silicate, and organic-rich soils. Chemosphere 365, 143349. https://doi.org/10.1016/j.chemosphere.2024.143349

Mignot, E.L., Siebenaller, L., Béziat, D., Salvi, S., Andrémayer, A., Reisberg, L., Velasquez, G., Zimmernann, C., Franceschi, G., 2014. The Paleoproterozoic Copper-Gold Deposit of Gaoua, Burkina Faso: Evidence for A Polyphased Mineralization. Acta Geol. Sin. - Engl. Ed. 88, 970–972. https://doi.org/10.1111/1755-6724.12378_5

Migration data portal, 2020. Understanding Migration to West African Artisanal Mines [WWW Document]. Migr. Data Portal. URL https://www.migrationdataportal.org/blog/understanding-migration-west-african-artisanal-mines (accessed 8.27.25).

Milési, J.P., Feybesse, J.-L., Pinna, P., Deschamps, Y., Kampunzu, H., Muhongo Lescuyer, J.L., Le Goff, E., Delor, C., Billa, M., Ralay, F., Heinry, C., 2004. Geological Map of Africa 110,000,000, SIGAfrique Project. In 20th Conference of African Geology. Orléans Bureau de Recherches Géologiques et Minières. - References - Scientific Research Publishing [WWW Document]. URL https://www.scirp.org/reference/referencespapers?referenceid=3325619 (accessed 10.14.25).

Milési, J.-P., Ledru, P., Feybesse, J.-L., Dommanget, A., Marcoux, E., 1992. Early proterozoic ore deposits and tectonics of the Birimian orogenic belt, West Africa. Precambrian Res. 58, 305–344. https://doi.org/10.1016/0301-9268(92)90123-6

MME, M. des mines et de l'énergie, 2017. Plus de 9 tonnes d'or produite dans l'orpaillage sur 438 sites répertoriés en 2016 – chambredesmines.bf. URL https://chambredesmines.bf/nvsite/plus-de-9-tonnes-dor-produite-dans-lorpaillage-sur-438-sites-repertories-en-2016/ (accessed 10.14.25).

MME, M. des mines et de l'énergie, Par-Gs, P. d'appui au renforcement de la gestion des finances publiques et des statistiques, 2014. Annuaire statistique 2012 du Ministère des mines et de l'énergie.

MMG, 2022. Bulletin de statistiques minières (14; p. 12). République de Guinée (Ministère des Mines et de la Géologie).
MMG, M. des M. et de la G., 2020. Bulletin de statistiques minières. N°10 de janvier décembre 2020.
MMG, M. des M. et de la G., 2019. Bulletin de statistiques minières. N°006 de l'année 2019 (Janver-Décembre).
MMG, M. des M. et de la G., 2010. Potentiel Minier de La GUINEE.
MOORE, S., 2018. Initiative pour la Transparence dans les Industries Extractives. ITIE Burkina Faso. ITIE Burkina FAso.
MUH, M. de l'Urbanisation et de l'Habitat, 2011. Schéma Directeur d'Aménagement et de l'Urbanisation de la ville de Gaoua au Burkina Faso.
Munson, K.M., Babi, D., Lamborg, C.H., 2014. Determination of monomethylmercury from seawater with ascorbic acid-assisted direct ethylation. Limnol. Oceanogr. Methods 12, 1–9. https://doi.org/10.4319/lom.2014.12.1
Muresan, B., Cossa, D., Richard, S., Dominique, Y., 2008. Monomethylmercury sources in a tropical artificial reservoir. Appl. Geochem. 23, 1101–1126. https://doi.org/10.1016/j.apgeochem.2007.11.006
Naharro, R., Esbrí, J.M., Amorós, J.A., Higueras, P.L., 2020. Experimental assessment of the daily exchange of atmospheric mercury in Epipremnum aureum. Environ. Geochem. Health 42, 3185–3198. https://doi.org/10.1007/s10653-020-00557-8
Naujokas, M.F., Anderson, B., Ahsan, H., Aposhian, H.V., Graziano, J.H., Thompson, C., Suk, W.A., 2013. The Broad Scope of Health Effects from Chronic Arsenic Exposure: Update on a Worldwide Public Health Problem. Environ. Health Perspect. 121, 295–302. https://doi.org/10.1289/ehp.1205875
N'Diaye, I.S., 2015. Le scandale géologique guinéen. L'Harmattan, Paris.
Ndzana, C.E., Emmanuel Mvondo, V.Y., Tchouta, K.D., Ngatcha, B.N., 2023. Assessment of the impact of small-scale mining on soil contamination by mercury and hydrocarbons in the kadey catchment (East Cameroon). Heliyon 9, e18786. https://doi.org/10.1016/j.heliyon.2023.e18786
Nelson, G., 2013. Occupational respiratory diseases in the South African mining industry. Glob. Health Action 6, 19520. https://doi.org/10.3402/gha.v6i0.19520
Némery, J., Mano, V., Coynel, A., Etcheber, H., Moatar, F., Meybeck, M., Belleudy, P., Poirel, A., 2013. Carbon and suspended sediment transport in an impounded alpine river (Isère, France). Hydrol. Process. 27, 2498–2508. https://doi.org/10.1002/hyp.9387
Nevondo, V., Malehase, T., Daso, A., Okonkwo, O., 2019. Leachate seepage from landfill: a source of groundwater mercury contamination in South Africa. Water SA 45. https://doi.org/10.4314/wsa.v45i2.09
Ngom, N.M., Baratoux, D., Bolay, M., Dessertine, A., Abass Saley, A., Baratoux, L., Mbaye, M., Faye, G., Yao, A.K., Kouamé, K.J., 2023. Artisanal Exploitation of Mineral Resources: Remote Sensing Observations of Environmental Consequences, Social and Ethical Aspects. Surv. Geophys. 44, 225–247. https://doi.org/10.1007/s10712-022-09740-1
Niane, B., 2014. Mercury distribution and speciation in soil profiles and various forms of Hg in water around artisanal small-scale gold mining areas in Kedougou region, Senegal (Thesis). Geneva, Switzerland: Université de Genève.
Niane, B., Devarajan, N., Poté, J., Moritz, R., 2019a. Quantification and characterization of mercury resistant bacteria in sediments contaminated by artisanal small-scale gold mining activities, Kedougou region, Senegal. J. Geochem. Explor. 205, 106353. https://doi.org/10.1016/j.gexplo.2019.106353
Niane, B., Guédron, S., Feder, F., Legros, S., Ngom, P.M., Moritz, R., 2019b. Impact of recent artisanal small-scale gold mining in Senegal: Mercury and methylmercury contamination of terrestrial and aquatic ecosystems. Sci. Total Environ. 669, 185–193. https://doi.org/10.1016/j.scitotenv.2019.03.108

Niane, B., Guédron, S., Moritz, R., Cosio, C., Ngom, P.M., Deverajan, N., Pfeifer, H.R., Poté, J., 2015. Human exposure to mercury in artisanal small-scale gold mining areas of Kedougou region, Senegal, as a function of occupational activity and fish consumption. Environ. Sci. Pollut. Res. 22, 7101–7111. https://doi.org/10.1007/s11356-014-3913-5

Niane, B., Moritz, R., Guédron, S., Ngom, P.M., Pfeifer, H.R., Mall, I., Poté, J., 2014. Effect of recent artisanal small-scale gold mining on the contamination of surface river sediment: Case of Gambia River, Kedougou region, southeastern Senegal. J. Geochem. Explor. 144, 517–527. https://doi.org/10.1016/j.gexplo.2014.03.028

Nicolas, K., Sayouba, S., Ousmane, B., Prosper, Z., Rosa, G., 2014. ACID MINE DRAINAGE AND HEAVY METALS CONTAMINATION OF SURFACE WATER AND SOIL IN SOUTHWEST BURKINA FASO–WEST AFRICA.

Noble, M.J., Decker, S.L., Zane Horowitz, B., 2016. Inhalational mercury toxicity from artisanal gold extraction reported to the Oregon poison center, 2002–2015. Clin. Toxicol. 54, 847–851. https://doi.org/10.1080/15563650.2016.1199029

Nriagu, J.O., Blankson, M.L., Ocran, K., 1996. Childhood lead poisoning in Africa: a growing public health problem. Sci. Total Environ. 181, 93–100. https://doi.org/10.1016/0048-9697(95)04954-1

Nugraha, W.C., Jeong, H., Phan Dinh, Q., Ishibashi, Y., Arizono, K., 2022. Combination of Vortex Agitation and Ultrasonic Irradiation for Mercury Removal from Sediment by Acid Extraction. Bull. Environ. Contam. Toxicol. 108, 1118–1123. https://doi.org/10.1007/s00128-022-03471-0

Nzihou, J.F., Bouda, M., Hamidou, S., Diarra, J., 2013. Arsenic in Drinking Water Toxicological Risk Assessment in the North Region of Burkina Faso. J. Water Resour. Prot. 05, 46–52. https://doi.org/10.4236/jwarp.2013.58A007

Obiri, S., Dodoo, D.K., Essumang, D.K., Armah, F.A., 2010. Cancer and Non-Cancer Risk Assessment from Exposure to Arsenic, Copper, and Cadmium in Borehole, Tap, and Surface Water in the Obuasi Municipality, Ghana. Hum. Ecol. Risk Assess. Int. J. 16, 651–665. https://doi.org/10.1080/10807031003788907

OCDE, 2018. L'or à la croisée des chemins: Étude d'évaluation des chaînes d'approvisionnement en or produit au Burkina Faso, au Mali et au Niger. OECD. https://doi.org/10.1787/fc17936e-fr

Omondi, G.Z.O., Nyamari, J., Mugo, J., 2023. Mercury Levels in Groundwater near Artisanal Small-Scale Gold Mines in Migori County, Kenya. East Afr. J. Environ. Nat. Resour. 6, 421–431. https://doi.org/10.37284/eajenr.6.1.1543

OMS, O.M. de la S., 2017. Santé et extraction minière artisanale et à petite échelle de l'or. Document technique N°1: Risque pour la santé au travail et l'environnement associés à l'extraction minière artisanale et à petite échelle de l'or. ISBN 978-92-4-251027-0.

OMS, O.M. de la S., 2003. Prévenir la maladie grâce à un environnement sain: l'exposition au mercure et ses conséquences sanitaires chez les membres de la communauté de l'extraction minière artisanale et à petite échelle de l'or (ASGM).

OMS, O.M. de la S., ONU, O. des Na.U. pour l'alimentation et l'agriculture, 2016. PROGRAMME MIXTE FAO/OMS SUR LES NORMES ALIMENTAIRES COMITÉ DU CODEX SUR LES CONTAMINANTS DANS LES ALIMENTS. DOCUMENT DE TRAVAIL SUR LES LIMITES MAXIMALES POUR LE MÉTHYLMERCURE DANS LE POISSON.

Oppong, S.O.B., Voegborlo, R.B., Agorku, S.E., Adimado, A.A., 2010. Total Mercury in Fish, Sediments and Soil from the River Pra Basin, Southwestern Ghana. Bull. Environ. Contam. Toxicol. 85, 324–329. https://doi.org/10.1007/s00128-010-0059-0

Ouédraogo, A., 2020. Les détentrices de hangars de traitement de l'or face à la technique de cyanuration (sud-ouest du Burkina Faso). J. Afr. 168–187. https://doi.org/10.4000/africanistes.9528

Ouédraogo, O., Amyot, M., 2013. Mercury, arsenic and selenium concentrations in water and fish from sub-Saharan semi-arid freshwater reservoirs (Burkina Faso). Sci. Total Environ. 444, 243–254. https://doi.org/10.1016/j.scitotenv.2012.11.095

Ouédraogo, O., Chételat, J., Amyot, M., 2015. Bioaccumulation and Trophic Transfer of Mercury and Selenium in African Sub-Tropical Fluvial Reservoirs Food Webs (Burkina Faso). PLOS ONE 10, e0123048. https://doi.org/10.1371/journal.pone.0123048

Oularé, F., Doumbouya, A., Konaté, A.A., Camara, S., Dembélé, N.D.J., 2025. Contribution of Remote Sensing to the Analysis of Land Cover and Surface Temperature: Case Study from the Siguirini Mining Area. J. Geol. Geogr. Geoecology 34, 377–392. https://doi.org/10.15421/112532

Padonou, E.A., Watson, C., Akakpo, B.A., Wichern, F., 2025. Impact of crop production on selected soil physicochemical properties in semiarid climate zone of Benin, West Africa. Discov. Soil 2, 11. https://doi.org/10.1007/s44378-025-00044-5

PAGSEM, MMG, 2017. Diagnostique de l'Exploitation Artisanale de l'Or en Republique de Guinée.

Pak, K.-R., Bartha, R., 1998. Mercury Methylation and Demethylation in Anoxic Lake Sediments and by Strictly Anaerobic Bacteria. Appl. Environ. Microbiol. 64, 1013–1017. https://doi.org/10.1128/AEM.64.3.1013-1017.1998

PAN, 2020. Plan d'Action National de réduction, voire d'élimination du mercure dans l'extraction minière artisanale et à petite échelle d'or conformément à la convention de Minamata sur le mercure.

Papadopoulos, A., 2023. RANKED: The World's Largest Gold Producing Countries, 2023. CEOWORLD Mag. URL https://ceoworld.biz/2023/08/29/ranked-the-worlds-largest-gold-producing-countries-2023/ (accessed 9.8.25).

Parks, J.M., Johs, A., Podar, M., Bridou, R., Hurt, R.A., Smith, S.D., Tomanicek, S.J., Qian, Y., Brown, S.D., Brandt, C.C., Palumbo, A.V., Smith, J.C., Wall, J.D., Elias, D.A., Liang, L., 2013. The Genetic Basis for Bacterial Mercury Methylation. Science 339, 1332–1335. https://doi.org/10.1126/science.1230667

Penglase, S., Hamre, K., Ellingsen, S., 2014. Selenium and mercury have a synergistic negative effect on fish reproduction. Aquat. Toxicol. 149, 16–24. https://doi.org/10.1016/j.aquatox.2014.01.020

Petit-Roulet, R., 2025. Sécurisation et distribution : évolutions de la gouvernance de l'orpaillage en Guinée. EchoGéo 71. https://doi.org/10.4000/140dt

PIF, P. d'Investissement F. du B.F., 2017. Notice communale de Boromo. Résultats des diagnostics socio-fonciers et des planifications participatives.

Pirrone, N., Keeler, G.J., Nriagu, J.O., Warner, P.O., 1996. Historical trends of airborne trace metals in Detroit from 1971 to 1992. Water. Air. Soil Pollut. 88, 145–165. https://doi.org/10.1007/bf00157419

PlanetGOLD, 2023. Annual Progress Report 2022-2023.

PNU, P. des N.U. pour l'Environnement, 2002. EVALUATION MONDIALE DU MERCURE.

Porgo, M., Gokyay, O., 2017. Environmental impacts of gold mining in Essakane site of Burkina Faso. Hum. Ecol. Risk Assess. Int. J. 23, 641–654. https://doi.org/10.1080/10807039.2016.1263930

PROJEG, 2018. L'OR EN PARTAGE. LA PARTICIPATION DES ORPAILLEURS AU DEVELOPPEMENT LOCAL.

PRPRSS, P.D.R.D.L.P.E.D.L.R.D.S.D.S., 2024. Cadre de gestion environnemental et sociétale.

Qiu, X., Liu, M., Zhang, Y., Zhang, Q., Lin, H., Cai, X., Li, J., Dai, R., Zheng, S., Wang, J., Zhu, Y., Shen, H., Shen, G., Wang, X., Tao, S., 2025. Declines in anthropogenic mercury emissions in the Global North and China offset by the Global South. Nat. Commun. 16, 1179. https://doi.org/10.1038/s41467-025-56274-2

Quispe Aquino, R., García Zúñiga, F.F., Malone, A., 2024. Soil and Urine Mercury Levels in Secocha: A Case Study of Artisanal and Small-Scale Gold Mining in Peru. Mining 4, 389–400. https://doi.org/10.3390/mining4020022

Raiswell, R., Vu, H.P., Brinza, L., Benning, L.G., 2010. The determination of labile Fe in ferrihydrite by ascorbic acid extraction: Methodology, dissolution kinetics and loss of solubility with age and de-watering. Chem. Geol. 278, 70–79. https://doi.org/10.1016/j.chemgeo.2010.09.002

Rajaee, M., Long, R., Renne, E., Basu, N., 2015a. Mercury Exposure Assessment and Spatial Distribution in A Ghanaian Small-Scale Gold Mining Community. Int. J. Environ. Res. Public. Health 12, 10755–10782. https://doi.org/10.3390/ijerph120910755

Rajaee, M., Obiri, S., Green, A., Long, R., Cobbina, S., Nartey, V., Buck, D., Antwi, E., Basu, N., 2015b. Integrated Assessment of Artisanal and Small-Scale Gold Mining in Ghana—Part 2: Natural Sciences Review. Int. J. Environ. Res. Public. Health 12, 8971–9011. https://doi.org/10.3390/ijerph120808971

Ramlal, P.S., Bugenyi, F.W.B., Kling, G.W., Nriagu, J.O., Rudd, J.W.M., Campbell, L.M., 2003. Mercury Concentrations in Water, Sediment, and Biota from Lake Victoria, East Africa. J. Gt. Lakes Res. 29, 283–291. https://doi.org/10.1016/S0380-1330(03)70555-3

Ravichandran, M., 2004. Interactions between mercury and dissolved organic matter—a review. Chemosphere 55, 319–331. https://doi.org/10.1016/j.chemosphere.2003.11.011

Razack, A.A., 2002. Proposals for optimising artisanal mining in Niger.

Reis, A.T., Coelho, J.P., Rodrigues, S.M., Rocha, R., Davidson, C.M., Duarte, A.C., Pereira, E., 2012. Development and validation of a simple thermo-desorption technique for mercury speciation in soils and sediments. Talanta 99, 363–368. https://doi.org/10.1016/j.talanta.2012.05.065

Reis, A.T., Coelho, J.P., Rucandio, I., Davidson, C.M., Duarte, A.C., Pereira, E., 2015. Thermo-desorption: A valid tool for mercury speciation in soils and sediments? Geoderma 237–238, 98–104. https://doi.org/10.1016/j.geoderma.2014.08.019

Rennert, T., 2019. Wet-chemical extractions to characterise pedogenic Al and Fe species – a critical review. Soil Res. 57, 1. https://doi.org/10.1071/SR18299

Reyes, I., Torrent, J., 1997. Citrate-Ascorbate as a Highly Selective Extractant for Poorly Crystalline Iron Oxides. Soil Sci. Soc. Am. J. 61, 1647–1654. https://doi.org/10.2136/sssaj1997.03615995006100060015x

Roamba, J., 2014. RISQUES ENVIRONNEMENTAUX ET SANITAIRES SUR LES SITES D'ORPAILLAGE AU BURKINA FASO : CYCLE DE VIE DES PRINCIPAUX POLLUANTS ET PERCEPTIONS DES ORPAILLEURS (CAS DU SITE ZOUGNAZAGMLIGNE DANS LA COMMUNE RURALE DE BOUROUM, REGION DU CENTRE-NORD).

Robertson, M., Peters, L., 2016. West African Goldfields. Episodes 39, 155–176. https://doi.org/10.18814/epiiugs/2016/v39i2/95773

Rodrigues, A.C.M., Torres-Rodriguez, N., Yuan, J., Dufour, A., Drude De Lacerda, L., Heimbürger-Boavida, L.-E., 2025. Mercury dynamics in the mangrove-influenced estuary of the Parnaíba Delta, Brazil. Chemosphere 376, 144262. https://doi.org/10.1016/j.chemosphere.2025.144262

Rodríguez Martín-Doimeadios, R.C., Wasserman, J.C., García Bermejo, L.F., Amouroux, D., Berzas Nevado, J.J., Donard, O.F.X., 2000. Chemical availability of mercury in stream sediments from the Almadén area, Spain. J. Environ. Monit. 2, 360–366. https://doi.org/10.1039/a909597g

Roulet, M., 2001. Methylmercury production and accumulation in sediments and soils of an Amazonian floodplain - effet of seasonal inundation 41–60. https://doi.org/10.1023/a:1010379103335

Roulet, M., Lucotte, M., 1995. GEOCHEMISTRY OF MERCURY IN PRISTINE AND FLOODED FERRALITIC SOILS OF A TROPICAL RAIN FOREST IN FRENCH GUIANA, SOUTH AMERICA. Kluwer Acad. Publ. 80, 1079–1088.

Rumayor, M., Diaz-Somoano, M., Lopez-Anton, M.A., Martinez-Tarazona, M.R., 2013. Mercury compounds characterization by thermal desorption. Talanta 114, 318–322. https://doi.org/10.1016/j.talanta.2013.05.059

Rumayor, M., Lopez-Anton, M.A., Díaz-Somoano, M., Maroto-Valer, M.M., Richard, J.-H., Biester, H., Martínez-Tarazona, M.R., 2016. A comparison of devices using thermal desorption for mercury speciation in solids. Talanta 150, 272–277. https://doi.org/10.1016/j.talanta.2015.12.058

Rumayor, M., Lopez-Anton, M.A., Díaz-Somoano, M., Martínez-Tarazona, M.R., 2015. A new approach to mercury speciation in solids using a thermal desorption technique. Fuel 160, 525–530. https://doi.org/10.1016/j.fuel.2015.08.028

Rutz, C., Schmolke, L., Gvilava, V., Janiak, C., 2017. Anion Analysis of Ionic Liquids and Ionic Liquid Purity Assessment by Ion Chromatography. Z. Für Anorg. Allg. Chem. 643, 130–135. https://doi.org/10.1002/zaac.201600437

Saha, A., Gupta, B.S., Patidar, S., Martínez-Villegas, N., 2023. Optimal GIS interpolation techniques and multivariate statistical approach to study the soil-trace metal(loid)s distribution patterns in the agricultural surface soil of Matehuala, Mexico. J. Hazard. Mater. Adv. 9, 100243. https://doi.org/10.1016/j.hazadv.2023.100243

Sako, A., Bamba, O., Gordio, A., 2016. Hydrogeochemical processes controlling groundwater quality around Bomboré gold mineralized zone, Central Burkina Faso. J. Geochem. Explor. 170, 58–71. https://doi.org/10.1016/j.gexplo.2016.08.009

Sako, A., Nimi, M., 2018. Environmental geochemistry and ecological risk assessment of potentially harmful elements in tropical semi-arid soils around the Bagassi South artisanal gold mining site, Burkina Faso. Cogent Environ. Sci. 4, 1543565. https://doi.org/10.1080/23311843.2018.1543565

Salonen, V.-P., Korkka-Niemi, K., 2007. Influence of parent sediments on the concentration of heavy metals in urban and suburban soils in Turku, Finland. Appl. Geochem. 22, 906–918. https://doi.org/10.1016/j.apgeochem.2007.02.003

Sanogo, I.S., Diabaté, D., Dara, Kone, I., Kone, A., 2019. Le secteur minier artisanal et le rôle du Service géologique au Mali,.

Sanogo, S., Kabre, J., Cecchi, P., 2014. Inventaire et distribution spatio-temporelle des macroinvertébrés bioindicateurs de trois plans d'eau du bassin de la Volta au Burkina Faso. Int. J. Biol. Chem. Sci. 8, 1005. https://doi.org/10.4314/ijbcs.v8i3.16

Sanoussi, A.A., 2020. Evaluation des impacts de l'exploitation artisanale de l'or sur le site d'orpaillage de Komabangou (Liptako, NIGER).

Sawadogo, E., 2011. Discours, pratiques et dynamiques environnementales autour de l'orpaillage dans la commune de Kampti (Sud-ouest du Burkina Faso) (Thèse en Géographie).

Sba-Ecosys, S. business association, 2011. Analyse économique du secteur des mines. Liens pauvrété et environnement. (Final), Ministère de l'Environnement et du Cadre de Vie (MECV) Projet Initiative Pauvreté Environnement (IPE).

Schön-Blume, N., Dolega, P., Buchert, M., Bodenmüller, B., Meyer, M., 2021. THE IMPACT OF GOLD "SUSTAINABILITY ASPECTS IN THE GOLD SUPPLY-CHAINS AND SWITZERLAND'S ROLE AS A GOLD HUB."

Schudel, G., Miserendino, R.A., Veiga, M.M., Velasquez-López, P.C., Lees, P.S.J., Winland-Gaetz, S., Davée Guimarães, J.R., Bergquist, B.A., 2018. An investigation of mercury sources in the Puyango-Tumbes River: Using stable Hg isotopes to characterize transboundary Hg pollution. Chemosphere 202, 777–787. https://doi.org/10.1016/j.chemosphere.2018.03.081

Schuster, E., 1991. The behavior of mercury in the soil with special emphasis on complexation and adsorption processes - A review of the literature. Water. Air. Soil Pollut. 56, 667–680. https://doi.org/10.1007/BF00342308

Seguin, J.J., 2005. Projet Réseau SIG-Afrique. Carte hydrogéologique de l'Afrique à l'échelle du 1/10 M.

Shapi, M., Jordaan, M.A., Nadasan, D.S., Davies, T.C., Chirenje, E., Dube, M., Lekoa, M.R., 2020. Analysis of the Distribution of Some Potentially Harmful Elements (PHEs) in the Krugersdorp Game Reserve, Gauteng, South Africa. Minerals 10, 151. https://doi.org/10.3390/min10020151

Si, Y., Zou, Y., Liu, X., Si, X., Mao, J., 2015. Mercury methylation coupled to iron reduction by dissimilatory iron-reducing bacteria. Chemosphere 122, 206–212. https://doi.org/10.1016/j.chemosphere.2014.11.054

Sidam-Minorex, E., 1998. Orrpaillage en Guinée.

Sissoko, M.F., 2019. Double rationalité sur l'orpaillage traditionnel au Mali. Rev. Afr. Sci. Soc. Santé Publique 1, 101–115.

Skyllberg, U., Bloom, P.R., Qian, J., Lin, C.-M., Bleam, W.F., 2006. Complexation of Mercury(II) in Soil Organic Matter: EXAFS Evidence for Linear Two-Coordination with Reduced Sulfur Groups. Environ. Sci. Technol. 40, 4174–4180. https://doi.org/10.1021/es0600577

Smedley, P.L., Kinniburgh, D.G., 2002. A review of the source, behaviour and distribution of arsenic in natural waters. Appl. Geochem. 17, 517–568. https://doi.org/10.1016/S0883-2927(02)00018-5

Smedley, P.L., Knudsen, J., Maiga, D., 2007. Arsenic in groundwater from mineralised Proterozoic basement rocks of Burkina Faso. Appl. Geochem. 22, 1074–1092. https://doi.org/10.1016/j.apgeochem.2007.01.001

Smith, L.J.D., Paktunc, D., Blowes, D.W., 2021. Trace elements in sulfides and release to porewater from sulfide oxidation in a historical waste-rock pile, Ontario, Canada. Appl. Geochem. 126, 104899. https://doi.org/10.1016/j.apgeochem.2021.104899

Somé, I., Sakira, A., Ouédraogo, M., Ouédraogo, T., Traoré, A., Sondo, B., Guissou, P., 2012. Arsenic levels in tube-wells water, food, residents' urine and the prevalence of skin lesions in Yatenga province, Burkina Faso. Interdiscip. Toxicol. 5, 38–41. https://doi.org/10.2478/v10102-012-0007-4

Somé, I.T., Sakira, A.K., Mertens, D., Ronkart, S.N., Kauffmann, J.-M., 2016. Determination of groundwater mercury (II) content using a disposable gold modified screen printed carbon electrode. Talanta 152, 335–340. https://doi.org/10.1016/j.talanta.2016.02.033

Song, X., Vanheyst, B., 2005. Volatilization of mercury from soils in response to simulated precipitation. Atmos. Environ. 39, 7494–7505. https://doi.org/10.1016/j.atmosenv.2005.07.064

Sonke, J.E., Angot, H., Zhang, Y., Poulain, A., Björn, E., Schartup, A., 2023. Global change effects on biogeochemical mercury cycling. Ambio 52, 853–876. https://doi.org/10.1007/s13280-023-01855-y

Soto-Jiménez, M.F., Páez-Osuna, F., 2001. Distribution and Normalization of Heavy Metal Concentrations in Mangrove and Lagoonal Sediments from Mazatlán Harbor (SE Gulf of California). Estuar. Coast. Shelf Sci. 53, 259–274. https://doi.org/10.1006/ecss.2000.0814

Stapper, D., Dales, K., Velasquez, P., Keane, S., 2021. Best Management Practices for Cyanide Use in the Small-Scale Gold Mining Sector (PlanetGOLD Programme (Global Environment Facility and United Nations Environment Programme)).

States, J.C., Srivastava, S., Chen, Y., Barchowsky, A., 2009. Arsenic and Cardiovascular Disease. Toxicol. Sci. 107, 312–323. https://doi.org/10.1093/toxsci/kfn236

Sultan, B., Janicot, S., 2003. The West African Monsoon Dynamics. Part II: The "Preonset" and "Onset" of the Summer Monsoon. J. Clim. 16, 3407–3427. https://doi.org/10.1175/1520-0442(2003)016<3407:TWAMDP>2.0.CO;2

Sunderland, E.M., Gobas, F.A.P.C., Branfireun, B.A., Heyes, A., 2006. Environmental controls on the speciation and distribution of mercury in coastal sediments. Mar. Chem. 102, 111–123. https://doi.org/10.1016/j.marchem.2005.09.019

Sunderland, E.M., Li, M., Bullard, K., 2018. Decadal Changes in the Edible Supply of Seafood and Methylmercury Exposure in the United States. Environ. Health Perspect. 126, 017006. https://doi.org/10.1289/EHP2644

Sunkari, E.D., Seidu, J., Ewusi, A., 2022. Hydrogeochemical evolution and assessment of groundwater quality in the Togo and Dahomeyan aquifers, Greater Accra Region, Ghana. Environ. Res. 208, 112679. https://doi.org/10.1016/j.envres.2022.112679

Sylla, M., Ngom, P.M., 1997. Le gisement d'or de Sabodala (Sénégal Oriental): Une minéralisation filonienne d'origine hydrothermale remobilisée par une tectonique cisaillante. J. Afr. Earth Sci. 25, 183–192. https://doi.org/10.1016/S0899-5362(97)00097-3

Szymczycha, B., Miotk, M., Pempkowiak, J., 2013. Submarine Groundwater Discharge as a Source of Mercury in the Bay of Puck, the Southern Baltic Sea. Water. Air. Soil Pollut. 224, 1542. https://doi.org/10.1007/s11270-013-1542-0

Tadiso, T.M., Borgstrøm, R., Rosseland, B.O., 2011. Mercury concentrations are low in commercial fish species of Lake Ziway, Ethiopia, but stable isotope data indicated biomagnification. Ecotoxicol. Environ. Saf. 74, 953–959. https://doi.org/10.1016/j.ecoenv.2011.01.005

Tankari Dan-Badjo, A., Ibrahim, O.Z., Guéro, Y., Morel, J.L., Feidt, C., Echevarria, G., 2019. Impacts of artisanal gold mining on soil, water and plant contamination by trace elements at Komabangou, Western Niger. J. Geochem. Explor. 205, 106328. https://doi.org/10.1016/j.gexplo.2019.06.010

Tankari Dan-Badjo, A., Tidjani, D., Idder, T., Guero, Y., Dan Lamso, N., Matsallabi, A., Ambouta, J., Feidt, C., Sterckeman, T., Echevarria, G., 2015. Diagnostic de la contamination des eaux par les éléments traces métalliques dans la zone aurifère de Komabangou – Tillabéri, Niger. Int. J. Biol. Chem. Sci. 8, 2849. https://doi.org/10.4314/ijbcs.v8i6.41

Tao, A., 2020. Production minière en 2019: Baisse de la production mais hausse des recettes. J. Econ. Faso. URL https://www.leconomistedufaso.bf/2020/06/23/production-miniere-en-2019-baisse-de-la-production-mais-hausse-des-recettes/ (accessed 10.25.22).

Taylor, H., Appleton, J.D., Lister, R., Smith, B., Chitamweba, D., Mkumbo, O., Machiwa, J.F., Tesha, A.L., Beinhoff, C., 2005. Environmental assessment of mercury contamination from the Rwamagasa artisanal gold mining centre, Geita District, Tanzania. Sci. Total Environ. 343, 111–133. https://doi.org/10.1016/j.scitotenv.2004.09.042

Telmer, K.H., Veiga, M.M., 2009. World emissions of mercury from artisanal and small scale gold mining, in: Mason, R., Pirrone, N. (Eds.), Mercury Fate and Transport in the Global Atmosphere. Springer US, Boston, MA, pp. 131–172. https://doi.org/10.1007/978-0-387-93958-2_6

Tetteh, S., Golow, A.A., Essumang, D.K., Zugle, R., 2010. Levels of Mercury, Cadmium, and Zinc in the Topsoil of Some Selected Towns in the Wassa West District of the Western Region of Ghana. Soil Sediment Contam. Int. J. 19, 635–643. https://doi.org/10.1080/15320383.2010.515626

The European Commission, 2023. COMMISSION REGULATION (EU) 2023/915 of 25 April 2023 on maximum levels for certain contaminants in food and repealing Regulation (EC) No 1881/2006.

Thiombane, M., De Vivo, B., Niane, B., Watts, M.J., Marriott, A.L., Di Bonito, M., 2023. A new hazard assessment workflow to assess soil contamination from large and artisanal scale gold mining. Environ. Geochem. Health 45, 5067–5091. https://doi.org/10.1007/s10653-023-01552-5

Tiffreau, C., Lützenkirchen, J., Behra, P., 1995. Modeling the Adsorption of Mercury(II) on (Hydr)oxides. J. Colloid Interface Sci. 172, 82–93. https://doi.org/10.1006/jcis.1995.1228

Tisserand, D., Daval, D., Truche, L., Fernandez-Martinez, A., Sarret, G., Spadini, L., Némery, J., 2024. Recommendations and good practices for dissolved organic carbon (DOC) analyses at low concentrations. MethodsX 12, 102663. https://doi.org/10.1016/j.mex.2024.102663

Tisserand, D., Guédron, S., Viollier, E., Jézéquel, D., Rigaud, S., Campillo, S., Sarret, G., Charlet, L., Cossa, D., 2022. Mercury, organic matter, iron, and sulfur co-cycling in a ferruginous meromictic lake. Appl. Geochem. 146, 105463. https://doi.org/10.1016/j.apgeochem.2022.105463

Tissot, S., Pichard, A., 2005. Seuils de Toxicité Aiguë Acide Cyanhydrique (HCN) (Rapport finale No. 01–25590), 02DR06. Ministaire de l'Ecologie et du Developpement Durable-INERIS.

Tomicic, C., Vernez, D., Belem, T., Berode, M., 2011. Human mercury exposure associated with small-scale gold mining in Burkina Faso. Int. Arch. Occup. Environ. Health 84, 539–546. https://doi.org/10.1007/s00420-011-0615-x

Tomiyasu, T., Kono, Y., Kodamatani, H., Hidayati, N., Rahajoe, J.S., 2013. The distribution of mercury around the small-scale gold mining area along the Cikaniki river, Bogor, Indonesia. Environ. Res. 125, 12–19. https://doi.org/10.1016/j.envres.2013.03.015

Tomiyasu, T., Matsuyama, A., Imura, R., Kodamatani, H., Miyamoto, J., Kono, Y., Kocman, D., Kotnik, J., Fajon, V., Horvat, M., 2012. The distribution of total and methylmercury concentrations in soils near the Idrija mercury mine, Slovenia, and the dependence of the mercury concentrations on the chemical composition and organic carbon levels of the soil. Environ. Earth Sci. 65, 1309–1322. https://doi.org/10.1007/s12665-011-1379-z

Torkaman, P., Veiga, M.M., 2023. Comparing cyanidation with amalgamation of a Colombian artisanal gold mining sample: Suggestion of a simplified zinc precipitation process. Extr. Ind. Soc. 13, 101208. https://doi.org/10.1016/j.exis.2022.101208

Tri Santosa, Y., 2025. 30 World's Largest Country Producers of Gold. Sci. Agric. URL https://www.scienceagri.com/2025/01/30-worlds-largest-country-producers-of.html (accessed 9.8.25).

Trivedi, P., Axe, L., 2001. Ni and Zn Sorption to Amorphous versus Crystalline Iron Oxides: Macroscopic Studies. J. Colloid Interface Sci. 244, 221–229. https://doi.org/10.1006/jcis.2001.7970

Tulasi, D., Fajon, V., Kotnik, J., Shlyapnikov, Y., Adotey, D.K., Serfor-Armah, Y., Horvat, M., 2021. Mercury methylation in cyanide influenced river sediments: A comparative study in Southwestern Ghana. Environ. Monit. Assess. 193, 180. https://doi.org/10.1007/s10661-021-08920-7

Turetsky, M.R., Harden, J.W., Friedli, H.R., Flannigan, M., Payne, N., Crock, J., Radke, L., 2006. Wildfires threaten mercury stocks in northern soils. Geophys. Res. Lett. 33, 2005GL025595. https://doi.org/10.1029/2005GL025595

Ullrich, S.M., Tanton, T.W., Abdrashitova, S.A., 2001. Mercury in the Aquatic Environment: A Review of Factors Affecting Methylation. Crit. Rev. Environ. Sci. Technol. 31, 241–293. https://doi.org/10.1080/20016491089226

Ummel, M., Schulz, Y., 2024. Sur la piste de l'or africain. Quantifier la production et le commerce afin de lutter contre les flux illicites.

UNECA, U.N.E.C. for A., 2011, 2011. Minerals and Africa's Development: The International Study Group Report on Africa's Mineral Regimes.

UNEP, 2023. COMMISSION REGULATION (EU) 2023/915 of 25 April 2023 on maximum levels for certain contaminants in food and repealing Regulation (EC) No 1881/2006. Official Journal of the European Union.

UNEP, 2013. Global Mercury Assessment 2013: Sources, Emissions, Releases and Environmental Transport (No. 3593). UNEP Chemicals Branch, Geneva, Switzerland.

UNEP, U.N.E.P., 2018. Global mercury assessment 2018. United Nations Environment Programm.

UNEP/OCHA, 2010. Lead Pollution and Poisoning Crisis Environmental Emergency Response Mission Zamfara State, Nigeria. Switzerland, Joint UNEP/OCHA Environment Unit.

U.S. Environmental Protection Agency, 1998. Methyl Mercury in Water by Distillation, Aqueous Ethylation, Purge and Trap, and Cold Vapor Atomic Fluorescence Spectrometry (Method 1630).

USEPA, 2001. Water Quality Criterion for the Protection of Human Health: Methylmercur.

USEPA, 1997. Mercury study report to congress; VolumeV: Health effects of mercury and mercury compounds.

Van Straaten, P., 2000. Mercury contamination associated with small-scale gold mining in Tanzania and Zimbabwe. Sci. Total Environ. Elsevier.

Vasters, J., Schütte, P., 2023. D1.4 – Country profiles of artisanal and small-scale ECRM mine production and processing developments.

Veiga, M.M., Baker, R.F., Fried, M.B., Withers, D., 2004. Protocols for environmental and health assessment of mercury released by artisanal and small-scale gold miners. Global Mercury Project, UNIDO, Vienna.

Veiga, M.M., Siegel, S., Schein, P., Camara, C.S., Dejean, J., Kamara, D., Diouf, A., 2006. Technical Mission to the Artisanal Gold Mines in Upper Guinea.

Velásquez-López, P.C., Veiga, M.M., Klein, B., Shandro, J.A., Hall, K., 2011. Cyanidation of mercury-rich tailings in artisanal and small-scale gold mining: identifying strategies to manage environmental risks in Southern Ecuador. J. Clean. Prod. 19, 1125–1133. https://doi.org/10.1016/j.jclepro.2010.09.008

Verbrugge, B., Geenen, S. (Eds.), 2020. Global Gold Production Touching Ground: Expansion, Informalization, and Technological Innovation. Springer International Publishing, Cham. https://doi.org/10.1007/978-3-030-38486-9

Verbrugge, B., Lanzano, C., Libassi, M., 2021. The cyanide revolution: Efficiency gains and exclusion in artisanal- and small-scale gold mining. Geoforum 126, 267–276. https://doi.org/10.1016/j.geoforum.2021.07.030

Verma, S.K., Chaurasia, S., 2024. Implicating the effects of consuming water with a high level of arsenic content: highlighting the cause and consequences of arsenic contamination in drinking water. Water Pract. Technol. 19, 1071–1083. https://doi.org/10.2166/wpt.2024.072

Vic, G., Billa, M., 2015. Geological setting and types of carbonate-hosted gold deposits in the Birimian of West Africa.

Wang, S., Feng, X., Qiu, G., Wei, Z., Xiao, T., 2005. Mercury emission to atmosphere from Lanmuchang Hg–Tl mining area, Southwestern Guizhou, China. Atmos. Environ. 39, 7459–7473. https://doi.org/10.1016/j.atmosenv.2005.06.062

Wang, T., Driscoll, C.T., Hwang, K., Chandler, D., Montesdeoca, M., 2020. Total and methylmercury concentrations in ground and surface waters in natural and restored freshwater wetlands in northern New York. Ecotoxicology 29, 1602–1613. https://doi.org/10.1007/s10646-019-02155-6

Wannous, M., Osenbrück, K., Tanimoun, B., Koeniger, P., 2024. Hydrochemical Characterisation of the Basement Aquifer with a Focus on the Origin of Nitrate in the Highly Urbanised Niamey Region, SW of Niger. Water 16, 3016. https://doi.org/10.3390/w16213016

Wasserman, J.C., Hacon, S., Wasserman, M.A., 2003. Biogeochemistry of Mercury in the Amazonian Environment. AMBIO J. Hum. Environ. 32, 336–342. https://doi.org/10.1579/0044-7447-32.5.336

WAXI Africa, 2023. West African Mineral Systems.

Webster, R., 2001. Statistics to support soil research and their presentation. Eur. J. Soil Sci. 52, 331–340. https://doi.org/10.1046/j.1365-2389.2001.00383.x

Werthmann, K., 2013. Gold mining in Burkina Faso since the 1980S.

Wiatrowski, H.A., Das, S., Kukkadapu, R., Ilton, E.S., Barkay, T., Yee, N., 2009. Reduction of Hg(II) to Hg(0) by Magnetite. Environ. Sci. Technol. 43, 5307–5313. https://doi.org/10.1021/es9003608

Williams, C.R., Leaner, J.J., Nel, J.M., Somerset, V.S., 2010. Mercury concentrations in water resources potentially impacted by coal-fired power stations and artisanal gold mining in Mpumalanga, South Africa. J. Environ. Sci. Health Part A 45, 1363–1373. https://doi.org/10.1080/10934529.2010.500901

Windmöller, C.C., Silva, N.C., Morais Andrade, P.H., Mendes, L.A., Magalhães Do Valle, C., 2017. Use of a direct mercury analyzer® for mercury speciation in different matrices without sample preparation. Anal. Methods 9, 2159–2167. https://doi.org/10.1039/C6AY03041F

Winkler, M.S., Divall, M.J., Krieger, G.R., Balge, M.Z., Singer, B.H., Utzinger, J., 2011. Assessing health impacts in complex eco-epidemiological settings in the humid tropics: The centrality of scoping. Environ. Impact Assess. Rev. 31, 310–319. https://doi.org/10.1016/j.eiar.2011.01.003

World Gold Council, 2021. Global mine production by country [WWW Document]. World Gold Counc. URL https://www.gold.org/goldhub/data/gold-production-by-country (accessed 10.25.22).

World Health Organization, 2017. Guidelines for drinking-water quality: fourth edition incorporating first addendum, 4th ed., 1st add. ed. World Health Organization, Geneva.

World Health Organization, 2011. Guidelines for drinking-water quality.

World Health Organization/FAO, 2007. METHYLMERCURY (Evaluations of the Joint FAO/WHO Expert Committee on Food Additives (JECFA) No. TRS 940-JECFA 67/57), 67th_2007_methyl mercury.pdf.

Wurl, J., Mendez-Rodriguez, L., Acosta-Vargas, B., 2014. Arsenic content in groundwater from the southern part of the San Antonio-El Triunfo mining district, Baja California Sur, Mexico. J. Hydrol. 518, 447–459. https://doi.org/10.1016/j.jhydrol.2014.05.009

Yin, R., Feng, X., Wang, J., Li, P., Liu, J., Zhang, Y., Chen, J., Zheng, L., Hu, T., 2013. Mercury speciation and mercury isotope fractionation during ore roasting process and their implication to source identification of downstream sediment in the Wanshan mercury mining area, SW China. Chem. Geol. 336, 72–79. https://doi.org/10.1016/j.chemgeo.2012.04.030

Yonlihinza, I.A., 2017. Mines - Niger : jusqu'où la ruée vers l'eldorado minéral ? [WWW Document]. Le Point. URL https://www.lepoint.fr/economie/mines-niger-jusqu-ou-la-ruee-vers-l-eldorado-mineral-16-05-2017-2127668_28.php (accessed 10.14.25).

Yu, R.-Q., Flanders, J.R., Mack, E.E., Turner, R., Mirza, M.B., Barkay, T., 2012. Contribution of Coexisting Sulfate and Iron Reducing Bacteria to Methylmercury Production in Freshwater River Sediments. Environ. Sci. Technol. 46, 2684–2691. https://doi.org/10.1021/es2033718

Yu, X., Driscoll, C.T., Warby, R.A.F., Montesdeoca, M., Johnson, C.E., 2014. Soil mercury and its response to atmospheric mercury deposition across the northeastern United States. Ecol. Appl. 24, 812–822. https://doi.org/10.1890/13-0212.1

Zabsonré, A., Agbo, M., Somé, J., Haffin, I., 2016. Impact de l'exploitation de l'or sur les conditions de vie des populations au Burkina Faso (No. 145). Pep Policy brief.

Zhang, C., Gan, C., Ding, L., Xiong, M., Zhang, A., Li, P., 2020. Maternal inorganic mercury exposure and renal effects in the Wanshan mercury mining area, southwest China. Ecotoxicol. Environ. Saf. 189, 109987. https://doi.org/10.1016/j.ecoenv.2019.109987

Zhang, H., Lindberg, S.E., 1999. Processes influencing the emission of mercury from soils: A conceptual model. J. Geophys. Res. Atmospheres 104, 21889–21896. https://doi.org/10.1029/1999JD900194

Zhang, L., Wright, L.P., Blanchard, P., 2009. A review of current knowledge concerning dry deposition of atmospheric mercury. Atmos. Environ. 43, 5853–5864. https://doi.org/10.1016/j.atmosenv.2009.08.019

Zhang, S., Xia, M., Pan, Z., Wang, J., Yin, Y., Lv, J., Hu, L., Shi, J., Jiang, T., Wang, D., 2024. Soil organic matter degradation and methylmercury dynamics in Hg-contaminated soils: Relationships and driving factors. J. Environ. Manage. 356, 120432. https://doi.org/10.1016/j.jenvman.2024.120432

Zhang, Y., Zhou, X., Ma, W., Yin, D., Wang, Y., Zhang, C., Wang, D., 2022. Distribution of Mercury and Methylmercury in Farmland Soils Affected by Manganese Mining and Smelting Activities. Int. J. Environ. Res. Public. Health 19, 10288. https://doi.org/10.3390/ijerph191610288

VI

Appendices

Appendix 1

VI.1. Appendix 1 : Synthèse en Français « Impact de l'orpaillage sur les écosystèmes aquatiques et les populations au Burkina Faso et en Guinée »

VI.1.1. Introduction

L'exploitation aurifère ou orpaillage est une activité ancienne dont les traces remontent au quatrième ou troisième millénaire avant J-C, et qui a une longue histoire dans les sociétés humaines (Hauptmann and Klein, 2009). Aujourd'hui encore, l'orpaillage occupe une place prépondérante avec une production mondiale représentant environ 20% de la production totale d'or qui inclue l'exploitation industrielle (AMAP/UNEP, 2019). En Afrique de l'Ouest, et plus particulièrement au Burkina Faso et en Guinée, cette activité connaît une expansion notable depuis plus d'une décennie, alimentée par l'augmentation du prix de l'or et par des crises socio-économiques successives (Choquet, 2018).

Le Burkina Faso, désormais l'un des principaux producteurs africains, a vu sa production artisanale passer d'environ 0,1-0,5 tonne en 2014 à plus de 8 tonnes en 2024 (ATI, 2025). Une croissance similaire est observée en Guinée, où l'exportation d'or artisanal a été multipliée par plus de dix entre 2013 et 2021 (MMG, 2022; WAXI Africa, 2023; Bortnikov et al., 2024). Cette croissance rapide de l'orpaillage montre son importance comme source de revenus.

L'orpaillage est une pratique regroupant un ensemble de processus impliquant l'extraction du minerai, suivi du concassage, du broyage, du lavage, et enfin de l'amalgamation au mercure (Hg) (Donkor et al., 2006; Telmer and Veiga, 2009). L'utilisation intensive et non réglementée du Hg liquide dans l'orpaillage conduit à la libération de grandes quantités de Hg dans l'environnement, et amplifie profondément la partie anthropique de son cycle biogéochimique (Sonke et al., 2023). Ce cycle biogéochimique lui permet d'exister sous différentes formes dans l'environnement, à savoir sous forme élémentaire inorganique (Hg0) et Hg^{2+} ou HgII, et sous forme organique comme le méthylmercure (MeHg). Ce Hg libéré par l'orpaillage se dépose principalement sous forme de gouttelettes de Hg0, qui s'accumulent dans les sols à proximité des sites d'amalgamation en raison de leur faible réactivité, de leur lente solubilité dans l'eau, de leur densité élevée et faible taux d'oxydation (Ariya et al., 2015). Une partie du mercure émis lors de la combustion de l'amalgame or-Hg se volatilise et se disperse dans l'atmosphère, où il peut être transporté sur de longues distances avant de se redéposer au sol et dans l'eau sous forme de dépôts secs et/ou humides (Fu et al., 2010; Tomiyasu et al., 2012; Yu et al., 2014; Noble et al., 2016). Une autre partie de ce Hg atmosphérique est absorbée ou adsorbée par les feuilles des arbres, puis incorporée dans le sol lors de la sénescence (litière), constituant ainsi une source d'apport exogène de Hg dans ces sols (Jiskra et al., 2015). À la suite d'épisodes de ruissellement après des précipitations, sur des sols nus dû à la déforestation, ces particules riches en Hg sont drainées dans les écosystèmes aquatiques, constituant une cause importante de contamination. Une fois dans le milieu aquatique, le Hg inorganique peut être transformé par différents types de microorganismes, comme les bactéries sulfato-réductrices et ferri-réductrices en méthylmercure (CH_3Hg^+), un composé toxique qui s'accumule et se bioamplifie dans les chaînes alimentaires (Parks et al., 2013; Mason et al., 2019; Compaore et al., 2020). Le Burkina Faso a

enregistré une utilisation particulièrement élevée de Hg dans l'orpaillage, estimée à 78 tonnes en 2020 (PAN, 2020). Ce qui entraine une contamination de l'environnement avec des vapeurs Hg0 qui sont potentiellement dangereuses pour la santé humaine. Cette contamination affecte les poissons par une accumulation et biomagnification du MeHg entraînant un risque direct pour les populations consommateurs intensifs de poissons (Ouédraogo et al., 2015; Sunderland et al., 2018). Les orpailleurs utilisent également le cyanure, pour dissoudre l'or, principalement sous forme de cyanure de sodium, qui génère des composés toxiques tels que le CN^- et l'acide cyanhydrique (Tissot and Pichard, 2005; Kouadio et al., 2025). Son usage intensif est associé à des effets neurologiques chez les mineurs et à une contamination environnementale touchant agriculture, élevage et pêche (Knoblauch et al., 2020; Koné, 2021). D'autres métaux comme le plomb et l'arsenic, parfois libérés lors de l'extraction, peuvent également contaminer les eaux souterraines au-delà des normes de l'OMS, exposant les communautés locales à des risques sanitaires chroniques et aigue (Hilson, 2002; UNEP/OCHA, 2010; UNEP, 2013; Bretzler et al., 2017). Les sols jouent alors un double rôle dans la dynamique de la contamination agissant comme des réservoirs de contaminants et la source potentiels de transfert vers les eaux de surface et souterraines par l'action des vecteurs « vent et eau » (Aleksander-Kwaterczak and Ciszewski, 2016). Il est donc essentiel de comprendre la spéciation et la distribution du Hg dans les sols, sa réactivité et les précurseurs de la méthylation dans les sédiments, et sa bioaccumulation dans les poissons pour comprendre les risques sanitaires associés aux activités d'extraction de l'or. Malgré la contribution socio-économique majeure de l'orpaillage, les connaissances sur la dynamique du Hg et des autres métaux (As, Pb) dans ces environnements restent limitées et peu documentées. Les flux, la spéciation, les voies d'exposition et les risques pour la santé humaine sont encore insuffisamment étudiés, en particulier dans le contexte ouest-africain.

Face à ces enjeux majeurs, cette thèse s'inscrit dans un partenariat entre l'Université Joseph KI-ZERBO (UJKZ) et l'Université Grenoble Alpes (UGA), soutenu par le réseau African Centers of Excellence (ACE-Partner). Elle répond également aux besoins du Centre Emergent pour les Mines et la Société (CEMS, Guinée) et de l'Institut International d'Ingénierie de l'Eau et de l'Environnement (2IE, Burkina Faso), tous deux engagés dans la formation d'experts capables de traiter les problématiques environnementales et sociales liées à l'exploitation minière en Afrique de l'Ouest.

L'objectif général de cette étude est d'évaluer le devenir environnemental des contaminants métalliques associés à l'exploitation aurifère et leurs risques pour l'écologie et la santé humaine au Burkina Faso et en Guinée, en s'intéressant particulièrement au mercure, au cyanure, à l'arsenic et au plomb, ainsi qu'à leurs impacts sur l'environnement et les populations locales. Pour atteindre cet objectif, trois objectifs spécifiques sont formulés visant à :

- Déterminer les niveaux de base des contaminants et l'impact des activités minières artisanales sur les concentrations (Hg, CN, As, Pb) dans les différents compartiments écologiques de l'environnement. Il

s'agira notamment de déterminer si ces éléments sont naturellement élevés dans les eaux souterraines et si l'orpaillage entraine une remobilisation, en particulier pour l'As et le Pb.

- Étudier le transfert de la réactivité du Hg des zones minières vers les villages et les cours d'eau, en suivant l'évolution des concentrations et des formes chimiques du mercure de l'amont vers l'aval des sites d'exploitation, ainsi que la part respective des sources géogéniques de l'As et du Pb.

- Évaluer les risques sanitaires associés aux niveaux mesurés, en identifiant les principales voies d'exposition humaine, notamment la consommation de poisson, et l'inhalation de vapeurs ou de poussières.

La problématique étudiée a été abordé à travers trois axes principaux :

I- Étude des niveaux de contamination au Hg dans les sols miniers et les rivières du sud-ouest du Burkina Faso, ainsi que les concentrations d'arsenic et de plomb dans les eaux, les sols et les sédiments.

II- Évaluation de la contamination des sites miniers et des villages aurifères, en mettant particulièrement en évidence les principales voies d'exposition des populations aux poussières et aux vapeurs de Hg, ainsi que la mobilité du métal dans les sols et son potentiel de contamination des eaux souterraines en République de Guinée.

III- Étude de l'impact de l'orpaillage sur le fleuve Niger et ses affluents en Guinée en évaluant la distribution spatiale et verticale du Hg dans les sédiments, sa spéciation, sa mobilité et sa bioaccumulation dans les espèces de poissons, ainsi que les risques associés pour la santé humaine.

VI.1.2. Description des sites d'étude

VI.1.2.1. Sites d'étude et échantillonnage au Burkina Faso

En raison de la dégradation de la sécurité dans les régions du Nord et de l'Est du Burkina Faso, les zones initialement ciblées ont été abandonnées au profit de régions plus sûres au Sud-Ouest grâce à la présence de l'ANEEMAS (Agence Nationale d'Encadrement des Exploitations Minières Artisanales et Semi-mécanisés) crée en 2015. Ainsi, les sites d'étude ont été redéfinis en 2022 focalisés sur trois localités situées le long du fleuve Mouhoun : Boromo, Dano et Gaoua dont le choix repose sur leur accessibilité, leur potentiel minier et les techniques d'orpaillage utilisées. Les détails sur les sites miniers et les types d'orpaillage utilisés sont repris dans le **Tableau VI-1**.A. En bref, deux sites dont B1 (Siby) et B2 (Siggnoghin) ont été échantillonné à Boromo situé dans la boucle de la rivière Mouhoun à 175 km de Ouagadougou. Deux autres sites nommés B3 (Gnikpière) et B4 (Memer1) ont été échantillonnés dans la région de Dano située au Sud-Ouest entre Ouagadougou, Bobo-Dioulasso et Gaoua. Un dernier site minier nommé B5 (Djikando) a été prélevé dans le Sud-Ouest à Gaoua situé dans la province de Poni. D'autres échantillons ont été prélevés en 2018 par Robert Mason dans la

région de Gaoua sur les sites B6 (Quadaradoua) et B7 (Bandediera–Banfara–Poniro), dont les analyses n'avaient jamais été diffusées avant leur intégration à ce travail.

Dans l'ensemble des sites étudiés, l'amalgamation au Hg est la technique dominante pour l'extraction de l'or, à l'exception du site de Siggnoghin où la cyanuration est également utilisée. En 2022, une rivière permanente (Poni) et intermittente non impactée (à Dano, à 3 km des sites), les puits et forages (sites et villages en aval) et des échantillons composites de 5 sous-échantillons de sols (sites et villages) et des sédiments (berges) sur ~12 m² (0-5cm de profondeur) ont été prélevés. Les sols de surface en dehors des sites miniers et les roches de la ceinture des roches verte de Boromo ont également été prélevés. En 2018, les minerais broyés, résidus de lavage du minerai, le concentré solide après lavage et l'amalgame ont été échantillonnés. L'échantillonnage des eaux de surface et souterraine a été effectué dans des flacons FEP Teflon® de 250 mL, à la fois des échantillons bruts et filtrés (filtre Sterivex 0.45 µm) suivant un protocole ultra-traces de prélavage acide. Les eaux filtrées et non filtrées pour l'analyse du Hg total (THg) et du méthylmercure (MeHg) ont été acidifiées au HCl (0.5% v/v, qualité trace) et celles filtrées pour les majeurs et traces (Fe, Al, S, Mn, As, Pb) acidifiées au HNO_3 (2% v/v). Celles pour les anions (SO_4^{2-}, Cl^-, PO_4^{3-}) ont été filtrées et congelées, et enfin pour le carbone organique dissous DOC, le prélèvement a été effectué dans des flacons borosilicates ambrés pré-calcinés (550°C) et acidifiées au HCL 0.1N (Némery et al., 2013). Des analyses de paramètres physico-chimiques (pH, conductivité, température et turbidité) ont été réalisées directement sur le terrain en utilisant le multi-paramètre Hach® (HQ4300). Pour le contrôle qualité, les échantillons de blanc d'eau milliQ ont également été prélevés dans les mêmes flacons et dans les mêmes conditions que les échantillons sur le terrain.

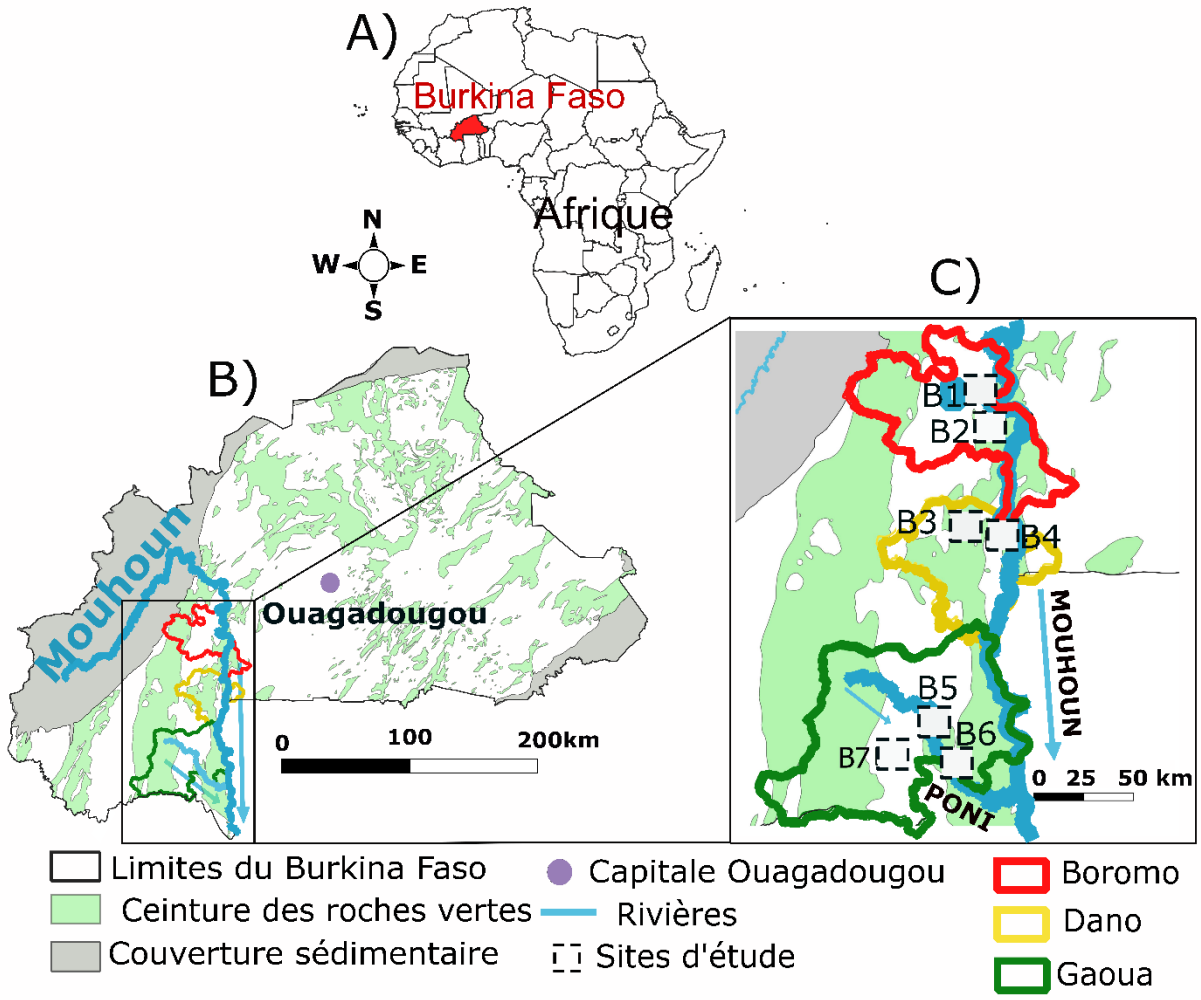


Figure VI.1. Carte du site étudié avec A) La localisation du Burkina Faso en Afrique. B) Carte géologique du Burkina Faso montrant la ceinture de roches vertes, les fleuves Mouhoun et Poni, et les trois districts miniers étudiés : Boromo, Dano et Gaoua. C) Extrait agrandi.

Tableau VI-1. *Informations synthétiques pour tous les sites étudiés concernant le type de processus d'extraction de l'orpaillage (mercure et/ou cyanuration), le nombre de mineurs, l'année de création, la superficie à la date de l'échantillonnage et la source d'eau utilisée dans le processus d'extraction A) au Burkina Faso et B) en Guinée. N.D signifie non déterminé. Les coordonnées sont exprimées en UTM où X correspond à l'abscisse est et Y à l'abscisse nord. Au Burkina Faso, les coordonnées UTM sont exprimées en zone 30N (WGS84). Les sites étudiés dans la région de Kouroussa (Haute Guinée) sont situés en zone UTM 29N (WGS84).*

A) Burkina Faso								
sites miniers	Nom site	X	Y	orpaillage type	Miners (nombre)	création année	surface (ha)	Lavage minerais type d'eau
B1	Siby	503938	1311725	Hg	~300	2009	6	Rivière
B2	Siggnoghin	508059	1295615	Hg+CN	~1000	2006	24	Eau souterraine
B3	Gnikpière	496842	1239977	Hg	~300	2019	100	Eau souterraine
B4	Memer1	510432	1234596	Hg	~500	1997	100	Eau souterraine
B5	Djikando	479243	1145849	Hg	~1200	1995	100	Rivière
B6	Quadaradouo	490536	1123049	Hg	N.D	N.D	N.D	Eau souterraine
B7	Bandediera-Banfara-Poniro	453332	1125884	Hg	N.D	N.D	N.D	Eau souterraine
B) Guinée								
G1	Bankan	396806	1175470	Hg	~1500	2021	1	Eau souterraine
G2	Djaragbela	394600	1170434	Hg	~300	2021	0.05	Eau souterraine
G3	Saman	408423	1166318	Hg+CN	~500	1983	3	Rivière
G4	Dionko	394157	1189522	Hg	~500	1993	2	Eau souterraine

VI.1.2.2. Sites d'étude et échantillonnage en Guinée

L'insécurité dans la région de Siguiri, proche de la frontière Malienne, a empêché l'accès à cette zone en 2023 et 2024, faisant basculer l'étude vers les régions plus sûres à Kouroussa en Haute Guinée. Cette zone est composée de savane soudano-guinéenne à relief doux drainée par le fleuve Niger et ses affluents Saman et Niandan. Kouroussa est une zone abritant des orpailleurs Burkinabè (29%) et Maliens (38%) en plus des natifs. Quatre sites d'orpaillage artisanal ont été étudiés en 2023 dont trois situés près du fleuve Niger et un plus éloigné dans la préfecture de Sanguiana. Les détails sur les sites échantillonnés sont présentés dans le **Tableau VI-1**.B. En bref, les sites G1 (Bankan), G2 (Djaraguela),

G3 (Saman), proches du fleuve Niger et le site G4 (Dionko) situé à plus de 5 km du fleuve Niger, font tous l'extraction minière sur place, mais le broyage, lavage et amalgamation s'effectuent dans les villages. Tous ces sites miniers utilisent l'amalgamation sauf le site G3 (Saman) qui utilise en plus la cyanuration qui est faite directement sur les berges (<100 mètres) du fleuve Niger. Contrairement au Burkina Faso, la gestion locale des sites d'orpaillage repose sur le système traditionnel du « Tomboloma », chargés de délimiter les zones d'orpaillage et collecter les taxes. Deux campagnes d'échantillonnage ont été réalisées en 2023 sur les quatre sites d'orpaillage, puis uniquement sur deux sites (G3 et G4) en 2024 mais avec une spatialisation intégrant le fleuve Niger et ses tributaires. Des échantillons composites de 5 sous-échantillons de sols de surface (sites et villages) et des sédiments (berges) sur ~12 m² (0-5cm de profondeur) ont été prélevés et homogénéisés. Les eaux de surface et souterraines ont été prélevées dans les villages miniers ainsi que dans le fleuve Niger et ses tributaires. En 2024, les eaux porales, les carottes de sédiments, les profils de sols, ainsi que les poissons ont également été prélevés dans les mines, les villages miniers et dans le fleuve Niger et ses tributaires. Les matières en suspension ont été prélevées par filtration des eaux sur filtre PVDF 0.45 µm, puis les eaux porales par microbougies poreuses (Rhizon®) entre 0 à 5 cm dans le sédiment. Les sols ont été échantillonnés selon la lithologie et le changement de couleur jusqu'à 50 cm en profondeur tandis que les sédiments ont été prélevées avec un carottier manuel en PVC (66 mm de diamètre), puis découpés en tranches de 2 cm.

Tous les échantillonnages ont été réalisés selon le même protocole et les analyses correspondantes sont décrites dans la section 6.2.1.

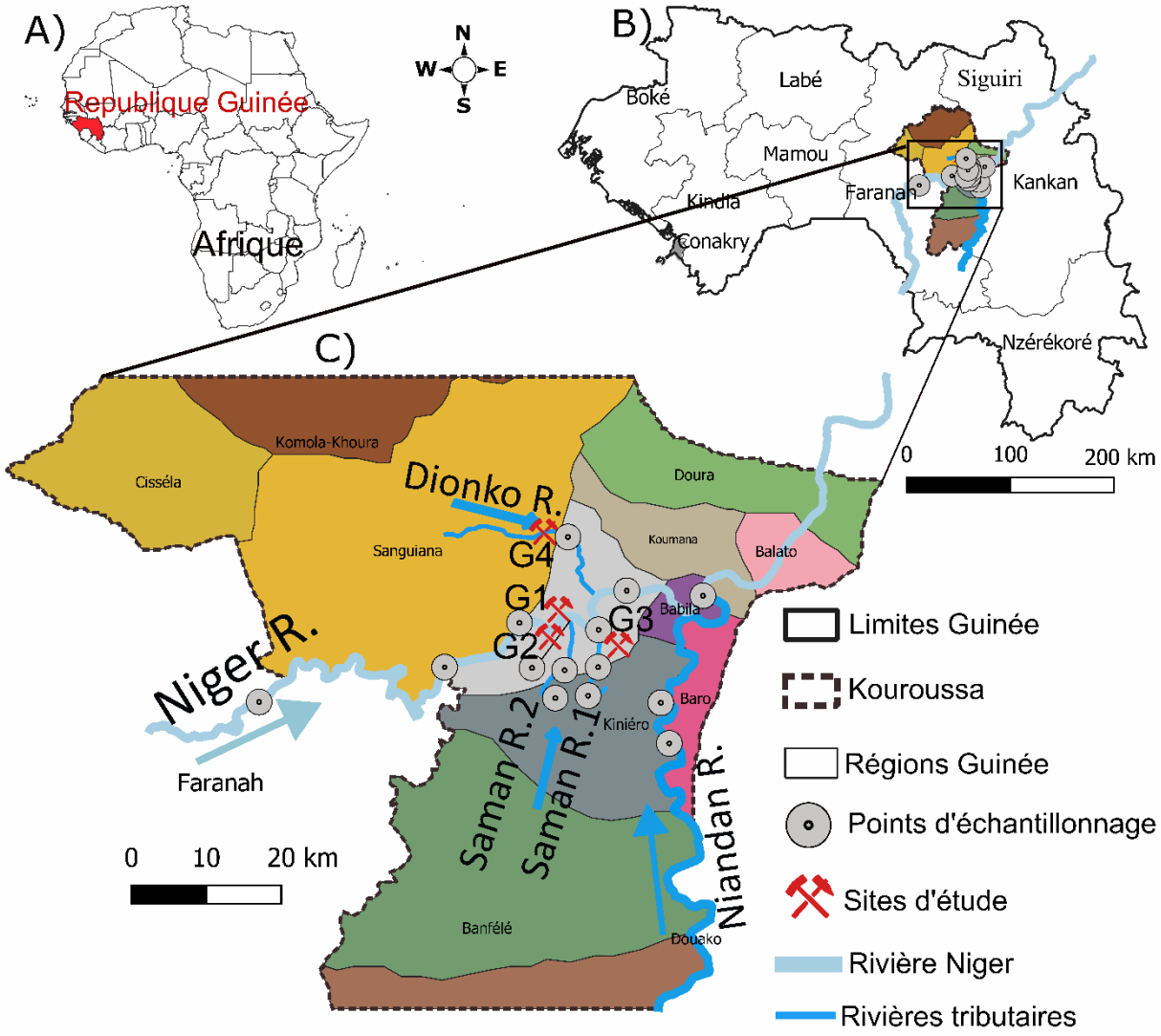


Figure VI.2. Carte de la zone d'étude montrant A) la Guinée en Afrique ; B) la région d'étude, située à Kouroussa en Guinée, et C) les points d'échantillonnage avec les principaux cours d'eau.

VI.1.3. Méthodes analytiques

Procédure d'extraction du méthylmercure dans les sols et sédiments

L'extraction du méthylmercure (MeHg) dans les sols et sédiments a été réalisée sur 2–2,5 g de sédiments et sur du matériel de référence certifié (CRM). Pour assurer la qualité des données, des blancs réactifs et des échantillons dopés ont été inclus et les analyses ont été faites en triplicats.

Les réactifs préparés comprenaient du $CuSO_4$ 1 M, pour la complexation du mercure, et une solution KBr/H_2SO_4 à 18%/5% avec hydroxylamine hydrochloride, servant à l'extraction sélective du MeHg, protégée de la lumière et conservée au réfrigérateur.

L'extraction s'effectuait en ajoutant les réactifs aux échantillons puis 10 mL de dichlorométhane (DCM). Après agitation et centrifugation, la phase organique contenant le MeHg était séparée de la phase inorganique. Le DCM était transféré dans des flacons pour évaporation sous azote à 60°C, puis reconstitué avec de l'eau déionisée pour l'analyse.

Cette procédure permet de séparer le méthylmercure de la matrice solide, garantissant une analyse précise et reproductible. Les échantillons étaient conservés à l'obscurité et analysés idéalement dans les 48 h suivant l'extraction.

Procédure de minéralisation du poisson pour l'analyse du methylmercure

Les tissus dorsaux des poissons ont été disséqués, lyophilisés pendant 3 à 5 jours, puis homogénéisés par broyage. Une masse de 15 à 25 mg de matière sèche a été pesée dans des contenants en Téflon, incluant des matériaux de référence certifiés (CRM : TORT-3 et DORM-2), puis digérée dans 5 mL d'acide nitrique 4,5 N à 60°C pendant environ 18 h. Les digestats ont ensuite été dilués avec de l'eau ultrapure et le pH ajusté entre 4,2 et 4,7 à l'aide d'un tampon acétate et de KOH. Les étalonnages ont été réalisés avec des standards de MeHg couvrant 0,05 à 4 ppt, en incluant blancs, CRM, duplicatas et des échantillons enrichis pour garantir exactitude et reproductibilité. Avant analyse, chaque flacon a reçu 30 µL de tétraéthylborate de sodium (NaTEB) pour réaliser l'ethylation du méthylmercure, préparant ainsi les échantillons pour la quantification analytique.

Procédure de détermination des phases porteuses du mercure dans les sols et sédiments

Une thermodésorption basée sur la détermination des phases de transport du mercure a été réalisée sur la fraction fine des sols et sédiments lyophilisés et broyés. Les différentes phases du Hg ont été déterminées par paliers de température à 80°C pour Hg0 (Hg élémentaire) ; entre 100 à 180°C (HgII associé à la matière organique) et 180-550°C (HgII plus réfractaire) selon le protocole adapté à la méthode décrite (Windmöller et al., 2017; Biester and Scholz, 1997; Meloni et al., 2024). Nous avons réalisé ces attaques en pesant environ 50 à 100 mg de sols et de sédiments (en fonction de la concentration initiale en Hg) dans des nacelles chauffées dans un four pendant 48 heures à 100°C et 180°C, puis les culots ont été analysés par spectroscopie d'absorption atomique (AMA : Advanced Mercury Analyzer) à 550°C, tout comme l'échantillon brut. La concentration de $Hg_{désorbé}$ a été calculée à l'aide de la formule suivante : $[Hg]_{desorbé}(ng.g^{-1}) = \frac{[THg]-[Hg]_{Pyrolisé}}{[THg]}$ avec [THg] et $[Hg]_{pyrolisé}$ en $ng.g^{-1}$ suivant le protocole décrit dans (Guedron et al., 2009). La concentration en HgII réfractaire a été déterminée en soustrayant la concentration de Hg mesurée à 180°C de la concentration totale en Hg (550°C) de l'échantillon brut.

Deux extractions sélectives ont été réalisées afin d'identifier et de quantifier les principales phases mercurifères dans les échantillons. Ces méthodes s'appuyaient sur l'expérience passée rapportée dans la littérature utilisant des sous-alcalis provenant d'échantillons de sols et de sédiments. Les extractions sélectives ont été réalisées dans une hotte à flux laminaire dans des flacons traces de 15 ml à un rapport solide/liquide de 1:100 (Bloom et al., 2003). Pour éliminer au mieux les chevauchements de pics de Hg, les extractions sélectives ont été réalisées sur les échantillons bruts ainsi que les échantillons dont le Hg0 a été préalablement éliminé à 80°C. Sur ces échantillons, la matière organique

associée aux composés humiques a été extraite en ajoutant 4 ml de NH_4OH 1M à 40 mg d'échantillons sous agitation pendant 1h (Rodríguez Martín-Doimeadios et al., 2000). L'extraction de la fraction de Hg liée aux minéraux d'oxydes de Fe(III) faiblement cristallisés et à la ferrihydrite a été réalisée en ajoutant de l'ascorbate. L'ascorbate a été préparé à des proportions de 50 g L^{-1} de citrate de sodium et 50 g L^{-1} de bicarbonate de sodium dans de l'eau déionisée puis le mélange a été dégazé à l'azote toute une nuit. À ce mélange dégazé, 10 g L^{-1} d'acide ascorbique ont été ajoutés donnant un pH final de 8,0. Tous les réactifs utilisés sont des produits de haute pureté que nous avons préalablement pyrolysés afin d'éliminer les impuretés et analysés pour déterminer leur teneur en THg, qui s'est avérée inférieure à 2 ng g^{-1}. Les sols et sédiments ont été extraits à un rapport solide/liquide de 1:100 dans 10 ml du mélange d'ascorbate pendant 24 heures à température ambiante, sous agitation à 125 tr/min. Les extractants de NH_4OH et d'ascorbate ont ensuite été centrifugés pendant 20 minutes à 3000 tours/minutes, et le surnageant a été retiré avec soin avec des pointes de pipettes préalablement lavées au HNO_3 et HCl pour éviter toute contamination. Le culot a été rincé trois fois avec de l'eau déionisée et le surnageant a été acidifié avec du HNO_3 supra pur à un pH inférieur à 5 et gardé pour l'analyse des traces et majeurs. Ces protocoles ont été adaptés de différents articles (Kostka and Luther, 1994; Veiga et al., 2004; Rodríguez Martín-Doimeadios et al., 2000; Guedron et al., 2009; Raiswell et al., 2010). Les culots ont ensuite été lyophilisés et analysés à l'AMA 254 pour déterminer la concentration de Hg. Ainsi, le Hg lié à chaque fraction (ce qui est extrait) a été obtenu par soustraction du Hg dans le culot au Hg total de l'échantillon brut ou après pyrolyse à 80°C obtenu à l'AMA selon le protocole (Guedron et al., 2009).

Protocole d'analyse de l'isotopie du carbone dans les échantillons de sols et sédiments

Les échantillons de sols et sédiments ont été décarbonatés avec du HCl afin d'éliminer le carbone minéral et ne conserver que le carbone organique. Le processus consistait en l'ajout progressif de HCl (1 N et 6 N) avec des temps d'attente pour permettre le dégazage complet du CO_2. Les échantillons étaient ensuite séchés à ≤50°C et conservés dans un dessiccateur pour éviter l'humidité.

Les analyses isotopiques ont été effectuées à l'aide d'un spectromètre Picarro sur des échantillons bruts et décarbonatés placés dans des capsules en étain. Chaque échantillon, pesé en fonction de sa teneur en carbone, était brûlé à 980°C pour libérer le CO_2, qui était ensuite analysé par CRDS. Les mesures incluaient le carbone total (en g/g d'échantillon) et le rapport isotopique $\delta^{13}C/\delta^{12}C$, normalisé au standard VPDB pour le carbone.

Des matériaux de référence certifiés (Benz 19, CMB 19-4, CalR 19) ont été utilisés pour corriger les biais analytiques et assurer la précision des mesures. La masse de carbone des échantillons a été ajustée à partir des courbes d'étalonnage et des signaux du $^{12}CO_2$ mesuré, garantissant des valeurs fiables pour la teneur en carbone et la signature isotopique. La formule standard utilisée pour calculer

la signature isotopique est : $\delta X = [\frac{Rech}{Rstd} - 1] * 1000.$ où $R_{échantillon}$ et $R_{standard}$ sont les rapports isotopiques $^{13}C/^{12}C$ pour l'échantillon et le standard, respectivement.

Protocole de digestion des échantillons de sols et de sédiments pour l'analyse des éléments majeurs et traces

Environ 50 mg d'échantillons solides (sédiments ou sols), préalablement humidifiés avec quelques gouttes d'eau dans des tubes en téflon, ont été digérés avec 5 mL de HNO_3 14 N et 2 mL de HF au micro-onde (UltraWAVE, Milestone) à 250°C pendant 1 h. Les digestats ont été évaporés à 120°C, repris deux fois dans 5 mL de HNO_3 14 N et évaporés, avant d'être dilués définitivement dans du HNO_3 2% pour constituer les solutions mères. Les solutions filles ont été préparées par dilution (×5000 pour les éléments majeurs, ×10 000 pour les traces).

Des standards certifiés (JSD3, IAEA-405, BR24 pour les sédiments ; ERM CC 141 pour les sols) ont été traités dans les mêmes conditions pour vérifier la reproductibilité.

Pour l'ICP-AES, les solutions filles ont été introduites via une pompe péristaltique dans un nébuliseur, formant un aérosol transporté vers la torche à plasma (≈6000–10 000 K) grâce au flux d'argon. Les grosses gouttes sont éliminées et les fines particules atomisées, excitant les atomes qui émettent des photons. Ces photons sont séparés par un système optique (prisme/réseau) et détectés, produisant un signal proportionnel à la concentration des éléments. Les analyses ont été effectuées en mode radial (one-NEB) pour garantir l'exactitude et la précision. Pour l'ICP-MS, les échantillons sont également convertis en aérosol et introduits dans le plasma, où ils sont désolvatés, vaporisés, atomisés et ionisés. Les ions mono-chargés sont extraits par un cône sous vide, focalisés par des lentilles ioniques, puis séparés selon leur rapport masse/charge (m/z) dans l'analyseur de masse. La détection par multiplicateur d'électrons fournit une intensité directement proportionnelle à la concentration, permettant une analyse multi-élémentaire à haute sensibilité.

Ces techniques ont été également appliquées directement aux eaux filtrées et acidifiées à 2% de HNO_3, en utilisant des standards certifiés SLRS4 et SLRS6 pour le contrôle qualité.

VI.1.4. Résultats

VI.1.4.1. Transport du mercure des sols miniers vers les sédiments de rivière et rôle des oxydes de fer amorphes dans le processus de méthylation dans le Sud-Ouest du Burkina Faso.

Introduction

L'Extraction minière artisanale et à petite échelle est une source majeure d'émissions de Hg dans le monde, notamment en Afrique de l'Ouest. Pensant augmenter leurs gains, les orpailleurs utilisent fréquemment de grandes quantités de Hg pour amalgamer l'or exposant les mineurs et les populations locales à des risques sanitaires graves et entrainant une contamination durable des sols et des cours d'eau. Les pertes de Hg sous forme liquide combinées aux retombées atmosphériques issues de la combustion de l'amalgame entrainent une contamination des sols, avec des concentrations de Hg souvent supérieures aux niveaux géochimiques naturels à proximité des sites d'extraction. La contamination des hydrosystèmes est induite par le rejet de Hg lié aux particules dans les rivières. Ce Hg peut être transformé en méthylmercure (MeHg) par des processus biogéochimiques dans des environnements suboxiques ou anoxiques, un composé hautement toxique, pour lequel les données sur les concentrations sont limitées en Afrique de l'Ouest. La spéciation et le comportement du Hg dans les sols tropicaux riches en fer restent peu documentés, tout comme les interactions possibles entre le Hg, la matière organique et les oxydes de fer. Cette étude examine la distribution et le transfert de Hg et d'autres contaminants géogéniques, tels que l'arsenic et le plomb, entre les sols miniers et les sédiments de cinq sites d'orpaillage le long de la Rivière Mouhoun, au Sud-Ouest du Burkina Faso.

Méthodes

Les échantillons de sols et les sédiments ont été lyophilisés, puis broyés et tamisés en différentes granulométries de sable (0,5 mm-2 mm) et d'argile + limon (<0,5 mm) homogène permettant une bonne reproductibilité des analyses. Sur la fraction argile + limon, la diffraction des rayons X (DRX) a été réalisée afin de déterminer les phases minérales par broyage de 1 g d'échantillons dans 15 ml d'éthanol absolu pendant 10 minutes. À l'aide d'un instrument Bruker D8, utilisant une source de rayons X Co ou Cu et un détecteur SolX, des analyses en géométrie Bragg-Brentano dans la plage de 5 à 80º avec un pas de 0,026º et un temps de comptage de 8 secondes par pas ont été effectuées. L'identification des minéraux a été réalisée à l'aide du logiciel EVA de Bruker, et la quantification a été effectuée à l'aide du logiciel PROFEX par affinement de Rietveld, en exploitant en plus les bases de données internes, conformément au protocole publié (Doebelin and Kleeberg, 2015). Le carbone organique et la signature isotopique ont été déterminés selon la technique décrite dans la section 7.3. Le Hg total a été analysé par AMA 254 (Automatic Mercury Analyzer) qui permet une détection des traces de Hg dans les échantillons solides (~ 100 mg) à une longueur d'onde de 254 nanomètres et le MeHg par digestion selon le protocole décrit dans la section 7.3. Les phases porteuses du Hg ont été

déterminées par thermodésorption (Windmöller et al., 2017; Biester and Scholz, 1997; Meloni et al., 2024), et les extractions sélectives selon (Kostka and Luther, 1994; Veiga et al., 2004; Rodríguez Martín-Doimeadios et al., 2000; Raiswell et al., 2010), et selon la technique décrite dans la section 7.3. Les concentrés de minerais et d'amalgame, ont été analysés par pyrolyse à 550°C et amalgamation de l'or à l'aide d'un Nippon DMA-3000, conformément à la procédure publiée (Nugraha et al., 2022), après digestion dans 5 ml d'eau régale (mélange d'acide nitrique et de HCl).

Sur les eaux filtrées et non filtrées, la concentration en Hg totale (THg) a été déterminée par spectrométrie de fluorescence atomique à vapeur froide (CV-AFS) après conversion de toutes les espèces de Hg en Hg0 par oxydation avec du BrCl et réduction avec du $SnCl_2$, puis détection à l'aide d'un Tekran® modèle 2500 suivant le protocole (Guedron et al., 2011; Guédron et al., 2020). Le MeHg a été analysé à l'aide d'un chromatographe en phase gazeuse avec purge et piégeage par éthylation par spectroscopie de fluorescence atomique à vapeur froide (GC-CVAFS) (Tekran®, modèle 2700) suivant le protocole (U.S. Environmental Protection Agency, 1998; Munson et al., 2014).

Résultats

Les résultats montrent que les concentrations en Hg total dans les sols des sites d'orpaillage artisanal sont nettement plus élevés (0,9 à 4,5 µg g^{-1}) que dans les sols non impactés (≈ 0,3 ± 0,1 µg g^{-1}). Ces derniers présentent des niveaux comparables aux concentrations de fond géochimiques rapportées pour divers sols tropicaux à l'échelle mondiale (Guedron et al., 2009; Leiva G. and Morales, 2013; Rajaee et al., 2015a; Verma and Chaurasia, 2024). Environ 10% du Hg total est présent sous forme thermiquement instable, principalement du Hg élémentaire (Hg0), aussi bien dans les sols vierges que dans les sols orpaillés. Les fortes proportions de Hg0 observées dans les sols orpaillés, notamment à proximité des zones de brûlage des amalgames, suggèrent un dépôt par condensation locale. Ceci induit un potentiel de réémission atmosphérique sous climat chaud et sec, faisant de ces sols des sources à long terme de Hg0. Un transfert de la contamination vers les hydrosystèmes est alors observé par la présence de Hg0 (10%) dans les sédiments en aval des sites miniers.

Dans l'ensemble des sols étudiés, le Hg divalent est majoritairement associé aux oxydes de fer amorphes ou faiblement cristallins (≈ 58% du Hg total), soulignant leur rôle clé dans la rétention du Hg. L'association du Hg avec la matière organique est plus faible que dans les sols amazoniens (≈ 34%), mais reste significative, avec une corrélation positive avec le soufre total, suggérant une complexation via des groupes fonctionnels soufrés. Ces résultats indiquent que le HgII est principalement lié à la matière organique et aux oxydes de fer amorphes, possiblement sous forme de revêtements *organiques sur les oxydes métalliques, contribuant au contrôle de sa mobilité et de sa persistance dans les sols (Guedron et al., 2009; Grimaldi et al., 2015)*.

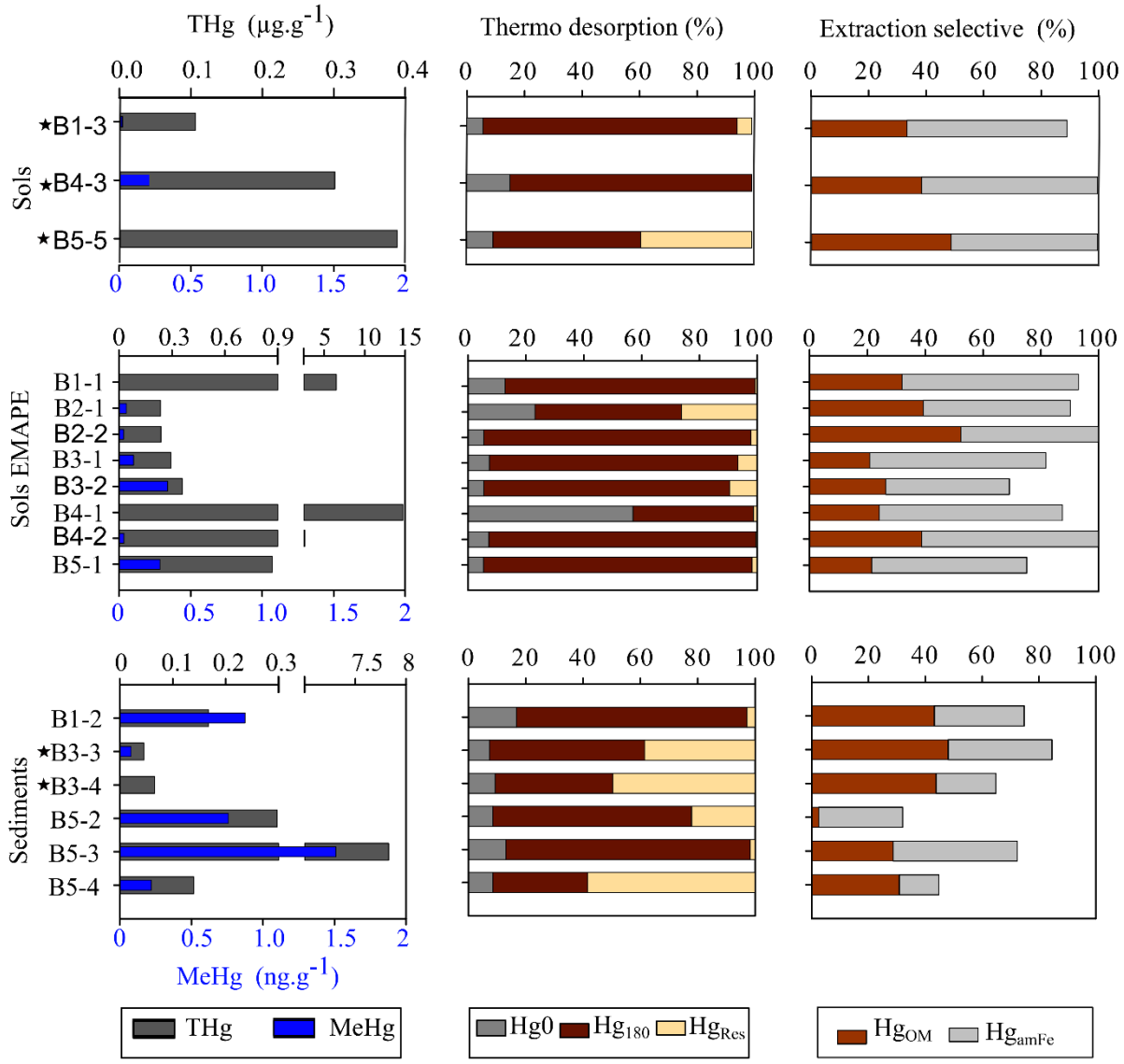


Figure VI.3. *De gauche à droite : concentrations de méthylmercure (MeHg) et de mercure total (THg). Proportions de THg (%) libérées par thermodésorption à 80°C (Hg0), 180°C (Hg180) et la différence entre 180 et 550°C (HgRes), extraction sélective par NH_4OH (HgOM) ou ascorbate (HgamFe) dans le sol loin des sites d'orpaillage (en haut) ; sol influencé par l'orpaillage (au milieu) et sédiments fluviaux (en bas). Les étoiles indiquent un environnement vierge, c'est-à-dire que les échantillons de sol à Boromo, Dano et Gaoua (sites B1-3, B4-3 et B5-5, respectivement) ont été prélevés à quelques kilomètres en aval du site orpaillé, et les échantillons de sédiments ont été prélevés en amont du site d'orpaillage à Dano (sites B3-3 et B3-4). Tous les échantillons de sédiments de Gaoua (site B5) ont été prélevés en aval du site d'orpallage.*

La comparaison entre la thermodésorption et les extractions sélectives montre que le Hg libéré à 180°C (Hg_{180}), initialement attribué à la matière organique, correspond en réalité à un mélange de Hg lié à la matière organique et aux oxydes de fer amorphes, avec une affinité plus forte pour ces derniers. La forte corrélation entre Hg_{180} et la somme de ces deux fractions confirme que le chauffage à 180°C permet de relarguer l'essentiel du Hg divalent associé à ces phases. Le Hg des sols orpaillagés est majoritairement associé aux particules fines (limons et argiles), facilement érodées et transportées

vers les rivières. Dans les hydrosystèmes, les oxydes de fer amorphes qui assuraient la fixation du Hg dans les sols peuvent être réduits en conditions réductrices, libérant le Hg et augmentant sa biodisponibilité. En revanche, la fraction de Hg associée à la matière organique reste similaire entre sols et sédiments. La proportion de Hg lié aux oxydes de fer amorphes ou faiblement cristallisés (HgII-oxydes de fer amorphes) diminue de moitié, passant de 50% dans les sols à 29% dans les sédiments et s'accompagne d'une augmentation marquée du MeHg dans les sédiments, avec des proportions au moins cinq fois plus élevées que dans les sols, indiquant une méthylation plus active en milieu sédimentaire. Par contre, une prédominance de Hg sous forme élémentaire de Hg0 (Hg0 = 13% THg) est associée à une très faible concentration de MeHg, ces formes étant potentiellement moins disponibles pour la méthylation microbienne. Ces résultats indiquent que l'accumulation du MeHg dans les sédiments dépend principalement de la nature et de la réactivité des phases porteuses de Hg présents, des conditions géochimiques (potentiel redox) et des micro-organismes présents, notamment les bactéries réductrices du sulfate (SRB) et du fer (IRB), qui possèdent les gènes impliqués dans la méthylation du Hg (Gilmour et al., 2013; Parks et al., 2013). Par ailleurs, le pompage des eaux souterraines provenant des puits d'orpaillage sont enrichies en arsenic géogénique, et peuvent atteindre des niveaux très élevés (60 µg L^{-1}), bien supérieures aux normes de l'OMS, dans les puits utilisés pour l'eau de boisson à Dano.

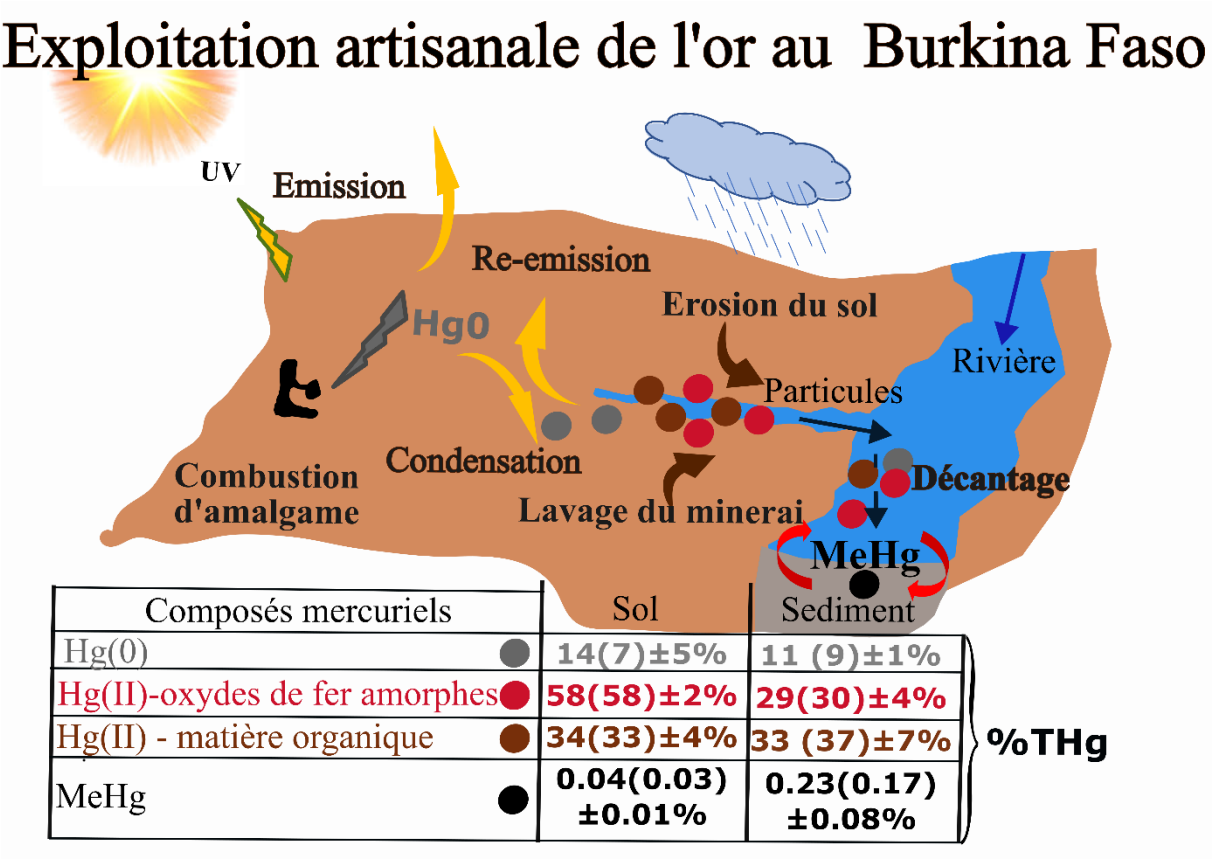


Figure VI.4. Figure de synthèse illustrant les processus environnementaux liés à l'exploitation aurifère et les pourcentages des différents composés du mercure dans les sols et les sédiments en aval des sites miniers au Burkina Faso.

Conclusion

Les sols issus de l'orpaillage artisanal au Burkina Faso présentent des concentrations de Hg bien supérieures aux niveaux naturels, principalement sous forme de HgII associé aux oxydes de fer amorphes et à la matière organique. En aval des sites, la mobilisation de ce HgII favorise la production de MeHg dans les sédiments. Dans les contextes d'un pays en voie de developpement avec à des ressources limitées, la thermodésorption permet d'évaluer efficacement et conjointement le Hg lié à ces fractions, à coût bas.

VI.1.4.2. Transfert de la contamination au mercure depuis la mine vers le village en Guinée: le cas de l'exploitation aurifère artisanale et à petite échelle

Introduction

Comme documenté dans le chapitre précédent, où les concentrations de Hg dans l'environnement au Burkina Faso étaient lié à l'exploitation minière artisanale et à petite d'échelle de l'or, ce chapitre transpose les mêmes études en Guinée. L'orpaillage y constitue une activité économique majeure, impliquant une utilisation intensive de Hg, exacerbée par l'augmentation du prix de l'or, entrainant une accumulation du Hg dans les sols. De plus, les pratiques locales, consistant à déplacer le traitement du minerai vers les villages, exposent directement les populations au mercure et favorisent la dispersion des polluants dans les sols et les eaux en milieu rural. Malgré cette longue tradition minière et la présence de nombreux sites orpaillés en Haute Guinée, les données sur la contamination au Hg restent très limitées. Pour combler cette lacune, des mesures de Hg total ont été effectuées dans les sols de surface et les profils de sols provenant de sites miniers et de sites témoins, prélevés le long d'un transect allant de Conakry vers la Haute Guinée. Afin de mieux comprendre la dispersion de la contamination au Hg et pour évaluer l'impact sur la santé humaine, des échantillons d'eaux souterraines ont également été analysés et la réémission possible de Hg a été estimée en déterminant la fraction du Hg élémentaire.

Méthodes

La distribution granulométrique des sol distinguant les argiles (<2 µm), les limons (2-63 µm) et les sables (>63 µm), a été réalisée sur les sols de surface (inférieure à 2 mm) à l'aide d'un granulomètre laser (Malver, Mastersizer 2000) selon le protocole (Fisher et al., 2017). Les concentrations en Hg total ont été analysées avec l'analyseur AMA 254 selon la méthode décrite dans la section 7.2. Le Hg total et la concentration en arsenic a également été analysé dans les eaux souterraines. Le MeHg a été analysé dans les sols de surface et les eaux souterraines suivant le même protocole de digestion des sols et d'analyse de MeHg décrit dans la section 7.2. Une thermodésorption et les extractions sélectives ont également été réalisées sur les sols de surface afin de confirmer les observations faites au Burkina Faso et de mieux comprendre la réactivité du Hg dans ces milieux. Enfin le stock de Hg accumulé dans les sols des sites miniers depuis leur création a été estimé.

Résultats

Les résultats montrent que les sols des villages miniers constituent les principaux réservoirs de Hg (jusqu'à 10 µg g^{-1}) à Dionko, avec des teneurs en moyenne 17 fois supérieures à celles des sites d'extraction. Cette contamination s'explique par les pratiques d'amalgamation et surtout de la combustion des amalgames au cœur des zones habitées. Le Hg est majoritairement concentré dans les horizons superficiels, sous une forme récente, mobile et réémissible, avec une forte proportion de Hg0

comprise entre 40 et 70%, et est associé principalement à la matière organique (~30%) et aux oxydes de fer réactifs (~10%), conférant au Hg une forte biodisponibilité. Cette fraction mobile favorise une réémission continue de Hg0 vers l'atmosphère, particulièrement sous les conditions climatiques chaudes de la Guinée. Les stocks de Hg élémentaire ont été estimés à environ 985 kg dans le village Saman et 200 kg environs dans celui de Dionko, pour des surfaces respectives de 1.05 et 0.12 km^2. La contamination diffuse observée dans les sols forestiers périphériques suggère un transfert atmosphérique régional (**Figure VI.5**). Compte tenu de la persistance des stocks dans les sols et de leur déplétion très lente, les impacts environnementaux et sanitaires sont durables, même après l'arrêt de l'orpaillage. La proximité entre habitats et activités minières expose directement les populations, y compris femmes et enfants, à l'inhalation répétée de Hg0 neurotoxique.

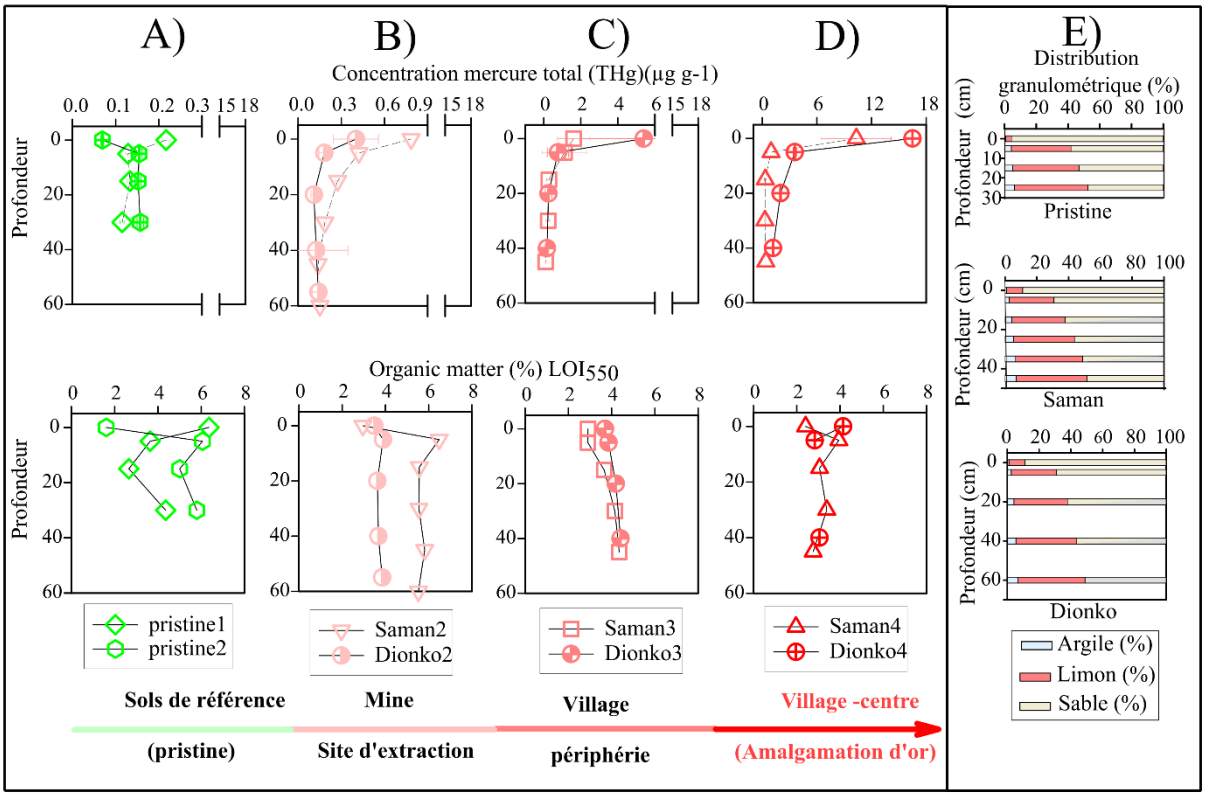


Figure VI.5. Mercure (en haut) et matière organique (en bas) dans le profil du sol dans A) un site vierge ; B) des sites miniers où le minerai est extrait ; C) un village situé à la périphérie et D) un village où se produit l'amalgamation et E) distribution granulométrique dans les sols vierges (en haut), Saman (au milieu) et Dionko (en bas).

De plus, les épisodes de vents et de pluie remobilisent le Hg vers les eaux souterraines, où il est majoritairement lié aux particules en suspension, la fraction dissoute restant faible et contrôlée par le carbone organique dissous. La méthylation du Hg dans ces eaux demeure ainsi limitée. L'arsenic quant à lui est généralement peu présent dans les eaux, avec quelques dépassements ponctuels des normes, suggérant un risque localisé pour certaines zones.

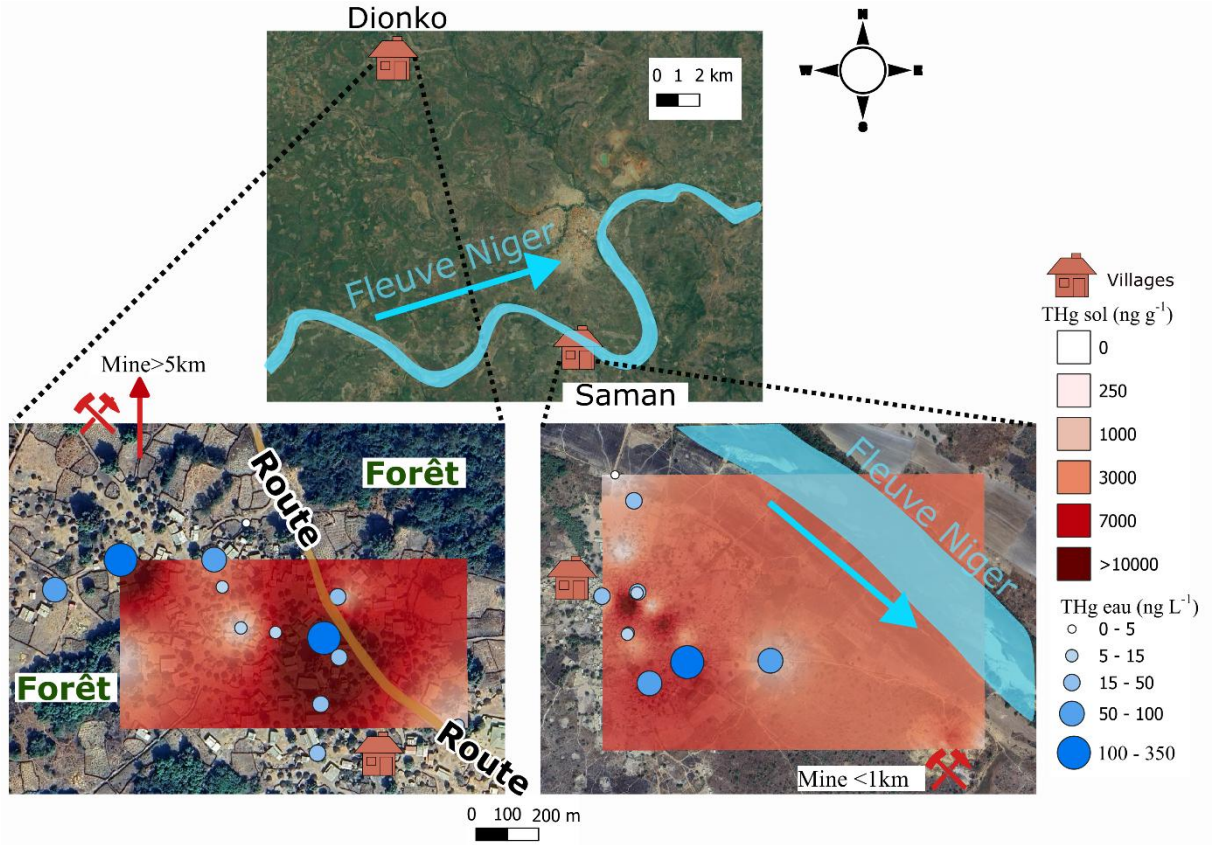


Figure VI.6. *Carte interpolée IDW (Interpolation par Pondération Inverse de la distance) des concentrations de mercure dans les sols superficiels à Dionko et Saman. En haut : carte indiquant l'emplacement des deux villages par rapport au fleuve Niger. En bas à gauche : carte interpolée des sols du village de Dionko en arrière-plan, avec l'eau non filtrée superposée en bleu. En bas à droite : carte interpolée des sols du village et de la mine de Saman avec l'eau non filtrée superposée en bleu.*

Conclusion

Les sols des villages d'orpaillage constituent le principal compartiment de stockage et de transfert du Hg, avec des concentrations très élevées issues des pratiques d'amalgamation et de brûlage des amalgames à Kouroussa. L'accumulation préférentielle dans les horizons superficiels, associée à la matière organique et aux oxydes de fer, confère au Hg une forte biodisponibilité environnementale. Les eaux souterraines apparaissent moins affectées, le Hg y étant majoritairement particulaire et faiblement présent sous forme dissoute, avec une méthylation limitée, bien que des risques localisés existent, notamment pour l'arsenic. Dans l'ensemble, ces résultats montrent que les sols jouent un rôle central comme puit et source de Hg issus des activités minières. Par conséquent, ces sols représentent une source durable de Hg atmosphérique, favorisant la dispersion, le redépôt et la transformation potentielle en méthylmercure, constituant ainsi un risque de transfert vers les chaînes alimentaires et notamment les hydrosystèmes aquatiques.

VI.1.4.3. Impact de l'exploitation artisanale et à petite échelle de l'or sur la contamination au (méthyl)mercure du fleuve Niger en République de Guinée: rôle des sédiments et bioaccumulation dans les poissons.

Introduction

Suite au chapitre précédent qui a mis en évidence une contamination significative des sols des villages miniers à Kouroussa, agissant également comme source de pollution des eaux souterraines, la question du transfert vers les hydrosystèmes se pose. Une fois dans les sédiments de surface, le Hg peut se transformer en méthylmercure, une forme hautement toxique qui se bioaccumule et se biomagnifie le long de la chaîne trophiques, exposant ainsi les populations qui consomment du poisson. Dans ce contexte, une attention particulière est portée au fleuve Niger, le plus grand fleuve d'Afrique de l'Ouest, traversant Kouroussa et alimenté par des tributaires susceptible d'être perturbés par l'orpaillage artisanale. Bien que plusieurs études aient documenté des niveaux élevés de Hg et MeHg dans les sédiments et les poissons des rivières tropicales, aucune donnée fiable n'est disponible pour le fleuve Niger. Cette étude vise donc à quantifier les concentrations de Hg et de MeHg, à identifier leurs vecteurs géochimiques et à évaluer les risques sanitaires pour les populations locales via l'exposition alimentaire, notamment à travers la consommation de poisson.

Méthodes

Les analyses ont principalement porté sur les eaux de surface, les eaux porales, les sédiments de surface, les carottes de sédiments ainsi que sur les poissons collectés dans le fleuve Niger et ses tributaires à Kouroussa, en Haute Guinée. Le Hg total (THg), et le méthylmercure (MeHg) ont été analysés dans les eaux filtrées et non filtrées, suivant le protocole décrit en 7.2, avec des procédures de contrôle qualités (QC) et d'assurance qualités (QA) effectuées à l'aide des standards ORMS 5 et des ajouts dosés, présentant des erreurs <5% pour le Hg et le MeHg respectivement. Le cyanure libre (CN^-) et les complexes cyanurés présents dans l'eau pouvant être décomposés par le chlore ont été mesurés in situ à l'aide du QUANTOFIX®. Pour les profils de sols, les sédiments ainsi que le poisson, le THg et le MeHg ont été analysés suivant les protocoles décrit en 7.2. Pour les poissons, les QA/QC ont été réalisés également avec des standards certifiés de Dogfish (DORM-4) et TORT-3 pour le THg et le TORT-3 et DORM-2 pour le MeHg, avec des valeurs toujours dans une fourchette d'erreur de 5% par rapport aux valeurs certifiées, conformément aux protocoles décrit (Mason et al., 2019, 2022). Le Hg élémentaire a été analysé dans les sédiments par thermodesorption selon le protocole décrit dans la section 7.2.

Résultats

La cartographie des concentrations de Hg dans le fleuve Niger et ses tributaires (**Figure VI.7**) révèle que l'orpaillage artisanal affecte principalement l'écosystème via des apports particulaires. Le Hg total dans les eaux de surface est majoritairement transporté sous forme particulaire, ce qui se reflète dans les sédiments riches en Hg situés en aval des zones d'orpaillage (**Figure VI.7**A et B). Les concentrations de Hg total (THg_F) et de MeHg ($MeHg_F$) dans les eaux de surface en aval des sites miniers ont montré une forte corrélation, suggérant une source commune de Hg. L'orpaillage modifie ainsi les concentrations et la spéciation du Hg dans les sédiments, et la remise en suspension des sédiments contaminés durant les crues pourrait favoriser sa dispersion vers l'aval.

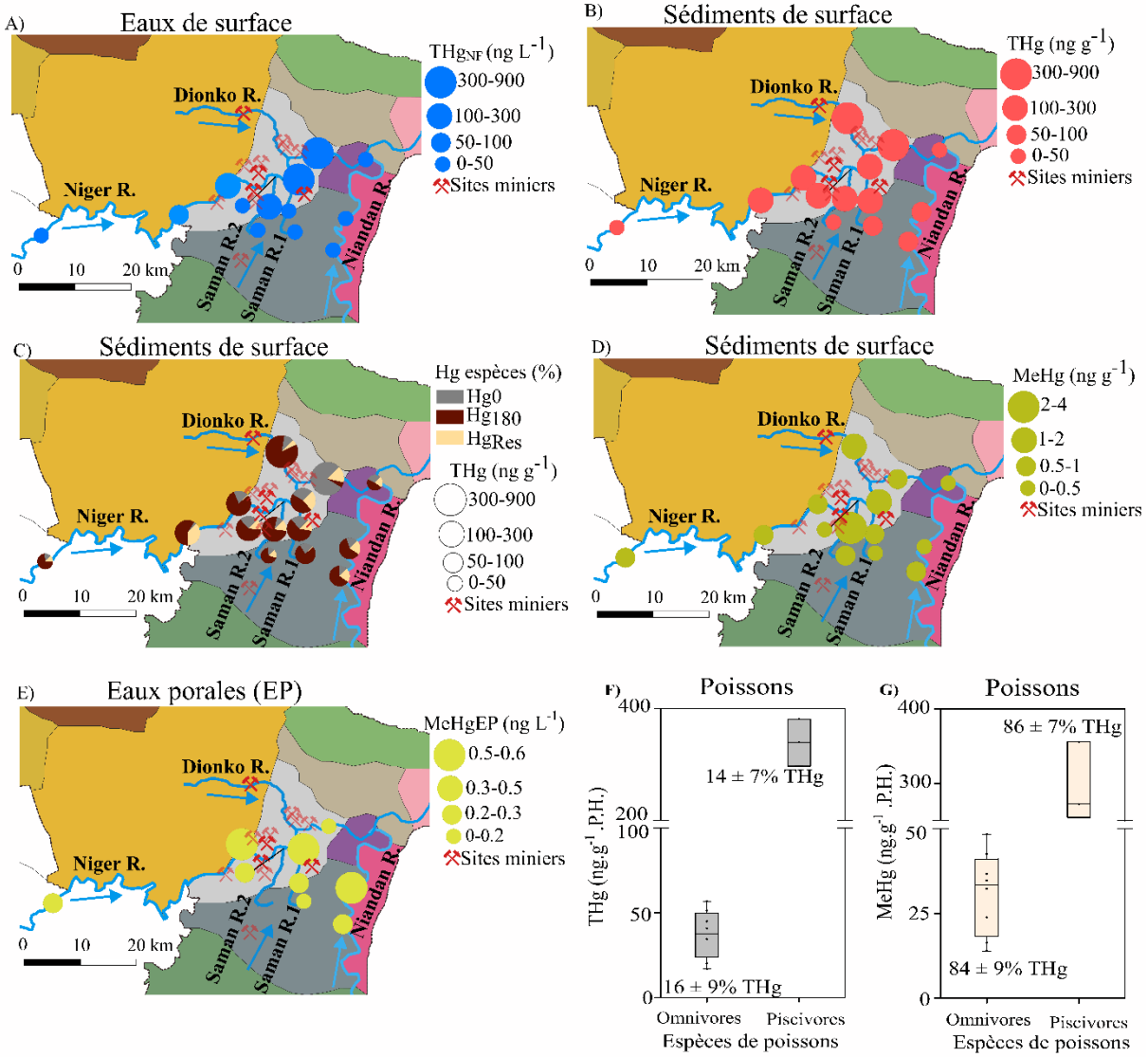


Figure VI.7. Répartition spatiale de la concentration totale en mercure dans A) les eaux non filtrées (THg_{NF}); B) les sédiments de surface. Spéciation du Hg dans les sédiments de surface avec C) phases porteuses du mercure, D) méthylmercure. E) méthylmercure dans les eaux porales. Concentration totale du mercure F) et méthylmercure G) dans les poissons.

En aval des zones minières, la présence accrue de Hg0, peu biodisponible pour les microorganismes méthylants, limite la méthylation du mercure (**Figure VI.7**C et D). L'analyse indique que le MeHg et le Hg inorganique sont transportés par des ligands différents, sans lien direct avec le carbone organique dissous. Les sédiments représentent la principale source de MeHg, libéré vers l'eau par diffusion ou remobilisation, et les relations entre THg, la matière organique et oxydes de fer dans les sédiments influencent fortement cette méthylation. La distribution du THg dans les sédiments et l'eau interstitielle montre qu'il existe un équilibre de partitionnement, tandis que l'accumulation de MeHg dépend des conditions géochimiques, de l'abondance des phases réactives au cours de la diagenèse précoce (Ullrich et al., 2001; Guédron et al., 2020). Les phases porteuses du Hg dans les sédiments déterminent sa mobilité et sa biodisponibilité, en particulier lors des épisodes de crues. Le MeHg a été bioaccumulé dans les 11 poissons prélevés dans le fleuve Niger, dont 18% dépassaient le seuil mondial de qualité de 100 ng Hg g^{-1}, exposant potentiellement les poissons à des risques reproductifs (Crump and Trudeau, 2009; Penglase et al., 2014). De plus, 67% des espèces piscivores, dépassaient le seuil de 300 ng g^{-1} de MeHg, exposant les populations locales de Kouroussa pour qui le poisson est une source importante de protéines, à un risque sanitaire lié au MeHg (Mason et al., 2022). Les estimations de consommation montrent une ingestion hebdomadaire de MeHg comprise entre 54,8 et 85,5 µg, avec des enquêtes de terrain indiquant jusqu'à deux repas de poisson par jour. Ainsi, un adulte de 70 kg pourrait ingérer des niveaux de MeHg dépassant les recommandations de sécurité de 49 µg MeHg/semaine, suggérant un risque important pour la santé, en particulier pour les femmes enceintes, en raison des effets néfastes possibles sur le développement du système nerveux du fœtus (Clarkson and Magos, 2006).

Conclusion

La contamination en Hg du Niger et de ses affluents provient principalement des activités aurifères artisanales, sous forme de particules riches en Hg. Une fois déposés dans les sédiments, le Hg lié à la matière organique et aux oxydes de fer non cristallins peut subir une biométhylation. Les poissons piscivores accumulent davantage de MeHg que les espèces omnivores, représentant plus de 85% du Hg total. Environ 18% des poissons échantillonnés dépassent les normes de protection de la santé humaine, indiquant un risque élevé pour les populations dépendantes de la pêche. Des études supplémentaires, portant sur un nombre plus important de poissons sont nécessaires pour confirmer ces résultats. Néanmoins, il est impératif d'instaurer un suivi régulier de la contamination des poissons et de formuler des recommandations alimentaires adaptées, afin de minimiser l'exposition humaine, tout en tenant compte des pratiques de consommation locales et de l'importance socio-économique de la pêche.

VI.1.5. Conclusion générale, recommandations et perspectives

Cette étude a permis de documenter de manière approfondie la contamination environnementale liée à l'utilisation du mercure dans l'orpaillage artisanal et à petite échelle en Afrique de l'Ouest, au Burkina Faso et en Guinée. Elle fournit des données essentielles sur la distribution et la spéciation du Hg dans les sols et sédiments, en identifiant les phases porteuses (matière organique et oxydes de fer amorphes) favorisant sa méthylation. L'étude a démontré que les pratiques d'orpaillage génèrent des sols fortement contaminés en mercure, impactant les eaux souterraines et de surface. Les villages miniers deviennent ainsi des hotspots de Hg. La contamination mercurielle se reflète également dans les poissons consommés par les populations locales. Ces résultats constituent une base solide pour les scientifiques, les gestionnaires de l'environnement et les décideurs politiques, permettant d'évaluer les risques environnementaux et sanitaires et orienter les politiques de gestion de l'orpaillage.

Pour réduire l'exposition des populations et limiter l'impact environnemental du Hg, plusieurs mesures sont recommandées :

- former les orpailleurs à une utilisation modérée du mercure et les sensibiliser aux dangers des produits chimiques utilisés dans l'extraction de l'or.
- Introduire progressivement des techniques sans Hg, telles que l'usage du borax pour la fusion, et développer des méthodes adaptées de récupération et de condensation du Hg afin de réduire les émissions de Hg.
- Formaliser et suivre régulièrement l'orpaillage pour limiter le transfert des pratiques minières vers les villages.
- Mettre en place des systèmes de traitement des effluents et explorer des solutions de phytoremédiation qui pourrait être une voie prometteuse pour réduire les flux de Hg vers les écosystèmes aquatiques.

Parmi les perspectives scientifiques, il apparaît nécessaire de différencier plus précisément les sources anthropiques et naturelles de Hg via l'utilisation des isotopes du Hg et la cartographie spatiale ; de quantifier les émissions atmosphériques et l'exposition par inhalation. Il est également primordial d'évaluer le potentiel de méthylation en lien avec les communautés microbiennes, et d'étendre les analyses des poissons et des biomarqueurs humains (urine, sang, cheveux) afin de mieux caractériser l'exposition cumulée et les risques pour la santé des populations.

Appendix 2

VI.2. Appendix 2 : Protocole d'étude épidémiologique

Evaluations des niveaux d'exposition au mercure des populations travaillant dans l'extraction minière artisanale et à petite échelle d'or et leur communauté à Kouroussa

Intérêt du thème de l'étude

Selon l'article 7 de la convention de Minamata sur le mercure (Hg), un plan d'action national doit être mené sur les territoires où l'extraction minière artisanale et à petite échelle d'or (EMAPE) sont répandues. Sur la base de cette convention, notre étude sera dirigée vers l'élaboration d'une stratégie de santé publique basé sur l'exposition des mineurs travaillant dans l'extraction aurifère artisanale et à petite échelle et de leurs communautés.

Version préliminaire du 18/12/2023

RÉSUMÉ DU PROTOCOLE

Intitulé de l'étude	Évaluations des niveaux d'exposition au mercure des populations travaillant dans l'extraction minière artisanale et à petite échelle d'or et leur communauté à Kouroussa
Contexte de l'étude	L'exploitation minière artisanale ou l'orpaillage traditionnel est une activité qui joue le premier rôle dans l'économie de la Guinée et est la seule activité de subsistance de la population à Kouroussa. Cette exploitation minière artisanale est réalisée dans huit préfectures dont Kouroussa qui est la troisième préfecture la plus productrice de la Guinée après Siguiri et Mandiana. En Guinée, la population impliquée dans l'orpaillage est estimée à 243 187 acteurs, composée en moyenne de 15% de citoyens ressortissants des pays voisins de la CEDEAO, de 40% de nationaux guinéens et 45% des autochtones. Cette activité implique l'utilisation des produits chimiques comme le mercure pour la récupération de l'or qui a un impact considérable sur la santé humaine et l'environnement.
Objectifs de l'étude	<u>Objectif principal :</u> Evaluer les niveaux d'exposition au mercure des populations travaillant dans l'extraction minière artisanale et à petite échelle d'or et leur communauté à Kouroussa. <u>Objectifs spécifiques</u>: Evaluer les niveaux de connaissances, attitudes et pratiques de la population sur l'utilisation du mercure dans l'EMAPE à Kouroussa. Déterminer les niveaux d'expositions des populations au mercure sur les sites miniers à Kouroussa : mesurer les taux de mercure chez les populations travaillant dans l'extraction minière artisanale et leurs proches à Kouroussa. Mesures effectuées sur les cheveux et urine de chaque communauté pour les amener à changer leur pratique en adoptant des techniques plus sécurisées. Analyser les vapeurs de Hg sur le terrain dans les zones de brûlage de l'amalgame dans l'EMAPE à Kouroussa. Afin de voir les niveaux de vapeurs de Hg potentiellement présent dans l'air de ces zones
Méthodologie	Il s'agira d'une étude transversale réalisée sur un intervalle d'un mois allant du 01 au 31 octobre 2024 sur un échantillon de 250 personnes. Un questionnaire et une collecte des échantillons de cheveux et d'urine seront réalisés chez des personnes âgées d'au moins 18 ans permettant d'abord d'évaluer le niveau de connaissance, attitude et pratique et ensuite de doser le niveau de concentration du mercure chez les populations vivant dans les sites d'extraction artisanale des mines à Kouroussa. Un appareil d'analyse des vapeurs de mercure sera utilisé pour doser la concentration du mercure dans l'air ambiant.
Justification du caractère d'intérêt public de l'étude	Elle permettra de déceler les niveaux de contamination au mercure des personnes impliquées dans l'orpaillage. Les résultats serviront de base aux politiques environnementales nationales visant à protéger les populations vivant dans un environnement minier.
Durée de l'étude	1 an et 6 mois

Financement ACE-Partner; Labex OSUG

Mots clés Pollution minière artisanale, Mercure, risque sanitaire, Kouroussa

Equipe d'étude, structures administratives & signatures

Type d'étude	Étude ayant recours à la collecte de de matériel biologique humain (cheveux et urines).
Investigateur principal	Pr TOURE Abdoulaye, Pharmacien épidémiologiste : Chaire de santé publique et législation pharmaceutique, Centre de recherche et de formation en infectiologie de Guinée à l'Université Gamal Abdel Nasser de Conakry ; courriel (; abdoulaye.toure@cerfig.org/ abdoulaye.toure@ird.fr); Numéro de téléphone (+ 224 623 85 26 58/ 666 64 65 66) Signature:
Co-investigateur	Mr Guédron Stéphane, HDR, Géochimiste à l'institution de des Sciences de la Terre (ISTerre) ; Courriel (stephane.guedron@ird.fr) ; Numéro de téléphone (04 76 63 59 28). Signature:
Coordinateur(s) de projet	Jacques Gardon, HDR, épidémiologiste à l'Hydosciences Montpelier (HSM) ; Courriel (Jacques.gardon@ird.fr) ; Numéro de téléphone (+33 4 49 33 82 32). DABRE Djamilatou ; Doctorante en 2ème année de thèse à ISTerre France ; ACE-Partner (African Center Excelences) ; courriel (djamilatou.dabre@univ-grenoble-alpes.fr); Numéro de téléphone (+33743014049) Signature:
Partenaires	Abdoulaye TOURE et équipe Signature :
Responsable de l'évaluation sanitaire,	Jacques Gardon, HDR, épidémiologiste à l'Hydosciences Montpelier (HSM) ; Courriel (Jacques.gardon@ird.fr) ; Numéro de téléphone (04 67 14 90 32). Signature:
Durée de l'étude	Cette étude sera menée en automne et ne durera que 1 mois pour le prélèvement humain, mais les données seront utilisées pendant une thèse de doctorant qui durera 3 ans jusqu'en fin 2025.
Version et date du protocole	Version préliminaire du 18/12/2023

VI.2.1. Introduction

Depuis le milieu des années 2000, l'Afrique sub-saharienne connait une véritable ruée vers l'or (Chevrillon-Guibert and Magrin, 2018). En 2017, l'Afrique sub-saharienne est le second producteur aurifère du continent après l'Afrique du sud avec une production annuelle de 70 tonnes devant le Mali et le Burkina Faso (Chevrillon-Guibert and Magrin, 2018). L'Afrique de l'Ouest se situe désormais au troisième rang des zones les plus riches en terrains aurifères sur la planète, avec un sous-sol a une réserve d'or dépassant largement 700 tonnes d'or en Guinée Conakry (ITIE, 2020). L'extraction minière artisanale et à petite échelle d'or (EMAPE) consiste en l'utilisation des outils rudimentaires ou peu mécanisés par des petits groupes ou des individus pour extraire l'or des petits gisements (Hentschel et al., 2003). Pratiquée dans plus de 70 pays, l'EMAPE serait traditionnelle et historique en Guinée, puisqu'elle remonte au 9ème siècle où ces activités étaient déjà pratiquées en Haute Guinée, plus particulièrement dans le Bouré et le Séké souvent de façon saisonnière et complémentaire des activités agricoles (G.Sidam-Minorex, 1988; Mbodj, 2009). Depuis 2000, l'exploitation de l'or est devenue l'activité économique principale de la Haute Guinée, avec une production aurifère de 400 000 - 500 000 onces soit entre 12 et 15 tonnes/ans (PAGSEM and MMG, 2017). La Guinée occuperait le 7éme rang africain des producteurs d'or après l'Afrique du Sud, le Soudan, le Ghana, le Burkina, le Mali et la Tanzanie (PAGSEM and MMG, 2017). Selon une étude en Guinée, l'EMAPE impliquerait 3720 habitants par village minier dont 1336 femmes, 1009 hommes et 1375 enfants. La montée des cours de l'or et les difficultés économiques poussent des populations toujours plus nombreuses vers cette activité rémunératrice, dont les externalités négatives sur l'environnement et la santé sont peu évaluées. Les procédés d'extraction de l'or et les produits chimiques utilisés pour sa récupération entrainent des contaminations diverses et complexes impliquant des contaminants tels que le mercure (Hg), le cyanure (CN) mais aussi l'arsenic (As). Les risques sanitaires liés à l'EMAPE sont diverss et variés allant des risques chimiques (mercure, cyanure, arsenic, plomb) aux risques biologiques, biomécaniques, physiques et psychosociaux (Lennett and Gutierrez, 2014).

Depuis la convention de Minamata, de nombreux pays prennent des mesures concrètes pour réduire et, si possible, éliminer l'utilisation du mercure dans les processus d'EMAPE. Cependant, un coût faible, une utilisation facile et une grande disponibilité font de l'amalgamation au mercure la pratique privilégiée pour l'extraction minière artisanale et à petite échelle d'or avec une utilisation estimée à environ 1 600 tonnes par an. L'EMAPE est également considérée comme la plus grande source d'émissions anthropiques de mercure dans l'environnement (OMS, 2017) .

Revue documentaire

La première étape de l'évaluation de la situation sanitaire a consisté à passer en revue la littérature et les rapports disponibles concernant l'EMAPE en Guinée afin de synthétiser ce qui a déjà été fait du

point de vu épidémiologique. La revue de la littérature non seulement constituera la pierre angulaire de la base factuelle de l'évaluation, mais permettra en outre d'affiner les questionnaires. Les émissions de mercure proviennent de deux sources : les émissions naturelles et anthropiques. Celle naturelle provient de l'environnement lui-même et celles anthropiques sont de deux types dont les réémissions de mercure déjà présent dans l'environnement, résultant d'activités humaines antérieures et émissions directes provenant des activités humaines récentes. Ces émissions représentent respectivement 10% ; 30% ; 60% des apports de mercure dans l'environnement(PNU, 2002). En 2018, un inventaire national du mercure effectué en Guinée a permis d'identifier et de quantifier les apports ; émissions et rejets de mercure dans l'environnement Guinéen. Il a été ainsi montré que le secteur de l'EMAPE et industriel contribuait à environs 6450 kg aux apports de mercure dans la société Guinéenne. En effet, l'orpaillage (industriel et artisanal) contribuent à environs 2588 kg en apport de Hg/an dans l'air ; 2054 kg Hg/an dans l'eau ; et à 8752 Kg Hg/an dans les sols (MEEF and DNE, 2018). Ce mercure relargué dans l'environnement représente des risques sanitaires pour les populations environnantes. Dans cette étude les femmes enceintes et les enfants sont identifiés comme le groupe à risque (European Environment Agency, 2028). En effet, au XXIe siècle, il apparaît clairement que les membres des communautés vivant dans les zones contaminées sont exposés aux vapeurs de mercure, au mercure inorganique et au méthylmercure contenus dans les poissons et les aliments locaux. Mais ces effets du mercure sur la santé vont au-delà des poissons et des fruits de mer et la compréhension de ces contextes socio-environnementaux complexes nécessite des approches multidisciplinaires, intersectorielles et participatives. La biosurveillance humaine du mercure, telle que les mesures dans les cheveux, l'urine et le sang, est une mesure clé pour évaluer l'impact de l'ASGM. Des recherches épidémiologiques menées aux Seychelles, dans les îles Féroé, dans l'Arctique et en Amazonie ont établi des liens entre l'exposition au methylmercure au début de la vie et des effets néfastes sur la santé, en particulier sur le développement neurologique (Basu et al., 2023). Aux Iles Féroé, une étude a révélé des effets cognitifs à l'âge de 7 ans pouvant être associés à des expositions prénatales, qui pouvaient persister jusqu'à l'âge de 14 ans chez l'enfant (Grandjean et al., 1997). En Amazonie, l'exposition humaine au mercure est fortement associée à la consommation de poisson, car la forêt tropicale amazonienne a un potentiel de méthylation élevé. Ce qui montre bien que les voies d'exposition au mercure dépendent de l'environnement et de la spéciation du mercure. Par exemple au Burkina Faso, des études menées sur l'exposition au mercure ont révélés des taux anormalement élevés dans l'urine dont 69% des mesures dépassant l'indice biologique d'exposition de l'ACGIH (American Conference of Industrial Hygienists) (Tomicic et al., 2011).

Il est à noter que jusqu'à ce jour, les informations sur l'orpaillage en Guinée sont essentiellement données par le ministère des mines et de la Géologie de Guinée ainsi que le fond monétaire international (FMI), plus spécifiquement sur le potentiel minier et la production minière. Les données

concernant le volet émission de mercure et risque sanitaire est abordé plus particulièrement par de rares articles existants en Géochimie et le PAN. Selon l'inventaire National d'EMAPE en 2017-2018, 42 tonnes de mercure a été utilisé en Guinée dont 5 tonnes à Kouroussa et 18 tonnes à Siguiri qui est la potentielle région émettrice de mercure en Guinée. Selon la même étude, l'orpaillage a un impact sur la santé des Guinéen représentant notamment 20% des affection nerveuse due aux vapeurs de mercure, mais également la consommation de poisson car 60% de la population en consomme (MEEF, 2018). Pourtant, plusieurs études montrent un effet néfaste du mercure pour la santé humaine allant du mercure à sa spéciation dans le monde, ce volet est abordé superficiellement en Guinée par des enquêtes de terrain et les Sciences Humaines et Sociales. Nous ne sommes pas sans savoir que ces enquêtes de terrain par les questionnaires sont très subjectives et loin d'être objectifs comme des analyses d'échantillons réels en Géochimie et épidémiologie qui ne sont pas sans faiblesse bien sûr, mais donnent des résultats fiables qui peuvent être vérifiés par des standards internationaux.

Fondements de l'étude

Cette étude se base sur la convention de Minamata, du nom de la ville Japonaise de Minamata ayant connu un évènement d'empoisonnement au méthylmercure. Cette convention a été adoptée en 2013 dans le but de protéger la santé humaine et l'environnement contre les émissions et rejets anthropiques de mercure et de ses composés (Winkler et al., 2011) . Cependant, un problème ne peut être résolu sans avoir déjà conscience de son existence et de son ampleur. C'est dans ce cadre que s'inscrit ce projet de recherche basé sur l'évaluation des problèmes de santé liés au mercure dans les communautés d'extraction minière artisanale et à petite échelle d'or de la préfecture de Kouroussa en Guinée Conakry. Selon les textes intégraux de la convention de Minamata sur le mercure, du paragraphe 3(a) de l'Article 7, chaque Partie qui constate que les activités d'EMAPE menées sur son territoire sont non négligeables est obligée d'élaborer et de mettre en œuvre un plan d'action national (PAN) conformément à l'Annexe C de la convention. Pour ce faire, des études doivent être menées afin de confirmer ou pas l'état non négligeable des activités de l'EMAPE et de leurs dégâts en termes de santé humaine et environnementale. Cette étude aidera les instances gouvernementales à connaitre et prendre consciences du danger réel des activités de l'EMAPE avec des données concrètes et réelles épidémiologiques des communautés de 2 sites miniers à Kouroussa. Ainsi, des stratégies visant à prévenir l'exposition des populations vulnérables, des stratégies pour informer et protéger les mineurs travaillant dans l'extraction aurifère artisanale et à petite échelle et les communautés touchées pourront être élaborés. La protection humaine commençant par celle de l'environnement où elle vit, cette étude aidera également à mettre en place des systèmes pilotes de phytostabilisation afin de réduire l'impact environnemental de l'EMAPE. Cette présente étude consiste en une étude préliminaire épidémiologique pour déceler les niveaux d'exposition au mercure afin de disposer d'une

base factuelle initiale des taux de mercure chez les mineurs travaillant dans l'extraction aurifère artisanale et à petite échelle et leurs communautés. Ensuite ces informations vont ainsi permettre d'identifier les priorités et les interventions à intégrer dans la stratégie de santé publique de la Guinée Conakry. Cette étude n'a pas vocation à offrir un aperçu épidémiologique détaillé des impacts de l'EMAPE sur la santé, mais de juste faire un état des lieux de l'exposition humaine au mercure à Kouroussa où aucune étude de ce type n'existe encore. Car Kouroussa est la troisième préfecture en Guinée ayant une grande population minière préfectorale de 30750 et une grande utilisation de mercure de 5,317 tonnes après Siguiri et Mandiana d'après l'inventaire national d'EMAPE, 2017-2018.

Questions de recherche:

Quelles sont les connaissances, attitudes et pratiques de la population sur l'utilisation du mercure dans les sites d'extraction artisanale des mines à Kouroussa?

Quelles sont les niveaux d'expositions des populations au mercure sur les sites miniers à Kouroussa ?

Objectif Général :

Evaluer les niveaux d'exposition au mercure des populations travaillant dans l'extraction minière artisanale et à petite échelle d'or et leur communauté à Kouroussa.

Objectifs spécifiques :

Décrire l'ampleur de l'utilisation et l'exposition du mercure dans l'EMAPE, à travers leur mode de vie et leur alimentation (eau de boisson, poissons et crustacés, …).

Décrire les perceptions des mineurs et de leurs proches concernant les risques sanitaires associés à l'utilisation du mercure dans l'EMAPE.

Montrer les taux respectifs de mercure de chaque communauté pour les amener à changer leur pratique en adoptant des techniques plus sécurisées.

Analyse des vapeurs de Hg sur le terrain dans les zones de brûlage de l'amalgame afin de voir les niveaux de vapeurs de Hg potentiellement présent dans l'air de ces zones sera effectué.

Ces résultats permettront de mettre en place les lignes directrices de la sensibilisation des communautés de l'EMAPE par un retour à la population des niveaux de contamination au mercure. Cette étude sera complètement anonyme pour le respect de la vie personnelle.

VI.2.2. Méthodologie

Zone d'étude

L'étude sera mise en œuvre en Guinée, un pays dont les activités d'EMAPE menées sur son territoire sont non négligeables, faisant partie actuellement des grands producteurs mondiaux d'or. Le secteur Guinéen de l'EMAPE englobe des mineurs informels et sans qualification, ayant recours à des procédés et méthodes d'extraction de minerai artisanaux. Les régions pratiquant l'EMAPE sont généralement situées dans des zones rurales et isolées, en haute Guinée dans 5 préfectures dont Siguiri, Kouroussa, Mandiana, Dinguiraye et Kankan. Cette étude sera exactement menée à Kouroussa où une étude géochimique sur les taux de mercure dans 3 compartiments (eaux, sols et sédiment) a déjà été effectué en février 2023. Il s'agit d'une étude transversale, mesurant l'exposition chez des sujets impliqués dans les activités d'orpaillage et non impliqués, appartenant aux mêmes communautés. L'étude consistera à comparer les niveaux d'exposition et à décrire les facteurs de risques associés à l'exposition au mercure. Ainsi, une enquête par un questionnaire basé sur les habitudes nutritionnelles sera effectuée en plus des prélèvements de cheveux et d'urine et des taux de mercure dans l'air des endroits de brûlage du mercure. Cette triangulation méthodologique combinant différents types de données, montre un aspect efficace de cette étude en suivant le guide pas-à-pas de l'OMS sur l'évaluation de la situation sanitaire dans les EMAPE.

Les sites choisis sont présentés au Tableau 1.

Tableau VI-2. *Sites potentiels de l'étude en Guinée Conakry à Kouroussa*

État	Préfecture	Village	Mines	Observations
Guinée Conakry	Kouroussa	Samankoura	Saman	Utilisation accrue de mercure (Hg) par les mineurs, femmes (amalgamation ; brûlage) et Djatis (brûleurs du minerais). Taux de mercure dans les sols entre 2 et 8 mg/kg. THg eaux souterraines & surface entre 0,5-2,7ng/l. (compléter peut-être par l'EMAPE)
Guinée Conakry	Kouroussa	Dionko	Dionko	Utilisation directe de mercure sur le site minier par les orpailleurs. Taux de mercure dans les sols entre 2 et 16 mg/kg. THg eaux souterraines & surface entre 100-900ng/l.

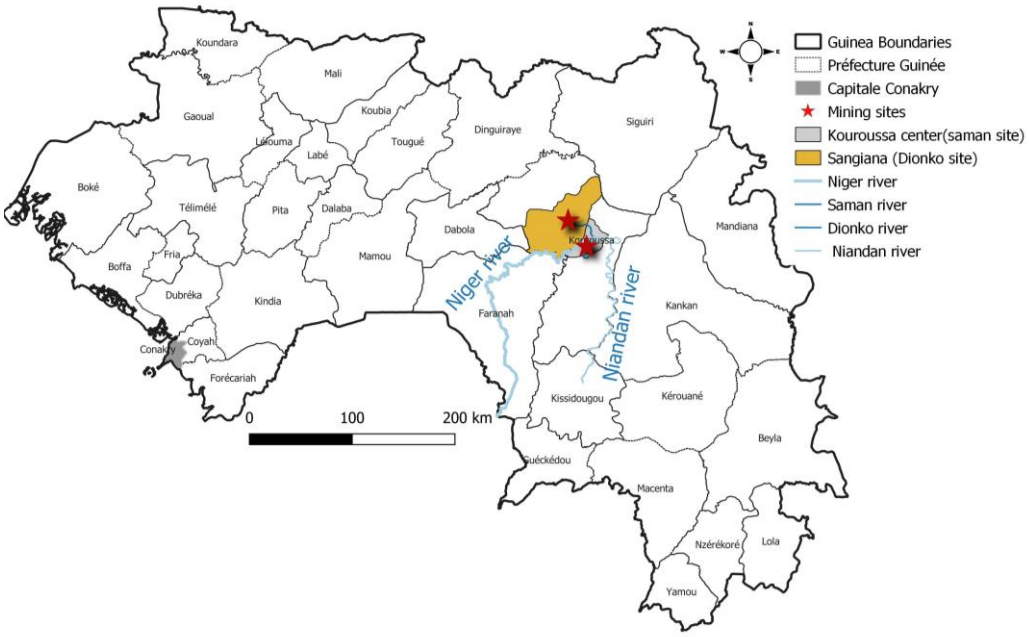


Figure 1. *Carte de la Guinée montrant les sites d'étude à Kouroussa. Source : Qgis réalisée par Djamilatou Dabré.*

Dans ces deux sites, il n'y a eu aucune étude préalable sur les communautés de l'EMAPE. Ces communautés ne vivent principalement que de l'orpaillage et de maraichage. L'agriculture est peu ou pas du tout pratiquée dans ces villages miniers. L'EMAPE étant presque le seul moyen de subsistance des populations à Kouroussa, les mineurs et artisans impliqués dans cette pratique ne portent aucun équipement de protection individuel augmentant ainsi les risques sanitaires.

Méthodes

Cette partie sera développée en fonction des deux questions de recherche

VI.2.3. Question 1 : Evaluer les connaissances, attitudes et pratiques de la population sur l'utilisation du mercure dans les sites d'extraction artisanale des mines à Kouroussa

Schéma d'étude :

Une étude transversale dans les différents sites d'extraction artisanale des mines à Kouroussa sera menée pour évaluer les connaissances, attitudes et pratiques de la population sur l'utilisation du mercure.

Période de l'étude :

Cette étude se déroulera sur un intervalle d'un (1) mois allant du 01 au 30 octobre 2024 auprès de la population des sites miniers des villages de Saman et Dionko dans la préfecture de Kouroussa.

Population d'étude :

Dans cette étude, seules les personnes présentes dans la région d'étude pendant au moins 6 mois seront éligibles pour participer aux questionnaires et aux prélèvements de sorte que les participants

aient été exposés suffisamment longtemps aux conditions locales. Ainsi, pour les exposées la sélection concernera le rang d'âge entre 18 et 75 ans avec une ancienneté de 1 an au moins dans l'orpaillage. Pour les témoins (non exposées), les mêmes conditions d'âge précédemment spécifiées s'appliquent. De plus ils ne doivent pas avoir participé à l'orpaillage depuis 10 ans et doivent être bien portant au moment de l'étude.

Un formulaire d'information détaillant les objectifs de l'étude et les méthodes employées sera remis aux participants et expliqué dans la langue de leur choix pour s'assurer d'une bonne compréhension des attentes de l'équipe et du déroulé de l'étude. Un formulaire de consentement, sera ensuite signé par les participants à l'étude. La confidentialité des participants sera maintenue en attribuant un code unique à chacun des participants.

Calcul de la taille d'échantillon

La taille des échantillons a été calculée en fonction d'une marge d'erreur et d'un intervalle de confiance selon la formule suivante :

$$n = \frac{tp^2 * \mathrm{P}(1-\mathrm{P}) * \mathrm{N}}{tp^2 * P(1-P) + (N-1) * y^2}$$

Avec :

- n : taille de l'échantillon.
- N : taille de la population cible (nombre de mineurs estimé) =1000 personnes
- P : proportion attendue d'une réponse de la population ou proportion réelle. Dans notre cas s'agissant d'une étude multicritère où aucune autre étude n'a été réalisée, elle est fixée à 0,5 par défaut, ce qui permet d'avoir le plus grand échantillon possible.
- tp : intervalle de confiance d'échantillonnage : dans notre cas on prendra 95% d'intervalle de confiance donnant un tp de 1,96 à considérer.
- y : marge d'erreur d'échantillonnage : nous prendrons une marge d'erreur de 5%.

Ainsi en effectuant le calcul nous obtenons un nombre total n=278 pour une population totale estimée à 1000 au départ dans les deux villages miniers.

Ainsi en se basant sur ce calcul, nous allons considérer une taille d'environ 150 personnes mineurs (hommes et femmes amalgameuses, laveuses et brûleuses) et environs 100 témoins (hommes comme femmes).

Variables d'étude :

Variable dépendante : Le niveau d'exposition des populations au mercure que nous nommons outcome sera décelé. Ce niveau sera annoté de non exposés ; moyennement exposé à très exposés.

Variables indépendantes :

Dans cette étude, plusieurs groupes de variable seront analysés :

Les caractéristiques sociodémographiques et professionnelles comprenant : le genre, l'âge, la profession, le statut matrimonial, la religion, le mode de vie, le niveau d'instruction.

Méthode de collecte :

Des entretiens individuels seront réalisés sur la base d'un questionnaire anonyme et standardisé qui seront pré testé avant de mener le travail sur le terrain. Le questionnaire comprendra : les caractéristiques socio-démographiques, la connaissance sur l'utilisation du mercure dans l'extraction minière artisanale d'or, les attitudes et pratiques dans les sites d'extraction artisanale de Saman et Dionko. Des assistants de recherche seront recrutés et formés sur l'objectif et les méthodes de l'étude afin d'assurer la cohérence et la fiabilité de la collecte des données. Le chercheur principal supervisera toutes les activités associées. L'instrument d'enquête sera initialement conçu en français, traduit en langue Malinké (par un natif de la région), puis retraduit en français par un autre traducteur pour s'assurer que la version traduite saisit correctement les questions. Les entretiens seront menés en Malinké, qui est la langue principale des enquêteurs et des personnes interrogées. Toutes les données de terrain seront enregistrées sur des fiches de données de terrain et seront saisies deux fois pour garantir leur exactitude. Les enquêtes se dérouleront au sein des maisonnées auprès des sujets, dans la rue et sur les sites d'extraction minières. Cette participation aux questionnaires sera bien évidemment libre et volontaire.

Analyses

Les données recueillies seront saisies et analysées à l'aide des logiciels Microsoft Office Excel 2019 et R Studio. Le nettoyage des données sera effectué en exécutant des fréquences pour chaque variable dans R Studio afin de vérifier les valeurs aberrantes, les incohérences et les valeurs manquantes. Des statistiques descriptives seront calculées pour obtenir les fréquences et les pourcentages qui seront présentés sous forme de tableau et figure. Pour l'analyse statistique, les niveaux de connaissances seront dichotomisés en bon et mauvais sur la base d'un seuil de 80 % du score total. La régression logistique sera utilisée pour analyser l'associations entre les co-variables et les niveaux de connaissances pour les deux seuils. Initialement, toutes les co-variables seront analysées séparément, et les variables avec $p \leq 0,20$ à cette étape seront incluses dans l'analyse multivariée. Les mesures d'association seront estimées par les rapports de côte (RC) avec leurs intervalles de confiance (IC) à 95 %. Toutes les « valeurs p » seront considérées comme statistiquement significatives à « $p < 0,05$ ».

VI.2.4. Question 2 : Quelles sont les niveaux d'expositions des populations au mercure sur les sites miniers à Kouroussa :

Schéma et Période de l'étude

Dans cette étude, nous allons évaluer le niveau d'exposition au mercure sur deux échantillons biologiques (urine et cheveux) ainsi que dans l'air du 01 au 30 octobre.

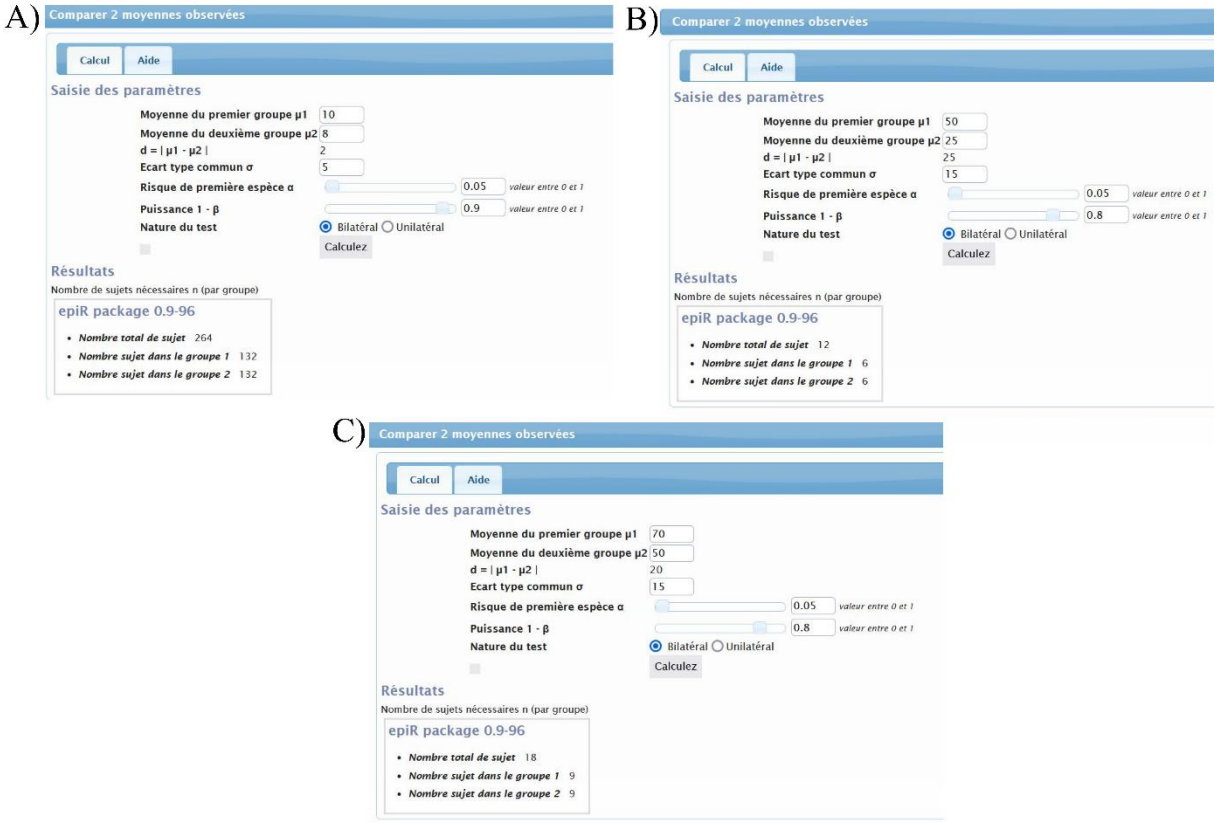
Calcul de la taille d'échantillon

Dans un souci de représentativité des échantillons, une analyse statistique a été effectué en fonction du nombre total de notre population étudiée estimé au cours de la première campagne géochimique

(février 2023). Pour ce faire la méthode basée sur le teste de comparaison de deux moyennes observées de BiostaTGV a été utilisée (https://biostatgv.sentiweb.fr/?module=etudes/sujets#) .

Cette méthode consiste à faire des hypothèses sur les moyennes attendues et leurs variances dans les groupes que l'on souhaite comparer pour en déduire le nombre de sujets nécessaires, tout en fixant les risques alpha et la puissance de l'étude. Avec une moyenne de 10µg/g Hg de cheveux dans le groupe exposé et de 8µg/g d'Hg dans le groupe non exposé, avec un écart type de 5, notre population totale doit être estimée à 264 au total pour un test Bilatérale. Ainsi la population à considérer doit être de 132 pour les mineurs et 132 pour les témoins (Figure. 2A).

Figure 2. *Taille d'échantillon extimée par la méthode Biosta*



Pour le méthylmercure, la population totale a été déterminée avec les niveaux d'exposition des orpailleurs au mercure mesuré dans les urines. Deux simulations ont été effectuées :

-Avec une moyenne de 50µg/g de créatinine pour les orpailleurs et 25µg/g de créatinine pour les témoins et un écart-type de 15 la population totale à considérer est de minimum 10 personnes (Figure.2B).

Ces chiffres changent considérablement lorsque la différence de moyenne est plus ou moins grande avec toujours le même écart-type (Figure.2.C). Ci-dessous la simulation

Ainsi, les simulations ci-dessus montrent que nous avons besoin de moins de 25 personnes dans la population totale pour mener à bien l'étude épidémiologique liée au méthylmercure dans les urines des orpailleurs. Ces chiffres s'inscrivent bien dans les 250 personnes à considérer pour toute l'étude épidémiologique.

Tableau VI-3. *Synthèse du nombre d'échantillon à considérer*

Participants	**Nombre de personnes**		**Total**
	Saman	**Dionko**	
Sous-préfectures	Kouroussa centre	Singuara	
Mineurs travaillant dans l'extraction minière artisanale et à petite échelle d'or (Homme comme Femmes laveuses, amalgameuses et brûleuses)	75	75	150
Périphériques des sites d'EMAPE : Hommes et femmes témoins (non mineurs)	50	50	100

Données à collecter:

Cheveux

Urines

Méthode de collecte:

Pour la collecte, les cheveux seront coupés par un ciseau en inox et mis dans une poche zip stérile. Les urines seront ensuite collectées dans des flacons traces en polypropylène de 15ml. Ces échantillons seront collectés dans les villages et sur les sites miniers de Saman et Dionko. Les urines seront traités en inactivant les bactéries pathogènes selon la méthode SODIS (Solar DISinfection), couplé à l'acidification avec du HNO3 suprapur à 3% pour détruire le potentiel biologique (3ml HNO3 dans 15ml d'urine) et mis immédiatement au frais (Antonini et al., 2012; Laur et al., 2021). Une autre méthode plus simple serait un ajout de TMAH (tétramethylammonium) dans les solutions biologiques d'urine, puis chauffé dans une étuve pendant 2h à 80°C (Cerqueira et al., 2024). Le dichromate sera ajouté aux échantillons d'urine pour stabiliser le mercure. Ces échantillons seront collectés au même moment que les questionnaires.

Circuit des échantillons

Les échantillons ainsi collectés et acidifiés pour détruire le potentiel biologique sur place seront rapidement mis dans des glacières frigorifiées de terrain puis acheminés rapidement dans la ville de Conakry. Ensuite ils seront acheminés à Grenoble en France au laboratoire de l'Institut des Sciences de

la Terre de l'université Grenoble-Alpes où ils seront analysés. Ces échantillons seront ainsi sans danger ni pour la personne qui collecte, ni pour la personne qui effectuera les manipulations au laboratoire.

A l'issue des analyses et après publication des résultats dans un délai maximum de 2 ans, les échantillons seront détruits.

Analyses :

Les analyses seront réalisées dans le laboratoire de l'Institut des Sciences de la Terre.

Analyses du mercure : Les analyses seront réalisées grâce à l'AMA 254 qui est un analyseur de mercure totale disponible à Isterre.

Analyses du methylmercure : Les analyses seront réalisées grâce à l'appareil Tekran 2700 disponible à Isterre.

Mesure de mercure dans l'air : L'analyseur de Mercure JEROME J405 de AMETEK sera utilisé pour mesurer les vapeurs de mercure dans l'air ambiant.

Activités de mobilisation et de sensibilisation des communautés

Il est primordial d'effectuer des activités de sensibilisation des communautés avant l'étude. Au vu des croyances traditionnelles de l'utilisation des cheveux et urine pour des pratiques de sorcelleries, il est important de rassurer la population des caractères scientifique de l'utilisation de ces échantillons et surtout de l'importance de cette étude pour leur santé et celle de leur descendance. Pour ce faire, nous allons d'abord par l'aide d'un guide et d'un natif de la région, présenter le projet pilote à la communauté concerné en commençant par obtenir l'autorisation de la préfecture de Kouroussa comme fait au précédant pour l'étude géochimique. Ensuite nous leur expliqueront la portée de l'étude (les motifs), le déroulement de l'étude (durée et période d'évaluation, processus de sélection des participants) et de son importance, ainsi que l'utilisation des données. Nous les rassurerons que ces données ne soient pas divulguées et ne seront utilisées que dans le cadre de cette thèse ainsi que dans l'élaboration du protocole sanitaire dans les pratiques de l'EMAPE. De plus, nous présenterons un descriptif des processus de collecte et d'utilisation des données, avec la garantie d'un anonymat entièrement préservé.

Respect des principes d'éthique

L'étude sera réalisée conformément au présent protocole et aux principes énoncés dans les lignes directrices d'éthique pour la recherche en matière de santé impliquant des participants humains élaborées par le Conseil des Organisations internationales des Sciences médicales (CIOMS) (Conseil des Organisations internationales des et al., 2016). Les lignes directrices suivantes seront suivies :

Dans un premier temps, le protocole d'étude initial sera soumis à l'approbation du Comité national d'éthique pour la recherche en santé (CNERS). Les procédures d'étude et les principes éthiques

présentés dans le protocole seront suivis dans les 2 sites étudiés. Les activités du projet ne pourront démarrer sur le terrain que lorsque le protocole d'étude, les formulaires de consentement et d'information des participants auront reçu l'approbation du CNERS. Ainsi, les procédures de terrain seront établies en collaboration étroite avec les partenaires institutionnels locaux (Pr Abdoulaye TOURE, pharmacien épidémiologiste en Guinée).

Protection des données, confidentialité et communication

Les formulaires de consentement seront complétés par les noms des participants mais ne seront associés à aucune photographie. Aucun nom ne sera divulgué dans le document ni les communications des résultats. À l'égard du souhait de l'OMS de promouvoir autant que possible la communication de données sanitaires, y compris de données épidémiologiques et de surveillance, le comité d'éthique et les instances gouvernementales doivent donner leur accord afin de publier les données, dépourvues de tout élément d'identification personnelle et de les mettre à la disposition de toute partie intéressée, sur demande (dans la mesure où elles n'auront pas, ou pas encore, été publiées par l'OMS) ("Lignes directrices d'éthique pour la recherche en matière de santé impliquant des participants humains, quatrième édition. Genève : Conseil des Organisations internationales des Sciences médicales et Organisation mondiale de la Santé," 2016), selon des modalités autorisant leur utilisation non commerciale et sans but lucratif à des fins de santé publique. Également d'utiliser, de compiler, d'agréger d'évaluer et d'analyser les données rendues anonymes et de publier les résultats obtenus grâce à ces données en rapport avec des travaux de l'OMS et conformément aux politiques et pratiques de l'Organisation. Une restitution des résultats sera faite aux communautés des sites d'orpaillage par des partenaires en Guinée avec l'appui de la chaire de santé publique et législation pharmaceutique après approbation du comité d'éthique

Impact et pertinence de l'étude

Caractère innovant et originalité de la contribution scientifique

Son caractère innovateur et original réside sur le fait que aucune étude de ce genre n'existe encore dans notre zone d'étude. Elle permettra de connaitre les niveaux d'exposition au mercure via la poussière et vapeur de mercure et au methylmercure via l'alimentation (poisson). Elle permettra ainsi de mettre en évidence la spéciation du mercure dans les écosystèmes aquatiques de ces sites et de confirmer les résultats géochimiques précédemment obtenus. Ces résultats serviront de base aux instances gouvernementales et sanitaires pour mettre en place la stratégie de santé publique et affiner leur plan d'action visant à protéger la santé humaine contre la pollution minière.

Pertinence scientifique et sociétale

Cette étude permettra de :

Comprendre les liens entre les mines, la santé et l'environnement dans les zones minières

Comprendre les facteurs de contamination liés au mercure et son ampleur sur les sites miniers en comparaison avec les témoins.

Formuler des recommandations allant dans le sens d'une exploitation minière qui s'inscrit dans le développement durable et qui protège à la fois la santé et l'environnement

Formuler des solutions alternatives et mesures d'atténuation des effets environnementaux et sanitaires

Budget et ressources pour le projet

Budget pour la collecte des données d'enquête et de relèvement épidémiologique				
Rubriques	**Nbre. Jours**	**Quantités**	**Prix Unitaire**	**Montant GNF**
Formation des enquêteurs				
Formation des enquêteurs				**860 000**
Collation (Petit-dej+Déjeuner)	1	4	100000	400 000
Outils de formation (Bloc-notes+Stylo)	1	4	40000	160 000
Transport participants (forfait)	1	3	100 000	300 000
Enquête terrain Saman et Dionko (Kouroussa)				
Outils de collecte				**8 800 000**
Impressions (Fiches d'information et consentement) Recto-verso (6 pages)	1	300	10 000	3 000 000
Location de tablettes	4	29	50 000	5 800 000
Location de véhicule et Carburant				**37 372 000**
Location véhicule	31	1	1 000 000	31 000 000
Carburant véhicule Conakry-Kouroussa Aller-retour	1	270	12 000	3 240 000
Carburant véhicule courses internes	29	9	12 000	3 132 000
Frais de séjour				**100 375 000**
Frais de séjour doctorant	31	1	800 000	24 800 000
Frais téléphonique doctorant	1	1	300 000	300 000
Connexion internet doctorant	1	1	260 000	260 000

Frais de séjour enquêteurs	31	3	800 000	74 400 000
Frais téléphonique enquêteurs	1	3	100 000	300 000
Connexion internet enquêteurs	1	3	105 000	315 000
Frais de terrain				**600 000**
Guide local	1	2	300 000	600 000
Total				**148007000**

Calendrier

Activités	Chronogramme											
	Année 2023				Année 2024				Année 2025			
	T1	T2	T3	T4	T1	T2	T 3	T4	T1	T2	T3	T4
Rédaction de protocole de recherche et obtention d'approbation éthique												
Collecte des données pour l'enquête et les échantillons de cheveux et d'urine												
Analyse des données de l'enquête et des échantillons de cheveux et urine												
Analyse, rédaction et soumission pour publication de l'étude des taux de mercure chez les populations vivants sur les sites d'extraction artisanale d'or à Kouroussa												
Restitution des résultats à la communauté												
Formations												
Ecriture et défense de la thèse												

PROFIL DES INVESTIGATEURS

Doctorante Djamilatou Dabre

MasterII en Hydroressources, Sciences de la Terre et des Planètes Environnement. Doctorante en Géochimie et Sciences de l'Environnement des Centres d'Excellence Africains. Très engagée dans la recherche dans le domaine des pollutions minières et ayant un très bon esprit d'équipe et une adaptabilité très facile.

Stéphane Guédron

Stéphane Guédron est chercheur en biogéochimie et paléoenvironnement à l'Institut de Recherche pour le Développement (IRD) au sein de l'Institut des Sciences de la Terre (ISTerre) - Université Grenoble-Alpes, France, depuis 2011. Il a obtenu son doctorat en géochimie environnementale en 2008 à l'Université de Grenoble (France), et a poursuivi par 3 années de post-doctorat à l'Institut Forel (Suisse), avant d'être recruté à l'IRD en 2011. Il a obtenu son HDR en 2021 à l'Université Grenoble Alpes.

Jacques Gardon

Médecin épidémiologiste de formation, je m'intéresse à la santé humaine en lien avec l'exposition aux éléments traces métalliques. Au cours des quinze dernières années, j'ai abordé plusieurs contextes, notamment l'exposition au mercure des populations riveraines des grands fleuves amazoniens, l'impact de la pollution métallique dans le contexte minier en Afrique et en Amérique Latine et l'imprégnation à l'arsenic des populations qui vivent dans des régions où l'eau est contaminée. Dans certains contextes, les études ont consisté en un simple diagnostic de situation pour préciser l'imprégnation afin d'évaluer le risque sanitaire. Dans d'autres, où un risque avait été identifié du fait de la présence de contaminants toxiques, nous avons conduit des études prospectives pour étudier le développement de l'enfant sur les aspects anthropométrique et psychomoteur. Très peu d'information est disponible en Afrique de l'Ouest sur les questions abordées dans cette thèse. Cependant, nous avons une première expérience acquise dans une étude pilote réalisée au Nord du Burkina Faso et interrompue pour des questions d'accessibilité.

Pr TOURE Abdoulaye

Abdoulaye Touré est un pharmacien épidémiologiste et professeur à l'Université Gamal Abdel Nasser de Conakry, en Guinée. Après des études en pharmacie, il poursuit une formation en France, obtenant un diplôme en VIH, puis deux masters en gestion des systèmes de santé et épidémiologie. En 2012, il soutient un doctorat en santé publique-épidémiologie. De retour en Guinée, il enseigne et recherche, collaborant avec l'ONG Solthis sur le projet OPP-ERA. Il a joué un rôle clé lors de l'épidémie d'Ebola de 2014 et cofonde le Centre de recherche et de formation en infectiologie de Guinée (CERFIG) en 2016. Entre 2018 et 2022, il dirige l'Institut national de santé publique de Guinée, contribuant à la réponse à la pandémie de Covid-19. En 2022, il participe à la création de la plateforme PRISME pour la recherche en santé mondiale et en 2023, rejoint le groupe technique de l'ANRS-MIE. En 2024, il devient membre correspondant de l'Académie des Sciences de Guinée et en 2025, lauréat du prix Christophe Mérieux.

VI.2.5. ANNEXE

NOTE D'INFORMATION DES PARTICIPANTS

Titre du projet : **EVALUATIONS DES NIVEAUX D'EXPOSITION AU MERCURE DES POPULATIONS TRAVAILLANT DANS L'EXTRACTION MINIÈRE ARTISANALE ET À PETITE ÉCHELLE D'OR ET LEUR COMMUNAUTÉ À KOUROUSSA**

RECHERCHE auprès des travailleurs des mines et population environnante

Introduction :

L'extraction artisanale des mines est une activité qui joue un rôle important sur le plan socio-économique. Cette pratique regroupe un grand nombre de personne de tout âge, de tout sexe et de toute origine. Le mercure est utilisé dans l'amalgamation de l'or et peut être à l'origine d'une exposition directe lors du brulage de l'amalgame suite à l'inhalation de vapeurs. Il peut également être le résultat d'une exposition indirecte, par l'ingestion de poissons si l'environnement est le siège de phénomènes de méthylation. Pour ce contaminant, nous proposons de doser le mercure élémentaire dans les urines, après une exposition chez les travailleurs et dans les cheveux, chez des travailleurs et des riverains du site d'orpaillage. Cette étude permettra de connaître les impacts de de l'utilisation du mercure sur la santé des communautés et surtout des personnes vulnérables et aidera les décideurs et les organismes de Santé Publique de mieux surveiller, prévenir et contrôler cet impact sanitaire.

Les objectifs de ce projet sont :

Principal:

Evaluer les risques pour la santé associés à l'exposition des travailleurs de la zone d'extraction artisanale des mines à la mercurielle à Kouroussa

Secondaires:

Evaluer les niveaux de connaissances, attitudes et pratiques de la population sur l'utilisation du mercure dans les sites d'extraction artisanale des mines à Kouroussa

Déterminer le niveau d'exposition des populations au mercure sur les sites d'extraction artisanales de l'or à Kouroussa.

Monsieur/Madame,

Aujourd'hui, nous aimerions vous inviter à participer à une enquête dans le cadre de cette étude sur la santé des personnes vivant dans les sites d'extraction artisanale des mines.

Ce document vous donnera des informations qui vous aideront à décider si vous voulez participer à cette étude ou non. Veuillez lire attentivement les informations suivantes. Si vous avez des questions, n'hésitez pas à les poser aux chercheurs dont les contacts sont à la fin du document.

Réalisation de l'entretien :

Cette étude cherche à connaître les risques de santé de la communauté liés à la pollution mercurielle dans les zones d'extraction artisanale des mines. Elle vise à évaluer les niveaux de connaissances

attitudes et pratiques lié à l'utilisation du mercure et à prélever des échantillons biologiques dont l'urine et les cheveux afin d'en déterminer les taux de mercure.
L'enquête sera réalisée par nous-même (enquêteurs) accompagné par un agent de santé suivant votre disponibilité à domicile.
Elle durera de 30 à 45 minutes et sera enregistrée de façon anonyme.

Qu'est ce qui se passe si je participe ?

La participation est entièrement volontaire. Elle consiste à prendre part à une enquête sur la santé de la population. En cas d'acceptation vous réaliserez un entretien individuel où l'on vous posera des questions concernant votre santé et votre mode vie.
Vous avez la possibilité de quitter l'étude à n'importe quel moment sans fournir d'explication, mais si le questionnaire est soumis, il n'y a pas de possibilité de retirer les données de l'étude car il n'y a pas de possibilité de repérer les données, car elles sont anonymisées.

Quels sont les risques de participation ?

Les risques de cette recherche impliquent le fait de donner des informations personnelles qui peuvent créer l'inconfort émotionnel et peut-être psychique. Mais les mesures prises sont le fait de répondre sous anonymat et de pouvoir se retirer de l'étude sans fournir d'explication.
Cependant la participation à l'étude pourra permettre de déterminer les niveaux d'imprégnation par le mercure des mineurs impliqués dans l'extraction artisanale et chercher des solutions pour y remédier.

Comment sera traitée l'information recueillie ?

L'information recueillie selon votre consentement seront gardées secrètes et anonymes pour être utilisées à des fins uniquement scientifiques. Tous les membres de l'équipe du projet seront tenus de respecter des règles strictes en matière de confidentialité, et vos données personnelles seront toujours gardées secrètes. L'utilisation commerciale de vos données ou le transfert des informations ne seront pas autorisés.
Les données seront collectées et stockées par l'ISMBG & Isterre. Elles seront partagées via un serveur sécurisé et protégé par un mot de passe. Le risque de vol et où de piratage sont très réduits par de nombreuses mesures de sécurité à savoir : le contrôle de l'entrée dans les bâtiments, le contrôle de l'accès aux ordinateurs, des règles sur le partage des données et d'autres moyens d'éviter la destruction ou la perte des données.
Dans le formulaire de consentement ci-dessous, vous trouverez plus d'informations sur vos droits concernant le traitement des données personnelles et le droit de retirer votre consentement à tout moment.

L'analyse des données sera réalisée par le chercheur principal *et par/en collaboration avec* les encadrants et les contributeurs.

Les résultats seront utilisés dans le cadre de la thèse et peuvent éventuellement être publiés.

Que dois-je faire si je veux participer ?

Veuillez lire la page suivante. Si vous acceptez de participer à l'étude, veuillez noter vos initiales et signer au bas de la page pour confirmer votre accord. Si vous avez des questions, n'hésitez pas à contacter un membre de l'équipe de recherche à la page 5 de ce protocole et présenté ci-dessous :

Type d'étude	Étude ayant recours à la collecte de de matériel biologique humain (cheveux et urines).
Investigateur principal	Pr TOURE Abdoulaye, Pharmacien épidémiologiste, et professseur titulaire en santé Publique à l'Université Gamal Abdel Nasser de Conakry en Guinée; courriel (abdoulaye.toure@ird.fr); Numéro de téléphone (00224 623 85 26 58)
Co-investigateur	Mr Guédron Stéphane, HDR, Géochimiste à l'institution de des Sciences de la Terre (ISTerre) ; Courriel (stephane.guedron@ird.fr) ; Numéro de téléphone (04 76 63 59 28).
Coordinateur(s) de projet	Jacques Gardon, HDR, épidémiologiste à l'Hydosciences Montpelier (HSM) ; Courriel (Jacques.gardon@ird.fr) ; Numéro de téléphone (+33 4 49 33 82 32). DABRE Djamilatou ; Doctorante en 2ème année de thèse à ISterre France ; ACE-Partner (African Center Excelences) ; courriel (djamilatou.dabre@univ-grenoble-alpes.fr); Numéro de téléphone (+33743014049)
Partenaires	Abdoulaye TOURE et équipe
Responsable de l'évaluation sanitaire,	Jacques Gardon, HDR, épidémiologiste à l'Hydosciences Montpelier (HSM) ; Courriel (Jacques.gardon@ird.fr) ; Numéro de téléphone (+33 4 49 33 82 32).
Durée de l'étude	Cette étude sera menée en automne et ne durera que 1 mois pour le prélèvement humain, mais les données seront utilisées pendant une thèse de doctorant qui durera 3 ans jusqu'en fin 2025.
Version et date du protocole	Version préliminaire du 18/12/2023

FORMULAIRE DE CONSENTEMENT

TITRE DU PROJET : EVALUATIONS DES NIVEAUX D'EXPOSITION AU MERCURE DES POPULATIONS TRAVAILLANT DANS L'EXTRACTION MINIERE ARTISANALE ET A PETITE ECHELLE D'OR ET LEUR COMMUNAUTE A KOUROUSSA

Merci de noter vos initiales dans chaque case :

Je confirme avoir lu et compris l'information ci-dessus et que j'ai eu la possibilité de poser des questions. ☐

Je comprends que ma participation est totalement volontaire et que je suis libre de sortir de l'étude à tout moment, sans avoir à fournir de raison et sans que mes soins de santé et mon droit légal soient affectés. ☐

Je suis d'accord sur le fait que toutes les informations que je fournis seront conservées, stockées et utilisées pour des recherches futures, sous réserve d'une approbation éthique ultérieure. ☐

Je comprends que l'ISMBG fera tous les efforts raisonnables pour garder mes données personnelles privées. J'ai reçu des informations claires sur la protection des données. ☐

Je donne mon consentement à l'utilisation éventuelle mais totalement anonyme de mes informations dans une thèse ou dans une publication. ☐

Je suis d'accord pour participer à l'étude. ☐

Signature (participant)_____	Signature (investigateur)_____
Date_____	Date_____
Nom_____	Nom_____

Questionnaire individuel

Annexe 1 : Fiche de recueil des données de l'étude

Date de remplissage du formulaire (jj/mm/aaaa)	____/____/_____/
Nom complet de l'enquêteur	_____
Nom du district	
Caractéristiques socio-démographiques	
Q1. Sexe	☐ Masculin ☐ Féminin
Q2. Date de naissance (jj/mm/aaaa)	___/___/_____/ □ Ne sait pas (Recueillir l'âge révolu) : ____/
Q3. Situation Matrimoniale	☐ Célibataire ☐ En couple ☐ Marié (e) ☐ Veuf (ve) ☐ Divorcé (e)
Q4. Profession	☐ Mineur ☐ Commerçant ☐ Cultivateur ☐ Fonctionnaire ☐ Eleveur ☐ Ménagère
Q5. Niveau d'instruction	☐ Non scolarisé ☐ Primaire ☐ Secondaire ☐ Universitaire
Q6. Provenance	☐ CEDEAO ☐ Guinéen: ☐ Autochtone ☐ Nationaux
Q7. Religion	☐ Sans religion ☐ Féticheur ☐ Chrétien ☐ Musulman
Connaissances sur l'orpaillage et le mercure	
Q1. Connaissez-vous l'orpaillage ?	☐ Oui ☐ Non ☐ Ne sait pas

Q2. Depuis combien d'année pratiquez vous l'orpaillage	☐ 1an ☐ 2ans ☐ > 3 ans ☐ 10 ans ☐ Ne sait pas
Q3. Combien d'heure travaillez-vous par jour ?	☐ 7h ☐ <7h ☐ >7h ☐ Ne sait pas
Q4. Combien de jours travaillez-vous par semaine ?	☐ <5 ☐ >5 ☐ 7 ☐ Ne sait pas
Q5. Pratiquez-vous une autre activité rénumératrice ?	☐ Non ☐ Oui ☐ laquelle?()
Q6. Mangez-vous des produits de la pêche ?	☐ Non ☐ Oui ☐ Ne sait pas
Q7. Si oui lesquels ?	☐ poisson ☐ autres ☐ Ne sait pas
Q8. Combien de fois mangez-vous du poisson par jour ?	☐ 1 ☐ 2 ☐ 3 ☐ jamais
Q9. Mangez-vous des légumes racines ?	☐ igname ☐ Manioc ☐ Carotte ☐ pomme de terre
Q10. Savez-vous ce que c'est que le mercure ?	☐ Non ☐ Oui ☐ Ne sait pas
Q11. Utilisez-vous le mercure ?	☐ Non ☐ Oui ☐ Ne sait pas
Q12. Avez-vous déjà été en contact avec le mercure ?	☐ Non ☐ Oui ☐ Ne sait pas
Q13. L'Utilisez-vous dans l'amalgamation ?	☐ Non ☐ Oui
Q14. Faites-vous le brûlage de l'amalgame ?	☐ Non ☐ Oui
Q15Combien de fois l'utilisez-vous par jour ?	☐ 1 ☐ >1 ☐ Noter le nombre
Q16. Quelle quantité de mercure utilisez-vous par jour ?	☐ 1ml ☐ >1ml ☐ Noter la quantité
Q17. Le mercure est-il dangereux ?	☐ Oui ☐ Non ☐ Ne sait pas
Q18. Le mercure peut se retrouver dans le sang les cheveux et l'urine ?	☐ Non ☐ Oui ☐ Ne sait pas
Q19. On peut être exposé au mercure par inhalation ?	☐ Non ☐ Oui ☐ Ne sait pas
Q20. Savez-vous qu'on peut utiliser le mercure et le condenser sans le libérer dans l'air ?	☐ Oui ☐ Non
Q21. Le mercure est-il dangereux pour les animaux aquatiques ?	☐ Oui ☐ Non ☐ Ne sait pas

Appendix 3

VI.3. Appendix 3 : Article on master's thesis work: “Source, fate, and budget of mercury species in the high-altitude watershed of a fast-developing Andean city (El Alto, Bolivia)”

Science of the Total Environment 998 (2025) 180239

Contents lists available at ScienceDirect

Science of the Total Environment

journal homepage: www.elsevier.com/locate/scitotenv

From mine to lake: Source, fate and budget of mercury species in the high-altitude watershed of a fast-developing Andean city (El Alto, Bolivia)

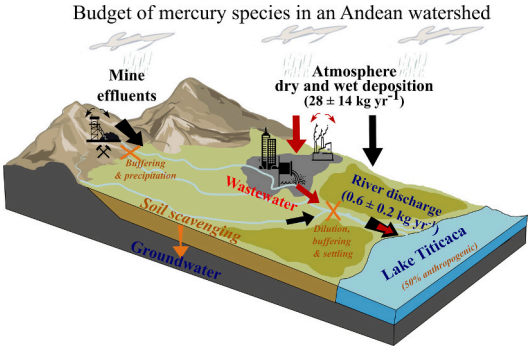
Stéphane Guédron [a,b,*], Djamilatou Dabre [a], Céline Duwig [c], David Amouroux [d], Jonathan Fin [a], Sylvain Campillo [a], Romain Biron [c], Hélène Guyard [c], Emmanuel Tessier [d], Isabel Moreno [e], Jimena Yupanqui [b], Gaëlle Uzu [c], Dario Acha [f]

[a] Univ. Grenoble Alpes, Univ. Savoie Mont Blanc, CNRS, IRD, UGE, ISTerre, 38000 Grenoble, France
[b] Instituto de Investigaciones Quimicas (IIQ), Universidad Mayor de San Andrés, 303 La Paz, Bolivia
[c] Univ. Grenoble Alpes, IRD, CNRS, UGA, INP, INRAE, IGE, 38000 Grenoble, France
[d] Univ. de Pau et des Pays de l'Adour, E2S UPPA, CNRS, IPREM, Institut des Sciences Analytiques et de Physico-chimie pour l'Environnement et les Matériaux, Pau, France
[e] Laboratorio de Física de la Atmósfera (LFA), Universidad Mayor de San Andrés, 303 La Paz, Bolivia
[f] Instituto de Biología, Laboratorio de Calidad Ambiental (LCA), Universidad Mayor de San Andrés, 303 La Paz, Bolivia

HIGHLIGHTS

- Mercury (Hg) speciation was assessed in several compartments of an Andean watershed.
- Atmospheric fallout and gaseous deposition are major sources of Hg species for soil.
- Hg contamination is restricted to the mining area.
- Urban wastewaters dominate (methyl-) Hg fluxes to the lake through the Katari River.
- Lake Titicaca sediment allows the reconstruction of historical urban Hg discharge.

GRAPHICAL ABSTRACT



ARTICLE INFO

Keywords:
Mercury species budget
High-altitude Andean watershed
Soil, river, atmosphere and lake

ABSTRACT

The rapid growth of cities and mines in developing countries has a major impact on the environment, through the discharge of untreated wastewater and mining waste. In the high-altitude tropical Andes, the Katari watershed combines a fast-developing urban area, upstream mining sites, and a downstream agricultural area, which are drained by the Katari River to Lake Titicaca. To assess the respective contribution of these areas to the watershed mercury (Hg) budget, Hg and monomethyl-Hg (MMHg) were measured in soil, sediment, surface water, groundwater, and the atmosphere (airborne fallout and total gaseous Hg). Further, two well-dated sediment cores collected in Lake Titicaca were used to reconstruct Hg accumulation rates over the last centuries. From instrumental river discharge, air and rainfall monitoring, the contribution of Hg originating from the atmosphere and the river was assessed. Results show that the mining area is a locally restricted main Hg hotspot. Although less contaminated, the urban area is the main source of MMHg for surface water through wastewater discharge,

* Corresponding author at: Univ. Grenoble Alpes, Univ. Savoie Mont Blanc, CNRS, IRD, UGE, ISTerre, 38000 Grenoble, France.
E-mail address: stephane.guedron@ird.fr (S. Guédron).

https://doi.org/10.1016/j.scitotenv.2025.180239
Received 28 March 2025; Received in revised form 15 July 2025; Accepted 7 August 2025
Available online 20 August 2025
0048-9697/© 2025 Elsevier B.V. All rights are reserved, including those for text and data mining, AI training, and similar technologies.

and the atmosphere the main source of total Hg through particulate and gaseous Hg emissions. Total Hg inventories in lake sediment from a bay at the outlet of the watershed show that at least one half of the Hg input originated from the river discharge, the rest being deposited from the atmosphere. The increasing development of the urban area without improvement of wastewater treatment implies that river discharge will be a source of Hg for the lake for many years.

1. Introduction

The rapid demographic growth of large cities in developing countries over the last decades is accompanied by numerous issues related to water resources management (Jury and Vaux Jr., 2005). Urban growth is generally linked to industrial and mining development that generates wastewater discharges to aquatic ecosystems with low or non-existent levels of wastewater treatment strategies. In megacities of Latin America and Asia (e.g., Mexico City or Hô Chi Minh City), the combination of such anthropogenic discharges has resulted in the polymetallic and organic contamination of surrounding ecosystems combined with eutrophication issues, both generating public health problems (Guédron et al., 2014a; Strady et al., 2016, 2017). Combustion processes (e.g., domestic, industrial and traffic) also release contaminants into the atmosphere, which disperse contaminants regionally or return to the local ground through dry and wet depositions. Amongst released pollutants, mercury (Hg) is one of the three most harmful highlighted by the WHO (2018) known for its adverse effects on the environment and human health especially under the methylmercury form (Fitzgerald and Clarkson, 1991).

To assess such contamination, direct measurements and monitoring of Hg speciation in precipitation, groundwater and river is needed to quantify Hg fluxes on a daily or monthly scale. Such approaches also provide information on the modes of transport and deposition and the species involved. As a complement to direct measurements, lake sediment records important information about historical natural and anthropogenic Hg emission from both the atmosphere and the lake catchment, and provide an archive of historical changes in the mine, industrial and urban discharge of Hg to the environment (Cooke et al., 2020). Therefore, the analyses of Hg from sediments can provide an insight into the temporal trends of Hg accumulation in lake ecosystems.

Recent studies in the Lake Titicaca region (Bolivia/Peru, South America) have shown evidence that human induced eutrophication of high-altitude lakes (above 3500 masl) of the altiplano (Heredia et al., 2022) has provoked the enhancement of mono-methylmercury (MMHg) production and accumulation (Achá et al., 2018; Alanoca et al., 2016; Guédron et al., 2020a, 2020b, 2017) through the increase in activities of methylating organisms and the decrease of MMHg photodegradation by water opacification (Bouchet et al., 2022). In addition, the recycling of atmospheric Hg has been proposed as one of the main Hg sources for these aquatic ecosystems (Guédron et al., 2018; Jiskra et al., 2022). This likely supports that enhanced local and regional anthropogenic atmospheric Hg may rise Hg levels in terrestrial and aquatic environments. Aside from the comprehensive inventory of Hg speciation levels including inorganic Hg(II), elemental Hg (Hg0) and MMHg, in the different compartments of Lakes Titicaca and Uru-Uru, to date there is no data on the levels of total Hg (THg) and MMHg in river, groundwater and rain in the watershed of these lakes.

To document these compartments, we studied the Katari watershed, which combines an upstream mining area, a fast-developing urban area, and a downstream agricultural area, which are all drained by the Katari River to Lake Titicaca. Hence, the first objective of this study was to quantify the concentrations and fluxes of Hg and MMHg present in the watershed, with the aim of assessing the relative contribution of anthropogenic activities (e.g., mining and urban) and natural processes implied in the Hg fluxes to watershed. For this purpose, Hg and MMHg concentrations and fluxes were monitored at the scale of the watershed through flood monitoring (surface water and particles) conducted in 2015 and 2016, together with atmospheric total gaseous Hg, and Hg speciation in atmospheric fallout, groundwater, soil and sediment. The second aim of this study was to document Hg historical fluxes from the Katari watershed to Lake Titicaca, through the use of well-dated sediment archives. The combination of these sediment records with instrumental record of the river discharge and precipitation monitored since the 1990s, allows to reconstruct annual Hg sedimentary and atmospheric fallout fluxes to the lake, and to provide an Hg speciation budget at the scale of the watershed.

2. Material and methods

2.1. Study site and environmental settings

The Katari catchment (2022 km^2) is located southwestern part of Lake Titicaca (Bolivia, Fig. 1), covers a large range of altitude from 4600 to 3810 masl, and drains more than thirteen municipalities including El Alto, the largest city in Bolivia accounting for more than >1.2 million inhabitants in 2020 (INE, 2024).

The Katari River is the main stream of the watershed, supplied by several tributaries listed hereafter (Fig. 1). Upstream El Alto city, the Seke and Seco rivers have their sources in the Cordillera Real. Then, the Seke Rivers drains the Milluni mining area (sites M in Fig. 1), which is impacted by acid mine drainage, and contributes to the polymetallic contamination of the surface waters (Archundia et al., 2017; Salvarredy-Aranguren et al., 2008). The Milluni area has been exploited during more than a century mainly for Tin (Sn) extraction with a known peak of activities in the 1970–1980s (Ríos, 1985). Downstream, both the Seke and Seco Rivers flow through the city of El Alto, an urban-industrial area (sites U in Fig. 1) accounting for more than 5000 industries [metallurgical, paint and tannery, food, laundries and dry cleaners (Poupeau and Hardy, 2016)]. The majority of wastewater from this industrial area is discharged directly into the environment, and less than 50 % of the wastewater (rate of ~500 L s^{-1}) is treated by the Puchukollo wastewater treatment plant (WWTP; site U3 in Fig. 1). The inefficiency of this WWTP, leads to the direct discharge of wastewater into surrounding soils and rivers (Archundia et al., 2017). Downstream El Alto city, the Seco River flows south through the city of Viacha, which hosts a cement factory (site CF in Fig. 1), and joins the Seke River to form the Palina River, which flows into the Katari River. In the downstream part of the watershed, the Katari River flows into the Cohana Bay, a eutrophic bay in the southern part of Lake Titicaca (Heredia et al., 2022).

2.2. Sampling strategy and sample preparation for chemical analysis

2.2.1. Soil profiles

Nine soil profiles were collected in 2017 along a transect from the upstream part of the Milluni Valley to the Lake Titicaca shores (Table S1). For each location, pedological pits were dug to characterize and collect the main soil horizons (Archundia et al., 2019). Soil samples were collected in plastic bags, homogenized on site and sieved at 2 mm to collect and weigh the coarse and fine soil fractions. The fine fraction below 2 mm was then freeze-dried and crushed to obtain a fine powder <63 μm for chemical analysis. The soil profiles are described in Archundia et al. (2021), including basic properties (mineralogy, texture, organic carbon, total nitrogen and iron oxide content).

2.2.2. Atmospheric fallout, river, and groundwater collection

Atmospheric fallout depositions were collected at 7 stations (Fig. 1) along the transect using 35 cm HDPE rain gauges covered with an opaque cover to prevent biological development. Samples were collected during the 2014/2015 and 2015/2016 rainy seasons (i.e., December to April), every 2 weeks. Additional fallout samples were collected after single rain events, at sampling stations L3 and A3, for comparison with samples collected after two weeks. River water samples were collected in May 2015 along the entire river network (Fig. 1). From March 2015 to the end of February 2016, the Katari river was sampled at the A3 hydrological station to document the rainy season floods. Katari River was gauged using a hydrological radar to provide a water height – flow relationship (Loayza Farrachol, 2022). Sample collection was performed with an automatic collector (ISCO 3700 sampler) into 500 mL polyethylene vials. Sample collection was parametrized with the water level to collect samples during river floods. Groundwater samples were collected at 7 locations in the watershed (Fig. 1 and Table S2) using an electrical water pump equipped with acid washed silicon tubing in wells used for irrigation or water supply for local inhabitants.

All containers for atmospheric fallout and river water collection were previously acid washed (HNO_3, 10 %, v/v) for 48 h. All water samples (filtered and unfiltered) for Hg speciation measurements were collected and stored in acid-washed FEP Teflon containers following ultra-trace procedures (Cossa et al., 1995). Groundwater samples were filtered on site with 0.45 μm membranes (PVDF, Millex). Fallout and river samples were filtered in the laboratory at 0.45 μm with 47 mm membranes (PVDF, durapore) in FEP filtration systems to recover the filtered solution and suspended particles. Samples for Hg speciation were acidified with HCl (0.5 %, v/v, Ultrex grade - Baker). Samples for filtered major and trace element analysis were stored in 15 mL PTFE vials and acidified with HNO_3 (2 %, v/v, Ultrex grade - Baker).

For atmospheric fallout samples, suspended solids (SS) collected on PVDF filters were freeze-dried and stored in petri dishes until analysis. Due to high suspended solids loads in river samples, collected samples were left to settle for a few hours in the laboratory, protected from light. The supernatant was then collected and filtered at 0.45 μm as described above. Settled coarse particles were then collected and frozen for freeze-drying, before being weighed and grind. The respective masses of the settled coarse fraction (defined in the manuscript as coarse suspended solids: SSC) and the fine fraction collected on the filter (fine suspended solids: SSF) were determined by weighing.

2.2.3. Sediment core collection

Two ca. 70 cm-long sediment cores, were collected with a Uwitech gravity corer few km from the Katari River outlet within the Cohana Bay (core W7) and in the shallow water of the eastern part of the Lake close to Huatajata (Core E6, Fig. 1) for historical THg reconstruction. All information for core collection, slicing, dating with short-lived radionuclides (^{210}Pb, ^{137}Cs), and age-depth model are published elsewhere (Guédron et al., 2023).

2.3. Elemental analysis

Mercury speciation analysis in solution was performed within two weeks after collection in the Laboratory of environmental quality (LCA, La Paz, Bolivia). Same analysis for solids (filters, soil and sediment) was performed within 6 months after collection in the LCA or in the analytical chemistry platform of ISTerre (OSUG-France).

Total mercury (THg) analysis in solids was determined by atomic absorption spectrophotometry (AAS) with an automatic Hg analyzer (Altec, model AMA 254) following a published procedure (Guédron et al., 2009). Concentrations obtained for repeated analyses of certified reference materials (CRMs) never exceeded the published range of concentrations for Mess-3 (mean ± SD = 90 ± 2 ng g^{-1}, $N = 13$; certified

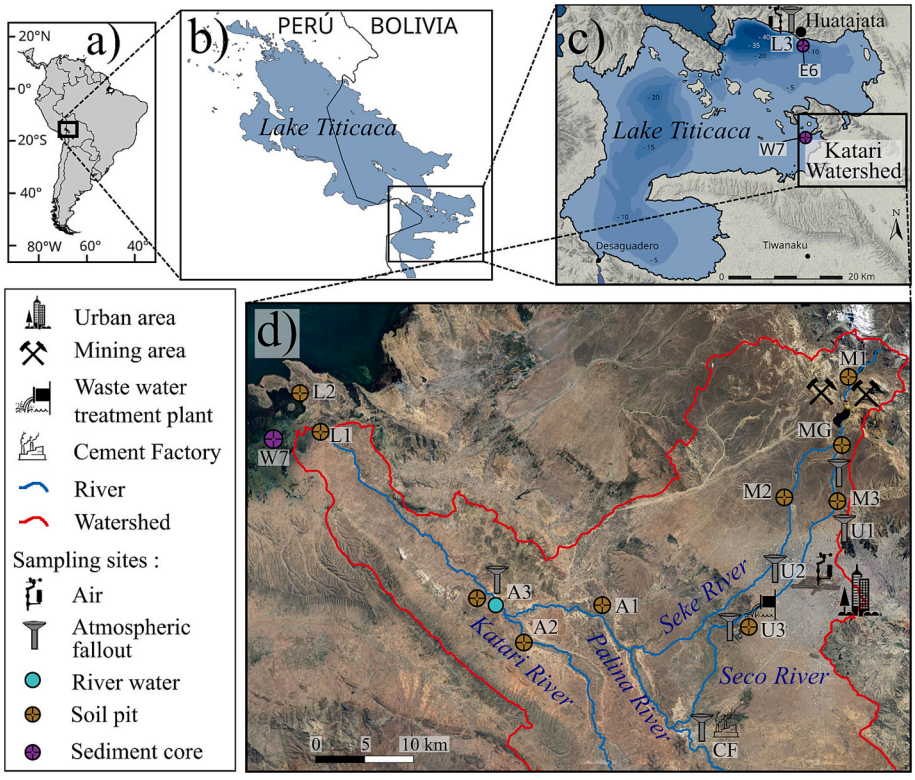


Fig. 1. Map of the geographical location of the Rio Katari in Bolivia, South America (a), in the southern part of the Lake Titicaca (b). Panel c) indicates the location of the Katari watershed and the sediment cores W7 (Cohana Bay) and E6 (Huatajata), and panel d) is a detailed map of the Katari watershed, with all sampling locations along the stream from the upstream mining area of Milluni (M), through the El Alto/La Paz urban area (U), the lower Katari agriculture plain (A), to the littoral area of the lake (L). All details for sampling sites are provided in Table S1.

value: 91 ± 8 ng g^{-1}), BCR 277 (126 ± 8 ng g^{-1}, $N = 7$; certified value: 128 ± 17 ng g^{-1}) and ERM-CC-141 (85 ± 5 ng g^{-1}, $N = 4$; certified value: 83 ± 17 ng g^{-1}). All samples were duplicated providing a residual standard deviation below 5 %.

Filtered (F) and unfiltered (UNF) THg in waters were determined by cold vapor atomic fluorescence spectrometry (CV-AFS) after conversion of all mercury species into Hg0 followed by detection using a Tekran® (Model 2500) (Bloom and Fitzgerald, 1988; Cossa et al., 2009; Guédron et al., 2015). Filtered and unfiltered mono-methylmercury (MMHg) concentrations were analyzed using an ethylation purge and trap gas-chromatograph-AFS analyzer (MERX System, Brooks Rand® or Tekran, model 2700). The detection limit (DL) defined as three time de SD of 25 blanks was 0.01 ng L^{-1}. For solids, MMHg was extracted from filters or from ~100 mg of solid samples (i.e., topsoil, sediment, or coarse suspended solids) with 5 mL HNO_3 (6 N) at 60 °C for 12 h (Guédron et al., 2020b, 2014a). Digestion aliquots were then analyzed in duplicates and quantified using the standard addition technique. Concentrations obtained for repeated analyses ($N = 10$) of certified reference materials (CRMs) never exceeded the published range of concentrations for IAEA-158 (Av. ± SD = 1.69 ± 0.13 ng g^{-1}, certified value: 1.41 ± 0.40 ng g^{-1}) and IAEA-405 (5.87 ± 0.57 ng g^{-1}, certified value: 5.50 ± 0.75 ng g^{-1}).

Total gaseous mercury (TGM) analysis in air was performed with a Tekran® (Model 2537) at three locations and altitudes in the urban La-Paz-El Alto and lake Titicaca regions, including i) the shore of Lake Menor (Huatajata, 3808 masl, from April 20th to May 1st 2014, and from October 6th to 18th 2014); ii) the El Alto airport weather station (El Alto, 4062 masl, from October 11th to 19th 2014), and iii) the UMSA Cota Cota Campus (La Paz, 3390 masl, from August 21st to September 12th 2014).

Dissolved organic carbon concentrations (DOC) were determined using a Non-Dispersive Infra-Red (NDIR) CO_2 Shimadzu® (Model VCSN) spectrometer after humid oxidation in a sodium persulfate solution at 100 °C. Organic carbon (C_{org}) and its isotopic composition ($\delta^{13}C_{org}$) in solids was measured after removal of the carbonates via aqueous acidification by Cavity Ring-Down Spectrometer (Picarro, Inc.®) coupled with Combustion Module (Costech, Inc.®) (CM-CRDS) using previously reported analytical methods, calibration, and sample preparation (Guédron et al., 2019; Heredia et al., 2022).

Major elements (S, Fe, Al, Ti, Ca and Mg) and trace metal(loid)s (Pb, As, Cr and Cu) analysis in solids were analyzed after acid digestion with 10 mL of a mixture of pure acids (HF/HCl/HNO_3, 1:6:2), sonicated for 2 h, and heated on a hot-block (120 °C, 4 h) following a published procedure (Guédron et al., 2021). Concentrations obtained for repeated analyses of CRMs never exceeded the published range of concentrations for SLRS-4 (Guédron et al., 2024). Major and trace metal analysis in solution and solids was performed by inductively coupled plasma optical spectrometer (ICP-OES, Varian 720-ES) within the analytical chemistry platform of ISTerre (OSUG-France).

2.4. Statistical analysis

Because the geochemical data were not normally distributed, the following parameters are reported in the manuscript: mean, and standard deviation (SD) or standard error on the mean (SEM), and the number (N) of observations (Webster, 2001). Data are presented as mean ± SD when N is small (≤6), and as mean ± SEM for higher N values with large data dispersion in order to better represent the dispersion of data and better indicate the reliability of the mean estimates. Non-parametric Mann–Whitney rank sum test (*U* test) and Kruskal–Wallis one-way analysis of variance on ranks (H test) were used to compare two or more than two data sets, respectively. Pearson correlations were applied to compare multiple data set pairs. Correlation coefficient (R^2) and *p* values (p) are reported. All statistical analysis was performed with the Sigmaplot 15.0 package.

2.5. Historical sediment reconstruction, river and wet deposition flux modelling

Historical reconstruction of Hg accumulation rates (HgARs) in sediment cores were performed by multiplying the Hg concentrations by the sedimentation rate and the sediment dry bulk density (Guédron et al., 2019). Historical modelling of Hg inputs from the Katari River and from wet depositions over the watershed was reconstructed from instrumental monitoring data provided by the Servicio Nacional de Meteorología e Hidrología de Bolivia (INE, 2024; SENAMHI, 2024). Historical Hg fluxes from the Katari River were modelled from the instrumental record of the river discharge since 1992, and the relationship obtained between THg flux and water discharge of this study. Historical atmospheric wet depositions of Hg were modelled from the annual precipitation recorded at El Alto from 1990 onward, multiplied by the average Hg concentrations in fallout depositions of this study. All details are given in Section 3.6, and in Supplementary Information.

3. Results and discussion

3.1. Point source mercury contamination in soils of mining district

Mean THg levels in soil profiles of the Katari watershed downstream the Milluni area (Fig. 2) are low (mean ± SEM = 26 ± 3 ng g^{-1}), and within the world geochemical baseline for pristine environment (Guédron et al., 2013, 2014b; Zhang et al., 2013). Highest THg concentrations are found in top-soils of the upstream Milluni mining area, where concentrations reached up to 766 ng g^{-1} at station M2. Downstream, littoral soil profiles show little variation of THg with depth, whereas agricultural soils exhibit baseline values in top-soils with a slight in-depth increase below the till layer. In both littoral and agricultural soil profiles, with the exception of the L1 top-soil sample, THg is found positively correlated with C_{org} ($R^2 = 0.70$, $p < 0.01$), and S ($R^2 = 0.69$, $p < 0.01$, Fig. S1) supporting the organic matter (OM) sulfur functional groups as a major carrier phase of Hg (Skyllberg, 2012). Both agricultural and littoral soils show large variability in $\delta^{13}C_{org}$ (i.e., from −19.9 to −25.6 ‰) and S (i.e., from below 0.1 to 1.4 mg L^{-1}, Fig. S1), indicating different sources and quality of OM, for which Hg affinity is reported to vary (Guédron et al., 2020b; Hammerschmidt et al., 2008). The urban soil profile collected on the wastewater treatment plant (WWTP) site only shows a surface Hg enrichment (Fig. 2), which suggests little in-depth Hg transfer. In the upstream mining area, the rapid downstream decrease of soil THg concentrations indicates point source contamination within the mining area, where Hg is potentially hosted by various carrier phases including OM, sulfides and iron (Fe) oxides reported to be the main metal carrier in the Milluni Valley (Salvarredy-Aranguren et al., 2008).

Methylmercury concentrations in topsoil are relatively low (Fig. S1), and decrease from the Milluni mining area (mean ± SEM = 0.56 ± 0.06 ng g^{-1}) to urban (0.17 ± 0.09 ng g^{-1}) and the agricultural and littoral areas (0.12 ± 0.02 ng g^{-1}), which represents 0.52 ± 0.34 % of THg for all the samples ($N = 9$). Consistently with THg, MMHg in topsoil is also found positively correlated with C_{org} ($R^2 = 0.74$, $p < 0.01$), and S ($R^2 = 0.81$, $p < 0.01$, Fig. S1) supporting its binding onto OM sulfur functional groups.

3.2. Atmospheric total gaseous mercury at urban and lake locations

Total gaseous mercury (TGM) concentrations measured on the shore of Lake Titicaca (station L3) are overall low, averaging 1.10 ± 0.17 ng m^{-3} (mean ± SD) during the rainy season, and 0.82 ± 0.09 ng m^{-3} during the dry one (Fig. 3a and b). These values are in the range of the remote regional pristine background measured in the Andes (Koenig et al., 2021).

In contrast with measurements performed at the nearby Chacaltaya mountain sites, a slight seasonal increase in average concentration is

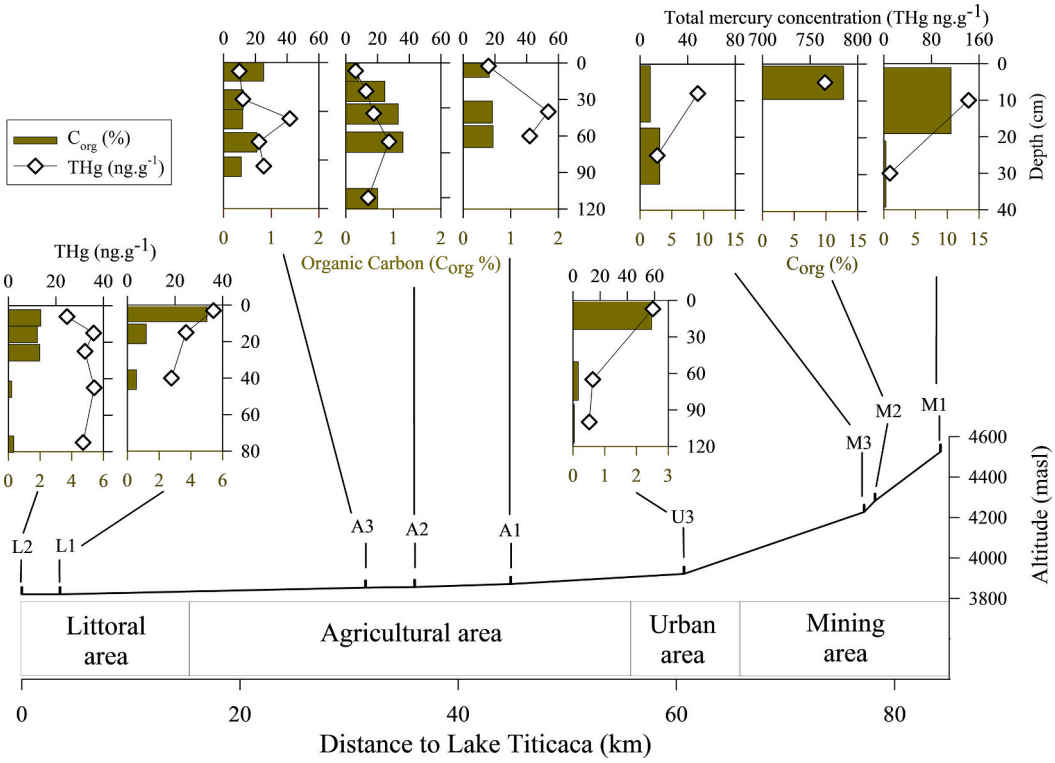


Fig. 2. Soil total mercury (THg, white diamond) and organic carbon (C_{org}, dark green bars) concentration profiles along the transect from Milluni mining area (M1, M2 and M3), to the urban area (U3), the agricultural plain (A1, A2 and A3), and the lacustrine coast (L1 and L2).

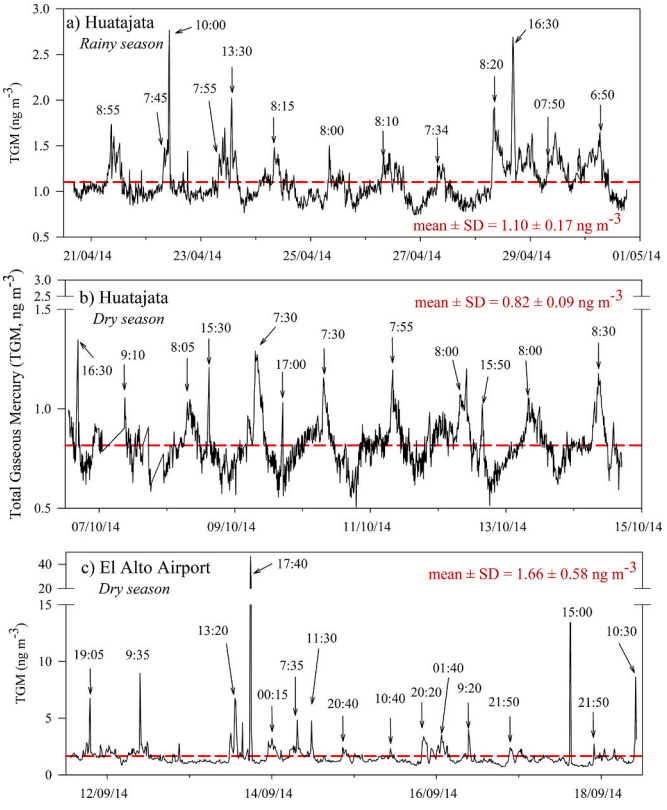


Fig. 3. Total gaseous mercury (TGM) measurement performed a) on the shore of Lake Titicaca (station L3) during the rainy (March 20th to April 1st), and b) the dry season (November 6th to 15th) 2014, and c) at the El Alto airport during the 2014 dry season (September 11th to 19th). Data obtained at the Cota Cota campus in La Paz are provided in Fig. S3.

found between the 2014 dry and wet season at Lake Titicaca. The largest increases in concentration are however found at the diurnal scale, with the lowest concentrations measured during the night (i.e., 0.7 to 1.0 ng m^{-3} during the rainy season, and 0.5 to 0.9 ng m^{-3} during the dry season), and the highest ones at the sunrise (i.e., around 8:00 AM) up to 1.9 and 1.3 for the rainy and dry seasons, respectively. Such diurnal patterns can be attributed to changes in air masses. Lower TGM concentration has been linked to westerly Altiplanic air masses, whereas higher TGM concentrations have been related to northerly air masses from the Amazonian area, or to southerly air masses of Altiplanic origin (Koenig et al., 2021). One cannot exclude the lake effect, as intense solar radiation above 3800 masl [i.e., UV-A from 800 to 1150 KJ m^{-2}, and PAR from 8 to almost 16 MJ m^{-2} (Helbling et al., 2001)] favors lake water MMHg photodegradation and significant inorganic Hg photoreduction that results in the atmospheric release of TGM (Masbou et al., 2025). Average TGM concentrations are two times higher at the Airport station of El Alto (1.66 ± 0.58 ng m^{-3}, Fig. 3c) and at the Cota Cota campus in La Paz (1.53 ± 0.41 ng m^{-3}, Fig. S2) than at station L3 for the dry season of the same year, with much higher peak amplitudes, up to 46.7 and 11.5 ng m^{-3} for El Alto and Cota Cota, respectively. Such higher peak values, which are randomly distributed during the day, support significant anthropogenic TGM punctual emissions in the urban areas, independent from diurnal natural cycles, as reported in other urban areas worldwide (Gay et al., 2013; Zhu et al., 2012).

3.3. Mercury deposition due to atmospheric aerosol washout

Total mercury concentrations in atmospheric fallout are highly variable between locations and through time, and no significant relationship is observed with rain intensity although the lowest THg in atmospheric fallout is found during the wettest episodes (Fig. S3), i.e., when particles have been washed out of the atmosphere. Spatially, the highest unfiltered THg concentrations (THg_{UNF}, Fig. 4a), are found in the urban area (stations U2, U3 and CF, mean ± SEM = 18 ± 2 ng L^{-1}) with particles >0.45 μm contributing to 68 ± 11 % of THg in

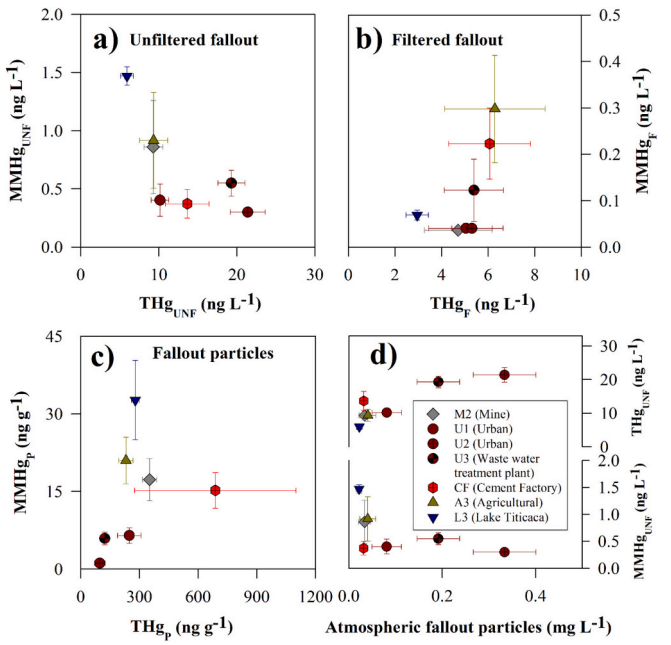


Fig. 4. Concentration in atmospheric fallout for the rainy season 2014/2015 and 2015/2016 (presented as mean ± SEM, $N = 14$ for each site). Biplots for a) Unfiltered (UNF) atmospheric fallout monomethylmercury (MMHg) and total mercury (THg), b) filtered (F < 0.45 μm) atmospheric fallout MMHg vs THg expressed in ng L^{-1}, c) particulate MMHg vs THg expressed in ng g^{-1}, and d) particulate THg (top panel) and MMHg (bottom panel) expressed in ng g^{-1} vs particles concentration in atmospheric fallout.

atmospheric fallout. In contrast, THg_{UNF} concentrations in the upstream part of the urban area (stations M1 and U1; $THg_{UNF} = 9.9 \pm 1.2$ ng L^{-1}), and in downstream remote stations (stations A3 and L3; $THg_{UNF} = 7.6 \pm 1.3$ ng L^{-1}) are at least two times lower, with a lower contribution of particles >0.45 μm (46 ± 9 %THg).

THg concentration in particles >0.45 μm (THg_P) increase from the urban area (110 ± 23 ng g^{-1}, Fig. 4c), which are in the upper range of THg found in soils, to the downstream remote stations, and the upstream part of the urban area. Finally, the highest THg_P concentration in particles >0.45 μm are found near the cement factory (CF, $THg_P = 688 \pm 413$ ng g^{-1}). Such levels are at least three times higher than the one outside the urban area (A3 and L3, $THg_P = 190 \pm 28$ ng g^{-1}), and four times those of the urban area. High THg_P concentration at CF is found associated with low fallout particles content, whereas a reverse trend is found for urban sites (Fig. 4d). This suggests that the cement factory (CF) is a major contributor of THg, likely as TGM (Goodarzi, 2004; Landis et al., 2014), which is washed out from the atmosphere during rain events associated to fine particle and dissolved species. In contrast, the contribution of THg in urban atmospheric fallout mainly originate from resuspended dust particles >0.45 μm, consistently with reported high levels of particles in the air at El Alto (Alvarez et al., 2013; Mardoñez-Balderrama et al., 2024; Mardoñez et al., 2023). Same trend is found for particulate THg in the mining area, although THg_P (290 ± 49 ng g^{-1}) are half those measured at CF. This indicates that the CF site, and in to lesser extent the mining, agricultural and littoral areas, are sources of fine Hg rich particles, whereas the urban area is a major source of particles depleted in Hg and probably coarser. Consistently with TGM data, higher concentrations for THg_P in atmospheric fallout of the urban area support anthropogenic emissions likely related to combustion processes, such as cement production and open waste burning (Mardoñez et al., 2023).

In contrast with THg, $MMHg_{UNF}$ exhibits higher concentrations in the downstream littoral and agricultural (A1, L3, mean $MMHg_{UNF}$ ± SEM = 1.2 ± 0.4 ng L^{-1}), and the upstream mining (M1, 0.9 ± 0.2 ng L^{-1}) areas than in the entire urban one (0.5 ± 0.1 ng L^{-1}). Highest $MMHg_F$ in atmospheric fallout are found in the agricultural area (0.3 ± 0.1 ng L^{-1}), and the lowest in the urban and littoral areas (0.07 ± 0.02 ng L^{-1}). Although the range of $MMHg_F$ concentrations is similar in samples collected during bi-weekly (0.05 ± 0.05 ng L^{-1}) and punctual (0.04 ± 0.02 ng L^{-1}) samplings for two events at station L3, we cannot rule out possible (de)methylation in rain collectors. As for THg, particles >0.45 μm are the major carrier of MMHg contributing to over 85 % of MMHg in atmospheric fallout collected in the upstream (M2, U1 and U2) and downstream part (L3) of the watershed, decreasing to 65 % at U3 and A3, and to 40 % at CF. Although differences in the partitioning and levels of MMHg in atmospheric fallout are found between sites, the percentage of $MMHg_{UNF}$ never exceed 1 % of THg_{UNF} for all sites, consistently with the range found in soils (see Section 3.1). This therefore supports wind erosion of soil as the most probable source for particulate MMHg in the atmosphere, as reported in other regions of the world (Ahmed et al., 1987; Huang et al., 2012b; Jiménez-Moreno et al., 2016; Liang et al., 2009).

In summary, precipitation leaches up to 10 times more atmospheric particles in the urban than in the rural area, which make THg fluxes in the urban area double those of the downstream part of the watershed. Conversely, MMHg fluxes are low in the urban area, whereas higher MMHg concentrations of atmospheric particles in rural areas, greatly increases the local deposition of atmospheric particles during rain events. The average wind direction over El Alto during the wet season is mostly easterly/southeasterly (Mardoñez-Balderrama et al., 2024), which likely reduces the dispersion of atmospheric particles from the urban to the agricultural area.

3.4. Groundwater

Mean THg_F concentration in groundwater collected in wells (mean ± SD; 1.5 ± 1.8 ng L^{-1}, Fig. 5) are in the lowest range for reported average background concentration [i.e., <10 ng L^{-1}; (Aleku et al., 2024; Laurier et al., 2007)]. $MMHg_F$ concentration in groundwater is also low (0.06 ± 0.03 ng L^{-1}), and represented 11 ± 13 % of THg (Table S2).

Overall, low concentrations of Hg species found in urban and rural wells, support that Hg is probably scavenged onto soil and sediment during water percolation, and that anthropogenic impact on Hg contamination of groundwater is limited.

3.5. Urban wastewater discharge as the main source of mercury for surface water

Filtered THg and MMHg measured in surface water along the Katari watershed during the wet season of May 2015 (Fig. 6), show evidence of a major contribution of the mining and urban areas in the rise of Hg levels in surface water.

THg concentrations are often above the range of reported levels in mine-contaminated rivers (1 to 100 ng L^{-1}) of the southern Bolivian Altiplano (Alanoca et al., 2016). THg concentrations increase abruptly along the Seke River, first within the mining area from the pristine sources (i.e., Janqo Khota outlet: 0.72 ± 0.77 ng L^{-1}) to the outlet of Lake Milluni Grande (MG: 132 ± 7 ng L^{-1}). Then, THg concentration sharply decreases between MG and M3 (0.4 ng L^{-1}), as a result from the dilution of acid mine drainage (AMD) waters with freshwaters, and from the treatment of water in the carbonate-based treatment plant of Achachicala (Driesen, 2012; Raffaillac, 2002). Downstream, THg rebound in the Urban area along the Seke and Seco Rivers (30.1 ± 17.5 ng L^{-1}). Strikingly, no significant difference is found between the inlet and outlet of the WWTP (station U3) for both THg_F (41.5 and 41.4 ng L^{-1} for the inlet and outlet, respectively) and $MMHg_F$ (1.1 and 1.0 ng L^{-1}), indicating the inefficiency of the plant for Hg removal. Percentage MMHg also exhibit a decrease from 2.5 ± 0.2 %THg at the station U3 to 0.5 ± 0.1 %THg in the downstream Palina River (CF and A1), indicating that wastewater is a probable source of MMHg for the stream. Then, THg

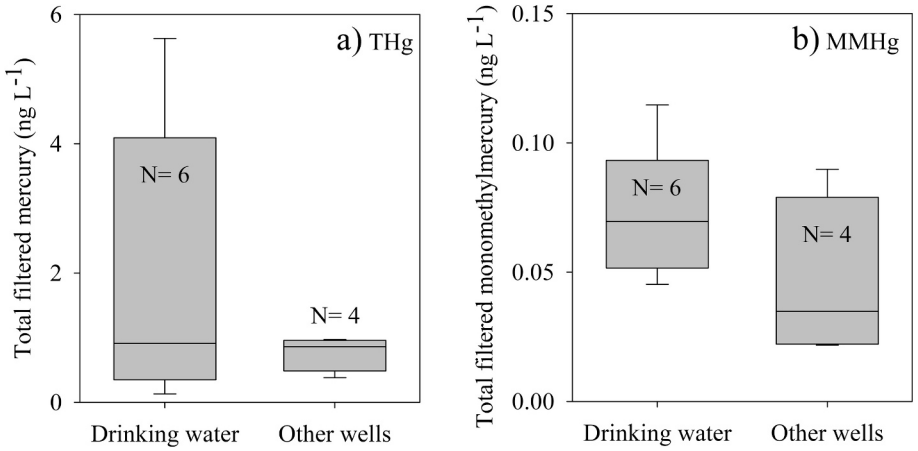


Fig. 5. Boxplot presentation of filtered a) total mercury, and b) methylmercury in groundwater in wells of the Katari watershed, showing the 25th and 75th percentile (upper and lower end of the box), mean (full line), minimum and maximum of each data set (N is the number of samples).

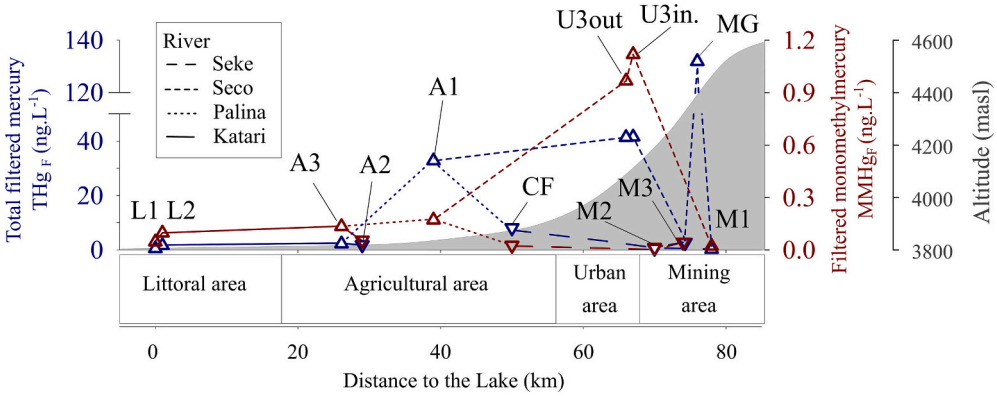


Fig. 6. Variations of total mercury (THg) and monomethylmercury (MMHg) in filtered surface water collected in May 2015, during the wet season, along the Katari watershed. Katari discharge during the sampling campaign was on average 5 times the baseline water discharge. Dashed lines indicate tributaries upstream their confluence with the Sece or Seco Rivers flowing through El Alto.

(mean ± SD = 1.35 ± 0.75 ng L^{-1}) and MMHg (0.08 ± 0.04 ng L^{-1}) return to baseline values in the agricultural and littoral area (stations A3 to L2), as a result of the dilution of urban water with the upstream Katari (site A2) and the Palina (site CF) Rivers. With the exception of the mining area, THg is found to be correlated with DOC ($R^2 = 0.95$, $p < 0.01$), indicating that the Seke and Seco Rivers are mainly impacted by urban wastewater enriched in organic matter and Hg, which are gradually diluted or buffered downstream the confluence with the Palina and Katari tributaries.

The monitoring of flood events in the Katari River at station A3, shows relatively high inter-seasonal variability for filtered THg and MMHg concentrations (Fig. 7), with MMHg representing 2.4 ± 1.5 % THg in average. The highest values are found at low water levels (i.e., $THg_F = 12.6 \pm 11.8$ ng L^{-1}, and MMHg = 0.12 ± 0.06 ng L^{-1}), indicating anthropogenic impact from the urban area (e.g., wastewater discharges), which are then diluted during the 2016 wet season (i.e., $THg_F = 2.3 \pm 0.8$ ng L^{-1}, and MMHg = 0.04 ± 0.03 ng L^{-1}), consistently with values obtained during the sampling campaign performed along the Katari watershed in May 2015 (Fig. 6).

These Hg and MMHg levels and inter-seasonal variability are consistent with other studies conducted on rivers impacted by urban effluents, such as the Saigon River (Strady et al., 2016), the Mississippi River (Balogh and Nollet, 2008), and rivers in Switzerland (Suess et al., 2020). A reverse trend is found for the suspended solids (SS) fractions, with the highest THg and MMHg found associated with fine (THg_{SSF} = 14.5 ± 6.3 ng L^{-1} and $MMHg_{SSF}$ = 0.20 ± 0.16 ng L^{-1}) and coarse (THg_{SSC} = 231.5 ± 85.5 ng L^{-1} and $MMHg_{SSF}$ = 14.0 ± 8.7 ng L^{-1}) suspended solids in high water discharge conditions during the wet season (Fig. 7). THg concentrations in the fine particles (74 ± 30 ng g^{-1}) tend to decrease with increasing turbidity ($R^2 = 0.47$, $p < 0.05$), likely resulting from inputs of fine soil particles during rain events (Archundia et al., 2021) with lower Hg content (see Section 3.1). In contrast, THg remains relatively constant in coarse particles (59 ± 14 ng g^{-1}). MMHg represent 3.7 ± 1.5 %, and 5.8 ± 2.9 %THg, for the fine (SSF) and coarse (SSC) suspended solids, respectively.

Overall, the highest concentrations in THg and MMHg are found at high particulate loads coincident with rising water discharge (Fig. 7a). Particulate THg represents 94 ± 3 % of the THg concentration in water, and is found correlated with C_{org} ($R^2 = 0.44$, $p < 0.05$). In contrast, both the filtered and fine fractions only represent 3 ± 3 %, and 7 ± 3 % of the THg concentration in water, respectively. Noteworthy, the highest SPM content along the transect are found in the urban area, and gradually decreased to the Lake (Fig. S4), indicating important SPM settling within the very gentle slopes of the downstream part of the watershed. Consistently, THg increases in the river sediment from A2 (5.9 ng g^{-1}), to A3 (24.5 ng g^{-1}), and L1 (42.3 ng g^{-1}), with MMHg representing 0.8 ± 0.6 %THg.

In summary, organic rich urban (waste)water is the main source of filtered Hg species for surface water, which are diluted by tributaries and runoff during flood events. In contrast, resuspension of fine and coarse particles during river flood enhances Hg concentrations in the stream, with fine particles as the main carrier for Hg to the lake

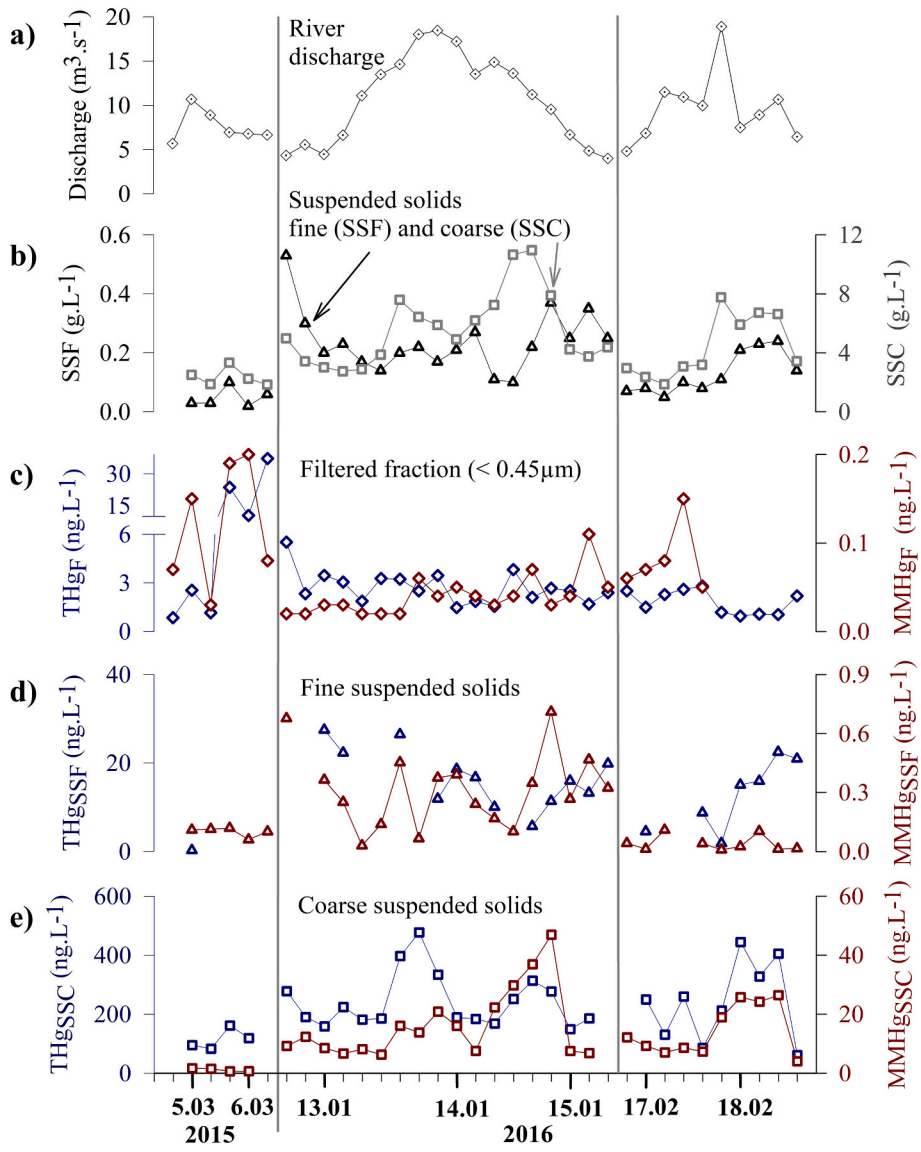


Fig. 7. Variations of water discharge of Katari river (A), fine (SSF) and coarse (SSC) suspended solids, total mercury (THg, blue symbols) and monomethylmercury (MMHg, red symbols) concentrations in the filtered (C, diamonds), fine (SSF, triangles) and coarse suspended solids (SSC, squares) during flood events monitored in 2015 and 2016 at station A3. Note that Katari discharge in early March 2015 was at least 5 time lower than during the sampling campaign performed along the Katari watershed during the wet season in May 2015 (Fig. 6).

(Archundia et al., 2017).

3.6. Historical reconstruction of Hg inputs to Lake Titicaca

The well-dated Lake Titicaca sediment core W7 (Fig. S5) allows the reconstruction of THg accumulation over the last past 120 years in the Cohana Bay at the outlet of the Katari River (Fig. 1). Both THg concentrations (mean ± SD = 58 ± 4 ng g^{-1}) and accumulation rates (HgAR = 27 ± 10 µg m^2 yr^{-1}) exhibit relatively stable values from 1920 to the modern period, with an increase during the last decades (Figs. 8a and S6). Surprisingly, no peak in THg or HgARs occurs during the main periods of tin (Sn) production in Milluni [i.e., from 1920 to 1980 CE (Mitre, 1993)], whereas other elements such as iron (Fe), lead (Pb), chromium (Cr) and titanium (Ti) broadly follow this trend (Figs. S5 and S6), indicating little THg contribution from the Milluni mining area to the Lake over this period. In contrast, the contribution of atmospheric Hg deposition from regional mining is found during the late 19th century (Fig. S7), a period marked by enhanced use of Hg in industrial silver (Ag) mining operations in Bolivia (Guédron et al., 2021; Hillman, 1984; Mitre, 1993). From 1990 onward, the rises in sediment, Hg, Pb and C_{org} accumulation rates (by at least a factor 2), indicate enhanced urban contribution of wastewater discharge in the Katari River to the Lake (Figs. 8 and S7) following the demographic increase at El Alto (Kinouchi et al., 2019).

To estimate the annual contribution of the Katari River discharge to the Lake Titicaca, we used the instrumental record of the Katari water discharge monitored since 1992 (SENAMHI, 2024), together with the relationship found between THg river flux and water discharge (Fig. S8) for the 2015/2016 wet season monitoring. This allows the reconstruction of annual THg exports from the Katari to the lake for the 1992–2015 period, considering that all particles settle within the Cohana Bay (area of the Bay = 44 km^2). Because the Cohana Bay is located at the outlet of the agricultural plain, we only consider the filtered and fine suspended solids as Hg carriers to the lake, making the assumption that all coarse particles have settled along the almost flat plain.

Annual riverine THg exports the Lake for the 1992–2015 period (17 ± 4 µg m^2 yr^{-1}) suggest that the Katari river has contributed to at least 43 ± 14 % of THg accumulated in the Cohana Bay sediment core W7 (34

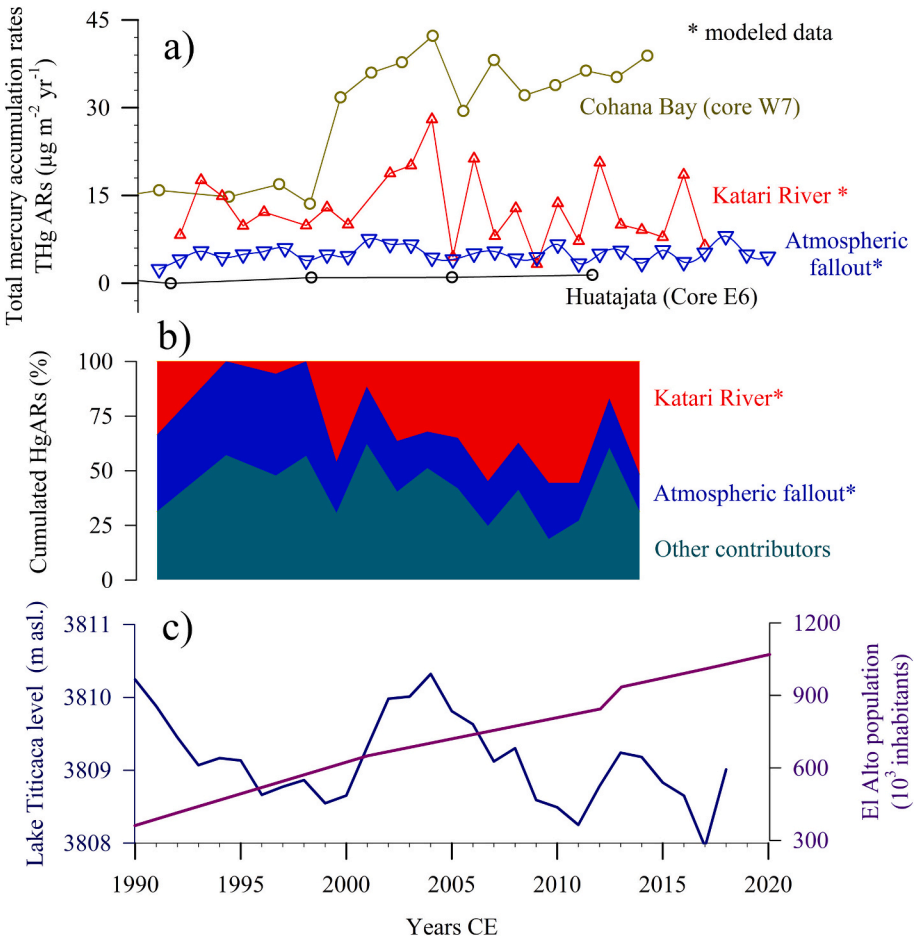


Fig. 8. a) Reconstruction for the 1990–2020 period of mercury accumulation rates (HgAR) from the Lake Titicaca sediment core W7 collected in the Cohana Bay and E6 collected at Huatajata, together with modelled (*) Hg fluxes discharged from the Katari river and from annual atmospheric fallout records (SENAMHI, 2024). b) Cumulated modelled HgARs from the Katari River (red), atmospheric fallout (bleu) and other sources (cyan) expressed in percentages of the total HgAR obtained from core E7. c) average Lake Titicaca annual water level (Senamhi, 2024), and demography of El Alto city (INE, 2024).

± 7 µg m^2 yr^{-1}, Fig. 7). It is worth mentioning that this contribution is likely overestimated for the period prior to the demographic boom (i.e., prior to 1990), as urban Hg discharges were certainly lower at that time. The contribution of annual Hg atmospheric fallout depositions are then estimated on the basis of the average Hg concentrations measured in the 2014–2016 rainfall samples, the recorded average annual precipitation at El Alto (INE, 2024), and the surface area of the bay. The resulting annual THg atmospheric fallout deposition rates over the bay (7 ± 2 µg m^2 yr^{-1}, Fig. 8a) have thus contributed to 16 ± 11 % of THg accumulated in the W7 sediment core (Fig. 8b). This range of calculated atmospheric fallout deposition is consistent with HgARs found in the remote core E6 (6 ± 1 µg m^2 yr^{-1}, Fig. 8a), and with values reported for sediment cores collected in a deep remote part of the lake [9 ± 2 µg m^2 yr^{-1} (Guédron et al., 2021; Jiskra et al., 2022)] away from river discharges, and for the same period. Finally, although impossible to reconstruct through time, the average annual dry deposition was assessed from TGM concentrations measured in the lake shores at station L3 (Fig. 3), and an average dry deposition velocity (V_d) between 0.01 and 0.03 cm s^{-1} reported for inland lake or uncovered and subalpine grassland soils (Zhang et al., 2009). This results in a rough estimate of TGM dry deposition of around 6 ± 4 µg m^2 yr^{-1} for the non-urban area, which is close to wet deposition fluxes. The sum of River (~44 %) and atmospheric sources (~38 %) account for ca. 82 % of the THg accumulated in core W7, and shows a rising contribution of the Katari discharge through time (Fig. 8b), consistently with the rise of wastewater effluxes with rising demography. To complete this budget, other potential contributors to the Cohana Bay sediment are the input of coarse particles during major floods, and the contribution of Hg uptake by lake biomass (Stern et al., 2009). For this latter contributor, the high primary productivity of the Cohana Bay (Achá et al., 2018; Heredia et al., 2022) supports important Hg bio-uptake within the bay as lake primary biological producers are known as important Hg scavengers in Lake Titicaca (Jiskra et al., 2022; Quiroga-Flores et al., 2021). Finally, groundwater contribution to Hg inputs to the lake is expected to be negligible as previous studies showed evidence of low contribution of the groundwater to the lake (Flores Avilès et al., 2020).

3.7. THg and MMHg at the scale of the Katari watershed (2014–2016): a budget

The annual wet and dry THg and MMHg fluxes were calculated at each site from measured average annual precipitation rates (INE, 2024), THg and MMHg content (filtered + unfiltered) in atmospheric fallout samples collected during the 2014/2015 and 2015/2016 rainy seasons, and TGM concentrations monitored in 2014. THg wet deposition fluxes (atmospheric fallout) found for the urban (14 ± 5 µg m^2 yr^{-1}) and the CF (11 ± 8 µg m^2 yr^{-1}) sites are at least two times higher than for the non-urban sites (7 ± 2 µg m^2 yr^{-1}). These latter fluxes are slightly higher than reported values for remote Tibetan regions [i.e., <2 µg m^2 yr^{-1} (Huang et al., 2012a)] and within the higher end of the global natural atmospheric Hg deposition rate [2 to 5 µg m^2 yr^{-1} (Swain et al., 1992)], but similar to those measured in the capital of Tibet [i.e., 19.3 µg m^2 yr^{-1}

(Huang et al., 2013)]. The estimated average TGM dry deposition for the urban area (11 ± 8 μg m^2 yr^{-1}) is almost double that of non-urban area (i.e., ca. 6 ± 4 μg m^2 yr^{-1}), and close to values obtained for wet deposition fluxes. Consistently, high dry Hg depositions fluxes have been reported at high elevations, and attributed to the enhanced Hg oxidation process with more intensive solar radiation (Zhang et al., 2019). These estimates of dry Hg depositions fluxes are in the range of reported values in Lhasa, Tibet [i.e., 14.3 μg m^2 yr^{-1} (Huang et al., 2013)], but lower than values obtained at measured in the high altitude forested Mt. Leigong (2178 m a.s.l.), China [i.e., 43.9 μg m^2 yr^{-1} (Fu et al., 2009)]. The annual atmospheric (wet and dry) Hg depositions are therefore 26 ± 11 μg m^2 yr^{-1} for the urban site, and 13 ± 7 μg m^2 yr^{-1} for the non-urban site. Reverse trend was found for MMHg with higher fluxes in non-urban sites (0.9 ± 0.3 μg m^2 yr^{-1}) compared to urban (0.3 ± 0.1 μg m^2 yr^{-1}) and CF (0.3 ± 0.4 μg m^2 yr^{-1}) sites, likely resulting from differences in atmospheric particle sources between sites (see discussion in Section 3.3). This estimate is however underestimated as dry MMHg fluxes are cannot be estimated here.

At the scale of the entire watershed (i.e., 2022 km^2), annual wet Hg depositions to the surface via atmospheric fallout represent 16 ± 6 kg per year of THg and 1.6 ± 1.5 kg per year of MMHg, and annual dry Hg depositions are 13 ± 8 kg per year of THg (Fig. 9). When normalized to the watershed scale, such annual THg wet and dry depositions over the Katari watershed (28.3 ± 13.8 kg yr^{-1}), is at least 3 times higher than reported values for the Chinese Lake Hongfeng watershed [7.9 ± 5.3 kg yr^{-1} (Zhang et al., 2025)], and similar to a small remote watershed in Scotland [33.0 ± 3.3 kg yr^{-1} (Yang et al., 2002)], which suggests a moderate atmospheric Hg pollution in this urban watershed.

In the Katari basin, most groundwater recharge results from the infiltration of precipitation and runoff on the high mountain ranges (Flores Avilès et al., 2020). The observed decrease in filtered THg and MMHg concentrations between atmospheric fallout and groundwater indicates that soil acts as a sink for atmospheric fallout Hg depositions. From the difference between the average filtered THg and MMHg concentration measured in fallout and groundwater, it can be assumed that at least 60 % of THg and MMHg deposited with fallout are stored in the soil. Annual amounts of THg and MMHg flowing through the Katari River to the lake represent less than 3 % of those deposited from the atmosphere at the scale of the watershed (Fig. 9). Hence, both the long distance and the very gentle slopes downstream the urban area make the river sediment another significant sink for Hg and MMHg through particle settling. The same hypothesis is also likely for the downstream part of the Milluni mining area (see discussion in Section 3.5).

4. Conclusion

This inventory of Hg and MMHg concentrations and fluxes in the compartments of the Katari river watershed allows documenting for the first time, the impact of anthropogenic activities (urban and mining) on the Hg budget of a high-altitude watershed. Although MMHg and THg levels are moderately low, we here show evidence that the rapid development of the urban area of El Alto has impacted the river and downstream lake environment mainly through wastewater discharge. This contribution accounts for almost one half of the riverine Hg emission to the lake. In this budget, wet and dry deposition appears as the major source of Hg species to watershed surface, and soils as the major sink, preventing Hg transfer to groundwater. Further research is required to improve the assessment of Hg dry deposition at the annual scale, and to provide more accurate values of TGM dry deposition velocity.

The unregulated and fast growth of the urban area has implications for continued Hg inputs to the lake as a result of possible enhanced wastewater emission. Therefore, the watershed will remain a source of Hg to the lake for many years if no efficient wastewater treatment is setup. Future works need to document the fate of Hg between the upstream mining area and the downstream river to better understand the mechanisms of deposition and storage of Hg. Sediment resuspension during high floods in the downstream part of the Katari River should also be studied as this area of the watershed is potentially a transient Hg stock to the lake.

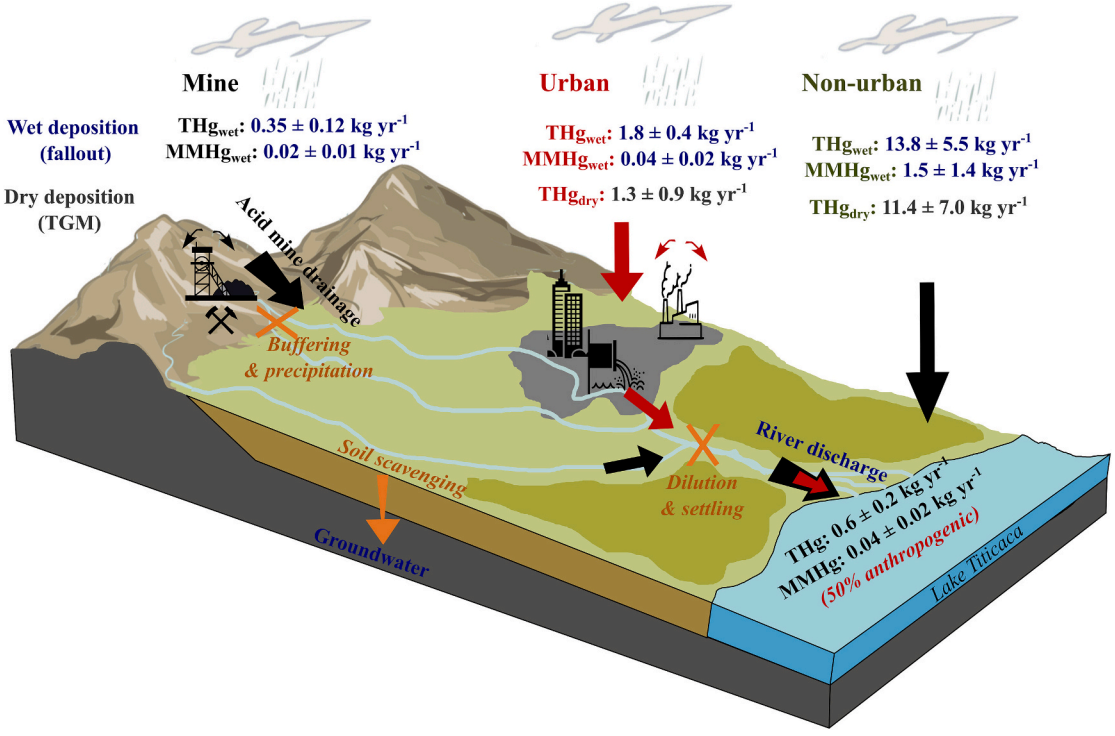


Fig. 9. Annual wet (blue) and dry (grey) total mercury (THg) and monomethylmercury (MMHg) budgets at the scale of the Katari watershed (2022 km^2) for the 2014–2016 period.

CRediT authorship contribution statement

Stéphane Guédron: Writing – review & editing, Writing – original draft, Visualization, Validation, Supervision, Software, Resources, Project administration, Methodology, Investigation, Funding acquisition, Formal analysis, Data curation, Conceptualization. **Djamilatou Dabre:** Writing – review & editing, Validation, Investigation, Formal analysis. **Céline Duwig:** Writing – review & editing, Resources, Investigation, Funding acquisition, Formal analysis. **David Amouroux:** Writing – review & editing, Validation, Supervision, Investigation, Funding acquisition, Formal analysis. **Jonathan Fin:** Formal analysis, Data curation. **Sylvain Campillo:** Validation, Formal analysis, Data curation. **Romain Biron:** Methodology, Investigation, Formal analysis. **Hélène Guyard:** Methodology, Investigation, Formal analysis. **Emmanuel Tessier:** Investigation, Formal analysis, Data curation. **Isabel Moreno:** Investigation, Formal analysis. **Jimena Yupanqui:** Investigation, Formal analysis. **Gaëlle Uzu:** Writing – review & editing, Project administration, Investigation. **Dario Acha:** Writing – review & editing, Supervision, Project administration, Investigation, Data curation.

Declaration of competing interest

The authors declare that they have no known competing financial interests or personal relationships that could have appeared to influence the work reported in this paper.

Acknowledgments

This work is a contribution to the TRACISOMER (PI: S. Guédron: stephane.guedron@ird.fr) and CONTITI (PI: C. Duwig: celine.duwig@ird.fr) projects supported by a grant from Labex OSUG@2020, and the LA PACHAMAMA project (ANR CESA program, No ANR-13-CESA-0015-01, PI: D. Amouroux: david.amouroux@univ-pau.fr). S. Guédron, S. Campillo, J. Fin (ISTerre/IRD/UGA), C. Duwig, R. Biron, H. Guyard and G. Uzu (IGE/IRD/UGA) are part of Labex OSUG@2020 (Investissements d'avenir ANR10 LABX56). This work is a contribution to the ALTIPLANO International Joint Laboratory (LMI ALTIPLANO), supported by a grant from the IRD (Institut de Recherche pour le Développement, France). We wish to thank, J. Gardon, A. Terrazas, C. Gonzalez, N. Clavijo, L. Salvatierra, R. Rios, J.C. Salinas, A. Castillo, M. Claure, and la Familia Catari (Don Ramon, Don Maximo, Don Eric, Don Ruben and Donia Maria) for their help and assistance during the field campaigns.

Appendix A. Supplementary data

Supplementary data to this article can be found online at https://doi.org/10.1016/j.scitotenv.2025.180239.

Data availability

Data will be made available on request.

References

Achá, D., Guédron, S., Amouroux, D., Point, D., Lazarro, X., Fernandez, P., et al., 2018. Algal bloom exacerbates hydrogen sulfide and methylmercury contamination in the emblematic high-altitude Lake Titicaca. Geosciences 8, 438.

Ahmed, R., May, K., Stoeppler, M., 1987. Wet deposition of mercury and methylmercury from the atmosphere. Sci. Total Environ. 60, 249–261.

Alanoca, L., Guédron, S., Amouroux, D., Audry, S., Monperrus, M., Tessier, M., et al., 2016. Synergistic effects of mining and urban effluents on the level and distribution of methylmercury in a shallow aquatic ecosystem of the Bolivian Altiplano. Environ. Sci. Process Impacts 18, 1550–1560.

Aleku, D.L., Lazareva, O., Pichler, T., 2024. Mercury in groundwater – Source, transport and remediation. Appl. Geochem. 170, 106060.

Alvarez, H.B., Echeverria, R.S., Alvarez, P.S., Krupa, S., 2013. Air quality standards for particulate matter (PM) at high altitude cities. Environ. Pollut. 173, 255–256.

Archundia, D., Duwig, C., Spadini, L., Uzu, G., Guédron, S., Morel, M.C., et al., 2017. How uncontrolled urban expansion increases the contamination of the Titicaca Lake Basin (El Alto, La Paz, Bolivia). Water Air Soil Pollut. 228, 44.

Archundia, D., Duwig, C., Spadini, L., Morel, M.C., Prado, B., Perez, M.P., et al., 2019. Assessment of the sulfamethoxazole mobility in natural soils and of the risk of contamination of water resources at the catchment scale. Environ. Int. 130, 104905.

Archundia, D., Martins, J., Lehembre, F., Morel, M.-C., Duwig, C., 2021. Sulfamethoxazole biodegradation and impacts on soil microbial communities in a Bolivian arid high altitude catchment. Chemosphere 284, 131335.

Balogh, S.J., Nollet, Y.H., 2008. Methylmercury input to the Mississippi River from a large metropolitan wastewater treatment plant. Sci. Total Environ. 406, 145–153.

Bloom, N.S., Fitzgerald, W.F., 1988. Determination of volatile mercury species at the picogram level by low-temperature gas chromatography with cold-vapor atomic fluorescence detection. Anal. Chim. Acta 208, 151–161.

Bouchet, S., Tessier, E., Masbou, J., Point, D., Lazzaro, X., Monperrus, M., et al., 2022. In situ photochemical transformation of Hg species and associated isotopic fractionation in the water column of high-altitude lakes from the Bolivian Altiplano. Environ. Sci. Technol. 56, 2258–2268.

Cooke, C.A., Martínez-Cortizas, A., Bindler, R., Gustin, M.S., 2020. Environmental archives of atmospheric Hg deposition–a review. Sci. Total Environ. 709, 134800.

Cossa, D., Sanjuan, J., Cloud, J., Stockwell, B., Corns, W., 1995. Automated mercury determination in waters. Water Air Soil Pollut. 80, 1279–1284.

Cossa, D., Averty, B., Pirrone, N., 2009. The origin of methylmercury in open Mediterranean waters. Limnol. Oceanogr. 54, 837–844.

Driesen, K., 2012. Contamination of Surface Waters by the Former Mining Industry in the Milluni Valley (Cordillera Real, Bolivia) and the Application of the Water Planning Model WEAP. University College Ghent. Bachelor in chemistry. Ghent, Ghent, Belgium, p. 64.

Fitzgerald, W.F., Clarkson, T.W., 1991. Mercury and monomethylmercury: present and future concerns. Environ. Health Perspect. 96, 159–166.

Flores Avilès, G.P.F., Descloitres, M., Duwig, C., Rossier, Y., Spadini, L., Legchenko, A., et al., 2020. Insight into the Katari-Lago Menor Basin aquifer, Lake Titicaca-Bolivia, inferred from geophysical (TDEM), hydrogeological and geochemical data. J. South Am. Earth Sci. 99, 102479.

Fu, X., Feng, X., Dong, Z., Yin, R., Wang, J., Yang, Z., et al., 2009. Atmospheric total gaseous mercury (TGM) concentrations and wet and dry deposition of mercury at a high-altitude mountain peak in South China. Atmos. Chem. Phys. Discuss. 9.

Gay, D.A., Schmeltz, D., Prestbo, E., Olson, M., Sharac, T., Tordon, R., 2013. The Atmospheric Mercury Network: measurement and initial examination of an ongoing atmospheric mercury record across North America. Atmos. Chem. Phys. 13, 11339–11349.

Goodarzi, F., 2004. Speciation and mass-balance of mercury from pulverized coal fired power plants burning western Canadian subbituminous coals. J. Environ. Monit. 6, 792–798.

Guédron, S., Grangeon, S., Lanson, B., Grimaldi, M., 2009. Mercury speciation in a tropical soil association; consequence of gold mining on Hg distribution in French Guiana. Geoderma 153, 331–346.

Guédron, S., Grangeon, S., Jouravel, G., Charlet, L., Sarret, G., 2013. Atmospheric mercury incorporation in soils of an area impacted by a chlor-alkali plant (Grenoble, France): contribution of canopy uptake. Sci. Tot. Environ. 445-446, 356–364.

Guédron, S., Duwig, C., Prado, B.L., Point, D., Flores, M.G., Siebe, C., 2014a. (Methyl) mercury, arsenic, and lead contamination of the world's largest wastewater irrigation system: the Mezquital Valley (Hidalgo state-Mexico). Water Air Soil Pollut. 225, 1–19.

Guédron, S., Tisserand, D., Garambois, S., Spadini, L., Molton, F., Bounvilay, B., et al., 2014b. Baseline investigation of (methyl)mercury in waters, soils, sediments and key foodstuffs in the Lower Mekong Basin: the rapidly developing city of Vientiane (Lao PDR). J. Geochem. Explor. 143, 96–102.

Guédron, S., Devin, S., Vignati, D.A.L., 2015. Total and methylmercury partitioning between colloids and true solution: from case studies in sediment overlying and pore waters to a generalized model. Environ. Toxicol. Chem. https://doi.org/10.1002/etc.3190.

Guédron, S., Point, D., Acha, D., Bouchet, S., Baya, P.A., Molina, C.I., et al., 2017. Mercury contamination level and speciation inventory in the hydrosystem of Lake Titicaca: current status and future trends. Environ. Pollut. 231, 262–270.

Guédron, S., Ledru, M.P., Escobar-Torrez, K., Develle, A.L., Brisset, E., 2018. Enhanced mercury deposition by Amazonian orographic precipitation: evidence from high-elevation Holocene records of the Lake Titicaca region (Bolivia). Palaeogeogr. Palaeoclimatol. Palaeoecol. 511, 577–587.

Guédron, S., Tolu, J., Brisset, E., Sabatier, P., Perrot, V., Bouchet, S., et al., 2019. Late Holocene volcanic and anthropogenic mercury deposition in the western Central Andes (Lake Chungará, Chile). Sci. Total Environ. 662, 903–914.

Guédron, S., Achá, D., Bouchet, S., Point, D., Tessier, E., Heredia, C., et al., 2020a. Accumulation of methylmercury in the high-altitude Lake Uru Uru (3686 m asl, Bolivia) controlled by sediment efflux and photodegradation. Appl. Sci. 10, 7936.

Guédron, S., Audry, S., Acha, D., Bouchet, S., Point, D., Condom, T., et al., 2020b. Diagenetic production, accumulation and sediment-water exchanges of methylmercury in contrasted sediment facies of Lake Titicaca (Bolivia). Sci. Total Environ. 723, 138088.

Guédron, S., Tolu, J., Delaere, C., Sabatier, P., Barre, J., Heredia, C., et al., 2021. Reconstructing two millennia of copper and silver metallurgy in the Lake Titicaca region (Bolivia/Peru) using trace metals and lead isotopic composition. Anthropocene 34, 100288.

Guédron, S., Delaere, C., Fritz, S.C., Tolu, J., Sabatier, P., Devel, A.-L., et al., 2023. Holocene variations in Lake Titicaca water level and their implications for

sociopolitical developments in the Central Andes. Proc. Natl. Acad. Sci. U. S. A. 120, e2215882120.
Guédron, S., Tolu, J., Amouroux, D., Tessier, E., Molina, C., Bueno, M., et al., 2024. Arsenic, selenium, and mercury speciation in hypersaline lakes of the Andean Altiplano: link between extreme levels and biodiversity repartition. J. Geochem. Explor. 267, 107577.
Hammerschmidt, C.R., Fitzgerald, W.F., Balcom, P.H., Visscher, P.T., 2008. Organic matter and sulfide inhibit methylmercury production in sediments of New York/New Jersey Harbor. Mar. Chem. 109, 165–182.
Helbling, E.W., Villafañe, V., Buma, A., Andrade, M., Zaratti, F., 2001. DNA damage and photosynthetic inhibition induced by solar ultraviolet radiation in tropical phytoplankton (Lake Titicaca, Bolivia). Eur. J. Phycol. 36, 157–166.
Heredia, C., Guédron, S., Point, D., Perrot, V., Campillo, S., Verin, C., et al., 2022. Anthropogenic eutrophication of Lake Titicaca (Bolivia) revealed by carbon and nitrogen stable isotopes fingerprinting. Sci. Total Environ. 845, 157286.
Hillman, J., 1984. The emergence of the tin industry in Bolivia. J. Lat. Am. Stud. 16, 403–437.
Huang, J., Kang, S., Zhang, Q., Yan, H., Guo, J., Jenkins, M.G., et al., 2012a. Wet deposition of mercury at a remote site in the Tibetan Plateau: concentrations, speciation, and fluxes. Atmos. Environ. 62, 540–550.
Huang, J., Kang, S., Wang, S., Wang, L., Zhang, Q., Guo, J., et al., 2013. Wet deposition of mercury at Lhasa, the capital city of Tibet. Sci. Total Environ. 447, 123–132.
Huang, M., Wang, W., Leung, H., Chan, C.Y., Liu, W.K., Wong, M.H., et al., 2012b. Mercury levels in road dust and household TSP/PM2.5 related to concentrations in hair in Guangzhou, China. Ecotoxicol. Environ. Saf. 81, 27–35.
INE, 2024. Clima y Atmósfera, Instituto Nacional de Estadística, La Paz, Bolivia. https://www.ine.gob.bo/index.php/medio-ambiente/clima-y-atmosfera/.
Jiménez-Moreno, M., Barre, J.P.G., Perrot, V., Bérail, S., Martin-Doimeadios, R.C.R., Amouroux, D., 2016. Sources and fate of mercury pollution in Almadén mining district (Spain): evidences from mercury isotopic compositions in sediments and lichens. Chemosphere 147, 430–438.
Jiskra, M., Guédron, S., Tolu, J., Fritz, S.C., Baker, P.A., Sonke, J.E., 2022. Climatic controls on a Holocene mercury stable isotope sediment record of Lake Titicaca. ACS Earth Space Chem. 6, 346–357.
Jury, W.A., Vaux Jr., H., 2005. The role of science in solving the world's emerging water problems. Proc. Natl. Acad. Sci. 102, 15715–15720.
Kinouchi, T., Nakajima, T., Mendoza, J., Fuchs, P., Asaoka, Y., 2019. Water security in high mountain cities of the Andes under a growing population and climate change: a case study of La Paz and El Alto, Bolivia. Water Security 6, 100025.
Koenig, A.M., Magand, O., Laj, P., Andrade, M., Moreno, I., Velarde, F., et al., 2021. Seasonal patterns of atmospheric mercury in tropical South America as inferred by a continuous total gaseous mercury record at Chacaltaya station (5240 m) in Bolivia. Atmos. Chem. Phys. 21, 3447–3472.
Landis, M.S., Ryan, J.V., ter Schure, A.F., Laudal, D., 2014. Behavior of mercury emissions from a commercial coal-fired power plant: the relationship between stack speciation and near-field plume measurements. Environ. Sci. Technol. 48, 13540–13548.
Laurier, F.J.G., Cossa, D., Beucher, C., Breviere, E., 2007. The impact of groundwater discharges on mercury partitioning, speciation and bioavailability to mussels in a coastal zone. Mar. Chem. 104, 143–155.
Liang, Y., Yuan, D., Lu, M., Gong, Z., Liu, X., Zhang, Z., 2009. Distribution characteristics of total mercury and methylmercury in the topsoil and dust of Xiamen, China. Journal of Environmental Sciences 21, 1400–1408.
Loayza Farrachol, K., 2022. Tratamiento de datos hidrologicos y evaluacion temporal de alteraciones hidrologicas en subcuencas del lago Ticicaca. Facultad de Ingeneria Civil. Master. Universidad Mayor de San Andrés, La Paz, Bolivia, p. 72.
Mardoñez, V., Pandolfi, M., Borlaza, L.J.S., Jaffrezo, J.-L., Alastuey, A., Besombes, J.-L., et al., 2023. Source apportionment study on particulate air pollution in two high-altitude Bolivian cities: La Paz and El Alto. Atmos. Chem. Phys. 23, 10325–10347.
Mardoñez-Balderrama, V., Močnik, G., Pandolfi, M., Modini, R.L., Velarde, F., Renzi, L., et al., 2024. Atmospheric black carbon in the metropolitan area of La Paz and El Alto, Bolivia: concentration levels and emission sources. Atmos. Chem. Phys. 24, 12055–12077.
Masbou, J., Point, D., Bouchet, S., Sonke, J.E., Molina, C., Ibanez, C., et al., 2025. Mercury compound-specific stable isotope fractionation in high-altitude lake ecosystems of the Bolivian Altiplano. Sci. Total Environ. 983, 179630.
Mitre, A., 1993. El enigma de los hornos: la economía política de la fundición de estaña: el proceso boliviano a la luz de otras experiencias. Asociación Nacional de Mineros Medianos.
Poupeau, F., Hardy, S., 2016. Water cooperatives in La Paz and El Alto, Bolivia: a complementary system. In: Water Regimes. Routledge, pp. 149–165.
Quiroga-Flores, R., Guédron, S., Acha, D., 2021. High methylmercury uptake by green algae in Lake Titicaca: potential implications for remediation. Ecotoxicol. Environ. Saf. 207, 111256.
Raffaillac, E., 2002. Estudio in Situ de la Contaminación Minera de la Cuenca Milluni, Mémoire de Stage en Aguas del Illimani. UMSA, La Paz, Bolivia, p. 96.
Ríos, C., 1985. Estudio de la Contaminación Ambiental por las Descargas Mineras de COMSUR en la Represa de Milluni. In: Andres, UMdS (Ed.), Ingenierîa Civil. La Paz, Bolivia, p. 120.
Salvarredy-Aranguren, M.M., Probst, A., Roulet, M., Isaure, M.-P., 2008. Contamination of surface waters by mining wastes in the Milluni Valley (Cordillera Real, Bolivia): mineralogical and hydrological influences. Appl. Geochem. 23, 1299–1324.
SENAMHI B, 2024. Servicio Nacional de Meteorología de Hidrología, Servicio Nacional de Meteorologia e Hidrologia, La Paz, Bolivia. http://www.senamhi.gob.bo.
Skyllberg, U., 2012. Chemical speciation of mercury in soil and sediment. In: Liu, G., Cai, Y., O'Driscoll, N. (Eds.), Environmental Chemistry and Toxicology of Mercury. John Wiley & Sons, Inc., Hoboken, New Jersey, pp. 219–258.
Stern, G.A., Sanei, H., Roach, P., Delaronde, J., Outridge, P.M., 2009. Historical interrelated variations of mercury and aquatic organic matter in lake sediment cores from a subarctic lake in Yukon, Canada: further evidence toward the algal-mercury scavenging hypothesis. Environ. Sci. Technol. 43, 7684–7690.
Strady, E., Dang, V.B.H., Némery, J., Guédron, S., Dinh, Q.T., Denis, H., et al., 2016. Baseline seasonal investigation of nutrients and trace metals in surface waters and sediments along the Saigon River basin impacted by the megacity of Ho Chi Minh (Vietnam). Environ. Sci. Pollut. Res. 1.
Strady, E., Dinh, Q.T., Némery, J., Nguyen, T.N., Guédron, S., Nguyen, N.S., et al., 2017. Spatial variation and risk assessment of trace metals in water and sediment of the Mekong Delta. Chemosphere 179, 367–378.
Suess, E., Berg, M., Bouchet, S., Cayo, L., Hug, S.J., Kaegi, R., et al., 2020. Mercury loads and fluxes from wastewater: a nationwide survey in Switzerland. Water Res. 175, 115708.
Swain, E.B., Engstrom, D.R., Brigham, M.E., Henning, T.A., Brezonik, P.L., 1992. Increasing rates of atmospheric mercury deposition in Midcontinental North America. Science 257, 784–787.
Webster, R., 2001. Statistics to support soil research and their presentation. Eur. J. Soil Sci. 52, 331–340.
Chemical safety - activity report. In: WHO, Organization WH (Eds.), 2018. WHO Chemical Safety. World Health Organization, Geneva, p. 20.
Yang, H., Rose, N.L., Battarbee, R.W., Boyle, J.F., 2002. Mercury and lead budgets for Lochnagar, a Scottish mountain lake and its catchment. Environ. Sci. Technol. 36, 1383–1388.
Zhang, H., Yin, R.-s., Feng, X.-b., Sommar, J., Anderson, C.W.N., Sapkota, A., et al., 2013. Atmospheric mercury inputs in montane soils increase with elevation: evidence from mercury isotope signatures. Sci. Rep. 3.
Zhang, H., Fu, X., Wu, X., Deng, Q., Tang, K., Zhang, L., et al., 2025. Watershed runoff as a dominant pathway for mercury loading into a karst lake as unraveled by a novel mercury isotope and flux balance model. Water Res. 283, 123820.
Zhang, L., Wright, L.P., Blanchard, P., 2009. A review of current knowledge concerning dry deposition of atmospheric mercury. Atmos. Environ. 43, 5853–5864.
Zhang, L., Zhou, P., Cao, S., Zhao, Y., 2019. Atmospheric mercury deposition over the land surfaces and the associated uncertainties in observations and simulations: a critical review. Atmos. Chem. Phys. 19, 15587–15608.
Zhu, J., Wang, T., Talbot, R., Mao, H., Hall, C., Yang, X., et al., 2012. Characteristics of atmospheric total gaseous mercury (TGM) observed in urban Nanjing, China. Atmos. Chem. Phys. 12, 12103–12118.